EDAPHOS

D2.5
Report on initial ecotoxicity and ecosystem services assessment (update)

WP2 – Task 2.2

February 2026 (M30)

Authors: Aleksandra Zgórska (GIG-PIB), Anna Borgulat (GIG-PIB), Paweł Łabaj (GIG-PIB), Mariusz Kruczek (GIG-PIB), Łukasz Pierzchała (GIG-PIB), Aleksa Warzecha (GIG-PIB), Nicolas Manier (INERIS)

Funded by the European Union

Disclaimer

Funded by the European Union. Views and opinions expressed are however those of the author(s) only and do not necessarily reflect those of the European Union or the European Research Executive Agency. Neither the European Union nor the granting authority can be held responsible for them.

Artificial Intelligence (AI) was used to enhance the clarity of certain aspects of this document. Open AI was used in to produce some figure in this documents The purpose was to facilitate the readability of the activity through graphical elements.

Document information

Grant Agreement	n°101112768
Project Title	Advanced mapping, risk assessment and nature-based depollution methods are combined to accelerate the recovery of contaminated soils and ensure that ecological restoration enters mainstream business
Project Acronym	EDAPHOS
Project Coordinator	Dr. Michel Chalot, UBFC
Project Duration	1 September 2023 – 31 August 2028 (60 months)
Related Work Package	WP2
Related Task(s)	T2.2. Acquiring ecotoxicological data and ESS data
Lead Organisation	GIG-PIB
Contributing Partner(s)	INERIS, UMLP, MIC, A21, CRES, CSIC, UNIBO, EVO
Due Date	28/02/2026
Submission Date	27/02/2026
Dissemination level	PU - Public

History

Date	Version	Submitted by	Reviewed by	Comments
20/02/2026	V1.0	A. Zgórska	N. Manier	

Funded by the European Union

22/02/2026	V2.0	A. Zgórska	M. Chalot	
27/02/2026	V2.1	L.Duivon;	A.Paul	Submitted to EC

Table of contents

Funded by the European Union

Funded by
the European Union

Funded by the European Union

List of figures

Funded by the European Union

List of tables

Funded by
the European Union

Funded by the European Union

Funded by
the European Union

Funded by the European Union

Funded by
the European Union

Funded by
the European Union

Summary

Within the EDAPHOS project, Task 2.2 was designed as a two-stream workflow for contaminated sites that serves as a starting point for understanding the relationship between ecosystem condition and the direction of site transformation needed to restore the capacity of land to deliver environmental, social, and economic benefits. This two-stream structure was intended to provide a comprehensive picture of the current status of each CS, not only in terms of contamination and ecosystem degradation, but also in terms of the CS's wider potential, shaped by its location, environmental settings, and the broader context in which it is embedded. The first Task2.2 work-stream focuses on soil ecotoxicity and soil functions. It provides a diagnostic baseline of the soil system, capturing contamination-related hazard signals and soil function limitations that are relevant for remediation planning and for tracking recovery over time. The second Task2.2 work-stream addresses ESS. It translates ecosystem state and land-cover structure into decision-relevant information on what a restored site can provide under alternative rehabilitation and future land-use trajectories. Together, these two perspectives enable a structured assessment of whether nature-based solutions (NBS) lead to measurable gains in soil integrity and to an improved capacity of regenerated ecosystems to generate benefits, while making constraints and trade-offs explicit.

Deliverable D2.2 (achieved in M18) reported the first consolidated results from WP2, Task 2.2 ("Acquiring ecotoxicological data and ESS data", M6–M42). In line with the project assumptions, it focused primarily on the initial condition of EDAPHOS soils under remediation by NBS, providing early evidence on contamination-related hazards and soil health status. This baseline is essential, because NBS performance can only be demonstrated credibly when the "starting point" is measured using consistent methods and comparable indicators.

Deliverable D2.5 is an updated and expanded version of D2.2. It complements the earlier reporting by strengthening the second pillar of Task 2.2 (i.e., the ESS assessment) and by framing results in a way that directly supports planning choices, scenario comparison, and downstream valuation. In this sense, D2.5 does not replace D2.2; it extends the same assessment chain from "*what is the current soil condition*?" to "*what benefits can be expected from restoration and alternative redevelopment pathways, and how can these be compared transparently*?".

D2.5 presents the EDAPHOS the results of ESS assessment as a harmonised, scenario-based evidence base to support decisions on contaminated and degraded sites. The main goal of D2.5 it to present (using the same approach across all CS), how NBS remediation solution and different redevelopment options may affect environmental, social, and economic outcomes, by clearly describing and comparing expected benefits, and trade-offs. To ensure traceability and consistency across sites, D2.5 applies a shared analytical framework. Ecosystem types are mapped using CORINE Land Cover, and ESS are identified and classified under CICES v5.2. The results are summarised as structured "service profiles", using comparable indicator sets for each scenario. This provides a clear baseline, supports transparent scenario comparison, and creates a robust basis for subsequent valuation and monitoring.

Task 2.2 results serve as a bridge between evidence generation and downstream use. It incorporates inputs from WP1 & WP3 (site characterisation, land status, level of contaminants, etc.) and produces outputs that are directly usable in WP4 and WP5. The ESS profiles provide a defensible basis for valuation, integrated indices, and appraisal workflows in WP4, while WP5 uses the same evidence base to support communication, stakeholder engagement, and uptake

pathways for NBS. D2.5 strengthens the project's ability to demonstrate, compare, and promote NBS as credible remediation and redevelopment pathways for contaminated and degraded land, supported by traceable metrics and a clear monitoring logic over time.

Keywords

Ecosystem services, Ecological indicators, CICESv5.2, spatial planning, redevelopment strategies

Funded by
the European Union

Abbreviations and acronyms

Acronym	Description
AGB	Above-ground biomass
AGBinc	Annual increment of above-ground biomass (t d.m.·ha^{-1}·year^{-1})
CICES	Common International Classification of Ecosystem Services
CLC	CORINE Land Cover
CS	Case Study
CV	Calorific value (GJ·t^{-1} d.m.)
DM	Dry matte
EP	Energy potential (GJ·ha^{-1}·year^{-1})
ESS	Ecosystem Services
EU	European Union
GIS	Geographic Information System
HM	Heavy Metals
IPCC	Intergovernmental Panel on Climate Change
MAES	Mapping and Assessment of Ecosystems and their Services
MEA	Millenium Ecosystem Assessment
NAI	Net Annual Increment
NBS	Nature-based solutions
NFI	National Forest Inventory
NIR	Near InfraRed domain
NUTS2	Nomenclature of Territorial Units for Statistics
PV_groundmounted	Photovoltaic
WP	Work Package
OSM	Open Street Map

Reference documents

Reference	Title
D2.2	Report on initial ecotoxicity and ecosystem services assessment (initial)

1 Ecosystem services in EU policies and international practice

1.1 EU directions on ecosystem restoration, soil recovery and degraded land management

EU directions on ecosystem restoration, soil recovery and degraded land management have moved from a primarily pollution-control and liability paradigm towards a more explicitly restorative and "*soil health*" orientation, in which soil functions, biodiversity recovery and land-use efficiency are treated as interdependent public goods. This shift is visible in the policy architecture linking soil to ESS (e.g. carbon storage, water regulation, habitat provision and nutrient cycling) and in the growing emphasis on monitoring, indicators and land take reduction as governance tools [European Commission, 2021a; Martinho et al., 2024; Robinson et al., 2024].

A durable regulatory baseline is provided by environmental liability, water protection and industrial permitting. The Environmental Liability Directive operationalises the polluter-pays principle through duties to prevent and remedy environmental damage, including land damage where contamination creates a significant risk to human health [Directive 2004/35/EC]. Industrial emissions governance complements this preventive logic by constraining cross-media pollution pathways and strengthening requirements that affect soil and groundwater protection at installations [Directive 2010/75/EU]. Water law provides the pathway lens: the Water Framework Directive and the Groundwater Directive require objectives, monitoring and measures that make soil degradation and contamination relevant beyond the site boundary, particularly where groundwater and surface waters are threatened [Directive 2000/60/EC; Directive 2006/118/EC]. In practice, this supports a risk-based approach to degraded land, where remediation and management are oriented to receptors and exposure pathways, rather than uniform removal ambitions.

Biodiversity protection and restoration increasingly shape the direction of travel, shifting from a constraint-based logic to an objective-based logic. The Habitats and Birds Directives remain the legal backbone for protecting habitats and species and for preventing deterioration in protected sites [Council Directive 92/43/EEC; Directive 2009/147/EC]. Over the last decade, EU policy has also elevated restoration as an explicit system goal, with a stronger emphasis on reversing biodiversity loss and recovering ecosystem functions across landscapes [European Commission, 2020]. Soil biodiversity has become more visible within this narrative, supported by monitoring initiatives and datasets that make ecological condition more legible to policy and appraisal [Orgiazzi et al., 2022; Zeiss et al., 2022]. The result is that soil recovery is no longer framed only as a remediation problem, but as an enabling condition for biodiversity outcomes. The Soil Strategy for 2030 consolidates this shift by treating *"healthy soils"* as a prerequisite for multiple ESS and by signalling concrete actions around monitoring, indicators and governance improvements [EC, 2021a]. The surrounding scientific-policy literature reinforces both the rationale and the design challenges of this approach: analyses of EU soil legislation and policy highlight fragmentation across instruments and the resulting need for more coherent monitoring and implementation pathways [Martinho et al., 2024], while long-term soil monitoring experience is increasingly used to inform principles for robust, comparable soil health measurement across regions [Robinson et al., 2024]. The proposed Soil Monitoring Law is widely discussed as

a potential step-change in the EU's capacity to move from aspiration to operational governance for soil condition, including by standardising monitoring and improving comparability for policy evaluation [European Commission, 2023; Kotschik et al., 2023; Wellbrock et al., 2024].

The "*zero pollution*" framing strengthens the restorative turn by linking soil contamination to exposure control, ecosystem protection and drinking water security. The EU Action Plan towards zero pollution positions soil as a central battleground and reinforces integrated, cross-policy governance for prevention, remediation and monitoring [European Commission, 2021b]. This is also where degraded land management, brownfields and contaminated sites become especially salient. In these cases, restoration is expected to be compatible with controls that prevent pollutant mobilisation and protect receptors, with monitoring obligations functioning as a core credibility mechanism [Directive 2000/60/EC; Directive 2006/118/EC; European Commission, 2021b].

Land take reduction and the brownfield-first logic represent the most direct bridge between restoration priorities and spatial development choices. The policy aim of "*no net land take*" (articulated in the resource-efficiency agenda) underpins subsequent debates on soil sealing, urban expansion and prioritising the reuse of already-taken land over greenfield conversion [European Commission, 2011]. While the land take objective is not, in itself a binding prohibition, it operates as a strategic constraint that supports brownfield redevelopment as a preferred pathway where feasible, particularly when coupled with assessment and permitting tools. Procedural planning instruments make these objectives operational. The EIA Directive (as amended) strengthens the assessment of effects on soil, land and biodiversity, helping to structure alternatives analysis and mitigation design for projects, including those on contaminated or previously used sites [Directive 2011/92/EU]. The SEA Directive performs a similar function at plan and programme level, ensuring that soil sealing, land take and ecosystem impacts are considered earlier, when strategic land allocations and restoration priorities can still be adjusted [Directive 2001/42/EC]. These mechanisms are important for evaluation because they require a clear and transparent description of baseline conditions, likely significant effects, mitigation measures, monitoring plans, and residual risks-key elements for judging whether restoration claims are credible in practice.

Climate and sustainable finance governance increasingly reinforces this direction. The European Climate Law strengthens the salience of land and soil in climate mitigation and resilience [Regulation (EU) 2021/1119]. The EU Taxonomy adds an investment governance layer through sustainability classification and "*do no significant harm*" expectations, which incentivise demonstrable safeguards and monitoring for activities affecting soil, biodiversity and pollution pathways [Regulation (EU) 2020/852]. In parallel, the EU's soil policy science infrastructure, including the EU Soil Observatory, is increasingly framed as a mechanism to translate restoration and soil-health objectives into measurable indicators and consistent evidence bases for policy and finance [Panagos et al., 2024; Robinson et al., 2024].

Within this architecture, Nature-based Solutions (NBS) are increasingly promoted as legitimate pathways to ecosystem recovery, but they remain conditional rather than universal. Policy and legal duties require that exposure pathways and long-term monitoring are addressed, particularly on contaminated land, and that restoration measures do not shift burdens to water bodies or protected habitats [Directive 2004/35/EC; Directive 2000/60/EC; Council Directive 92/43/EEC]. The scholarly discussion on NBS in EU environmental governance similarly stresses that uptake

depends on regulatory acceptability, evidence of performance and careful alignment with permitting and risk management [Fermeglia & Perisic, 2023; Zeiss et al., 2022]. In evaluation terms, the practical implication is clear: ESS can be used as a planning and appraisal language, but only where claims are tied to indicators, monitoring design and compliance constraints that reflect EU law and the strategic trajectory towards healthier soils, reduced land take and recovered ecosystems [EC, 2021a; EC, 2021b; Regulation (EU) 2020/852].

1.2 Ecosystem services in spatial planning for degraded and post-industrial sites

ESS are most useful in spatial planning when they act as a shared evidence language between disciplines that do not naturally "*speak*" to each other. That is precisely the situation on degraded and post-industrial sites. Here, planning decisions sit at the intersection of land condition (including soils, groundwater sensitivity and legacy contamination), urban development pressure, and public expectations regarding safety, fairness and long-term quality of place. The ESS framing helps to connect these dimensions without forcing planners to reduce everything to a single metric. It translates ecological functioning into outcomes that decision-makers routinely have to weigh cooling and shade during heatwaves, infiltration and flood buffering, habitat support, recreational access, and the everyday experience of living near a site that used to be industrial. This matters because brownfields are not empty canvases. The evidence shows that post-industrial landscapes can have "*unrealised ecological potential*" and, in some cases, carry meaningful biodiversity and service capacity even where assemblages are novel rather than historically "restored" [Merwin et al., 2022; Jacek et al., 2022]. In planning terms, this shifts the baseline. A credible redevelopment conversation cannot start from a simplistic "*before: nothing, after benefits*". It must ask what services already exist, what constraints limit them, and what would be lost or gained under each redevelopment pathway. ESS assessment offers a structured way to ask those questions while remaining compatible with real planning documents.

Planning on post-industrial sites often separates surface-level ambitions from subsurface realities. Contamination and unfavourable groundwater conditions are frequently treated as technical issues to be addressed after future land use has already been defined. This approach is risky. When subsurface constraints are not considered early, land-use options with high potential for regulating and cultural services, e.g. such as green space that reduces heat stress and supports water retention, may be excluded by default or become costly to implement once the design is fixed. [Rodríguez-Espinosa et al., 2021; Martinát et al., 2016]. The ESS perspective does not replace legal obligations or engineering constraints. It requires early, explicit statements on what the land is expected to deliver for people and nature, and on which risks and constraints must be respected. Trade-offs are therefore made transparent and intentional rather than incidental.

The ESS approach also strengthens the quality of scenario thinking. Redevelopment of contaminated sites is almost never a simple "*develop or not develop*" decision. It is usually a choice between bundles of land use, remediation pathway and long-term management obligations. The "*soft re-use*" literature demonstrates that non-built green uses can optimise value, particularly where sealing is avoided and where the site can deliver benefits while remaining manageable under residual constraints [Bardos et al., 2016]. Work on phytomanagement and practical contaminant management similarly shows that some strategies can manage risks while enabling wider benefits, although suitability is always site-specific and depends on governance and monitoring [Cundy et al., 2016]. Crucially, the literature also legitimises an option that planning

Funded by
the European Union

sometimes struggles to treat as a genuine alternative: allowing succession or partial non-intervention, where it produces strong ecological and social outcomes [Haase, 2021; Merwin et al., 2022]. ESS framing helps because it allows "do less" to be evaluated on its merits rather than dismissed as inaction.

Where ESS becomes especially practical is in making comparisons defensible. Planning processes often require alternatives assessment in one form or another, and even where the method is not called "*ecosystem services*", the logic is familiar: describe the baseline, compare alternatives, identify significant effects, propose mitigation, and commit to monitoring [Directive 2011/92/EU; Directive 2001/42/EC]. ESS assessment aligns naturally with this logic because it promotes the use of indicators that can be applied consistently across scenarios. It also provides a more honest way to handle valuation. The evidence base you provided supports the view that economic inputs can help, but that value is plural and contested, especially for green infrastructure and nature-based outcomes [Ameller et al., 2019; Haase et al., 2017; Zhong et al., 2020]. In practice, this means that good planning does not pretend that one number resolves a complex choice. It makes the criteria visible, documents the assumptions, and uses stakeholder-informed judgement where trade-offs are real. Another planning-relevant advantage is communication and legitimacy. Projects fail not only because they are technically weak, but because the public cannot see what the project is for, or because benefits are perceived as unevenly distributed. Evidence from co-creation and from operational monitoring practice shows that structured engagement and transparent performance tracking can support multifunctional outcomes and social acceptance over long redevelopment timelines [Kabisch, 2019; Laprise et al., 2018]. At the same time, the literature also makes clear that greening can carry equity risks, including eco-gentrification dynamics, if the distribution of benefits and burdens is not managed [Haase et al., 2017; Zheng & Masrabaye, 2023]. An ESS lens can help here by clarifying who gains access to services (cooler streets, accessible parks, safer environments), and where burdens may fall, but only if planners are willing to treat distribution as part of the appraisal rather than a peripheral social issue. For planners and decision-makers, the real test is whether ESS produces planning artefacts that can travel through local plans, redevelopment strategies, and assessment documents. In this context, ESS is most defensible when it results in a small set of tangible outputs:

- a clear baseline "*service profile*" of the site, including soils, sealing status, existing habitat or informal use, and known constraints linked to contamination and water pathways [Rodríguez-Espinosa et al., 2021; Palliwoda et al., 2020; Directive 2000/60/EC];
- a set of scenarios that describe not only end use but also the remediation and management logic that makes that end use credible over time [Bardos et al., 2016; Cundy et al., 2016; Martinát et al., 2016];
- a transparent comparison basis, typically indicator-led and often supported by structured appraisal tools, so that the decision can be explained and audited rather than asserted [Bardos et al., 2020; Bartke et al., 2016];
- a monitoring and communication plan that treats sustainability claims as commitments to be checked, adjusted and reported, not as one-off promises [Laprise et al., 2018; Çahantimur et al., 2010].

The EDAPHOS ESS approach responds directly to the planning problem described above. It provides the infrastructure needed to move from general claims about "*multiple benefits*" to evidence that can support real decisions under uncertainty: decisions that must be safe, explainable, and durable across time horizons and stakeholders [Zhong et al., 2020; Bardos et

al., 2020; Robinson et al., 2024]. In other words, ecosystem services add value not because they introduce new concepts, but because they strengthen the discipline of planning: making alternatives comparable, making trade-offs explicit, and keeping outcomes visible long after the ribbon cutting.

Funded by
the European Union

2 Ecosystem services assessment in the EDAPHOS project

2.1 Context and justification for ESS assessment and valuation within EDAPHOS

Within the EDAPHOS project, ESS and ESS valuation are used to make the benefits of NBS on degraded post-industrial and post-mining sites **visible, comparable and usable in decisions**. Therefore, remediation should not only be treated as a technical response to legacy pressures but also as an opportunity to restore soil and ecosystem functions that support biodiversity and human well-being. ESS framing helps to express that wider value in a way that planners, regulators, land managers and local communities can understand, without relying on vague claims of "*greening*" or "*added value*" [Wang, 2022; Seddon et al., 2020].

This approach is consistent with the direction of EU policy and regulation, which increasingly expects land management choices to be evidence-led, monitored and defensible. Soil health, ecosystem recovery and land-use efficiency are now treated as interdependent public goods, supported by stronger emphasis on indicators, monitoring and land take reduction [European Commission, 2011; European Commission, 2021a; Robinson et al., 2024]. At the same time, the regulatory baseline for degraded land remains firmly risk- and pathway-oriented. Environmental liability focuses on preventing and remedying environmental damage, including land damage where contamination creates significant risks to human health [Directive 2004/35/EC]. Water protection requires objectives, monitoring and measures that make pollutant mobilization and soil-water interactions relevant beyond the site boundary, especially where groundwater and surface waters may be affected [Directive 2000/60/EC; Directive 2006/118/EC]. Planning procedures reinforce the same logic: baseline conditions, alternatives, mitigation and monitoring are central both at project and plan level, creating a clear demand for traceable evidence on expected outcomes [Directive 2011/92/EU; Directive 2001/42/EC]. In this context, ESS assessment functions as an evidence bridge - linking ecological recovery to measurable outcomes that can be tested against constraints, documented in appraisal, and followed up through monitoring.

In practical terms, **ESS analysis in EDAPHOS supports consistent recognition and quantification of ecosystem contributions across environmental, social and economic dimensions**. These include, for example, changes in soil-related functions, carbon-related benefits, air-quality regulation, and the provision of spaces with recreational and social value. By making these effects explicit and comparable through the analyses performed in Task 2.2, the project strengthens the evidence base for NBS-based remediation pathways, including co-benefits that are often assumed but rarely demonstrated in a consistent format [Lai & Zoppi, 2024; Debele et al., 2023; Seddon et al., 2020]. This is particularly important on degraded land, where decisions involve trade-offs between risk management, land-use options and long-term stewardship, and where stakeholders may value outcomes differently. ESS valuation complements that assessment by supporting integration into planning and decision-making. It helps to express the value of restored ecosystem functions in ways that decision processes can use, especially when choices must balance environmental protection with future development opportunities. Valuation is treated here as a decision-support layer rather than a single decisive metric. It provides a structured basis for discussing trade-offs and longer-term benefits across land-use pathways, while recognising that different valuation approaches illuminate different aspects of value (economic, social, ecological, deliberative) [IPBES, 2012; Geneletti et al., 2018; Geneletti et al., 2020]. In EDAPHOS, the current

focus is on evaluating and scaling ESS potential consistently across sites. Monetisation, valorisation and guidance for uptake into business models will be developed in subsequent work within WP4 and WP5.

Finally, **ESS assessment supports restoration and conservation by evidencing what is gained through ecosystem recovery and by making the case for investment in NBS more concrete**. In practical terms, it helps demonstrate how remediation choices can contribute to resilience and well-being in the places where people live and work, while remaining compatible with regulatory duties and planning constraints that require transparency, monitoring and accountability [Baill et al., 2021; Directive 2004/35/EC; European Commission, 2021a].

2.2 Objectives of the EDAPHOS ecosystem services assessment

Main objective

The assessment of ESS within the EDAPHOS project is designed to provide a structured understanding of how nature-based remediation and redevelopment processes influence environmental, social, and economic outcomes across contaminated and degraded sites. By applying a consistent analytical framework across all case studies (CS), the ESS assessment supports the identification, classification, and evaluation of ecosystem contributions emerging from site restoration processes.

A key objective of the ESS assessment is to identify and classify ecosystem services using the CICES framework, supported by spatial delineation of ecosystem types based on CORINE Land Cover data. This approach enables the systematic mapping of ecosystem characteristics within study areas and provides a basis for selecting appropriate indicators reflecting ecosystem functions and contributions to human well-being.

Another important objective is to quantify ecosystem contributions through the collection of relevant environmental data across all CS. This includes measurements such as biomass production to support the assessment of provisioning services and soil parameters to inform regulating and maintenance services. By integrating quantitative data with scenario-based analysis, the project aims to capture interactions between ecosystem processes and societal benefits under different redevelopment pathways. The ESS assessment also supports the evaluation of future land-use scenarios by considering local soil conditions and key contextual factors influencing redevelopment, such as legal requirements, land use constraints, and accessibility. Through scenario-based analysis, the project evaluates the potential of restored sites to deliver ESS under different redevelopment options, including nature-based recreational use or renewable energy production.

A main objective of this work is to make the value of ESS more visible and measurable, thereby strengthening the evidence base for decision-making. By assessing ecosystem contributions across environmental, social, and economic dimensions, the ESS framework helps to understand how remediation strategies can support sustainable land management and long-term site regeneration. The ESS assessment provides also a foundation for subsequent valuation activities by identifying and scaling ecosystem service potential across sites. While some changes in ESS may extend beyond the project timeframe, the scenario-based approach allows the project to estimate the potential benefits associated with the restoration of soil functions and the recovery of ecosystem processes.

Funded by
the European Union

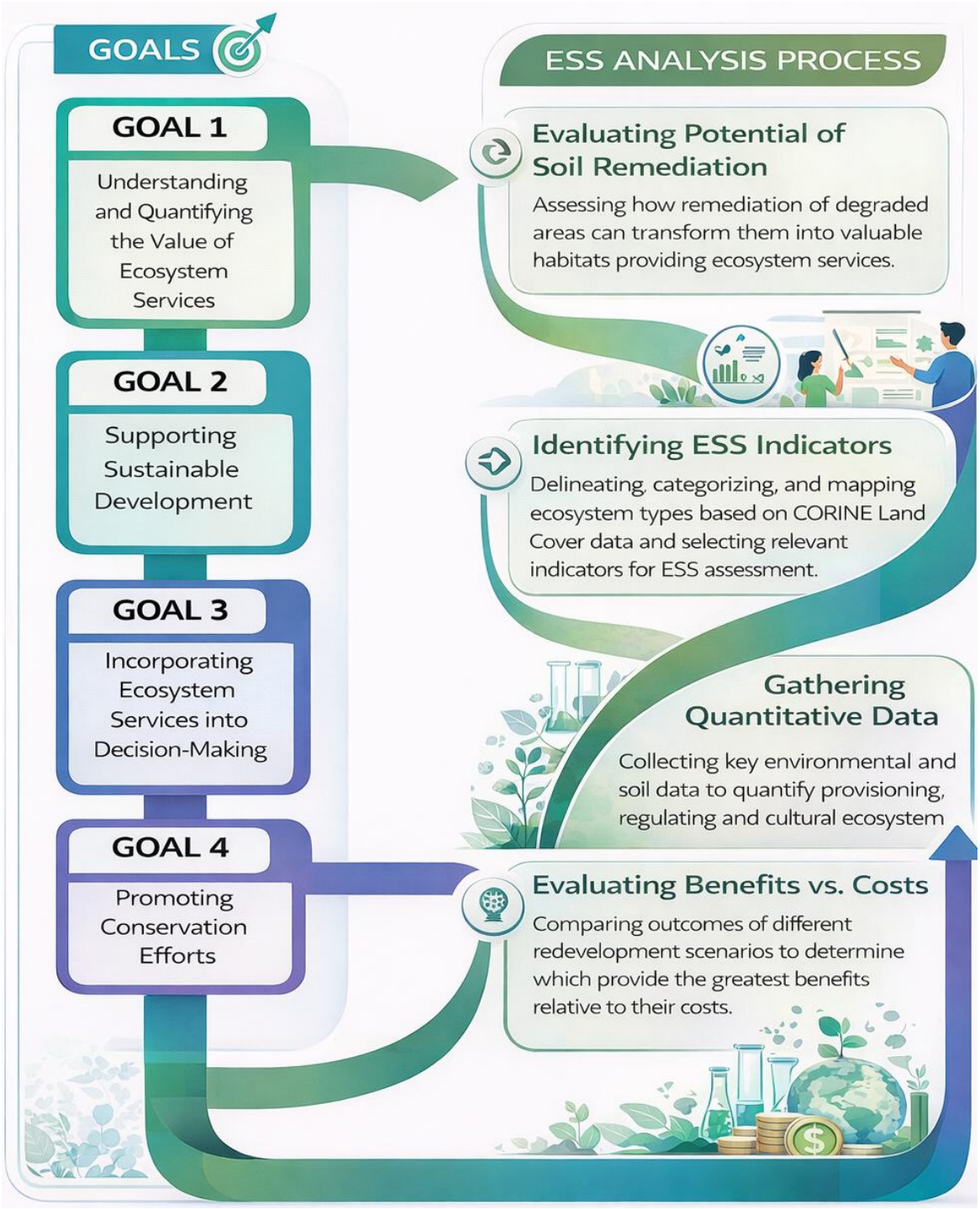

Figure 1 Main goals of ESS assessment within EDAPHOS project *[Source: OpenAI].*

Specific objectives

The ESS assessment in the EDAPHOS project aims to provide a clear and evidence-based understanding of how remediation processes based on NBS methods generate ecosystem benefits, support the comparison of redevelopment scenarios, and reinforce the role of ESS in sustainable site regeneration (Figure 1). Additionally, the results of the ESS assessment carried out within Task 2.2 (and further continued within WP4 & WP5) are intended to serve as a practical decision-support tool for stakeholders and decision-makers involved in planning, supervising, and

implementing activities across individual CS. By translating analytical results into structured and comparable information, the assessment helps inform decisions related to land use, remediation strategies, and future site development. The results of Task 2.2 will serve as a direct input to parallel activities within EDAPHOS project, particularly Tasks 4.2 and Task 5.2, where they will be further used for monetisation, valorisation, and integration into decision-making processes. In this context, the outputs are designed to be directly usable by landowners and land managers responsible for scenario approval and for defining system boundaries, as well as by stakeholders involved in planning and implementation. In this way, the results from Task 2.2 provide a practical knowledge base that supports subsequent analytical works across the project

2.3 Scope of the analysis

The ESS assessment within the EDAPHOS project is conducted across all seven CS, ensuring a consistent analytical approach across different geographical and environmental contexts. For each CS, the ESS analysis is performed for three alternative future land-use scenarios representing potential redevelopment pathways, including NBS, enabling comparison of ESS provision under different site futures. A harmonised methodological framework is applied across all CS, following a common workflow described in Section 4.1. This approach supports the comparability of results across all sites.

For each scenario the ESS assessment is carried out across the full set of selected ESS indicators, enabling the identification of services most relevant under different redevelopment options and providing a basis for comparing alternative land-use pathways. The detailed scope of analytical activities and methodological procedures is presented in Section 4 [4.2; 4.3]. The table below (Table 1) provides references to the sections of D2.5 where detailed ESS analysis for each CS is presented.

Table 1 Reference guide to ESS analysis sections by CS.

№	CS №	CS name	Site characteristic	ESS assessment
1	CS1	Carrières sous Poissy (FR)	Section 5.1*(Subsection 5.1.1)*	Section 6.1 *(Subsection 6.1.1-6.1.7)*
2	CS2	Kozani (GR)	Section 5.1 *(Subsection 5.1.2)*	Section 6.2 *(Subsection 6.2.1-6.2.7)*
3	CS3	Odiel Basin Area (ESSP)	Section 5.1*(Subsection 5.1.3)*	Section 6.3 *(Subsection 6.3.1-6.3.7)*
4	CS4	Upper Silesia Coal Basin (PL)	Section 5.1*(Subsection 5.1.4)*	Section 6.4 *(Subsection 6.4.1-6.4.7)*
5	CS5	Castelvetro (IT)	Section 5.1*(Subsection 5.1.5)*	Section 6.5 *(Subsection 6.5.1-6.5.7)*
6	CS6	Vieus_Charmont (FR)	Section 5.1*(Subsection 5.1.6)*	Section 6.6 *(Subsection 6.6.1-6.6.7)*
7	CS7	Lavrio (GR)	Section 5.1*(Subsection 5.1.7)*	Section 6.7 *(Subsection 6.7.1-6.7.7)*

2.4 Potential target users

The ESS results are primarily intended to demonstrate the value of applying NBS remediation techniques and rehabilitation approaches, by making their benefits visible and comparable. At the same time, the analysis also shows how different future land-use options may generate different bundles of ESS and co-benefits. In this way, the results support selecting site regeneration

Funded by the European Union

strategies and help identify options that deliver the highest overall benefits across the EDAPHOS CS. A list of potential target users of the results, together with a brief justification on their relevance for each group is provided below and in Figure 2:

- Landowners and land managers - responsible for defining redevelopment options, approving scenarios, and managing site operations, members of this group can use ESS results to better understand the environmental and economic implications of alternative land-use pathways.
- Urban and regional planners - ESS assessment provides clear evidence that can guide spatial planning and zoning decisions and helps incorporate ecosystem-based approaches into land-use planning policies and practice.
- Environmental authorities and regulators - public authorities responsible for environmental protection and permitting can use ESS results to compare remediation options, support permitting decisions, and check whether proposed actions meet environmental objectives and compliance requirement.
- Policy makers and public administrations - ESS valuation helps design and justify policies and strategies that support sustainable land management, use of NBS in remediation processes and the regeneration of brownfield sites.
- Project developers and investors -private sector actors involved in redevelopment can use ESS results to compare different redevelopment options, understand their long-term value and co-benefits, and make better-informed investment decisions.
- Local communities and civil society organisations - ESS assessment helps explain, in a clear way, the environmental and social benefits that site regeneration can deliver. This supports stakeholder engagement and makes decision-making more transparent.
- Researchers and scientific community -the results contribute to advancing knowledge on ESS in the context of contaminated land remediation and NBS.

Funded by the European Union

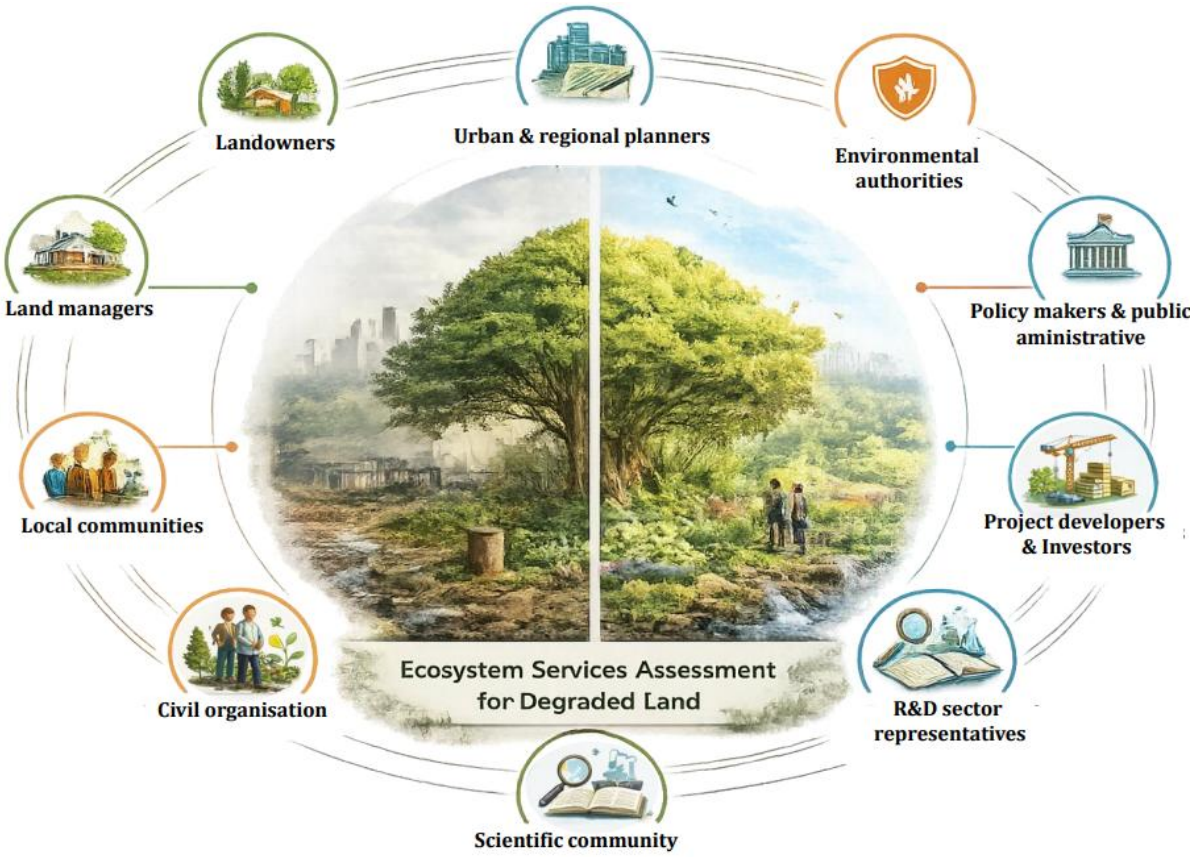

Figure 2 Potential stakeholders and beneficiaries of ESS valuation results within the EDAPHOS project *[Source:OpenAI]*.

Funded by the European Union

3 Methodological framework for ESS assessment and valuation

3.1 EU and international frameworks for ecosystem services assessment and valuation

Historical development and chronology

The concept of ESS emerged from the recognition that human well-being is fundamentally dependent on ecological systems and the functions they perform [Longato et al., 2021]. Over time, the understanding of these services has evolved from a primarily ecological perspective toward integrated ecological-economic frameworks aimed at supporting decision-making, policy development, and environmental management (Figure 3). Today, ESS valuation is widely used across science, policy, and planning to provide structured evidence on the benefits provided by ecosystems [EC, 2011, 2019], [IPBES, 2012].

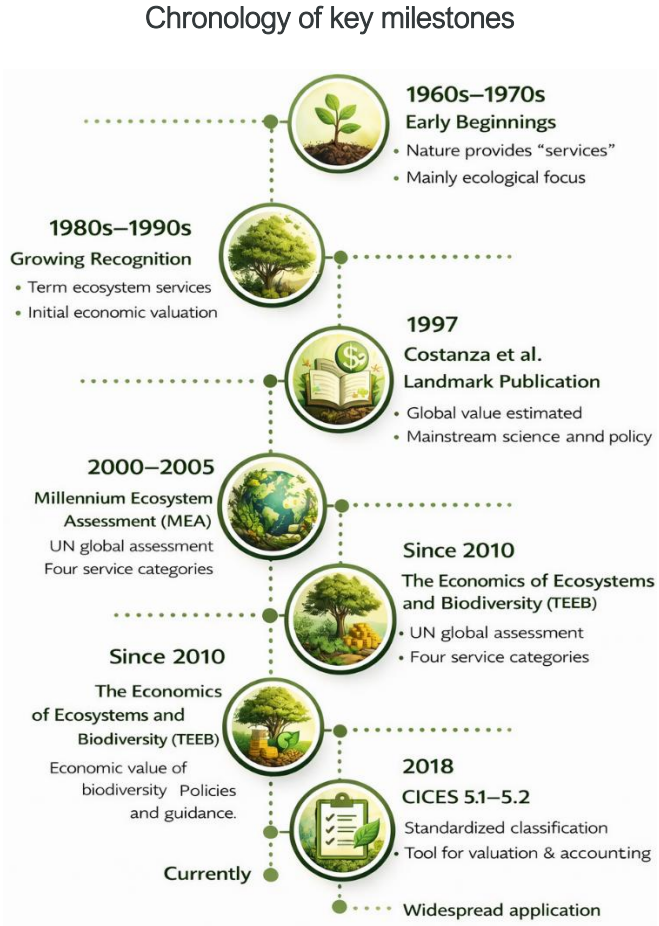

1960s-1970s - Early beginnings of ESS
Early research emphasized that nature provides essential functions supporting human survival, although the term "ecosystem services" was not yet widely used. The focus during this period remained largely ecological, with limited economic framing.

1980s-1990s - Growing recognition of ESS
The term ESS began to appear in scientific literature, accompanied by increasing awareness of the link between environmental protection and human well-being. Initial attempts were made to assign economic value to ecosystem functions to strengthen arguments for conservation.

1997 - Costanza et al. landmark publication
The publication '*The value of the world's ecosystem services and natural capital*" estimated the global value of ESS at trillions of dollars annually, bringing the topic into mainstream scientific and policy discourse [Costanza, 1997].

Figure 3 Development of ESS Valuation.

2000 - 2005 - Millennium Ecosystem Assessment (MEA)
The Millennium Ecosystem Assessment, a global UN initiative, classified ESS into four categories: provisioning, regulating, supporting, and cultural. The assessment demonstrated the direct link

between ESS and human well-being, providing a conceptual foundation for subsequent frameworks [MEA, 2025].

Since 2010 - The Economics of Ecosystems and Biodiversity (TEEB)
TEEB highlighted the global economic benefits of biodiversity and aimed to promote better understanding of the true economic value of ESS, as well as the growing costs of biodiversity loss. The initiative seeks to provide economic tools and policy guidance to integrate ecosystem values into decision-making [TEEB, 2013].

2018 - CICES 5.1 (updated to CICES v5.2)
The Common International Classification System of ESS introduced a standardized framework for classifying ESS and supporting measurement and valuation. The classification defines ESS as contributions that ecosystems make to human well-being and provides a hierarchical structure to enable consistent analysis and comparison [CICES, 2025].

Current status
Today, ESS frameworks are widely applied in policy, research, urban planning, and business. Valuation tools continue to evolve through spatial mapping, modelling, and integrated assessment approaches, with increasing attention not only to economic values but also to social and cultural dimensions.

Overview of major ESS assessment approaches

Different international frameworks are currently used to assess and value ESS. While they share a common objective to provide transparent, decision-relevant evidence, they differ in methodological emphasis, scope, and intended application. The main distinctions are characterized below.

- CICES (Common International Classification of Ecosystem Services)
  CICES provides a standardized classification system designed to support measurement, assessment, and valuation of ESS. It focuses on defining ESS as contributions to human well-being arising from ecosystem processes and offers a hierarchical structure that enables comparison across studies and policy contexts [CICES, 2025]. The framework is particularly useful as a reference classification because it allows translation between different ESS typologies and supports indicator development, mapping, and valuation exercises.
  Key distinguishing feature: A classification and structuring tool that facilitates comparability and consistency across assessments.

- EU MAES (Mapping and Assessment of Ecosystems and their Services)
  The MAES initiative was established to support EU Member States in mapping and assessing ecosystems and their services, providing a consistent evidence base for policy and planning. The approach emphasizes spatial assessment and integration into policy frameworks, particularly within biodiversity and environmental strategies [MAES. 2020].
  Key distinguishing feature: Strong focus on spatial mapping and policy implementation within the EU context.

- System of Environmental Ecosystem Accounting (SEEA EA)
  SEEA EA is an international statistical standard adopted by the United Nations Statistical Commission that provides an integrated framework for organizing environmental and

Funded by
the European Union

economic data. It supports measurement of ESS, tracking changes in ecosystem assets, and linking ecosystem information to economic activity and national accounts. The framework represents a major step toward incorporating ESS into national accounting systems and policy evaluation, emphasizing coherence with economic statistics and the environment-economy nexus.
Key distinguishing feature: A statistical accounting framework integrating ESS into national economic accounts.

- TEEB (The Economics of Ecosystems and Biodiversity)
  TEEB focuses on highlighting the economic value of biodiversity and ESS and providing practical tools for incorporating these values into decision-making. It analyses valuation case studies and promotes economic approaches to demonstrate the benefits of conservation and the costs of ecosystem degradation
  Key distinguishing feature: Strong emphasis on economic valuation and policy relevance [TEEB, 2015].

Examples of ESS provided by trees in urban areas are presented in the figure below (Figure 4).

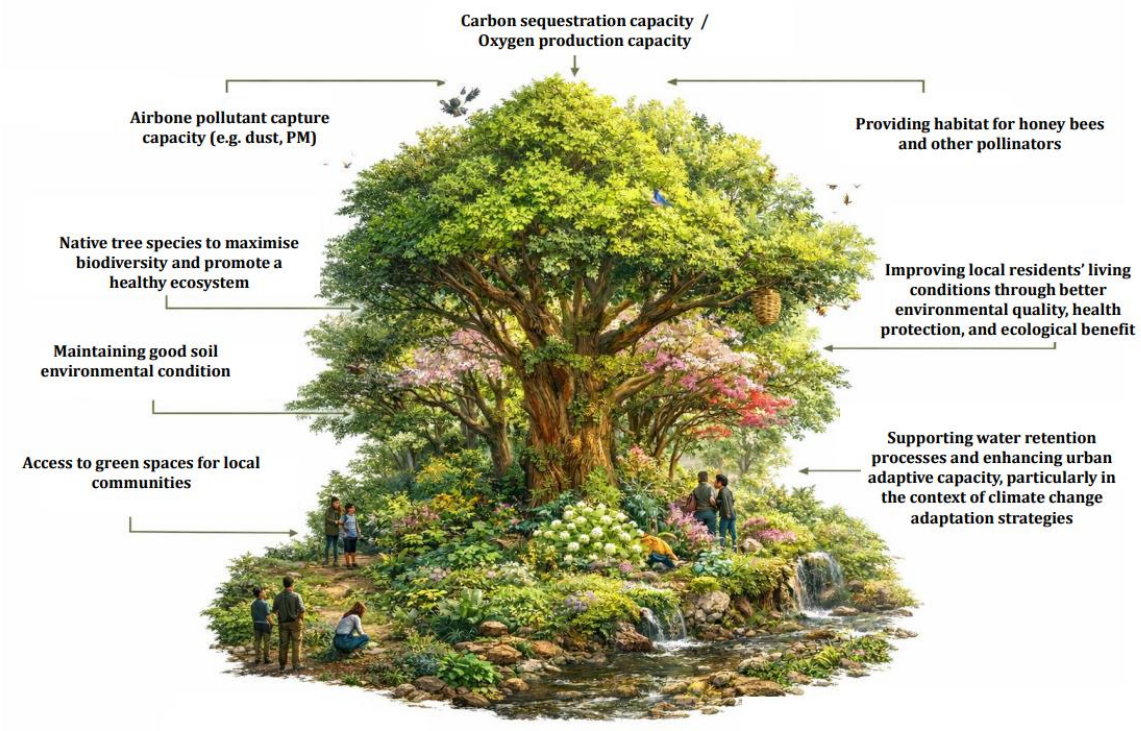

Figure 4 Example of ESS provided in urban landscapes *[Source: OpenAI].*

3.2 ESS definitions and categories

ESS definition

As described in the previous sections (Section 3.1) the ESS field has developed through several complementary frameworks (e.g. MEA, TEEB, CICES, SEEA EA). These approaches share a common purpose, but they operationalize the concept in slightly different ways (Figure 5). This is also visible in ESS definitions: some describe goods and services, others describe benefits, and newer classifications distinguish ecosystem contributions from the benefits delivered to people.

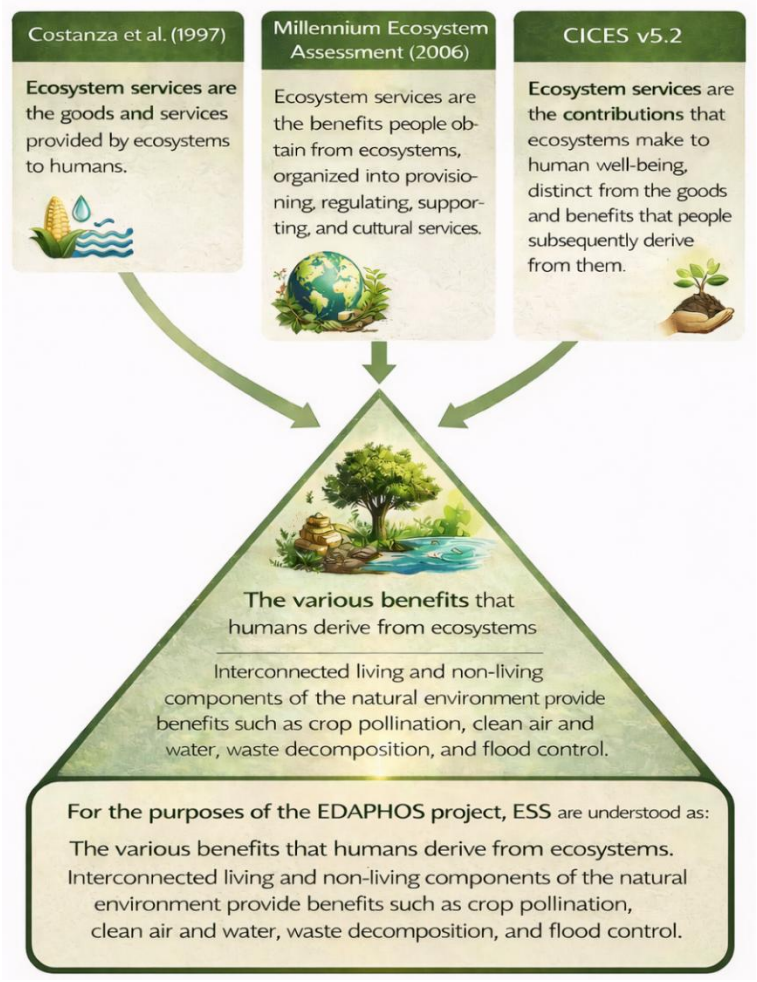

Figure 5 Various ESS definitions integrated into one common EDAPHOS approach *[Source: OpenAI].*

Differences in definitions mainly reflect the focus of each framework. Valuation and policy approaches usually emphasize the benefits people receive, while classification frameworks aim for conceptual clarity by distinguishing ecosystem contributions from the benefits derived from them. In this deliverable (D2.5), the ESS concept is used in a broad and practical sense, focusing on the benefits people obtain from ecosystems.

ESS categories according to MEA

ESS refers to the various benefits that humans derive from ecosystems. For better understanding the ESS are commonly grouped into categories based on the type of benefits they provide to society. The most widely used classification, developed through the MEA, distinguishes four main categories: provisioning, regulating, cultural, and supporting services, which are described below (Figure 6).

- Provisioning services are the tangible products obtained from ecosystems and are often referred to as ecosystem goods. They include food (such as crops, seafood, wild foods, and spices), raw materials (e.g., timber, fuelwood, and organic matter), genetic resources used in agriculture and medicine, biogenic minerals, medicinal resources, energy sources such as biomass and hydropower, and ornamental resources. These services directly support human livelihoods and economic activities.

Funded by
the European Union

- Regulating services are the benefits obtained from the natural regulation of ecosystem processes. They include air and water purification, climate regulation through carbon sequestration, waste decomposition and detoxification, biological control of pests and diseases, pollination of crops, and protection against natural hazards such as floods. These services play a crucial role in maintaining environmental stability and reducing risks to human societies.
- Cultural services encompass the non-material benefits that people gain from nature. These include inspiration in art and culture, spiritual and historical values, recreation and tourism, education and scientific discovery, as well as therapeutic benefits such as ecotherapy and animal-assisted activities. Cultural services contribute to human well-being by supporting mental health, cultural identity, and social cohesion.
- Supporting services are the fundamental ecological processes that enable all other ESS to exist. They typically have indirect and long-term impacts on humans and include nutrient cycling, primary production, soil formation, and habitat provision. By sustaining ecosystem functioning, supporting services ensure the continued delivery of provisioning, regulating, and cultural benefits [MEA, 2005].

Figure 6 Categories of ESS according to the Millennium Ecosystem Assessment *[MEA, 2005] [Source: OpenAI].*

ESS categories according to CICES

The MEA introduced a widely used framework that distinguishes ***four categories*** of ESS provisioning, regulating, cultural, and supporting services. In contrast, CICES adopts a different conceptual approach. Rather than including supporting services as a separate category, CICES focuses on final ESS, defined as the contributions that ecosystems make directly to human well-being. Supporting ecological processes are therefore treated as underlying ecosystem functions rather than services themselves [CICES, 2025]

Therefore, CICES is designed as a hierarchical reference classification that allows ESS to be measured, assessed, and compared across different analytical contexts, while maintaining conceptual clarity between ecosystem processes, services, goods, and benefits. At the highest

level, CICES groups ESS into ***three main*** groups (Figure 7). Those sections are based on the type of contribution ecosystems make to human well-being:

- **Provisioning** services refers to ecosystem contributions that meet material and energy needs. They represent outputs such as biomass or other ecosystem-derived materials that can be used directly or processed further. According to the guidance, these services relate to the provisioning of material and energy needs and are defined by ecosystem attributes that enable their use by people.
  Key characteristic: direct material contributions derived from ecosystems.
- **Regulation and Maintenances** include ecosystem contributions that regulate environmental conditions and maintain ecosystem functioning in ways that affect human health, safety, and comfort. CICES guidelines include processes such as mediation of wastes, regulation of water flows, erosion control, and maintenance of soil quality.
  Key characteristic: indirect contributions through regulation of environmental processes.
- **Cultural** services refer to the non-material contributions of ecosystems that influence people's physical and mental states. The classification describes these as contributions linked to interactions with ecosystems that provide experiential, symbolic, or intellectual benefits.
  Key characteristic: non-material contributions affecting human experience and well-being [CICES, 2025].

Figure 7 Categories of ESS according to the CICES approach *[CICES, 2025] [Source: OpenAI].*

CICES emphasizes that ESS should be understood within the cascade model, which links ecosystem structures and processes to services, goods, and benefits. The guidance highlights that:

- services retain a connection to underlying ecosystem functions and structures,
- services give rise to goods and benefits once the "production boundary" is crossed,
- a single ecosystem function may contribute to multiple services, and services may depend on multiple functions.

Importantly, CICES does not treat supporting ecological processes (e.g., nutrient cycling) as individual ESS. Instead, these processes are seen as the underlying mechanisms that enable services, rather than direct contributions to human well-being. CICES v5.2 provides a

Funded by
the European Union

conceptually precise classification focused on final ESS and their direct contributions to human well-being (Figure 8). Unlike the MEA framework, which includes supporting services as a separate category, CICES groups services into three main sections (provisioning, regulation and maintenance, and cultural) while treating underlying ecological processes as part of ecosystem functioning rather than services themselves.

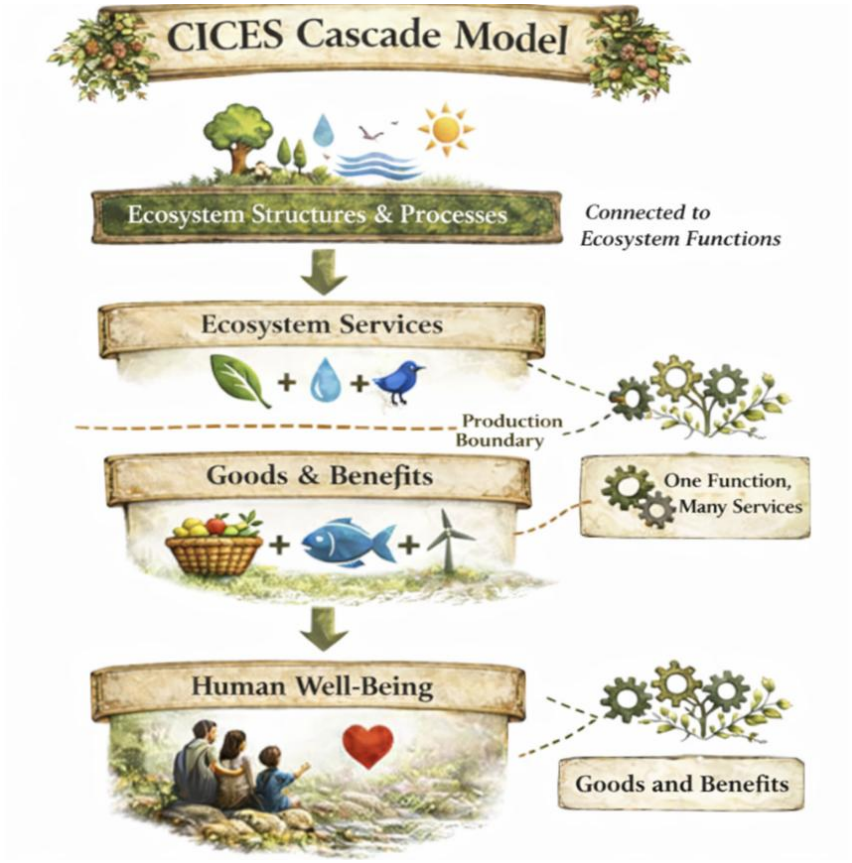

Figure 8 The CICES cascade model *[CICES, 2025] [Source: OpenAI].*

3.3 CICES as a reference classification for the EDAPHOS project

CICES provides a structured and internationally recognised framework for identifying, organising, and reporting ESS. The guidance presents CICES as a reference classification that supports consistent assessment and comparability across analytical and policy contexts, based on the cascade logic linking ecosystem structures and processes to services, and further to goods and benefits. Within the EDAPHOS project, a scenario-based and indicator-driven approach was adopted during the analytical work within WP2, WP4 & WP5 (Task 2.2; Task 4.2; Task 5.2) to ensure that results respond to decision-making needs across CS. In this context, CICES proved to be the most coherent and practical framework for organising ESS, structuring indicator selection, and ensuring that results remain comparable across scenarios and sites. Its hierarchical structure and clear terminology provided a consistent foundation for organising evidence and preparing results for subsequent valuation steps.

Following the logic of the CICES guidance, EDAPHOS adopted a clear step-by-step approach (Figure 9) that ensures transparent assessment and provides a traceable route from mapping to valuation:

- maps ecosystem types and define system boundaries;
- selects or develops indicators capturing ecosystem contributions;
- assesses ESS under alternative scenarios;
- compiles results as an evidence base for valuation and further monetization (WP4, Task 4.2).

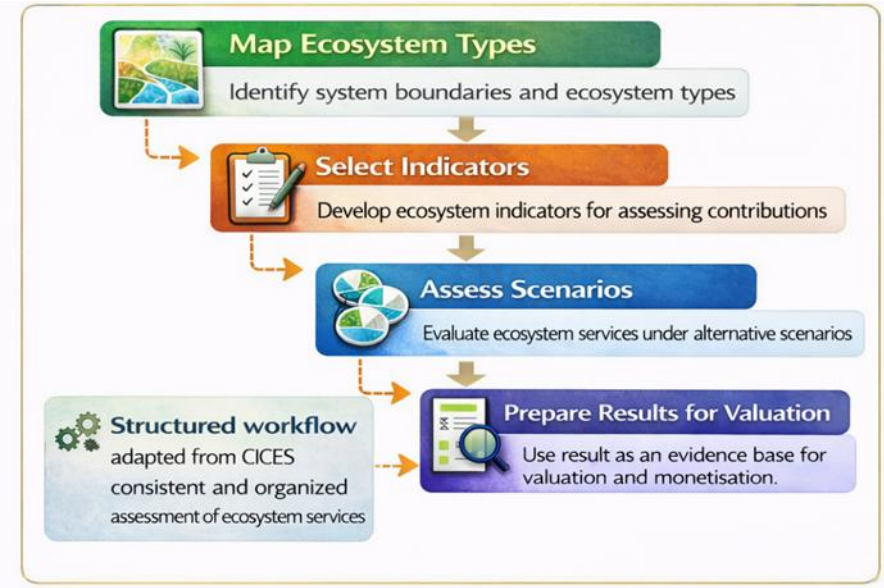

Figure 9 ESS assessment approach based on CICES 5.2 adapted within EDAPHOS WP2 (Task 2.2) *[CICES, 2025] [Source: OpenAI].*

The adopted workflow reflects the role of CICES as a practical reference structure for indicator-based assessment and systematic organisation of ESS information. As mentioned in previous section (section 3.2) CICES defines ESS as the contribution ecosystems make to human well-being and distinguishes these from goods and benefits derived later. This framing is particularly valuable in EDAPHOS, because it enables consistent description and quantification of ecosystem contributions across redevelopment variants, while avoiding conceptual ambiguity between functions, services, and subsequent benefits. The results of the ESS assessment performed within Task 2.2 may provide valuable insights for groups directly engaged in scenario definition, assessment, and downstream valuation work, including CS Leaders, landowners and land managers, planning stakeholders involved in approving scenarios and defining boundaries as well as experts and stakeholder's engagement processes, where CICES supports the organisation of views and evidence. Within Task 2.2, EDAPHOS project applies the CICES v5.2 methodology for ESS assessment. This framework offers a consistent and transparent basis for scenario-based, indicator-driven analysis. It also provides a clear pathway from assessment to valuation. This approach supports methodological coherence and clearer interpretation. It also improves comparability of results across case studies and scenarios.

3.4 ESS selected for the assessment

The selection of ESS was based on the CICES v5.2 classification framework and reflects the key ecosystem contributions relevant to the EDAPHOS project context. The performed ESS selection was focused on services that are directly linked to the functioning of phytoremediation systems and the restoration of degraded post-industrial or post-mining sites. The selected ESS were

Funded by
the European Union

grouped according to the three main CICESv5.2 (.xls sheet) categories: (1st) provisioning, (2nd) regulation and maintenance, and (3rd) cultural. Within the provisioning category, the ESS assessment includes e.g. biomass production (considering biomass-based energy). These services reflect the capacity of vegetation systems, including poplar plantations and (optional) accompanying plant species (*Brassica L., Lablab purpureus L.*), to generate biological resources that can be used as material or energy inputs. The regulation and maintenance category forms the core of the analysis, capturing ecosystem contributions directly related to environmental remediation processes. The assessment includes regulation of soil quality, climate change mitigation through carbon sequestration, air quality regulation, and temperature related to microclimate regulation. These services reflect the role of vegetation in improving soil conditions, reducing pollutants, regulating environmental parameters, and supporting ecosystem recovery processes on degraded land. Within this category, we also estimated the site's potential to supply energy under a ground-mounted photovoltaic (PV) installation scenario. Within the third, cultural category, the analysis considers direct in-situ interactions with living systems, reflecting the potential of restored sites to provide opportunities for recreation, health benefits, and experiential engagement with nature. A detailed classification of the selected ESS, together with the methodological approach used for their assessment, is presented in subsequent Section 4.2 and 4.3. The selected set of ESS reflects the main pathways through which NBS solutions implemented in EDAPHOS project generate environmental and societal benefits. By structuring the assessment, the analysis ensures conceptual consistency while capturing the ecosystem contributions most relevant to site restoration and sustainable land management.

4 ESS assessment methodology

4.1 Workflow and research stages

The work focuses on ESS as contributions of ecosystems to human well-being, assessed for contaminated (post-industrial/ post-mining) sites under alternative redevelopment pathways, highlighting how future land-use options may influence the range and level of provided services.

In EDAPHOS this valuation work was designed to support subsequent steps on valuation, monetization, and integration into decision-making, which are performed across parallel work packages, and will be delivered as results from WP4 (Task 4.2) & WP5 (Task 5.2).

To ensure methodological consistency across all seven case studies (CS1–CS7) and to generate results that are directly comparable between all sites a common scenario set was adopted for the ESS assessment in every CS. This decision was taken based on consultations with the PP (especially CS Leaders) and follows CICES v5.2 guidance, which promotes the use of a common reference framework ("*designed to help measure, account for and assess ecosystem services"* and has been *"used widely… for designing indicators, mapping and for valuation*"). The guidance also links such a framework to comparability, noting that the classification enables authors to "*position the target references work in a common framework so that comparison and analysis is possible".* In line with this rationale, EDAPHOS harmonises the assessment set-up across CS by standardising scenarios and the associated ESS indicator catalogue. This ensures a unified basis for cross-CS interpretation and synthesis.

Accordingly, for each CS, the ESS assessment was carried out for three alternative future land-use variants (Section 5.2), treated as a harmonised and comparable scenario set (including

Funded by the European Union

a NBS-based option). These scenarios were applied across all CS, even if a given variant was unlikely or not currently planned for a specific site. By applying a common assessment approach across all CS, it becomes possible to:

- compare results on a like-for-like basis across sites,
- identify site-specific constraints and opportunities that explain why a given pathway may (or may not) be feasible and beneficial,
- clearly and transparently show differences in expected benefits and trade-offs linked to alternative land-use and remediation strategies.

The methodology adapted by the GIG-PIB team to estimate ESS is aligned with the approach set out in the CICES v5.2 guidance. For this part of Task 2.2, the work was divided into four key stages, providing a clear and consistent workflow for the ESS assessment.

The adopted workflow is described and presented on Figure 10.

Figure 10 ESS assessment workflow *[Source:OpenAI].*

STAGE 1 - baseline mapping of relevant ecosystems

Baseline mapping defines the spatial area of analysis and provides a consistent description of ecosystem types within that area across all CS. In practice, it includes two subtasks:

Funded by
the European Union

Stage 1 (Subtask 1.1) Setting the assessment boundaries.

At this stage of work, the appropriate scale and geographic coverage were defined for the areas where planned activities could affect environmental, social, and economic aspects. The boundaries of the analysis area were typically aligned with administrative units, as this supported the collection of socio-economic data and facilitated the use of results in planning and decision-making, especially for cultural ESS. Depending on the CS location, the defined analysis boundaries either matched the administrative boundary of the municipality where the CS is located (CS2, CS4 see Figure 11) or covered two administrative units when the CS lies on a municipal border (CS1, CS3, CS5, CS6, CS7).

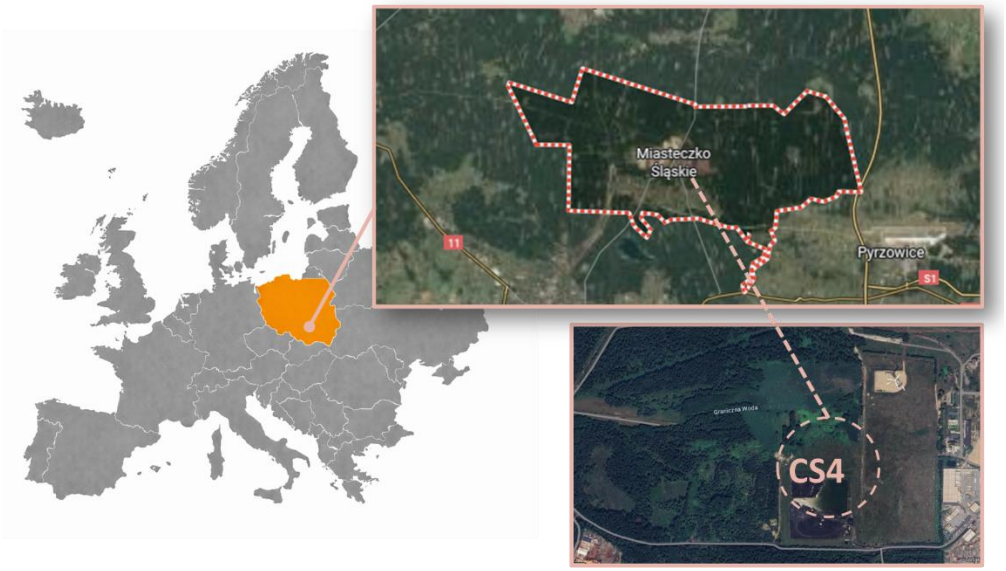

Figure 11 Delineation of the administrative boundaries for CS4 (Miasteczko Śląskie, PL) *[Source: GIG-PIB]*.

Stage 1 (Subtask 1.2) Delineating ecosystem types.

Delineating ecosystem types was an important step because it defined the spatial basis for the ESS assessment. Within this subtask, the CORINE Land Cover (CLC) classification was used as a harmonised basis to map ecosystem types and describe their potential functions and service provision. The CLC system is hierarchical and consists of three levels. Level 1 groups of land cover into five broad categories: artificial surfaces, agricultural areas, forests and semi-natural areas, wetlands, and water bodies. Level 2 further subdivides these into 15 categories that can be mapped at scales of 1:500,000 to 1:1,000,000. Level 3 provides the highest level of detail, with 44 classes used to build land cover databases across Europe. In Poland, 31 of these 44 classes are present (Figure 12). The CLC codes applied in this work are presented in section 5.3.

Funded by the European Union

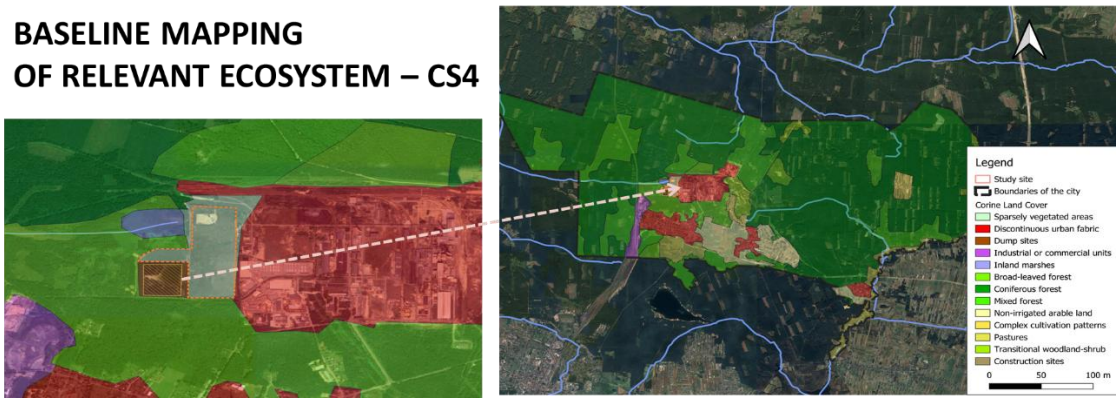

Figure 12 Example of delineated ecosystem types based on land cover for CS4 *[Source: GIG-PIB].*

Stage 2 Formulating alternative rehabilitation / redevelopment scenarios per CS (including NBS) to reflect feasible end-uses and planning recommendations.

Within WP2, Task 2.2, ESS provision was estimated for each CS under three alternative future land-use scenarios (Table 2). The scenario approach was adopted to capture different, realistic redevelopment pathways and to enable a structured comparison of their implications for ecosystem functions and benefits (Figure 13). Following internal PP consultations, in order to ensure consistency and comparability of results across all sites, a decision was taken to harmonise the scenario set and apply the same three scenario directions to every CS.

Table 2 Set of future land-use scenarios analysed.

Scenario	Characteristic
Scenario 1	Afforestation *(land cover by fores; for available data afforestation with Poplar was considered)*
Scenario 2	Industrial redevelopment *(installation of photovoltaic panels)*
Scenario 3	Grassland cover *(e.g., resulting from natural succession).*

Figure 13 Example of visualisation of potential redevelopment scenarios for CS4.

Stage 3 -Selection of ESS indicators

The selection of ESS for the EDAPHOS assessment was based on the CICES v5.2 classification and focuses on services that are most relevant for restoration of degraded post-industrial/post-mining sites, including the restoration based on NBS, like phytoremediation techniques. The selected ESS cover the three main CICESv5.2 categories: (1st) provisioning, (2nd) regulation and maintenance, and (3rd) cultural, and represent the key functions that EDAPHOS sites may deliver under different future land-

Funded by
the European Union

use scenarios. In the provisioning category, the assessment includes e.g. biomass production (including biomass-based energy potential), reflecting the capacity of vegetation systems (e.g., poplar plantations and accompanying species) to provide biological resources. The regulation and maintenance category is central to the analysis and captures services directly linked to remediation and recovery processes, such as soil quality regulation, carbon sequestration (climate mitigation), air quality regulation, and microclimate/temperature regulation. Within this category, the energy supply from PV electricity generation under Scenario 2 was also included. The cultural category addresses the potential for direct in-situ interactions with nature, including recreation and well-being benefits that may emerge as sites recover. The selected ESS and the methodology used to determine the indicators applied in the ESS assessment are presented respectively in sections 3.4 and 4.3 (Figure 3).

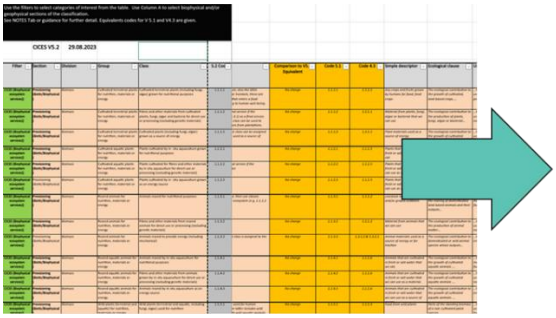

ESS ID	Ecosystem Service (EDAPHOS)	CICES Code (v5.1)	CICES Code (v5.2)
ESS 1	Biomass production	1.1.1.2	1.1.1.2
ESS 2	Regulation of soil quality	1.2.1.2	1.2.1.2
ESS 3	Mitigation of climate change (carbon dioxide sequestration)	2.1.1.2	2.1.1.2
ESS 4	Air quality mitigation	2.1.1.3	2.1.1.3
ESS 5	Temperature regulation	2.2.6.2	2.2.6.2
ESS 6	Direct in-situ interactions with living systems	3.1.1.1 /	3.1.1.1 3.1.2.2
ESS 7	Energy properties	4.3.2.4	4.3.2.4

Table 3 A fragment of the Excel sheet CICESv5.2 used for ESS selection in the EDAPHOS Task 2.2 assessment. *[Source: https://cices.eu/].*

Stage 4- Assessment of ESS provision under each scenario using the selected indicators.

The ESS valuation in EDAPHOS was based on an indicator-driven approach. For each selected ESS, a specific methodology was developed to define which indicators should be used, how the indicator should be assessed and quantified, and what kind of data are required. These indicator methodologies are grounded in scientific literature and established analytical models commonly applied in ESS assessment (e.g. EU tool for PV energy production). Following these methodologies, the necessary input data were collected from appropriate sources, including *desk research*, satellite and remote sensing data, geospatial datasets and geoportals, interactive tools and other available environmental and socio-economic data. The collected datasets were then processed in line with the agreed procedures to calculate indicators and assess the level of service provision. Each ESS was assessed separately for each land-use scenario, allowing a transparent comparison of expected benefits and trade-offs under alternative redevelopment pathways. Detailed information on the indicator methodologies, data acquisition procedures, and the full set of results for all sites are in further section of D2.5.

4.2 List of relevant ecosystem services identified for the CS

In the early stage of EDAPHOS project, the identification of ESS performed within Task 2.2 was initially based on the CICESv5.1 classification (methodological approach described in D2.2). In the present deliverable (D2.5), the updated CICES v5.2 classification has been adopted as the operational conceptual framework. The structure of CICES v5.2 was adapted to the specific objectives of the project, with a focus on soil-related processes and vegetation functions

underpinning the assessment of land-use scenarios. Following the approach defined in WP2, ESS were selected in collaboration with CS leaders, site managers and other project partners, based on their ecological relevance, their sensitivity to changes in land management, and their importance for subsequent process-based analyses in WP4 and valuation tasks in WP5.List of selected ESS is presented in table below (Figure 4).

Table 4 ESS matrix used in the assessment within Task 2.2.

ESS ID	Ecosystem Service (EDAPHOS)	CICES Code (v5.1)	CICES Code (v5.2)	Section	Division	Group	Class
ESS 1	Biomass production	1.1.1.3	1.1.1.3	Provisioning	Biomass	Cultivated terrestrial plants for nutrition, materials or energy	Cultivated plants (including fungi, algae) grown as a source of energy
ESS 2	Regulation of soil quality	2.1.1.2	2.1.1.2	Regulation & Maintenance	Transformation of biochemical or physical inputs to ecosystems	Reduction of nutrient loads and mediation of wastes or toxic substances of anthropogenic origin by living processes	Filtration /sequestration/ storage/ accumulation by micro-organisms, algae, plants, and animals
ESS 3	Mitigation of climate change (carbon dioxide sequestration)	2.2.6.1	2.3.6.1	Regulation & Maintenance	Regulation of physical, chemical, biological conditions	Atmospheric composition and conditions	Regulation of chemical composition of atmosphere and oceans, and the maintenance of continental atmospheric/oceanic circulation patterns
ESS 4	Air quality mitigation	2.1.1.2	2.1.1.2	Regulation & Maintenance	Transformation of biochemical or physical inputs to ecosystems	Reduction of nutrient loads and mediation of wastes or toxic substances of anthropogenic origin by living processes	Filtration /sequestration/ storage/ accumulation by micro-organisms, algae, plants, and animals
ESS 5	Temperature regulation	2.2.6.2	2.3.6.2	Regulation & Maintenance	Regulation of physical, chemical, biological conditions	Atmospheric composition and conditions	Regulation of temperature and humidity, including ventilation and transpiration at local scales
ESS 6	Direct in-situ interactions with living systems	3.1.1.1	3.1.1.1	Cultural	Physical and experiential interactions with natural environment	Direct, in-situ and outdoor interactions with living systems that depend on presence in the environmental setting, i.e. broadly recreational activitie	Elements of living systems that that enable activities promoting health, recuperation or enjoyment through active or immersive interactions
ESS 7	Energy properties	4.3.2.4	4.2.2.4	Provisioning	Non-aqueous natural abiotic ecosystem outputs	Non-mineral substances or ecosystem properties used for nutrition, materials or energy	Solar energy

Funded by the European Union

ESS 6 (Direct in-situ interactions with living systems) is reported as a combined cultural ecosystem service, aggregating experiential and educational interactions with nature, as both classes are closely linked in the context of in-situ learning and living laboratories.

4.3 ESS Data Sources and Methodological Limitations

This section summarises the main data sources and methodological considerations applied in the assessment performed for each ESS (ESS1–ESS7). For each service, key information is presented in a structured format ("data sheet"), including the ESS name, its classification and code according to CICES v5.2, the main indicator with units, and a concise description of the methodological approach used for quantification.

Detailed data sheets for each ESS are provided in the respective tables: EES1 (Table 5), ESS 2 (Table 6), ESS3 (Table 7) ESS4 (Table 8), ESS5 (Table 9), ESS6 (Table 10) and ESS7 (Table 11).

Funded by the European Union

Table 5 Data sheet for ESS1 -Biomass production.

ESS 1 – Biomass production	
Provision of plant biomass from contaminated sites intended for bioenergy purposes, following phytomanagement or restoration processes.	
CICES 5.2 Code & Division	1.1.1.3– Biomass
Main indicator	Energy potential derived from annual above-ground biomass increment (EP; GJ/ha/year).
Methodology	To estimate annual biomass production, annual above-ground biomass increment (AGBinc; t DM·ha^{-1}·yr^{-1}) is converted to energy potential using: EP = AGBinc × CV *where:* *CV (calorific value; GJ·t^{-1} DM) is fixed by biomass type and applied consistently across case studies: CV_woody = 18.5 GJ·t^{-1} DM for forests and woody crops, CV_herb = 17.5 GJ·t^{-1} DM for grassland and grassland-equivalent scenarios, and CV_topola = 18.56 GJ·t^{-1} DM when poplar is treated as a separate woody category.*
Methodology description: AGBinc values are assigned per land-use scenario (CLC classes) using a hierarchical approach to ensure cross-case-study comparability: **Scenario 1:** Forest scenarios (broad-leaved and coniferous forests) AGBinc is taken from literature and/or forest inventory–based sources that provide harmonised increments for forest types, ensuring consistent definition and comparability across countries and case studies. **Scenaruio 2:** industrial/commercial (PV energy production) In scenarios with partial vegetation cover, it was assumed that AGBinc is determined as a constant part of grassland productivity, proportional to the share of biologically active area. A uniform scenario assumption was used throughout the report: **PV = 0.8 × grassland (i.e., 80% of grassland productivity)** industrial/commercial = 0.2 × grassland (i.e., 20% of grassland productivity). **Scenario 3: Grassland** scenarios (natural succesion) AGBinc is assigned using a typological NUTS2 approach (climate and management intensity), where values reflect the expected order of magnitude for the specific grassland type (e.g., Mediterranean dry pastures vs temperate productive meadows). In this approach, AGBinc is primarily driven by water availability and use intensity rather than administrative boundaries. Poplar plantations (transitional woodland/shrub) AGBinc is assigned using literature-based yields for poplar energy plantations. When regional datasets are inconsistent or dominated by unusually high-yield conditions (e.g., highly irrigated sites), a harmonised value is used to maintain comparability across case studies. Special case: NAI-based conversion (applied only in Greece) For Greece, where consistent AGBinc values in a single increment definition were not available at the required scale, AGBinc for forest scenarios was derived from Net Annual Increment (NAI; m^3·ha^{-1}·yr^{-1}) using an internal harmonisation procedure. This procedure converts NAI to AGBinc using a conversion coefficient $\boldsymbol{k}$ calibrated from reference regions where both NAI and AGBinc were available $\left(\boldsymbol{k} = \frac{\boldsymbol{AGBinc_{ref}}}{\boldsymbol{NAI_{ref}}}\right)$, and applies this coefficient to Greece ($\boldsymbol{AGBinc_{GR} = k \times NAI_{GR}}$); the resulting AGBinc is then used to compute energy potential as $\boldsymbol{EP = AGBinc \times CV}$. Non-irrigated arable land - *Brassica juncae* or *Lablab purpureus* crop Where literature-based biomass increment/yield data were available, AGBinc was taken directly from literature.	
Applied ecosystem types (CLC)	▪ Broad-leaved forest ▪ Coniferous forest ▪ Mixed forest ▪ Shrublands / transitional woodland-shrub (poplar plantations) ▪ Grasslands (with limited use and lower biomass productivity) ▪ PV ground-mounted (grassland-equivalent fraction) ▪ Industrial/commercial units (grassland-equivalent fraction) ▪ Non-irrigated arable land - *Brassica juncae* or *Lablab purpureus* crop
Reference	1.Copernicus / CLC (land cover classes and spatial allocation). 2.National Forest Inventories / harmonised NFI outputs (NAI / increments for forest types). 3.Copernicus GPP/NPP only as supplementary screening layer, not as primary AGBinc input(Optional)

	4.Literaure: [Andresen et al., 2018], [Aravanopoulos, 2010], [Borreani et al., 2007], [CIP, 2020], [Dal Prà, et al., 2023], [Del Gatto et al., 2015], [Di Cosmo et al., 2023], [Feng et al., 2023], [Forest Ecology and Management, 562, 121913], [Gabryszuk et al., 2021], [Gasparini et al., 2022], [González-Díaz, et al., 2019], [Gschwantner, et al., 2024], [GUS, 2020], [Lazzeri et al., 2009], [Les Etudes Report, 2024], [Manzone et al., 2014], [Niemczyk, 2017], [Obermeier et al., 2018], [Oddi et al., 2024], [Shi et al., 2023], [Tao et al., 2015], [Zianis & Mencuccini, 2005], [Étude de nouveaux gisements de biomasse végétale fermentescible, et des conditions de leur mobilisation pour la méthanisation Rapport]

Funded by the European Union

Table 6 Data sheet for ESS2 - Regulation of soil quality.

ESS 2 – Regulation of soil quality	
The role of ecosystems in maintaining and improving soil quality, specifically through Nature-Based Solutions (NBS) as effective methods for pollutant removal (phytoremediation).	
CICES 5.2 Code & Division	2.1.1.2 – Transformation of biochemical or physical inputs to ecosystems
Main indicator	Potential annual accumulation of a representative soil pollutant in above-ground plant biomass (g/ha/year).
Methodology	Potential annual pollutant accumulation is calculated as: Pollutant Accumulation => **AGBinc × C_plant** *where:* *AGBinc - annual above-ground biomass increment (t DM/ha/year).* *C_plant- pollutant concentration in above-ground biomass (mg/kg DM), converted for calculation consistency.* *For afforestation scenariosC_plant is computed as a weighted value across tissue compartments:* *C_plant = f_leaf × C_leaf + f_wood × C_wood* *with f_leaf = 0.2 and f_wood = 0.8,* *where C_leaf refers to leaves/needles and C_wood refers to stem wood/shoots.*
Methodology description: **Biomass productivity assessment (AGBinc)** AGBinc is assigned per land-use scenario consistently with ESS1 (harmonised forest increments; typology-based grassland values; fixed grassland-equivalent fractions for PV and industrial/commercial). **Pollutant selection (representative metal)** For valuation and cross-scenario comparability, cadmium (Cd) is used as the representative pollutant (non-essential element, frequently reported, typically more mobile and translocated to above-ground tissues than Pb). Other metals may be used for range screening. **Tissue-specific concentration parameterisation** C_leaf and C_wood (or C_shoots for woody crops) are parameterised from peer-reviewed literature reporting tissue concentrations (mg/kg DM). Priority is given to datasets providing both compartments measured with consistent analytical procedures. **Scenario-level aggregation and calculation** For woody scenarios, concentrations are aggregated using fixed tissue fractions (0.2/0.8). Pollutant Accumulation is then computed as AGBinc × C_plant, enabling scenario-based comparison of phytomanagement potential	
Applied ecosystem types (CLC)	• Broad-leaved forest (especially Poplar/Willow natural forest) • Coniferous forest • Transitional woodland/shrub (poplar plantations) • Grasslands (with limited use and lower biomass productivity) • PV ground-mounted (grassland-equivalent fraction) • Industrial/commercial units (grassland-equivalent fraction Non-irrigated arable land - *Brassica juncae* or *Lablab purpureus* crop
Unit of measurement	g/ha/year (grams of pollutant accumulated in above-ground biomass per hectare per year).
Assumptions	Vegetation used in scenarios has sufficient accumulation potential for the representative pollutant (Cd). Tissue concentrations are parameterised from literature (moderate contamination) and aggregated for woody biomass using fixed fractions 0.2 (leaves/needles) and 0.8 (stem wood/shoots). Results describe potential accumulation; harvesting is a possible management option but is not required for the indicator.
Reference	1.Copernicus / CLC (land cover classes and spatial allocation). 2.National Forest Inventories / harmonised NFI outputs (NAI / increments for forest types). 3.Copernicus GPP/NPP only as supplementary screening layer, not as primary AGBinc input (Optional) 4. Literature: [Algreen et al.,2013], [Asare et al., 2025], [Bayçu et al., 2006], [Bierza & Bierza, 2024], [Budzyńska et al., 2023], [Carabulea et al., 2024], [Čeburnis & Steinnes, 2000], [Jakubiak et al., 2025], [Juranović Cindrić et al., 2019], [Kandziora-Ciupa et al., 2022], [Kaoukis et al., 2018], [Kicińska & Gruszecka-Kosowska, 2016], [Kicińska et al. 2019], [Li et al., 2024], [Nechita et al., 2025], [Pilipović et al., 2019], [Radojčić Redovniković et al., 2017], [Sawidis et al., 2011], [Skonieczna et al., 2014], [Sun et al., 2009], [Suo et al., 2021], [Teodoro et al., 2019]

Table 7 Data sheet for ESS 3 – Mitigation of climate change/ carbon dioxide sequestration.

ESS 3 - Mitigation of climate change/carbon dioxide sequestration	
Storage and sequestration of greenhouse gases (GHG) by ecosystems, specifically through the capture of atmospheric carbon dioxide (CO_2) in plant biomass on remediated and managed sites.	
CICES 5.2 Code & Division	2.2.6.1 – Atmospheric composition and conditions
Main indicator	Annual carbon sequestration expressed in t CO_2/ha/year
Methodology	Total carbon sequestration is calculated as the sum of above-ground and below-ground carbon accumulation. The methodology follows the carbon allocation models for poplar plantations: Total Seq CO_2 => **(AGBinc + BGBinc) × C_fraction × 3.67** *where:* *- AGBinc / BGBinc: annual above- and below-ground biomass increment (t d.m./ha/year).* *- C_fraction: carbon content in dry matter (assumed at 0.5 or 50%).* *- 3.67: conversion factor from Carbon (C) to CO_2 equivalent*
Methodology description: **Biomass Assessment:** estimation of annual growth using yield tables (NFI) and literature proxies (Kożuch et al. 2024). **Below-ground allocation:** application of the root-to-shoot ratio and biomass allocation patterns according to Oliveira Rodríguez et al. to account for carbon stored in the root systems and below-ground organs. **Carbon conversion:** converting the total accumulated dry matter into carbon mass and subsequently into t CO_2/ha/year equivalents to reflect the service's contribution to climate mitigation. The indicator reflects the annual flow of carbon sequestration associated with biomass growth, rather than long-term carbon stock changes. **Scenario-level aggregation and calculation** Similarly as for the ESS1, for woody scenarios, concentrations are aggregated using fixed tissue fractions (0.2/0.8). Pollutant Accumulation is then computed as AGBinc × C_plant, enabling scenario-based comparison of phytomanagement potential.	
Applied ecosystem types (CLC)	• Broad-leaved forest (including Poplar/Willow SRC) • Coniferous and mixed forest • Shrublands / transitional woodland-shrub • Grasslands (Carbon storage in perennial root systems).
Unit of measurement	t CO_2/ha/year (tons of carbon dioxide equivalent per hectare per year).
Assumptions	1. Carbon fraction is constant at 50% of dry mass for woody species. 2. Below-ground biomass is estimated using species-specific expansion factors when direct root measurements are unavailable.
Methodological limitations	Potential exclusion of long-term Soil Organic Carbon (SOC) changes in short-term assessments; variability of sequestration rates depending on stand age and site-specific contamination levels.
References	1.Copernicus Global Land Service (GPP/NPP data). 2.National Forest Inventory (local yield tables). 3.Literature-based proxy data: [Oliveira et. Al., 2018], [IPPC, 2006], [Mokany et al., 2006], [Dupouey et al., 2010], [Shiferaw et al., 2022], [Cañellas et al., 2018], [GIOŚ, 2019]

Table 8 Data sheet for ESS 4 – Air quality regulation.

ESS 4 - Air quality regulation	
Removal of atmospheric pollutants (specifically particulate matter PM_{10} and $PM_{2.5}$) by tree and shrub canopies in urban, peri-urban and rehabilitated post-industrial areas through dry deposition processes.	
CICES 5.2 Code & Division	2.1.1.2 – Transformation of biochemical or physical inputs to ecosystems
Main indicator	Annual removal of particulate matter (PM_{10} / $PM_{2.5}$) expressed in t/ha/year
Methodology	The methodology follows the dry deposition model for particulate matter (PM_{10}) established by Tallis et al. (2011): **Absorption of PM_{10} = Flux (V) x Surface (SA) x Period (t) (t/km²/year)** where: - Flux is the pollutant to the surface (amount removed per unit area and time), calculated by multiplying the deposition velocity of the pollutant (m/s), which depends on canopy structure and wind speed and the concentration of the pollutant in the atmosphere. - Surface is the considered surface area multiplied by the surface area index functioning in a given area (LAI). - Period accounts for the period of analysis in days, multiplied by the proportion of dry days and the proportion of non-leaf days. The total annual pollutant removal is calculated by integrating deposition fluxes over the vegetated surface area of each land-use scenario. The above contributes to the calculation as follows: - V = deposition velocity (m/s) x pollutant conc. (µg/m³) • Flux (µg/m³) was then converted to daily flux by multiplying it by 86400 - SA = LAI (m²/m²) x area of land considered (m²) - t = period of analysis (days) x proportion of dry days (fraction) x proportion of on-leaf days (fraction) • Afterwards the absorption of PM_{10} was converted from (µg/m²/year) to (t/km²/year) by x10^6
Methodology description: **Canopy assessment:** Calculation of the Tree Canopy Area (TCA) using Land Cover data and NFI (National Forest Inventory) to determine the active surface area for deposition. **Deposition modeling:** Applying the Tallis et al. approach, which considers the "filtering" effect of different tree types (broad-leaved vs. coniferous). Coniferous trees are generally more efficient due to higher Leaf Area Index (LAI) and year-round foliage. **Concentration data**: Integration of local air quality monitoring data (PM_{10}/$PM_{2.5}$ concentrations) to calculate the total annual removal load	
Applied ecosystem types (CLC)	▪ Broad-leaved forest ▪ Coniferous forest (highest efficiency according to Tallis et al.) ▪ Mixed forest ▪ Transitional woodland-shrub (urban greenery).
Unit of measurement	kg/ha/year (efficiency per area).
Assumptions	1. Deposition velocity (Vd) is estimated based on the average values for specific canopy types provided in the literature. 2. The model assumes dry deposition as the primary mechanism for PM removal in the assessed NBS scenarios.
Methodological limitations	Variability in removal efficiency due to local weather conditions (wind speed, precipitation) and the "saturation" effect of the canopy in highly polluted areas.
References	1.Copernicus Global Land Service (GPP/NPP data). 2.National Forest Inventory (local yield tables). 3. Satellite Imagery & Land Cover Data 4. National and Local Forest Statistics 5. National & Local Air Quality Monitoring 6.Literature: [Airparif, 2022], [AQI, 2021], [Borlaza-Lacoste et al., 2022], [Chen, 2015], [Chervenkov et al., 2025], [EU EMEP, 2016], [GIOŚ, 2018], [Khan et al., 2017], [Kuklinska et al., 2015], [Langner et al., 2011], [Le Dantec et al., 2010],[Leśny et al., 2007], [Lovett, 1994], [Marando et al., 2016], [Mariarosa et al., 2017], [Nowak et al., 2017], [Parker, 2020], [Pérez-Vizcaíno et al., 2026], [Schrader & Brümmer, 2014], [Sinan & Hasenauer, 2025], [Sówka et al., 2019], [Tomczyk & Szyga-Pluta, 2016], [Turner et al., 2000], [U.S. Forest Service, 2011], [Waza et al., 2025], [WHO,2013]

Table 9 Data sheet for ESS 5 – temperature regulation.

ESS 5 – Temperature regulation	
Regulation of local microclimate and mitigation of the Urban Heat Island (UHI) effect through vegetation-driven processes such as shading and evapotranspiration.	
CICES 5.2 Code & Division	2.3.6.2 – Regulation of physical, chemical, biological conditions
Main Inicator	Surface temperature reduction (ΔT, °C) between NBS sites and reference land-use areas.
Methodology	The methodology utilizes daylight surface temperature upscaling models as proposed by Radoux et al. (2025), correlating specific Land Cover (LC) types with their thermal signatures using remote sensing data.
Methodology description: **1. Surface temperature mapping**: Extracting Land Surface Temperature (LST) from thermal infrared satellite bands. **2. Land cover thermal profiling:** Applying the Radoux et al. (2025) model to assign specific thermal weights to various land cover classes (e.g., poplar plantations vs. bare soil/industrial concrete). **3. Health & comfort assessment:** Evaluating the cooling benefits on local environmental health and human comfort based on the framework by Mirzaei et al. (2020). Land Surface Temperature (LST) is used as a spatially consistent proxy for microclimate regulation, enabling comparative assessment across land-use scenarios.	
Applied ecosystem types (CLC)	▪ Broad-leaved and Coniferous forests ▪ Urban parks and greenery ▪ Transitional woodland-shrub on remediated post-industrial sites.
Unit of measurement	°C (temperature difference, ΔT)
Assumptions	1. Vegetation density (NDVI) is inversely proportional to surface temperature during daylight hours. 2. Established forest canopies provide significantly higher cooling than open grasslands due to vertical shading.
Methodological limitations	LST data represents surface skin temperature, which can differ from ambient air temperature; results are highly sensitive to cloud cover and soil moisture at the time of data acquisition.
References	1. National Forest Inventory (local yield tables). 2. Literature-based proxy data 3. National & Local Meteorological Monitoring 4.Copernicus Global Land Service (LST products)

Table 10 Data sheet for ESS 6 - Direct, in-situ and outdoor interactions with living systems.

ESS 6 - Cultural - Direct, in-situ and outdoor interactions with living systems	
The capacity of the ecosystem to provide opportunities for direct in-situ and outdoor interactions with living systems	
CICES 5.2 Code & Division	3.1.1.1 – Physical and experiential interactions with natural environment
Main indicator	Number of residents within 300 meters of a green recreational area (> 1 hectare).
Methodology description: **1. Accessibility analysis:** Spatial analysis of population density in the vicinity of areas that may serve recreational functions (Green recreational areas) This ecosystem service is assessed as a cultural service according to CICES, reflecting the role of living systems elements that enable activities promoting health, recuperation or enjoyment through active or immersive interactions (recreation service value). Green spaces for recreation have to be publicly accessible (not fenced areas). Agricultural land does not meet this criterion because recreational use of such land could lead to crop losses.	
Applied ecosystem types (CLC)	CLC types that could be used for outdoor recreation purposes: ▪ urban green areas ▪ deciduous forests ▪ coniferous forests ▪ mixed forests ▪ natural grasslands and meadows ▪ forests and shrub vegetation undergoing change ▪ scattered vegetation ▪ water courses and water bodies ▪ parks [Wales et al 2016]
Unit of measurement	Number of residents within 300 meters of a green recreational area (> 1 hectare).
Assumptions	Proximity to urban areas directly correlates with higher recreation service value of green areas for nature-based recreation.
Methodological limitations	A distance of 300 m in a straight line does not always reflect the possibility of reaching the area on foot in less than 15 minutes (criterion of green area accessibility for residents)
References	1.Copernicus Global Land Service (Corine Land Cover and Urban Atlas data). 2.OpenStreetMap Landcover 3.High Resolution Population Density Maps 4. Literaure: [Grunewal et al 2017], [Handley et al 2003], [Tobias G., et al. 2017] [Kabisch, Strohbach, Haase, & Kronenberg, 2016]

Table 11 Data sheet for ESS 7 – Energy properties (PV).

ESS 7 –Energy properties (PV)	
Provision of physical space and suitable environmental conditions (insolation, topography) for the production of renewable electricity via ground-mounted photovoltaic systems.	
CICES 5.2 Code & Division	4.2.2.4 Non-aqueous natural abiotic ecosystem outputs
Main indicator	Technical suitability for photovoltaic energy production expressed as site-scale total annual potential energy yield (GWh/year), aggregated over the developable area
Methodology	Spatial multicriteria analysis based on the framework of Casalegno et al. (2014), which prioritizes land for energy production based on solar radiation and land-use trade-offs.
Methodology description (PV performance and electricity production) **PV yield estimation (PVGIS):** PV performance for each CS was estimated with the PVGIS tool of the European Commission / Joint Research Centre using a harmonised reference setup. **Reference configuration**: Database PVGIS-SARAH3; technology crystalline silicon; 1 kWp; system loss 14%; mounting free-standing; tilt 35°; azimuth 0°. **Upscaling to CS capacity:** Maximum feasible installed capacity was derived from available area assuming 6 m² per 1 kWp. A Surface Coverage Ratio α = 50% was applied to account for non-deployable land (module spacing, roads, technical buildings, fencing, grid infrastructure), calibrated against operating PV farms (27–300 ha)	
Applied ecosystem types (CLC)	▪ Post-industrial brownfields ▪ Rehabilitated mining sites
Unit of measurement	GWh/y / or [kWp]
Assumptions	Reference configuration: ▪ Database: PVGIS-SARAH3; ▪ Technology: crystalline silicon; ▪ 1 kWp; ▪ system loss: 14%; ▪ mounting: free-standing; ▪ tilt:35°; ▪ azimuth:0°.
Methodological limitations	Energy potential does not account for seasonal cloud cover variability or future changes in grid capacity; focus is on the *physical space* as a provider of the service.
References	1.Copernicus Global Land Service (GPP/NPP data). 2. Local Spatial Planning & Grid Infrastructure 3. Global Solar Atlas / CAMS Radiation Service 4.Literature: [Walston et al., 2021], [Semeraro at. al., 2011] Databases: Photovoltaic Geographical Information System [https://re.jrc.ec.europa.eu/pvg_tools/en/tools.html]

5 EDAPHOS sites profile and land-use scenario framework

5.1 Sites characteristic

5.1.1 CS1 Carrières-sous-Poissy (FR) - site characteristics

CS1 is located at Carrières-sous-Poissy (48°57'35.9"N, 2°02'18.5"E) in the Northwest area of Paris (Figure 14). This 1-ha study site is owned by the Yveline Department. For over a century and a half, the region has been used for vegetable gardening, and from the end of the 19th century to the beginning of the 21st, it was irrigated with raw wastewaters to boost the soil's fertilization potential. This led to the accumulation of TE in the top 30 to 50 cm of soil, including Pb, Cu, Zn and Cd. Poly-metallic, polycyclic aromatic hydrocarbons (PAH) and pesticide pollution were identified following the site's agricultural past [Dère et al., 2007]. The ESS analysis is framed using the relevant commune-scale administrative boundary, because it provides a clear planning and governance unit for describing baseline conditions and interpreting who may benefit from ecosystem service changes [INSEE, 2025].

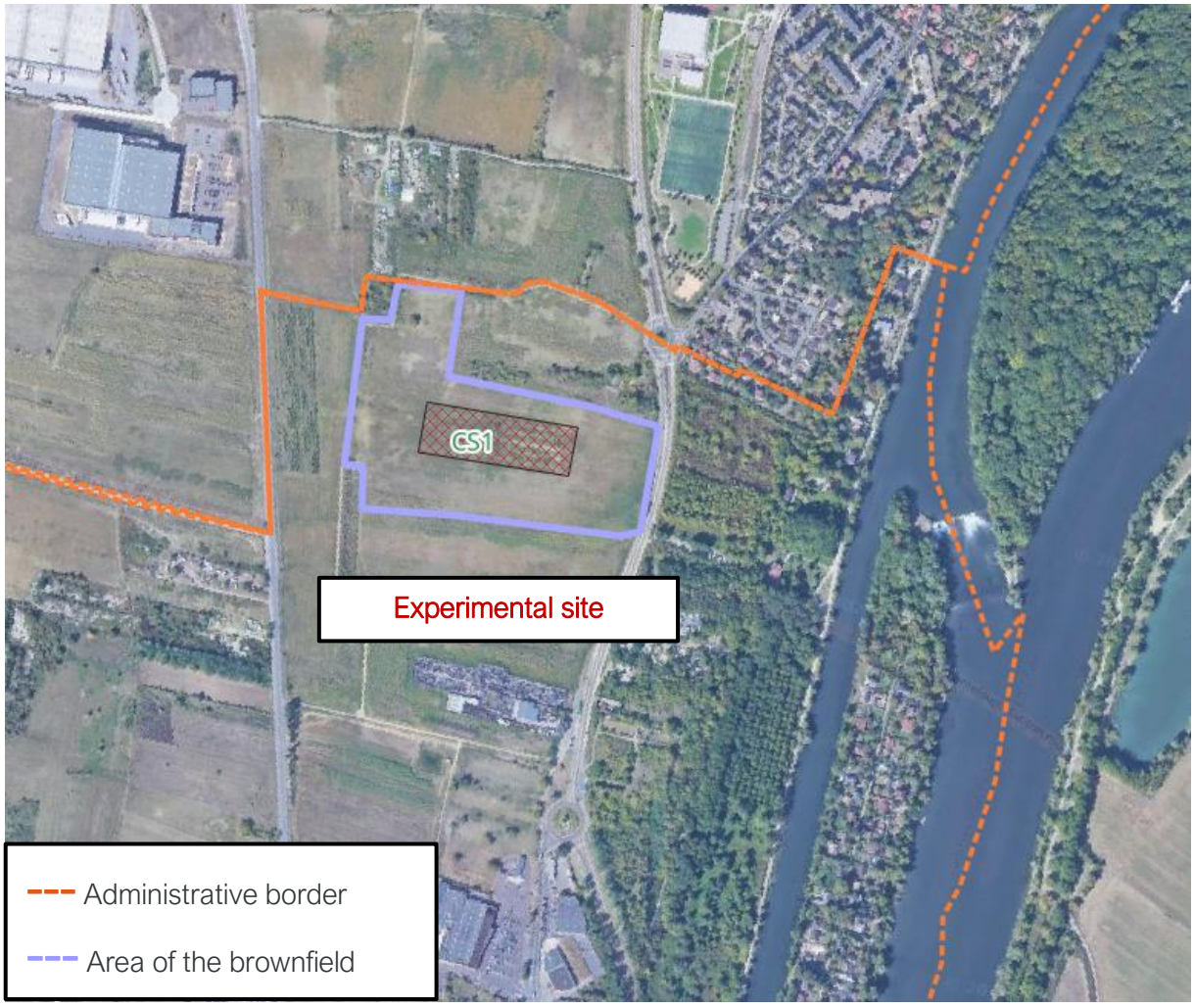

Figure 14 Location of CS1 within the indicative extent of the brownfield site (The red rectangle indicates the area of the experimental site; the violet line indicates the area of the brownfield; the orange line indicates the administrative border).

CS1 – site profile

The site is characterized as a rural area that received raw wastewater inputs during the 20th century, and it is considered representative of a wider affected agricultural extent in the north-western Paris area. Based on the available data, the site is moderately contaminated with heavy metals (e.g. Cd, Pb, Zn), PAHs, and pesticides related to crop cultivation; under these conditions, phytoextraction is indicated as the remediation pathway expected to deliver the highest depollution benefit. An area of ~1 ha is available for EDAPHOS trials, and the land is owned by the Yvelines Department, which foresees establishing a living lab in the 2026-2028 timeframe.

CS1 — baseline mapping for ESS assessment

The ESS assessment focuses on the entire contaminated part of the site that currently has no use, i.e., the area for which development scenarios will be prepared. The administrative framing explicitly covers Carrières-sous-Poissy and Chanteloup-les-Vignes communes, and the border-proximate location means remediation-related benefits (e.g., increased availability of safe green areas) may extend into the neighbouring commune (Figure 15).

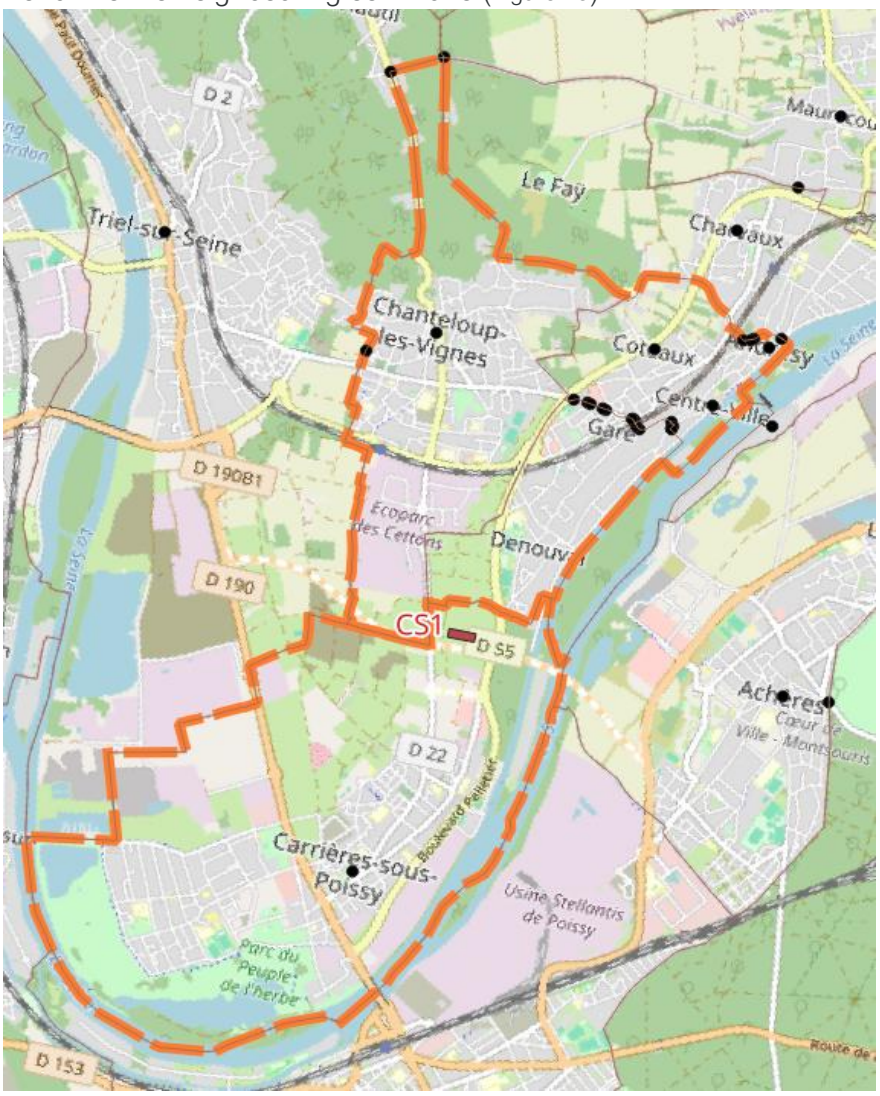

Figure 15 CS1 within the administrative boundaries of Carrières-sous-Poissy commune (The orange line indicates the administrative border of the Carrières-sous-Poissy commune and Chanteloup-les-Vignes commune.

Funded by the European Union

High-resolution land-cover data are available via Urban Atlas for Carrières-sous-Poissy, supporting baseline mapping across diverse land-cover types and allowing ecosystem-service potential to be estimated for different ecosystem types within the analysis boundary.
Boundary used for ESS analysis: Carrières-sous-Poissy commune and Chanteloup-les-Vignes commune.

Local socio-economic and industrial context relevant to ESS

Carrières-sous-Poissy is a dense peri-urban commune in Île-de-France, with about 19,900 residents in 2022 across ~7.2 km² (≈2,775 inhabitants/km²), and it has recorded strong recent population growth (average annual change 2016–2022: 3.7%). Nearby, Chanteloup-les-Vignes has 10,793 residents (2022) on ~3.3 km² (density ~3,241 inhabitants/km²). This settlement pattern matters for ESS interpretation because it points to a sizeable local beneficiary base for regulating and cultural services linked to safe green space, environmental quality, and risk reduction in the broader commune-scale impact zone. (INSEE, 2025). When defining the target ecosystem functions for CS1, two key aspects should be taken into account: (i) the site's moderate mixed contamination (heavy metals, PAHs, and pesticides) in an agricultural area historically influenced by wastewater, and (ii) the cross-boundary relevance resulting from the proximity of Chanteloup-les-Vignes, which will extend the potential beneficiary area beyond the administrative limit. A realistic pathway will be to develop the site as a phytoextraction-focused remediation testbed (supported by existing datasets and the planned living-lab set-up), and to translate depollution objectives into scenarios that will also strengthen locally relevant ESS.

5.1.2 CS2 Kozani (GR) - site characteristics

The CS2 site is located in a peri-urban lignite mining area near Prosilio, within the wider Kozani area in Western Macedonia (Figure 16). For the ESS assessment, the analysis will be framed using the administrative boundary of the Servia Municipal Unit (or a smaller unit where needed), as this provides the most practical scale for land-use governance and for compiling comparable local datasets.

Funded by
the European Union

Figure 16 Location of CS2 within the indicative extent of the brownfield site (The red rectangle indicates the area of the experimental site; the violet line indicates the area of the brownfield).

CS2 - site profile

The site is a contaminated brownfield with no current use, linked to lignite mining activities and managed by METE. A major environmental constraint is elevated nickel: available data indicate Ni concentrations at around 20 times above typical background levels, which strongly directs the site toward remediation-oriented land uses rather than soil-based provisioning functions. A 1 ha experimental plot will be available for EDAPHOS trials, and the site has already hosted phytostabilisation crop trials (e.g., sorghum, miscanthus, and switchgrass). Agroforestry trials are also planned using Ni-hyperaccumulating species, positioning the CS as a practical test ground for soil depollution pathways and for identifying plant (and potentially microbial) species relevant to Ni remediation. Historically, the surrounding area was used as pasture before mining; the current dominant land-use type is mining, and the expected future trajectory is land reclamation.

CS2 — baseline mapping for ESS assessment

The ESS assessment will cover the contaminated, currently unused brownfield area for which redevelopment scenarios will be developed. Because high-resolution land-cover data are not

Funded by the European Union

available (including Urban Atlas coverage), the analysis will be extended to a larger surrounding area to allow ecosystem service potential to be estimated across different ecosystem types (Figure 17).

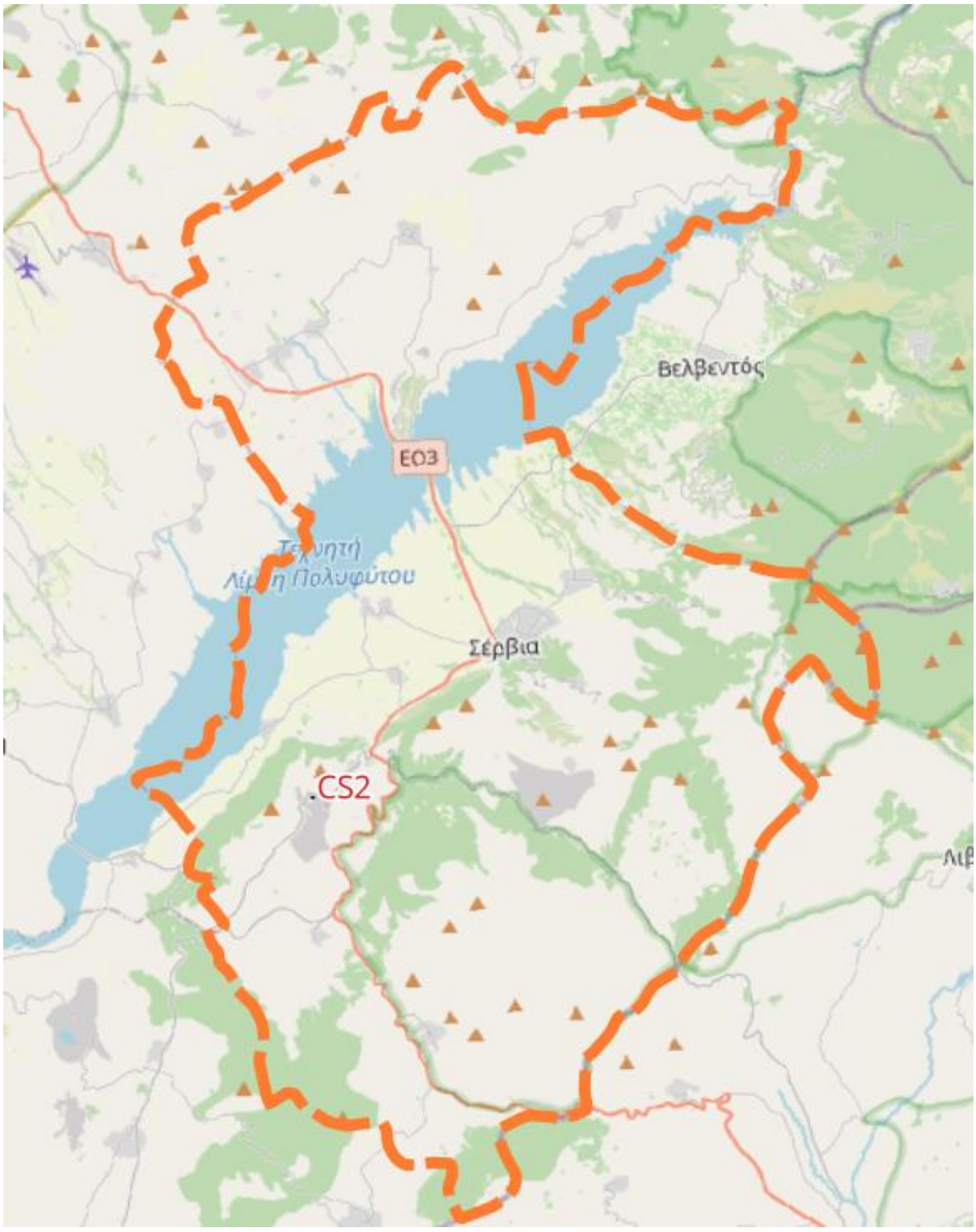

Figure 17 CS2 within the administrative boundaries of Servia Municipal Unit (The orange line indicates the administrative border of the Servia Municipal Unit.

Funded by
the European Union

The wider setting shows a moderate topographic constraint (average slope ~12% across the analysed area and ~8% at the point location), confirmed presence of technical infrastructure, and nearby settlements (nearest village ~1 km; the nearest small town—Servia—~7 km). Large-scale renewable energy infrastructure is also present in the broader Kozani area, including photovoltaic farms and a major PV power plant. For example, the Kozani solar park covers about 450 ha and is reported to generate around 320 million kWh per year [https://www.juwi.com/references/project-stories/article/pv-power-plant-kozani?utm_source=chatgpt.com].

Boundary used for ESS analysis: Servia Municipal Unit (or a smaller local administrative unit where applied).

Local socio-economic and industrial context relevant to ESS

The wider Kozani area in Western Macedonia is defined by a long history of lignite extraction, which has strongly shaped land use, infrastructure, and environmental pressures. The region is now moving toward a post-mining transition in which land reclamation and alternative development pathways are becoming the dominant planning direction. Within this context, the University of Western Macedonia is a relevant local knowledge and demand driver, supporting environmental education and applied research linkages. In the analysed area, industries with high electricity demand and toxic-waste-generating industries are reported as not present, and a biomass power plant is not reported within the local setting. In the future, two key drivers should shape ESS interpretation for CS2: (i) the strong nickel contamination signal (around 20× above typical levels) and (ii) the current mining-related land-use status combined with a clear reclamation trajectory. Together, these conditions will prioritise ESS pathways focused on risk reduction, soil stabilisation, and recovery of ecological functions rather than provisioning services.

5.1.3 CS3 Odiel Basin Area (ESSP) - site characteristics

CS3 is located in the Andalusia mining basin (Huelva province), within the Iberian Pyrite Belt (Figure 18). This is an area shaped by long-term sulphide mining and related environmental pressures. For the ESS assessment, the analysis will use the administrative boundaries of Minas de Riotinto and Nerva, because the brownfield extent and the expected benefits of remediation are relevant across this border-proximate setting.

Funded by the European Union

Figure 18 Location of CS3 within the indicative extent of the brownfield site (The red rectangle indicates the area of the experimental site; the violet line indicates the area of the brownfield; the orange line indicates the administrative border).

CS3 – site profile

The site is part of a very large sulphide mining district (>12,000 ha) with extensive abandoned mine areas and severe metallic pollution linked to acid mine drainage. The main contaminants are reported as As, Pb, and Cu, with additional contributions from Zn and Cd. For EDAPHOS field trials, the currently available experimental area is about 500 m², and the total area that can be allocated for experimentation is no more than ~1 ha. The land is not public. The area is currently managed by the mining company. Remediation-oriented land use is already represented by phytoremediation testing, including the use of poplars for phytoextraction of mobile metals (e.g., Zn and Cd). Based on local spatial indicators, the terrain is gently sloping (average ~2.5%). Photovoltaic farms and power plants/CHP are not present. Technical infrastructure (roads/railways and utility networks such as water, electricity, and communications) is not located within the experimental plot itself. The nearest village is ~0.8–1.0 km away, and economic/industrial zones are present nearby. Green features include surrounding forested areas (closest ~800 m). Blue features include the Río Tinto (~530 m) and reservoirs/dams: Marismilla Dam (~600 m), Zumajo reservoirs (~2.93 km), and Embalse del Sur (~1.26 km). Waste disposal sites are reported in Nerva (~1.44 km), including municipal and industrial facilities.

CS3 – baseline mapping for ESS assessment

Funded by
the European Union

The ESS analysis area was followed for the administrative boundaries of Minas de Riotinto and Nerva, covering the contaminated brownfield and its immediate zone of influence (Figure 19). CS3 lies within a wider brownfield landscape, and because high-resolution land-cover data are not available in this site context, a larger surrounding area will be included to represent multiple ecosystem types consistently in ESS calculations. This framing also reflects likely cross-boundary effects, where remediation outcomes (such as improved availability of safe green space) may extend to nearby settlements within the shared mining basin.
Boundary used for ESS analysis: Minas de Riotinto municipality and Nerva municipality.

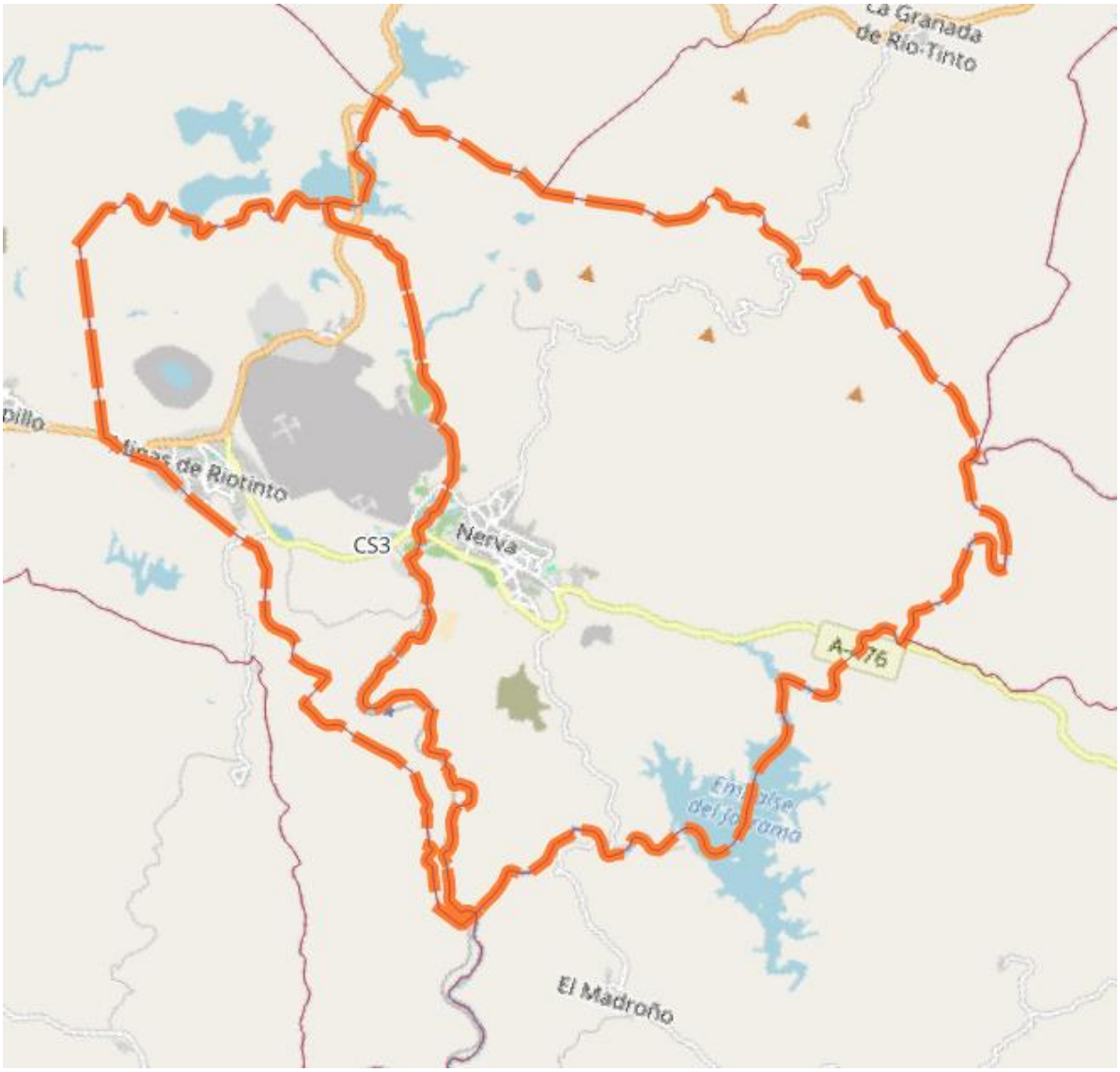

Figure 19 CS3 (red circle) within the administrative boundaries of Minas de Riotino town (location of the brownfield site); orange line indicates the administrative borders of the Minas de Riotinta town and Nerva municipality (potential area for consideration).

Local socio-economic and industrial context relevant to ESS

Minas de Riotinto and Nerva are part of the “Cuenca Minera” area of Huelva, where settlements and livelihoods have long been linked to metallic mining and its legacy. Mining heritage and visitor-oriented activities are also increasingly important in the local context. The population of Minas de

Riotinto is about 3,703, which indicates a small municipality where environmental quality and land reuse decisions can deliver clear community-scale benefits. At the broader regional level, Andalusia is a major European mining region (especially for metallic mining), which reinforces the importance of remediation, risk management, and socially accepted redevelopment pathways in mining-affected municipalities. In the future, two key drivers should shape ESS interpretation: (i) strong mining-related contamination and acid mine drainage pressures, which limit provisioning uses and increase the relevance of regulating services (especially exposure reduction, soil stabilisation, and recovery of soil functions), and (ii) the close connection to green and blue features (forests and nearby river/reservoirs), which influences both recreation potential and risk pathways. A realistic opportunity is to link remediation with multifunctional reuse (e.g., ecological restoration combined with education/heritage-oriented functions), consistent with a closure-and-restoration direction and the presence of a local environmental education actor. The Atalaya Mining Company also offers guided tours inside the mine, providing recreational and cultural ecosystem services.

5.1.4 CS4 Upper Silesia Coal Basin (PL) - site characteristics

CS4 is localised in Miasteczko Śląskie in the Silesian Voivodeship (Poland) (Figure 20), within the wider Upper Silesian Coal Basin (Upper Silesian industrial region). For the ESS analysis, the municipal administrative boundary was used as the assessment unit to ensure relevance for local planning and to enable a consistent, municipality-scale interpretation of ESS patterns and beneficiaries.

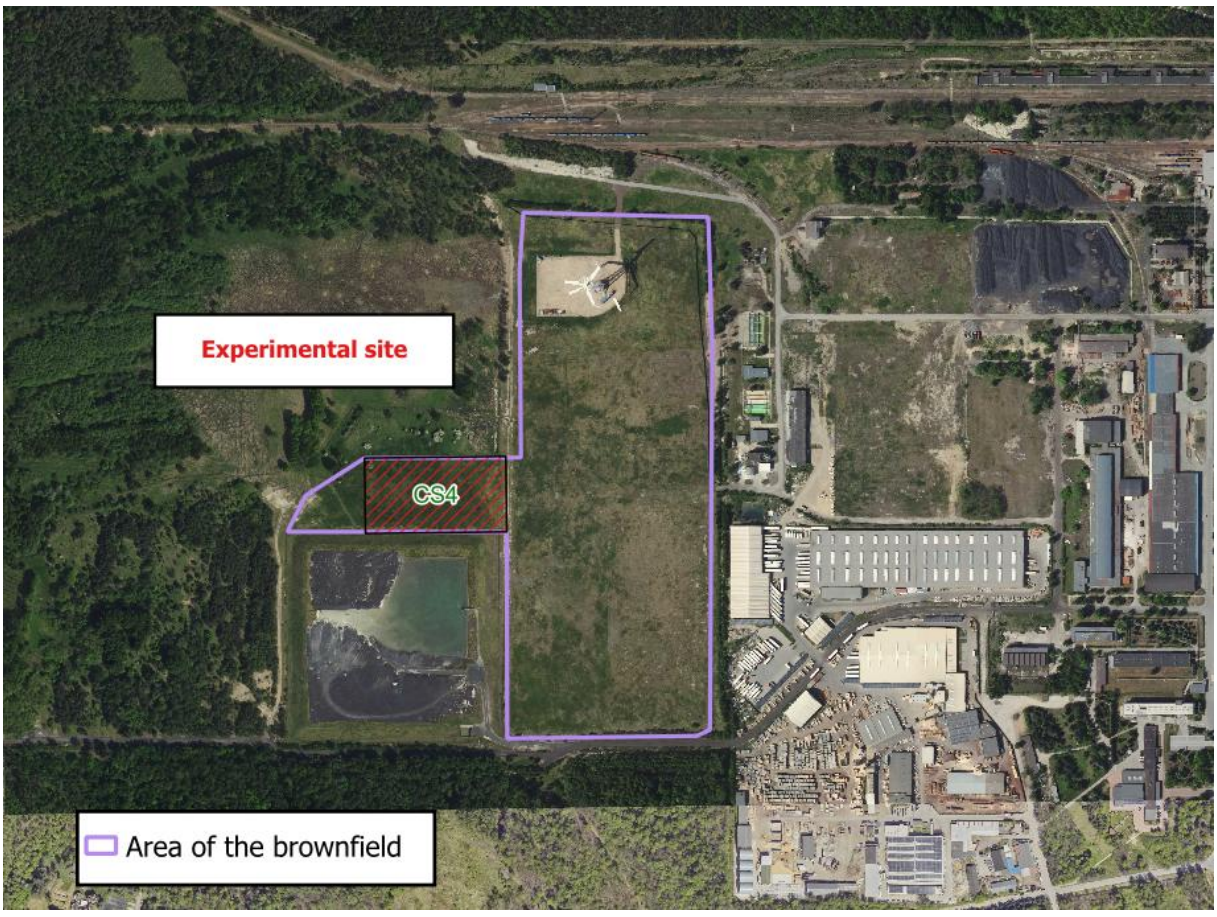

Funded by
the European Union

Figure 20 Location of CS4 within the indicative extent of the brownfield site (The red rectangle indicates the area of the experimental site; the violet line indicates the area of the brownfield).

CS4 – site profile

CS4 represents an industrial contaminated site resulting from past industrial activity. It is located in the immediate vicinity of a hazardous-waste landfill associated with the Zinc Smelter "Miasteczko Śląskie" and is characterised by significant HM contamination (e.g. Zn, Pb, Cd and Tl). Reported waste composition indicates elevated metal contents (Zn 2-5%, Pb 5-20%, Cd 5-15%, and Tl). The landfill is isolated, and leachate water are collected and treated in a treatment plant, which defines an important part of the site's current risk-management setup. **Boundary used for ESS analysis:** Miasteczko Śląskie municipal administrative boundary (Figure 21).

CS4 – baseline mapping for ESS assessment

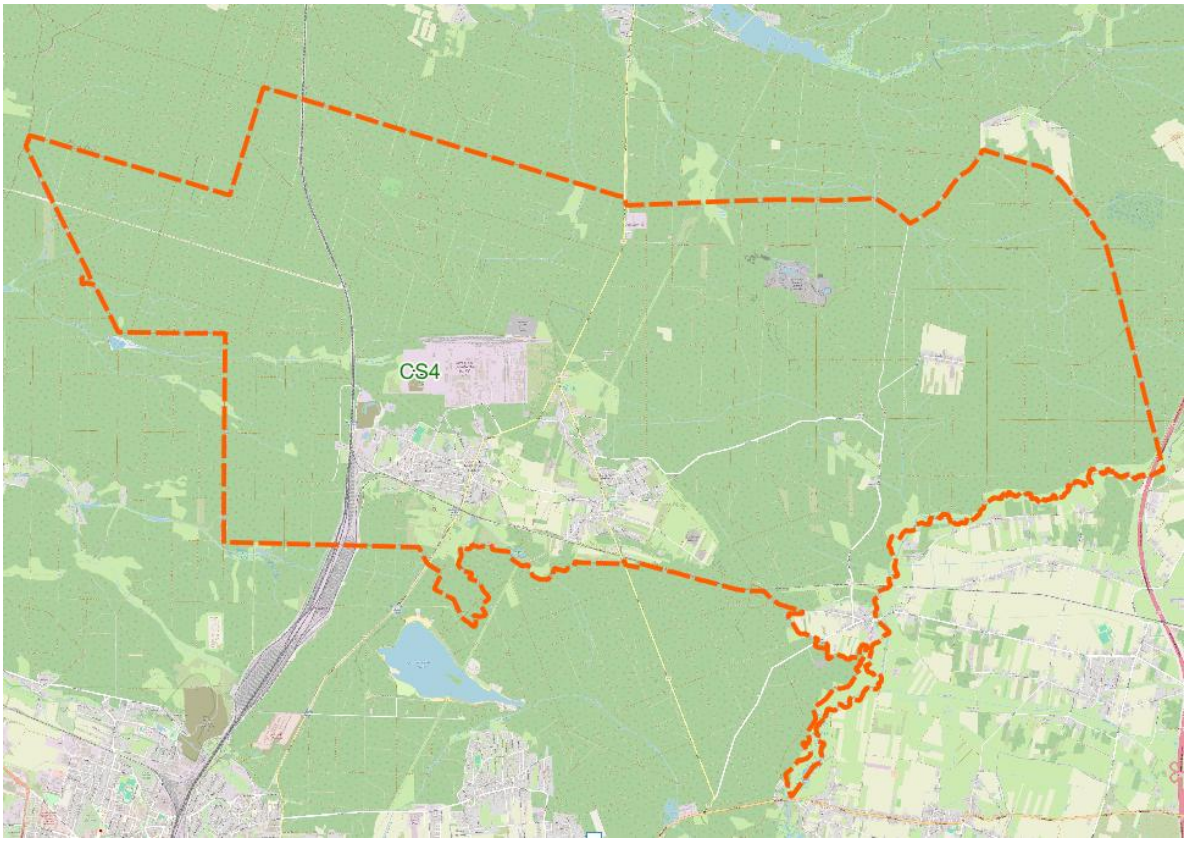

Figure 21 CS4 (marked on the map) within the administrative boundaries of Miasteczko Śląskie town (The orange line).

Local socio-economic and industrial context relevant to ESS

Miasteczko Śląskie is a small town with a strong industrial identity shaped by mining and metallurgy related development pathways. This context matters for ESS assessment because land-use options typically need to balance redevelopment and environmental safety with the functioning of the local economy and the surrounding forest landscape. Available socio-economic descriptors indicate a local labour-market profile broadly comparable to the region, with unemployment in 2023 reported at 4.4%, compared to 3.6% at the regional level. The wider municipal context includes production buildings and facilities, and the presence of renewable energy installations is

Funded by the European Union

reported, pointing to an ongoing diversification of land-use functions. In this context, ESS results can help to show what type of potential benefits can be delivered by remediation and site regeneration, especially where industrial contamination co-exists with extensive forest cover and little nearby housing.

5.1.5 CS5 Castelvetro (IT) - site characteristics

CS5 is located in the municipality of Castelvetro di Modena (Solignano 2, ex Frattina), in the Modena area of Emilia-Romagna, about 50 km from Bologna (Figure 22). The ESS analysis will use the administrative boundaries of Castelvetro di Modena and the neighbouring municipality of Maranello, because the brownfield is close to the municipal border and remediation benefits may extend across it.

Figure 22 Location of CS5 within the indicative extent of the brownfield site (The red rectangle indicates the area of the experimental site; the violet line indicates the area of the brownfield; the orange line indicates the administrative border).

Funded by
the European Union

CS5 – site profile:

The CS5 site is an urban brownfield with no current use, affected mainly by Pb, Zn and contamination linked to the local ceramic industry. The terrain is flat and considered suitable for the implementation of agroforestry and co-cropping systems involving tree species, perennial herbaceous species, and annual herbaceous species. The basic soil physical conditions (e.g., pH and texture), support remediation-oriented redevelopment pathways without increasing the risk of leaching the labile fraction of trace elements into nearby groundwater and surface water. Key spatial indicators show a low terrain slope (~1.93%), presence of technical infrastructure, and no photovoltaic farms. The site is close to sensitive receptors and pressure sources: the first residential area is ~200 m away and the first ceramic industry is also ~200 m away from the CS. Surface water is very close (the Torrente Tiepido ~50 m), while a municipal waste facility is reported at ~1.8 km (Isola ecologica di Maranello). Environmental requirement values relevant for ESS interpretation include soil thresholds Pb < 100 mg/kg and Zn < 150 mg/kg, surface water thresholds Pb 10 µg/L and Zn 3 mg/L, groundwater thresholds Pb 10–15 µg/L and Zn 1–3 mg/L, and an air Pb threshold of 0.5 µg/m³.

CS5 – baseline mapping for ESS assessment

The ESS study area will cover the entire contaminated, art of the brownfield (the area used to build redevelopment scenarios), which, outside the experimental site, is subject to dig-and-dump practices involving contaminated soil. The site will be mapped within the administrative border of Castelvetro di Modena, while the assessment will also consider Maranello because the site is border-proximate and remediation outcomes (e.g., improved availability of safe green areas) may be relevant on both sides of the boundary (Figure 23). High-resolution land cover information is available through Urban Atlas, supporting baseline mapping across land-cover types.
Boundary used for ESS analysis: Castelvetro di Modena municipality + Maranello municipality.

Funded by the European Union

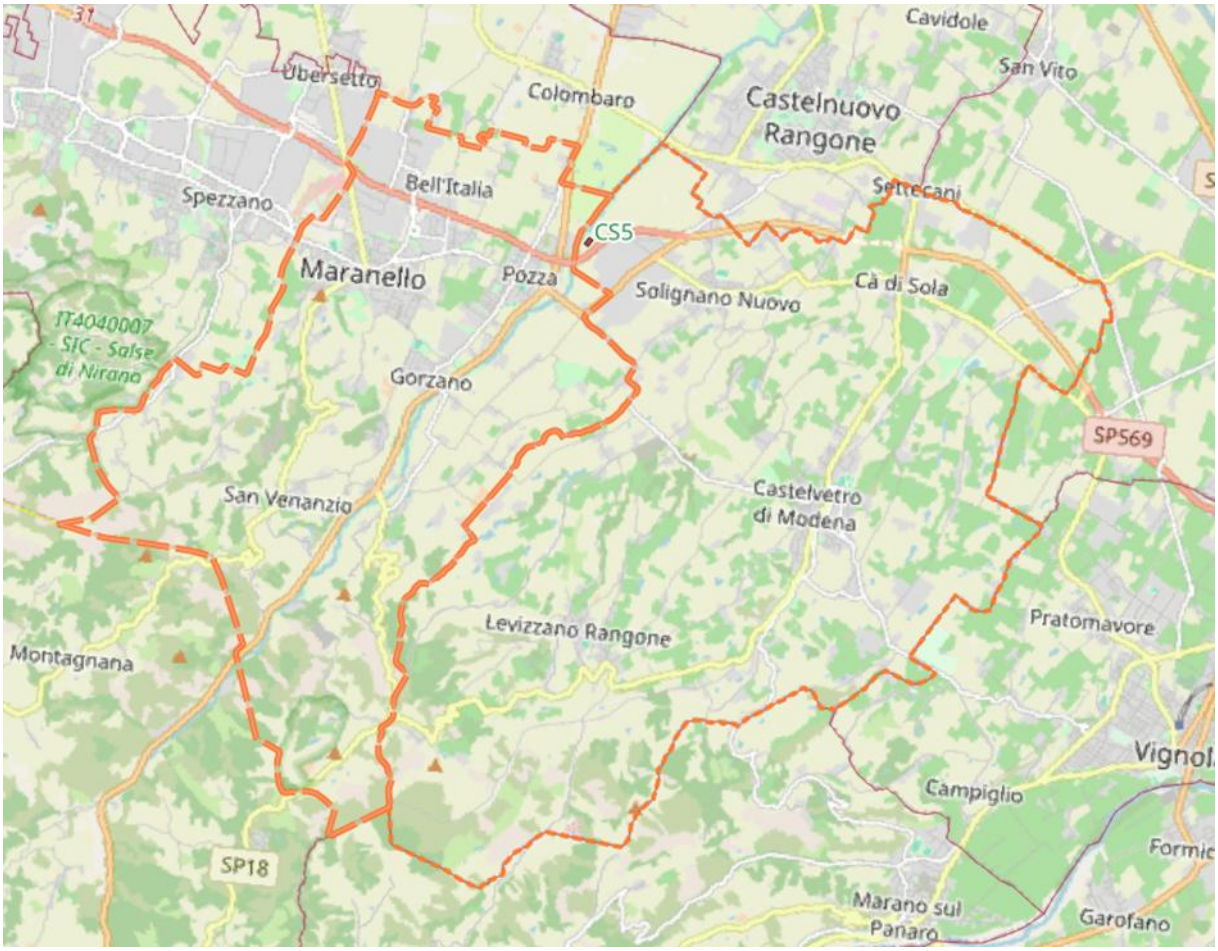

Figure 23 CS5 (red circle) within the administrative boundaries of Maranello and Castelvetro di Modena city (The red line indicates the administrative border of Castelvetro di Modena (location of the brownfield site; orange line indicates the administrative border of the Maranello city (potential area for consideration).

Local socio-economic and industrial context relevant to ESS

Castelvetro di Modena is a small municipality in the Province of Modena, within an area strongly influenced by the regional ceramic production cluster (including nearby municipalities such as Maranello within the wider district). This matters for ESS because ceramic-related industrial land use can shape local environmental pressures (e.g., soil quality constraints, transport and industrial footprint) and can increase demand for regulating services such as risk reduction, buffering of emissions, and safe, accessible green space. From a future land-use perspective, two factors will be key: (i) the confirmed Pb–Zn–Se contamination, and (ii) the site's very short distance to residential and industrial receptors (about 200 m). Together, these conditions will shift scenario priorities toward remediation-driven regulating services, especially exposure reduction, soil stabilisation, and recovery of soil functions, rather than soil-based provisioning uses. The site should be redeveloped in a way that supports phytoremediation and delivers clear local co-benefits. These benefits will also be able to extend into nearby Maranello, provided that exposure routes are controlled, and safe access and use are ensured in the scenario design

Funded by
the European Union

5.1.6 CS6 Vieux-Charmont (FR) - site characteristics

CS6 is located in the eastern French city of Vieux-Charmont (47°31'15.8"N, 6°50'23.8"E), the study site is a 2-ha industrial wasteland (Figure 24). The river "La Savoureuse," two active factories, a pond built in 1957, and residential areas encircle this wasteland. Since 1871, a variety of operations have been carried out in the facilities, including the production of precision parts, automobiles, heat-treated piston pins, and watches. Waste from homes and businesses, both buried and surfaced, was dumped carelessly at the location. Following a soil investigation that found pollution by organic (PAH, PCB) and inorganic (Zn, Pb, Cd, As, Cu, Ni, Cr, Hg) compounds, the wasteland was declared off-limits to the public in 2007 [Louzon et al., 2022]. The ESS analysis is framed at the commune level, which is the most relevant local unit for spatial planning, remediation decisions, and municipal-scale datasets.

Figure 24 Location of CS6 within the indicative extent of the brownfield site (The red polygon indicates the area of the experimental site; the violet line indicates the area of the brownfield) *[Source: GIG-PIB, 2026].*

CS6 – site profile

The site is a brownfield with a documented industrial legacy. The CS6 covers ~2 ha and is representative of a broader context of industrial wastelands in Bourgogne-Franche-Comté (estimated ~150 ha). The area is described as contaminated and currently unused, which makes it suitable for scenario-based redevelopment and restoration planning under EDAPHOS. Within the analysing area a living lab has been established to support co-development of site solutions with industrial partners, local residents, and public administration (operational since March 2023). This matters because it provides an existing governance setting for testing and evaluating remediation and land-use options with stakeholder involvement. The site is highly contaminated

with heavy metals (e.g. As, Cd, Pb, Zn) and PAHs, with reported pollution hot spots. This contamination profile can constrain soil-based provisioning uses, while increasing the relevance of remediation-linked regulating functions (e.g., exposure reduction, soil stabilisation, and recovery of soil functions).

CS6 – baseline mapping for ESS assessment

The ESS framing includes the administrative unit of Vieux-Charmont, with potential cross-boundary relevance for Sochaux due to proximity to the commune border (Figure 25). The mapped experimental site lies within a wider brownfield extent, and positive effects of remediation (*e.g.,* improved availability of green areas) may plausibly extend into neighbouring areas. High-resolution land-cover information for Vieux-Charmont is available via Urban Atlas, supporting spatial estimation of ESS potential across land-cover types. (Source:EEA, 2026).
Boundary used for ESS analysis: Vieux-Charmont commune (with cross-boundary effects potentially involving Sochaux).

Figure 25 CS6 (red circle) within the administrative boundaries of Vieux-Charmont commune (location of the brownfield site; orange line indicates the administrative borders of the Vieux-Charmont and Sochoux communes.

Local socio-economic and industrial context relevant to ESS

Vieux-Charmont is a small, dense commune (population 2,829 in 2022; area ~2.5 km²; density ~1,127 people/km²). Local employment at the place of work is reported as 536 jobs (2022), with an unemployment rate (15–64, census definition) of 12.4%, and 60 establishments recorded at end-2023 (industry share 10% of establishments). (Source: INSEE, 2025). The wider Pays de

Funded by
the European Union

Montbéliard area has a strong automotive-industrial identity, with approximately ~80 automotive-related firms and ~15,000 direct jobs reported in the sector. This regional industrial profile is relevant because it can shape local environmental pressures and the demand for regulating services (air quality buffering, safe green space, and risk mitigation near legacy industrial sites) (Source: Pays de Montbéliard Agglomération, 2023; INSEE, 2019). In the future analysis the ESS interpretation should be focused on: (i) the confirmed HM + PAH contamination and hotspot pattern, and (ii) the unused brownfield status, which together emphasise remediation-linked ecosystem functions (stabilisation, exposure reduction, soil function recovery) as key pathways of change. Given the border-proximate location, potential beneficiaries of improvements (e.g., increased availability of safe green areas) may extend into neighbouring communes, which is important when assessing ESS distribution at the local scale

5.1.7 CS7 Lavrio (GR) - site characteristics

CS7 is located in the Lavrio area within the Lavreatiki/Lavreotiki administrative unit in East Attica (Greece) (Figure 26). The ESS analysis is framed using the municipal administrative boundary to ensure local policy relevance and consistent municipal-scale interpretation of ecosystem service patterns and beneficiaries.

Figure 26 Location of CS7 within the indicative extent of the brownfield site (The red rectangle indicates the area of the experimental site; the violet line indicates the area of the brownfield).

Funded by the European Union

CS7 – site profile

The CS7 is described as a lignite mining area situated in a dense agricultural area, shaped by a long mining and metallurgical legacy (Figure 26). CS7 is a long-term multi-metal contaminated site, linked to ancient (c. 3000–200 BC) and more recent (1864–1982 AD) mining and metallurgical activities. Site profile thin a densely agricultural setting and functions as a contaminated brownfield with no current use. Long-term multi-metal contamination is reported, with hotspots of Pb and Zn linked to ancient and more recent mining and metallurgical activity. The area has supported phytostabilisation crop trials, indicating a remediation-oriented use pathway and the potential to identify plant and microbial species relevant to soil depollution. A detailed analysis of the CS and its immediate surroundings indicates that no photovoltaic farms or power plants/CHP facilities were identified in the area. By contrast, technical infrastructure is present, including road/rail connections and utility networks (water supply, electricity, gas, and communications). The nearest built-up area is located approximately 2 km from the site, and economic/industrial zones are recorded in the surroundings. Green-area features include a natura site at about 10 km, a park at about 2 km, and a swimming reservoir at about 15 km. No rivers or streams were reported nearby; however, the Aegean Sea is indicated as the closest surface water body. A municipal waste disposal site is reported at approximately 20 km from CS7 location, whereas no industrial waste sites were identified.

CS7 — baseline mapping for ESS assessment

The administrative unit used for baseline mapping is the Lavreatiki/Lavreotiki municipal boundary, with CS7 mapped within the municipality (Figure 27). Due to the lack of high-resolution land cover data, the analysed area is expanded beyond the immediate brownfield extent to allow estimation of ESS potential across different ecosystem types in and around the site.
Boundary used for ESS analysis: Lavreatiki/Lavreotiki municipal administrative boundary.

Funded by
the European Union

Figure 27 CS7 (red circle) within the administrative boundaries of Lavreatiki Municipality (location of the brownfield site; orange line indicates the administrative borders of the municipality.

Local socio-economic and industrial context relevant to ESS

The CS7 is embedded in a landscape with a strong post-mining identity, reflected in its recognition as a UNESCO Global Geoparks-related geopark designation (2023), which highlights the geoheritage value and cultural landscape functions of the broader area. This context is relevant for ESS assessment because local land-use options typically need to balance redevelopment ambitions with environmental risk management, while maintaining heritage-related place functions (UNESCO, 2023). A documented component of the local economic footprint is port activity. Lavrio Port Authority S.A. is responsible for the administration and operation of the Lavrio Port Zone,

supporting coastal transport connectivity and associated service functions (Lavrio Port Authority SA, 2020; IAPH, 2026). Performed site characteristic data analyses indicate the presence of industrial activities with significant electricity demand, suggesting an energy-intensive local profile, whereas toxic-waste-generating industries requiring storage are reported as absent. In addition, the area hosts substantial touristic infrastructure, which can further increase electricity and water demand, particularly during the summer season. The wider area also hosts higher-education institutions linked to environment- and agriculture-relevant competencies, including the Agricultural University of Athens and the National Technical University of Athens.

5.2 Land-use scenarios

Within the ESS assessment performed under WP2, Task 2.2, ESS provision was estimated for each CS under three alternative future land-use scenarios. The scenario approach was adopted to capture different, realistic redevelopment pathways and to enable a structured comparison of their implications for ecosystem functions and benefits. Following internal consultations, in order to ensure consistency and comparability of results across all sites, a decision was taken to harmonise the scenario set and apply the same three scenario directions to every CS. The selected redevelopment pathways are illustrated in Figure 28 and described in the section below.

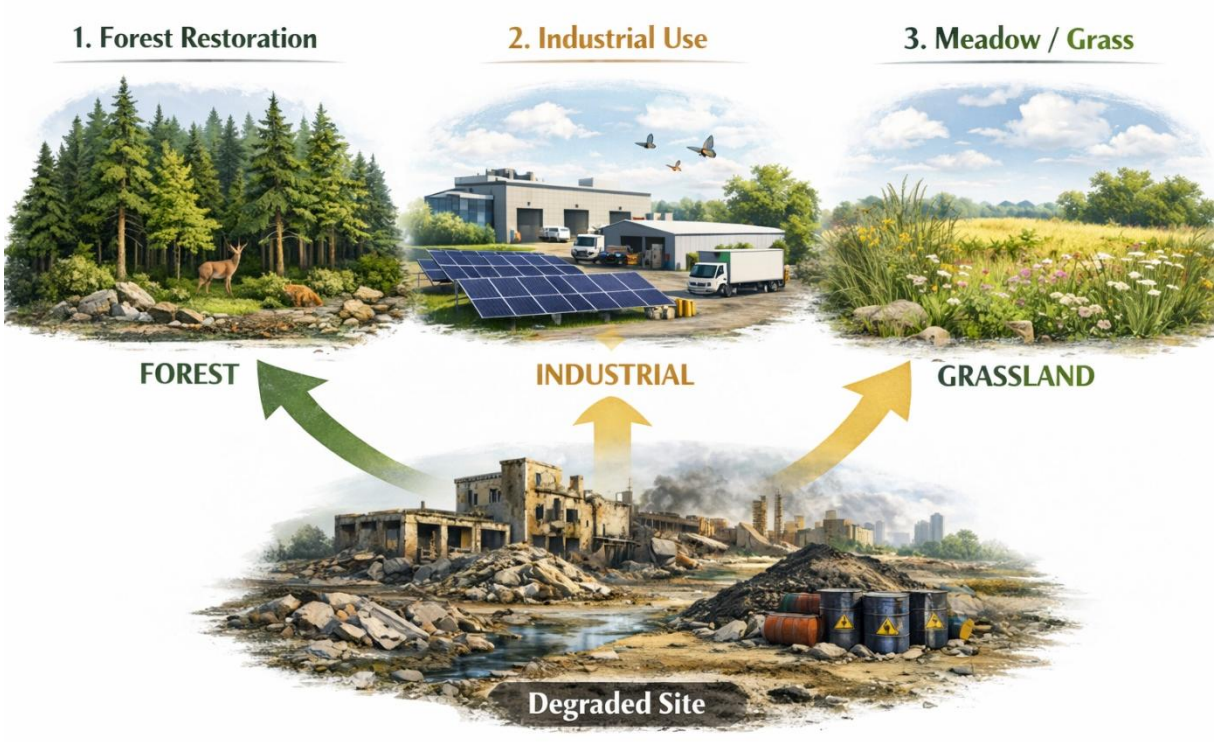

Figure 28 Potential future land-use scenarios for degraded land (CS).

Funded by
the European Union

The selection of the forest restoration scenario is directly aligned with the overarching objectives of the EDAPHOS project, which promotes NBS as effective remediation pathways enabling the recovery of degraded ecosystems and the restoration of soil functions. Within this framework, afforestation represents a well-established NBS approach that supports ecological regeneration while addressing contamination legacies through the gradual stabilisation and improvement of soil conditions. Furthermore, forest restoration strongly supports EU climate and biodiversity policies, including the European Green Deal and the EU Biodiversity Strategy for 2030, which recognise afforestation and reforestation as key NBS contributing to carbon sequestration, biodiversity enhancement, and increased ecosystem resilience. As highlighted in recent analyses of EU climate policy integration of NBS (e.g. https://www.climatescorecard.org), forests play a critical role as long-term carbon sinks while simultaneously delivering multiple co-benefits such as habitat creation, improved water regulation, and enhanced landscape connectivity. The ESS assessment for this scenario supports forest restoration as a realistic and sustainable remediation option within EDAPHOS and the policy context. It is assumed that, within the ESS assessment, afforestation will be shown to help transform a contaminated, degraded site into a high-value natural area. Under this pathway, the restored forest may deliver multiple ESS, including climate regulation, soil stabilisation, biodiversity support, and cultural and recreational benefits. The forest restoration scenario represents a scientifically grounded and policy-consistent pathway that supports both environmental recovery and long-term landscape resilience. This confirms its suitability as a preferred direction for the remediation and ecological rehabilitation of contaminated sites. The application of NBS using hybrid poplar varieties tested in the project can be used both for afforestation and for creating short-term plantations (short rotation coppice). In the first case, the scenario will aim to create a broad-leaved forest ecosystem, while in the second case, the crop structure will be classified as transitional woodland/shrub according to the land cover classification (CLC).

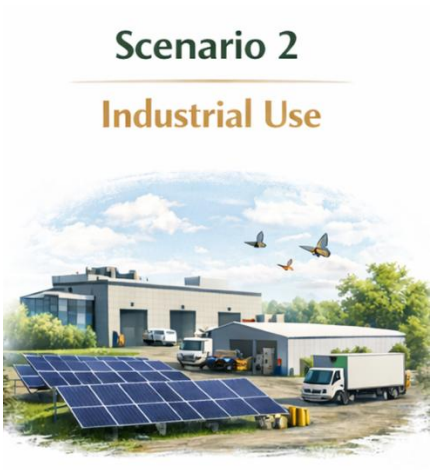

The industrial reuse scenario (e.g., a photovoltaic (PV) plant for energy generation, and optionally industrial or warehouse use) is included because it is often the most realistic option for heavily contaminated post-industrial land. On some sites, contamination levels and related risks may remain too high to meet threshold values required for more sensitive land uses. In such cases, land-use restrictions may limit the site to industrial functions even after mitigation measures. This scenario is also consistent with European Union policy directions. EU strategies promote the principle of “brownfield before greenfield” and aim to reduce pressure on undeveloped land. Reusing already degraded sites for new functions, including renewable energy, supports these

Funded by the European Union

goals and helps avoid additional land take. Finally, the scenario is used to show that a site can still deliver benefits to society even when the end-use remains industrial. In the PV option, the key benefit is the provision of clean energy. This can contribute to climate mitigation and energy transition targets. It also aligns with broader United Nations objectives linked to climate action, resilient infrastructure, and responsible land use.

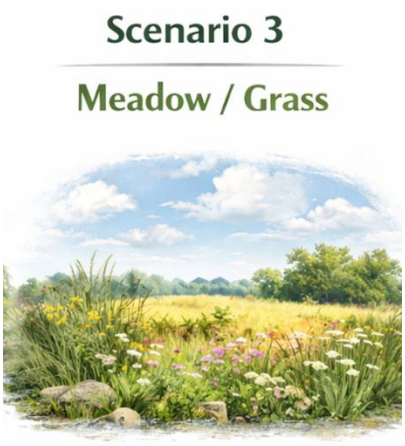

The grassland (e.g. grassland and meadow) scenario is selected as a natural (nature-based) pathway for degraded and post-industrial land, because it rebuilds ecological functions primarily through biological processes rather than intensive engineering. It supports the gradual recovery of soil structure and functioning (microbial activity, organic matter formation, infiltration and water cycling), while reducing erosion and dust mobilisation, improving local microclimate, and creating habitats that attract and reconnect local flora and fauna. This direction is strongly aligned with European Union guidance for soil renewal and brownfield regeneration, where priority is placed on restoring soil health and ecosystem functions, enhancing biodiversity, and promoting land recycling (reusing degraded sites instead of expanding onto greenfields). In this framing, natural succession and meadow establishment are treated as practical tools to restore the ecological value and spatial structure of post-industrial areas and to support long-term resilience.

5.3 Baseline mapping procedure

The first step of Task 2.2 was to determine the spatial scale and geographical coverage of areas where the planned activities could cause impacts on economic, environmental, and social aspects. ESS mapping studies were set on the administrative units that included all identified negative environmental impacts of the contaminated sites under consideration. In the next step, CORINE land cover classes were used to delineate different ecosystem types of land cover in the study areas. The CORINE Land Cover (CLC) project has been the responsibility of the European Environment Agency since 1995, with the fundamental objective of obtaining a European database of land use at a scale of 1:100,000, useful for territorial analysis and policy management. The CORINE Land Cover classes (Bossard et al., 2000) were used to delineate, categorize and map the different ecosystem types of land cover in the study areas (Figure 29). ESS Corine Land Cover map has too low spatial resolution for evaluation cultural ESS. Accounting indicators that quantity potential for *in-situ* and outdoor interactions with living systems, high spatial resolution data provide more useful information. **This applies in particular to small administrative units located in areas with a significant proportion of urbanized areas (CS 1, CS6). In this case, more detailed data was used: Urban Atlas and OpenStreetMap Landcover. The types of OSM land cover were assigned to CLC categories.** Correspondence between CLC Classes and ecosystem types is presented in Figure 30.

Funded by
the European Union

CLC Level 1	CLC Level 2	CLC Level 3	Ecosystem types level 2
1. Artificial surfaces	1.1. Urban fabric	1.1.1. Continuous urban fabric	Urban
		1.1.2. Discontinuous urban fabric	
	1.2. Industrial, commercial and transport units	1.2.1. Industrial or commercial units	
		1.2.2. Road and rail networks and associated land	
		1.2.3. Port areas	
		1.2.4. Airports	
	1.3. Mine, dump and construction sites	1.3.1. Mineral extraction sites	
		1.3.2. Dump sites	
		1.3.3. Construction sites	
	1.4. Artificial non-agricultural vegetated areas	1.4.1. Green urban areas	
		1.4.2. Sport and leisure facilities	
2. Agricultural areas	2.1.Arable land	2.1.1. Non-irrigated arable land	Cropland
		2.1.2. Permanently irrigated land	
		2.1.3. Rice fields	
	2.2. Permanent crops	2.2.1. Vineyards	
		2.2.2. Fruit trees and berry plantations	
		2.2.3. Olive groves	
	2.3. Pastures	2.3.1. Pastures	Grassland
	2.4. Heterogeneous agricultural areas	2.4.1. Annual crops associated with permanent crops	Cropland
		2.4.2. Complex cultivation patterns	
		2.4.3. Land principally occupied by agriculture, with significant areas of natural vegetation	
		2.4.4. Agro-forestry areas	
3. Forests and semi-natural areas	3.1. Forests	3.1.1. Broad-leaved forest	Woodland and forest
		3.1.2. Coniferous forest	
		3.1.3. Mixed forest	
	3.2. Shrub and/or herbaceous vegetation association	3.2.1. Natural grassland	Grassland
		3.2.2. Moors and heathland	Heathland and shrub
		3.2.3. Sclerophyllous vegetation	
		3.2.4. Transitional woodland shrub	Woodland and forest
	3.3. Open spaces with little or no vegetation	3.3.1. Beaches, dunes, and sand plains	Sparsely vegetated land
		3.3.2. Bare rock	
		3.3.3. Sparsely vegetated areas	
		3.3.4. Burnt areas	
		3.3.5. Glaciers and perpetual snow	
4. Wetlands	4.1. Inland wetlands	4.1.1. Inland marshes	Wetlands
		4.1.2. Peatbogs	
	4.2. Coastal wetlands	4.2.1. Salt marshes	Marine inlets and transitional waters
		4.2.2. Salines	
		4.2.3. Intertidal flats	
5. Water bodies	5.1 Inland waters	5.1.1 Water courses	Rivers and lakes
		5.1.2 Water bodies	
	5.2 Marine waters	5.2.1 Coastal lagoons	Marine inlets and transitional waters
		5.2.2 Estuaries	
		5.2.3 Sea and ocean	Marine

Figure 29 Correspondence between CLC Classes and ecosystem types.

Funded by the European Union

Corine Land Cover Class / Scenario	CS1 (FR)	CS2 (GR)	CS3 (ES)	CS4 (PL)	CS5 (IT)	CS6 (FR)	CS7 (GR)
Continuous urban fabric							
Discontinuous urban fabric							
Industrial or commercial units							
Road and rail networks and associated land							
Port areas							
Airports							
Mineral extraction sites							
Dump sites							
Construction sites							
Green urban areas							
Sport and leisure facilities							
Non-irrigated arable land							
Permanently irrigated land							
Rice fields							
Vineyards							
Fruit trees and berry plantations							
Olive groves							
Pastures							
Annual crops associated with permanent crops							
Complex cultivation patterns							
Land principally occupied by agriculture, with significant areas of natural vegetation							
Agro-forestry areas							
Broad-leaved forest							
Coniferous forest							
Mixed forest							
Natural grasslands							
Moors and heathland							
Sclerophyllous vegetation							
Transitional woodland-shrub							
Beaches, dunes, sands							
Bare rocks							
Sparsely vegetated areas							
Burnt areas							
Glaciers and perpetual snow							
Inland marshes							
Peat bogs							
Salt marshes							
Salines							
Intertidal flats							
Water courses							
Water bodies							
Coastal lagoons							
Estuaries							
Sea and ocean							

	Ecosystem type (according to CLC) not occurring within the analysed area.
	Ecosystem type (according to CLC) occurring within the analysed area.

Figure 30 CORINE Land Cover classes used in the ESS assessment (Task 2.2) [Source: GIG-PIB].

To evaluate some ESS Corine Land Cover map is in too low spatial resolution.

Funded by
the European Union

6 Valuation of Ecosystem Services

6.1 Ecosystem services assessment for CS1

In this section, the valuation of ESS for CS1 (France) is presented in relation to the local context, considering the site profile, current land-use conditions, and the defined land-use scenarios. At the same time, data preparation and processing were harmonised across all analysed CS to ensure that the results are comparable and based on consistent calculation assumptions.

6.1.1 Biomass production (ESS1)

The assessment of ESS1 (*biomass production*) for CS1 is based on the energy potential indicator EP (GJ·ha^{-1}·year^{-1}). EP is derived from the annual increment of above-ground biomass AGBinc (t d.m.·ha^{-1}·year^{-1}) using the following relationship:

$$EP = AGBinc \times CV \ [GJ \cdot ha^{-1} \cdot year^{-1}]$$

Where:
- CV is the calorific value of the biomass (GJ·t^{-1} d.m.), adopted in line with the ESS1 service card,
- AGBin above-ground biomass AGBinc (t d.m.·ha^{-1}·year^{-1}),
- EP is energy potential.

During the data preparation stage, the available sources of AGBinc were reviewed, including inventory data, literature sources, and proxy indicators. In practice, the data available for France were found to be fragmented and methodologically inconsistent, mainly due to differences in the definitions of increment/production, the units used, and the typological coverage. As a result, the potential for direct comparisons across land-cover types and between CS1–CS7 was substantially limited (Table 12).

To ensure consistency and comparability, the ESS1 (biomass production) assessment for all CS, under each of the three analysed land-use scenarios, was based on a single common reference source (benchmark). Harmonised forest increment results were adopted from the publication "*Improved large-area forest increment information in Europe through harmonisation of National Forest Inventories*" (Forest Ecology and Management, 562, 121913). This source provides comparable increment data across countries and forest types, including the above-ground biomass increment (AGBinc), and therefore supports a consistent calculation basis across case studies.

Table 12 Annual biomass production on different types of land in France.

Land type	Min (t/ha/year)	Max (t/ha/year)	Unit	Biomass type/notes	References
Broadleaved forests	4.03	4.03	t/ha/year	Above-ground biomass increment (GAI7)	[Gschwantner, et. al, 2024].
Mixed forests	4.20	4.20	t/ha/year	Above-ground biomass increment (GAI7)	[Gschwantner, et,al., 2024]
Coniferous forests	4.75	4.75	t/ha/year	Above-ground biomass increment (GAI7)	[Gschwantner, et,al., 2024]
Poplar monoculture (poplar plantations)	4.20	5.40	m³/ha/year	Wood mass at 12% moisture (stem/wood proxy); wood density 350–450 kg/m³ (12% moisture)	[CIP, 2020]

Land type	Min (t/ha/year)	Max (t/ha/year)	Unit	Biomass type/notes	References
Grassland – permanent productive grasslands	5.00	5.00	t/ha/year	Annual dry matter production (DM)	[Les Etudes Report,2024]
Grassland – temporary grasslands	6.00	6.00	t/ha/year	Annual dry matter production (DM)	[Les Etudes Report,2024]
Grassland – permanent low-productive (estives)	1.50	1.50	t/ha/year	Annual dry matter production (DM)	[Les Etudes Report,2024]

Due to the lack of consistent regional data for grasslands, a typology-based approach was adopted and a representative value was applied for productive lowland meadows in the temperate zone (Table 13):

$$AGBinc = 5.00\ t\ d.m.\cdot ha^{-1}\cdot year^{-1}$$

(a working value reflecting a typical level of dry-matter production for this type of land use).

Table 13 Estimated annual above-ground biomass increment (AGBinc) for grasslands in NUTS2 regions – assumptions and literature-based justification.

NUTS2	Region	Type of grassland	Estimated AGB increase (t DM·ha⁻¹·yr⁻¹)	Rationale (climate / intensity)	Citations
FR10	Île-de-France	temperate lowland meadows	4–6	Temperate C3 grasslands: lower precipitation and higher summer temperatures reduce productivity, but it still remains at a few t/ha/yr	[Obermeier et al., 2018], [Andresen et al., 2018]

For scenarios with partial vegetation cover, coefficients consistent with the scenario assumptions were applied:

$$PV\_groundmounted = 0.8 \times grassland\ and\ Industrial/commercial\ units = 0.2 \times grassland$$

This approach-maintained comparability across scenarios while reflecting the reduced biologically active area. Table 14 presents the input data used to calculate ESS1 (biomass production) for CS1, including AGBinc, CV and the resulting EP values for each land-cover component considered in the scenarios.

Table 14 ESS1 – Calculation parameters for the biomass energy potential for CS1 (FR10).

CLC clasification	Couling Land Cover	AGBinc (tDM/ha/yr)	CV (GJ/tDM)	EP (GJ/ha/yr)
3.1.1	Broad-leaved forest	4.03	18.5	74.6
1.4.1	Green urban areas -grassland or lawns	5.00	17.5	87.5
1.2.1	Industrial - PV installation (80% grassland)	4.00	17.5	70.0
3.1.2	Coniferous forest	4.75	18.5	87,9
3.2.4	Transitional woodland/shrub (poplar plantations)	6.60	18.6	122.5
1.2.1	Industrial - buildings and halls (20% grassland)	1.00	17.5	17.5
2.1.1	Non-irrigated arable land - *Brassica juncae*	7.20	17.5	126.0
2.1.1	Non-irrigated arable land - *Lablab purpureus*	na	na	na

Funded by the European Union

Table 15 provides a scenario-level summary of ESS1 results for CS1 by compiling the EP outcomes across the defined land-use scenarios. The reported values enable comparison between scenarios under a consistent calculation framework and a harmonised set of biomass increment assumptions.

Table 15 A summary of ESS1 (Biomass production) results for the different CS1 land-use scenarios.

Land-use scenario	Scenario 1	Scenario 2	Scenario 3
Energy potential [GJ/ha/year]	122.5	70	87.5

The reported values enable comparison between scenarios under a consistent calculation framework and a harmonised set of biomasses increment assumptions.

6.1.2 Regulation of soil quality (ESS2)

In this section, the ESS2 indicator (regulation of soil quality) for CS1 was estimated as the potential for metal accumulation in plant biomass under the analysed land-use scenarios. As part of the literature review, concentration ranges of several metals in plant biomass were compiled e.g. Cd, Pb, Zn, Cu, and Ni (Table 16). However, for valuation purposes, one representative metal was selected: (Cd), which is frequently reported in environmental studies, it has no nutrient function (unlike Zn or Cu), and its accumulation in plant tissues provides a useful indicator of contamination pressure. In addition, Cd is often more mobile and more readily translocated to above-ground plant parts than Pb, which increases its suitability for scenario comparisons based on AGB.

Table 16 Heavy metal concentrations in the biomass of broadleaf species.

Metal	Species	Leaves [mg/kg]	Stem Wood [mg/kg]	Source
Cd	Betula pendula, Fagus sylvatica, Acer pseudoplatanus	0.2 – 0.6	0.05 – 0.15	[Jakubiak et al., 2025], [Kandziora-Ciupa et al., 2022], [Bierza & Bierza, 2024] [Algreen et al.,2013], [Budzyńska et al., 2023]
Pb	Betula pendula, Quercus robur, Platanus orientalis	5.0 – 15.0	0.5 – 2.0	[Bayçu et al., 2006], [Jakubiak et al., 2025] [Kandziora-Ciupa et al., 2022], [Bierza & Bierza, 2024], [Algreen et al.,2013], [Budzyńska et al., 2023]
Zn	Betula pendula, Acer platanoides, Fagus sylvatica	50.0 – 150.0	5.0 – 30.0	[Bayçu et al., 2006], [Jakubiak et al., 2025], [Kandziora-Ciupa et al., 2022], [Bierza & Bierza, 2024], [Algreen et al.,2013], [Budzyńska et al., 2023]
Cu	Fagus sylvatica, Betula pendula, Tilia cordata	5.0 – 15.0	1.0 – 4.0	[Jakubiak et al., 2025], [Kandziora-Ciupa et al., 2022], [Algreen et al.,2013], [Budzyńska et al., 2023], [Bayçu et al., 2006], [Nechita et al., 2025]
Ni	Platanus orientalis, Betula pendula, Fraxinus excelsior	1.0 – 5.0	0.5 – 3.0	[Kandziora-Ciupa et al., 2022], [Algreen et al.,2013], [Budzyńska et al., 2023], [Bayçu et al., 2006], [Nechita et al., 2025] [Kaoukis et al., 2018]

As part of the parameterisation of metal concentrations in conifer biomass, relevant literature sources were reviewed. A literature review conducted to determine ESS1 show that data for needles are widely available, but they show high variability depending on species, site conditions, anthropogenic pressure, and the age of the assimilatory tissues. At the same time, many studies focus on needles or bark as biomonitors and do not provide comparable values for stem wood, nor a consistent "*needles versus stem wood*" dataset for the full set of metals. For this reason,

instead of averaging results from heterogeneous studies, an approach based on one internally consistent dataset was adopted, covering both needles and stem wood analysed with the same methodology. The study by Skonieczna et al. (2014) was selected as the baseline source. In that work, 15 *Pinus sylvestris* trees from five stands were analysed. The investigated forests were located in an area influenced by anthropogenic pressures, but not in the immediate vicinity of point emission sources.

For the assessment, mean concentrations of Cd, Zn, Pb, and Cu were introduced for needles (as a representative of the "leaf" fraction) and for stem wood (as a representative of the "stem" fraction). Cadmium was then used for the subsequent valuation step (Table 17).

Table 17 Heavy metal concentrations in the biomass of conifer species.

Metal	Species	Needles [mg/kg]	Wood [mg/kg]	Experimental Conditions / Location	Source
Cd	Pinus sylvestris	0.10	0.24	Natural forest background; NW Poland.	[Skonieczna et al., 2014]
Cd	Pinus nigra	0.14 – 0.42	n.d.	Urban centers (Salzburg, Belgrade); urban pollution.	[Sawidis et al., 2011]
Cd	Pinus massoniana	0.18 – 0.48	n.d.	Urban-rural gradient (China); highest in industrial zones.	[Sun et al., 2009]
Cd	Pinus sylvestris	0.12	n.d.	Urban parks; comparative study of pine species.	[Juranović Cindrić et al., 2019]
Pb	Pinus massoniana	4.80 – 12.40	n.d.	Industrial areas and road traffic; high surface deposition.	[Sun et al., 2009]
Pb	Pinus nigra	0.75 – 4.96	n.d.	Urban monitoring; high accumulation in bark (up to 17.4).	[Sawidis et al., 2011]
Pb	Pinus sylvestris	1.10	0.54	Clean forest habitat; low lead availability in soil.	[Skonieczna et al., 2014]
Pb	Picea abies	0.50 – 1.50	n.d.	Semi-natural ecosystems (Lithuania); atmospheric deposition.	[Čeburnis & Steinnes, 2000]
Zn	Pinus sylvestris	~ 45.00	13.00	Physiological levels required for natural growth.	[Skonieczna et al., 2014]

For poplar plantations, several literature sources were reviewed (Table 18). As in other cases, it was found that experimental conditions were often not comparable between studies. Therefore, the focus was placed on a single publication that reported concentrations in poplar leaves and shoots in a format suitable for comparison across case studies.

Based on the reviewed evidence, Pilipović et al. (2019) was adopted as the source of ESS2 parameters for poplar plantations, as it provides a coherent empirical dataset covering both leaves and shoots/stems, analysed using the same methodology and under the same experimental conditions (Table 18). This allowed the "leaf versus wood/shoots" fractions to be separated directly, without merging heterogeneous studies and without additional assumption-based conversions. In addition, the study reports several metals (including Cd, Zn, Pb, and Cu) in a way that supported the selection of values representative of moderate anthropogenic pressure, thereby improving comparability between land-use scenarios within the ESS2 assessment.

Table 18 Heavy metal concentrations in the biomass of poplar and willow crops.

Metal	Species / Variety	Leaves [mg/kg]	Wood/Shoots [mg/kg]	Experimental Conditions / Location	Source
Cd	Salix viminalis	5.50 – 10.20	2.50 – 4.00	Soil amended with contaminated river sediments (Serbia).	[Pilipovic et al., 2019]

Funded by the European Union

Metal	Species / Variety	Leaves [mg/kg]	Wood/Shoots [mg/kg]	Experimental Conditions / Location	Source
Cd	Populus deltoides	11.80 – 118.30	~ 36.60	4-year field study on toxic mine tailings.	[Suo et al., 2021]
Cd	Populus nigra	21.30 – 107.30	10.00 – 30.00	Pot experiment; soil artificially spiked (10–50 mg Cd/kg).	[Radojčić Redovniković et al., 2017]
Cd	Poplar Hybrids	1.50 – 15.00	n.d.	Experimental field; composite metal contamination (China).	[Li et al., 2024]
Pb	Populus deltoides	16.00 – 486.00	n.d.	Extreme field conditions; mine tailings (paddy/mineral).	[Suo et al. ,2021]
Pb	Populus nigra	60.00 – 160.00	15.00 – 45.00	Pot experiment; soil spiked with lead (400–1200 mg Pb/kg).	[Radojčić Redovniković et al., 2017]
Pb	Populus sp.	4.50 – 8.00	1.50 – 2.50	Sediment remediation; Pb shows low root mobility.	[Pilipovic et al., 2019]
Zn	Populus deltoides	200.00 – 606.00	~ 118.00	Very high zinc availability in mining substrate.	[Suo et al., 2021]
As	Poplar Hybrids	0.50 – 2.50	n.d.	Composite pollution; low arsenic translocation to leaves.	[Li et al., 2024]
Hg	Poplar Hybrids	0.05 – 0.15	n.d.	Experimental field; trace amounts of mercury in leaves.	[Li et al., 2024]

For scenario with grassland, an above-ground biomass (AGB)-based approach was applied, using metal concentration ranges in herbaceous plant tissues as reported in the literature (Table 19). To reflect the typical spread of values associated with different levels of anthropogenic influence, three pressure levels were compiled (moderate, heavy, and extreme), representing, respectively, urban and transport impacts, post-mining areas, and locations in the immediate vicinity of smelters.

However, for the purpose of the ESS2 valuation, the moderate contamination variant was adopted, as it was considered representative of the common anthropogenic background conditions observed across the CS landscape and the analysed land-use scenarios. This choice reduced the influence of extreme concentration values that could otherwise dominate the result, and it ensured that differences in ESS2 were driven primarily by land-cover type and AGB magnitude rather than by exceptional, localised point sources of pollution.

Table 19 Heavy metal concentrations in the aboveground biomass of grassland species.

Metal	Species (Latin name)	Leaves [mg/kg]	Scenarios & Conditions	Source
Cd	Dactylis glomerata, Festuca sp.	0.5 – 1.0	Moderate: urban/industrial areas; impact of city emissions and transport (e.g., Copșa Mică).	[Carabulea et al., 2024]
Cd	Agrostis capillaris	5.0 – 15.0	Heavy: post-mining sites; soils with high Zn-Pb content (e.g., Olkusz/Bukowno).	[Kicińska et al. 2019], [Teodoro et al., 2019], [Kicińska & Gruszecka-Kosowska, 2016]
Cd	Grassland mix	10.0 – 25.0	Extreme: direct vicinity of smelters and river floodplains contaminated by mining (e.g., Litavka).	[Asare et al., 2025]; [Kicińska and

Metal	Species (Latin name)	Leaves [mg/kg]	Scenarios & Conditions	Source
				Gruszecka-Kosowska,2016]
Pb	Dactylis glomerata, Festuca sp.	8.0 – 15.0	Moderate: historical industrial deposition; medium pollution index.	Carabulea et al. (2024)
Pb	Agrostis capillaris	20.0 – 40.0	Heavy: metalliferous grasslands on calamine waste heaps.	[Kicińska et al., 2019], [Teodoro et al., 2019], [Kicińska & Gruszecka-Kosowska, 2016]
Pb	Grassland mix	40.0 – 300+	Extreme: smelter-affected areas; high atmospheric deposition on leaf surfaces.	[Asare et al., 2025], [Kicińska & Gruszecka-Kosowska, 2016]
Zn	Dactylis glomerata, Festuca sp.	70.0 – 100.0	Moderate: areas with elevated geochemical background and urban pressure.	Carabulea et al., 2024]
Zn	Agrostis capillaris	300.0 – 600.0	Heavy: colonization of industrial tailings by metal-tolerant species.	[Carabulea et al., 2024]
Zn	Grassland mix	1000.0 – 2500.0	Extreme: hot spots of Zn-Pb mining; highly bioavailable metal forms in soil.	[Kicińska et al., 2019], [Teodoro et al., 2019] [Kicińska & Gruszecka-Kosowska, 2016]
Cu	Various species	3.0 – 7.0	Uniform: Low mobility across most grassland scenarios; often within physiological limits.	Asare et al. (2025); Kicińska and Gruszecka-Kosowska,2016

Table 20 presents the input parameters and calculation outputs used to estimate the ESS2 indicator for CS1 (FR10), expressed as the potential annual Cd accumulation in above-ground plant biomass. It combines AGBinc values (from ESS1) with tissue Cd concentrations and harvest fractions to derive Cd concentration in harvested biomass and the resulting Cd removal per ha and year, in accordance with the methodology described in Section 4.3

Table 20 Calculation sheet for ESS2 (Cd): biomass increment, concentration assumptions and annual removal.

Corine Land Cover	AGBinc (tDM/ha/yr) [from ESS1]	f_leaf (season harvest) [0-1]	Cd_C_leaf (mg/kg DM) [input]	Cd_C_stem (mg/kg DM) [input]	Cd_C_harvest (mg/kg DM) [calc]	Cd_Removal (g/ha/yr) [calc]
Broad-leaved forest	4.03	0.2	0.4	0.1	0.16	0.6
Green urban areas -grassland or lawns	5.00	1	0.4	0.1	0.48	2.4
Industrial - PV installation (80% grassland)	4.00	1	0.4	0.1	0.48	1.9
Coniferous forest	4.75	0.2	0.4	0.1	0.16	0.8

Funded by the European Union

Corine Land Cover	AGBinc (tDM/ha/yr) [from ESS1]	f_leaf (season harvest) [0-1]	Cd_C_leaf (mg/kg DM) [input]	Cd_C_stem (mg/kg DM) [input]	Cd_C_harvest (mg/kg DM) [calc]	Cd_Removal (g/ha/yr) [calc]
Transitional woodland/shrub (poplar plantations)	6.60	0.2	7.85	3.25	4.17	27.5
Industrial - buildings and halls (20% grassland)	1.00	1	0.4	0.1	0.48	0.5

Table 21 summarises the ESS2 results for CS1 across the analysed land-use scenarios, reported as the estimated potential annual cadmium (Cd) accumulation in above-ground biomass ($g \cdot ha^{-1} \cdot year^{-1}$).

Table 21 A summary of ESS2 (Regulation of soil quality) results for the different CS1 land-use scenarios.

Land-use scenario	Scenario 1	Scenario 2	Scenario 3
Potential annual pollutant accumulation [g/ha/year]	27.5	1.9	2.4

6.1.3 Mitigation of climate change (carbon dioxide sequestration) (ESS3)

Evaluation for ESS3 was based on annual carbon sequestration expressed in t CO_2/ha/year as its indicator. Total carbon sequestration was calculated as the sum of above-ground biomass and below-ground carbon accumulation, which was later converted to CO_2 equivalent. The methodology followed the carbon allocation models for poplar plantations, as specified in the ESS3 card earlier in the document.

Acquiring information about the AGBinc followed the same procedure as described in ESS1, which involved analysing the accessible sources of data such as literature, inventory data and indirect indicators. For the Carrières-Sous-Poissy site in France (CS1) the data proved methodologically inconsistent and dispersed, which resulted in various definitions of production, growth, typological ranges or units. Therefore, a direct comparison between the coverage types was limited. The values for AGBinc across the deliverable are based on the harmonized data sourced from the "Improved large-area forest increment information in Europe through harmonization of National Forest Inventories" (Forest Ecology and Management, 562, 121913), which provided comparable results regarding the annual growth across most of the countries regarding forest types.

The BGBinc value was derived from the AGBinc value by using the AGBinc / BGBinc, annual above- and below-ground biomass ratio. The root-to-shoot ratio was based upon the literature findings such as Oliveira Rodríguez et al. (2018) and Intergovernmental Panel on Climate Change in 2003 and 2006 due to their unified methodology across countries, to best estimate the BGBinc (Table 22). Based on those findings, the ratio for industrial and commercial land use scenario was calculated based on the value of about 20% of the grassland AGBinc to BGBinc ratio, and the scenario assuming the ground-mounted photovoltaic farm designation accounted for 80% of the grassland coverage value.

Funded by the European Union

Table 22 Sources used for the estimation of below ground - above ground ratio (%).

CS1 (FR) - types of management	AGBinc - BGBinc ratio (%)	Sources
Broad-leaf forest	0.43	IPCC (2003) Annex 3A.1.8
Coniferous forest	0.46	
Grassland	1.58	IPCC (2003) Annex 3A.1.8 Mokany, Raison & Prokushkin (2006)
Poplar cultivation	0.21	Oliveira (2018)

After calculating the values of the BGBinc from the ratio and the AGBinc values provided, the results were added and multiplied by the C fraction to account for the carbon content. The carbon content values in dry matter are assumed at approx. 50% values, supported by literature (Table 23).

In the next step the results were converted to the CO_2 equivalent by multiplying the final value by 3.67 (ratio of the atomic mass of the molecules). The indicator reflects the annual flow of carbon sequestration associated with biomass growth, rather than long-term carbon stock changes.

Table 23 Sources used for the estimation of C fraction of carbon content in dry mass.

CS1 (FR) - types of management	C fraction of carbon content in dry matter	Source/Reference
Broad-leaf forest	0.46	[IPPC, 2003]
Coniferous forest	0.46	
Grassland	0.48	[Shiferaw et al., 2022]
Poplar cultivation	0.48	[Shiferaw et al., 2022]

The results for the region of Carrières-Sous-Poissy site in France (CS1) show that the annual carbon sequestration for broadleaf forests is about 9.73 t (CO_2/ha/year), with similar results for coniferous forests: 11.71 t (CO_2/ha/year) and estimation for poplar plantation: 9.81 t (CO_2/ha/year) (Figure 31). The highest values for annual carbon sequestration resulted in grassland coverage, at 22.73 t (CO_2/ha/year), majorly due to much more potent root biomass, which had shown and increased ability in terms of accumulation of carbon than any the forest types of management. Those results were used to provide background land use values for the evaluation of the values for Scenarios 1, 2 and 3.

ESS: MITIGATION OF CLIMATE CHANGE

PL	Średnia roczna ilość biomasy nadziemnej z hektara (tDM/ha/yr)	Stosunek biomasy poniżej - powyżej gruntu	Średnia roczna ilość biomasy korzennej z hektara (tDM/ha/yr)	Średnie stężenie węgla w biomasie (%)	Sekwestracja węgla (kg/year/ha)	Roczna sekwestracja węgla wyrażona w t (CO_2/ha/year)
ENG	Average anual amount of above-ground biomass from ha (tDM/ha/yr)	Below ground - above ground ratio	Average annual amount of below biomass from ha (tDM/ha/yr)	Biomass mean concentration of carbon (%)	Carbon sequestration (t/year/ha)	Annual carbon sequestration expressed in t (CO_2/ha/year)
						Conversion factor from Carbon (C) to CO_2 equivalent
						3,67
CS1 (FR) - Carrières-Sous-Poissy						
Forest_broadleaf_poplar	4,03	0,43	1,733	0,46	2,651	9,729
Grassland	5,00	1,58	7,900	0,48	6,192	22,725
PV_groundmounted (80% grassland)	4,00	1,58	6,320	0,48	4,954	18,180
coniferous	4,75	0,46	2,185	0,46	3,190	11,708
poplar cultivation	4,80	0,21	1,008	0,46	2,672	9,805
Industrial of commercial units (20% grassland)	1,00	1,58	1,580	0,48	1,238	4,545

Figure 31 Calculations concerning the ESS3 indicator – annual carbon sequestration expressed in t (CO_2/ha/year) for the Carrières-Sous-Poissy site in France (CS1).

For the Scenario 1 – NBS solutions, the value of poplar plantations was assumed. The 2nd Scenario for ESS3 considered 80% vegetation in AGBinc and BGBinc value due to a decreased but still

Funded by the European Union

present level of low-vegetation growth. For Scenario 3, the value of grasslands was assumed as an option for low-vegetation, recreational approach (Table 24).

Table 24 A summary of ESS3 - Annual carbon sequestration expressed in t CO_2/ha/year for the different CS1 land-use scenarios.

Land-use scenario	Scenario 1	Scenario 2	Scenario 3
ESS3 - Annual carbon sequestration expressed in t CO_2/ha/year	9.805	18.18	22.725

6.1.4 Air quality mitigation (ESS4)

Evaluation of ESS4 considers the removal of atmospheric pollutants (specifically particulate matter PM_{10} and $PM_{2.5}$) by tree and shrub canopies in urban, peri-urban and rehabilitated post-industrial areas through dry deposition processes. The main indicator is the annual removal of particulate matter PM_{10} particles expressed in t/ha/year. The methodology is based on the dry deposition mode, established by Tallis et al. (2011), where:

$$\text{Absorption of } PM_{10} = \text{Flux (V) x Surface (SA) x Period (t) (t/km}^2\text{/year)}$$

where:

- Flux is the pollutant to the surface (amount removed per unit area and time), calculated by multiplying the deposition velocity of the pollutant (m/s), which depends on canopy structure and wind speed and the concentration of the pollutant in the atmosphere.
- Surface is the considered surface area multiplied by the surface area index functioning in a given area (LAI).
- Period accounts for the period of analysis in days, multiplied by the proportion of dry days and the proportion of non-leaf days.

The total annual pollutant removal is calculated by integrating deposition fluxes over the vegetated surface area of each land-use scenario. The above contributes to the calculation as follows:

- V = deposition velocity (m/s) x pollutant conc. (µg/m³)
  - Flux (µg/m³) was then converted to daily flux by multiplying it by 86400
- SA = LAI (m²/m²) x area of land considered (m²)
- t = period of analysis (days) x proportion of dry days (fraction) x proportion of on-leaf days (fraction)
  - Afterwards the absorption of PM_{10} was converted from (µg/m²/year) to (t/km²/year) by $x10^6$

The approach of Tallis et al. considers the "filtering" effect of different tree types regarding deposition velocity (broad-leaved vs. coniferous). Coniferous trees are generally more efficient due to higher Leaf Area Index (LAI) and year-round foliage. The canopy assessment considered Calculation of the Tree Canopy Area (TCA) using Land Cover data and NFI (National Forest Inventory) to determine the active surface area for deposition. To calculate the total annual removal load, the local air quality monitoring data (PM_{10}/$PM_{2.5}$ concentrations) were integrated.

The data for the Carrières-Sous-Poissy site in France (CS1) involved land use scenarios for the broad-leaf forest, coniferous forest, mixed forest, pastures, grasslands and photovoltaic farm. For each of the components of the model, the literature research was carried out to scope the best range of unified results to produce comparable values. In some cases, it was not possible to gather data regarding each of the components of the model, in which case an average was used from the data regarding countries or regions in the world with closest ecosystem type, for the results to be compatible.

Funded by the European Union

Regarding the deposition velocity by land use type, no data was found in the research for the Carrières-Sous-Poissy region, however, comparable data were used from European, U.S. and Italian databases to provide a baseline. Data gathered from Marando et al. (2016), investigated deposition velocity in various vegetation types in mediterranean climate, its main reference point being Rome, Italy, using the i-Tree Eco dry deposition model (Table 25).

Table 25 Estimated deposition velocity in mediterranean climate by Marando et al. (2016).

Vegetation Type	Deposition Velocity (cm s^{-1})	Additional observations
Broadleaf trees (in-leaf)	0.5–1.5	Higher during full leaf area
Coniferous trees	1.0–2.0	Year-round interception
Grass/shrubs	0.2–0.8	Lower aerodynamic roughness

Another study by Mariarosa et al. (2019) provided information in Dry deposition modelling and validation in urban and suburban Italy, representative of mediterranean and temperate climate (Table 26).

Table 26 Estimated deposition velocity in regions managed as low-vegetation or industrial/urban sites by Mariarosa et al. (2019).

Land use type	Deposition Velocity (cm s^{-1})	Additional observations
Industrial surfaces	0.1–0.5	Smooth surfaces lower deposition
Suburban vegetation	0.3–1.2	Higher roughness enhances capture
Grasslands	0.2–0.6	Moderate

Other studies which represented estimation of deposition velocity on a global scale in temperate and boreal regions, their focus on U.S and central Europe. Lovett (1994) investigated particle deposition velocity in coniferous forests, deciduous forests and grasslands, with results stated in Table 27.

Table 27 Estimated deposition velocity in temperate and boreal climate by Lovett (1994).

Land use	Particle Deposition Velocity (cm s^{-1})	Additional observations
Coniferous forest	1.0–3.0	High canopy roughness
Deciduous forest	0.5–2.0	Seasonal variation
Grassland	0.1–0.5	Lower surface roughness

Considering the site in Carrières-Sous-Poissy site in France lays in the temperate climate belt, a cross-study synthesis was performed to best account for the values of deposition velocity for the different types of vegetation in Carrières-Sous-Poissy region, and an average of values was used for following calculations (Table 28).

Table 28 Cross-Study Synthesis Deposition Velocity by Land Use Type.

Land Use	PM10 (cm s^{-1})	Represented regions	Sources/Reference
Broad-leaf forest	0.5–2.0	North America, Italy	Marando et al. (2016) Lovett (1994) Nowak et al. (2013) U.S. Forest Service. i-Tree Eco (2011). Mariarosa et al. (2019)
Coniferous forest	1.0–3.0	North America, Europe	
Grassland/ Pasture	0.1–0.5	North America, Europe	
Industrial land cover	0.1–0.5	Italy	

Funded by the European Union

The next component researched for the model was the pollutant concentration (µg/m³). The values for pollutant concentrations could not be recovered for the region; however, estimates were based on the information gathered over a period from the Airparif (2022) reports, and investigations by Waza et. al. (2025). Based on these results, a pollution concentration of 23 µg/m³ was assumed.

Regarding the surface area, the values of the leaf area index (LAI) in various types of land use were taken into consideration (Table 29). Due to the lack of specific data regarding the above-mentioned land use types for the region, European and global data were considered.

Table 29 References for the leaf area index concerning chosen types of land use.

Land use type	LAI values	Represented region	Sources / References
Broad-leaf forest	5–8 (max values) 3–6 (urban average 3–4.5) 2–10 (broad global range)	France (temperate deciduous) Primarily U.S., global review Global synthesis	[Le Dantec et al., 2000] [Nowak et al., 2017] [Parker, 2020]
Coniferous forest	6–11 3–6 (urban average 3–4.5) 2–10 (broad global range)	Pacific Northwest, U.S. Primarily U.S., global review Global synthesis	[Turner et al., 2000] [Nowak et al., 2017] [Parker, 2020]
Mixed forest	3–7 typical; up to 9 dense stands	Europe (multi-site comparison)	[Sinan & Hasenauer, 2025]
Pasture/ Grassland/ Shrub	2.0–4.5 (Wetland shrubs lower (2–3), wooded wetland stands up to 4.5)	Poland (Central Europe)	[Leśny et al., 2007]

Area assumed for the calculation at this stage was a m^2, after conversion km^2. Regarding the period component, it was calculated by taking average of the range of the vegetation period for each type of land use. For the Carrières-Sous-Poissy site the temperate values which were used for calculation according to different land use type are presented in Table 30.

Table 30 Number of vegetative days for each land use type according to the climate type.

Land Use Type	Boreal	Temperate	Mediterranean	Subtropical	References/Sources
Coniferous Forest	120–180	180–220	200–240	250–300	[EMEP, 2016] [GIOŚ, 2018] [Langner et al., 2011] [Chen, 2015] [Khan & Perlinger, 2017] [Vivanco et al., 2021]
Broadleaf Forest	140–190	190–220	220–260	280–320	
Grassland	150–190	200–240	220–300	280–320	
Cropland	140–180	180–220	250–320	280–330	

For the scenario regarding industrial land use type, including photovoltaic farm, the vegetative period was assumed to be the same as for grassland. The proportion of dry days was assumed at 60% according to Chervenkov & Slavov (2021), while the proportion of on-leaf days was assumed at 100%, due to already exclusively selected vegetative dry periods.

The results for the region of Carrières-Sous-Poissy site in France (CS1) presented in the figure below (Figure 32) show that the annual absorption of PM10 are as follow: 13.95 t/km²/year for broad-leaf forest, 33.38 t/km²/year for coniferous forest, 23.06 t/km²/year for mixed forest, 2.33 t/km²/year for pastures, 2.56 t/km²/year for grasslands and 0,17 t/km²/year for industrial land use/photovoltaic farm. Those results were used to provide background land use values for the evaluation of the values for Scenarios 1, 2 and 3.

Funded by the European Union

For the Scenario 1 – NBS values of broad-leaf forest was assumed. Concerning Scenario 2, the industrial/photovoltaic land use was considered and for Scenario 3 the values for pastures were assumed, as shown in Table 31.

ESS: AIR PURIFICATION							
Seconds/day (s)	86 400						
		CS1 (FR) - Carrières-Sous-Poissy					
PL	EN	Broad-leaf forest	Coniferous forest	Mixed forest	Pasture	Grassland	Photovoltaic farm
Prędkość osiadania (m/s)	Deposition velocity (m/s)	0,013	0,020	0,017	0,003	0,003	0,001
Stężenie PM10 (µg/m^3)	Pollutant conc. (µg/m^3)	23,000	23,000	23,000	23,000	23,000	23,000
Przepływ (µg/m^2/s) = Prędkość osiadania (m/s) x Stężenie PM10 (µg/m^3)	**Flux (µg/m^2/s) =** deposition velocity (m/s) x pollutant conc. (µg/m^3)	0,299	0,460	0,391	0,069	0,069	0,023
Dzienny przepływ (µg/m^2/dzień)	**Daily flux (µg/m^2/day)**	25833,6	39744	33782,4	5961,6	5961,6	1987,2
Wskaźnik powierzchni (m^2/m^2)	Surface area index (LAI) (m^2/m^2)	6,000	7,000	6,500	3,250	3,250	0,650
Powierzchnia brana pod uwagę (m^2)	Area of land (m^2)	1,000	1,000	1,000	1,000	1,000	1,000
Powierzchnia (m^2) = Wskaźnik powierzchni (m^2/m^2) x Powierzchnia brana pod uwagę (m^2)	**Surface (m2) =** LAI (m^2/m^2) x area of land (m^2)	6,000	7,000	6,500	3,250	3,250	0,650
Okres kwitnienia liści	Vegetation period (days)	150,000	200,000	175,000	200,000	220,000	220,000
Odsetek dni suchych	Proportion of dry days (fraction)	0,600	0,600	0,600	0,600	0,600	0,600
Odsetek dni wchłaniania przez dojrzały liść	Proportion of on-leaf days (fraction)	1,000	1,000	1,000	1,000	1,000	1,000
Okres = Okres kwitnienia liści (dni) x Odsetek dni suchych x Odsetek dni wchłaniania przez dojrzały	**Period =** period of analysis (days) x proportion of dry days (fraction) x proportion of on-leaf days	90,000	120,000	105,000	120,000	132,000	132,000
Wchłanianie PM10 (µg/m^2/rok)	**Absorption of PM10 = Flux x Surface x Period (µg/m^2/year)**	13950144	33384960	23056488	2325024	2557526	170501,8
Wchłanianie PM10 (t/km^2/rok)	**Absorption of PM10 = Flux x Surface x Period (t/km^2/year)**	**13,95**	**33,38**	**23,06**	**2,33**	**2,56**	**0,17**

Figure 32 Summary of the calculations involved in the calculations for ESS4 indicator – Absorption of PM10.

Table 31 A summary of ESS4 - Annual removal of particulate matter PM10 particles [t/km²/year] results for the different CS1 land-use scenarios.

Land-use scenario	Scenario 1	Scenario 2	Scenario 3
ESS4 – Annual removal of particulate matter PM10 particles expressed as t/km²/year	13.95	0.17	2.33

Funded by the European Union

6.1.5 Temperature regulation (ESS5)

The assessment of temperature regulation potential was based on Landsat 8 satellite data processed into a Land Surface Temperature (LST) map using the ASTER database. The Advanced Spaceborne Thermal Emission and Reflection Radiometer Global Emissivity Database (ASTER GED) was developed by National Aeronautics and Space Administration's (NASA) Jet Propulsion Laboratory (JPL), California Institute of Technology. The ASTER GED product provides global emissivity maps of the Earth's land surface in five spectral bands. In addition to the mean emissivity and standard deviation maps for all five ASTER thermal infrared bands, the product also provides maps for mean land surface temperature (LST) and standard deviation.

The analysis focused on the day with the highest air temperature recorded in the last 10 years. For CS1, this was 24 July 2019. The analysis was carried out for the entire municipality of Carrieres-Sous-Poissy, within which CS1 is located. The study area was divided into land-use categories according to CLC 2018 (Corine Land Cover). The following land-use categories were identified: water courses (511), water bodies (512), transitional woodland-shrub (324), discontinuous urban fabric (112), pastures (231), industrial or commercial units (121), mineral extraction sites (131), momplex cultivation patterns (242) (Figure 33).
Mixed forests (313) located closest to CS1 were also included in the analysis, because this land-cover category did not occur within the boundaries of the commune under study.

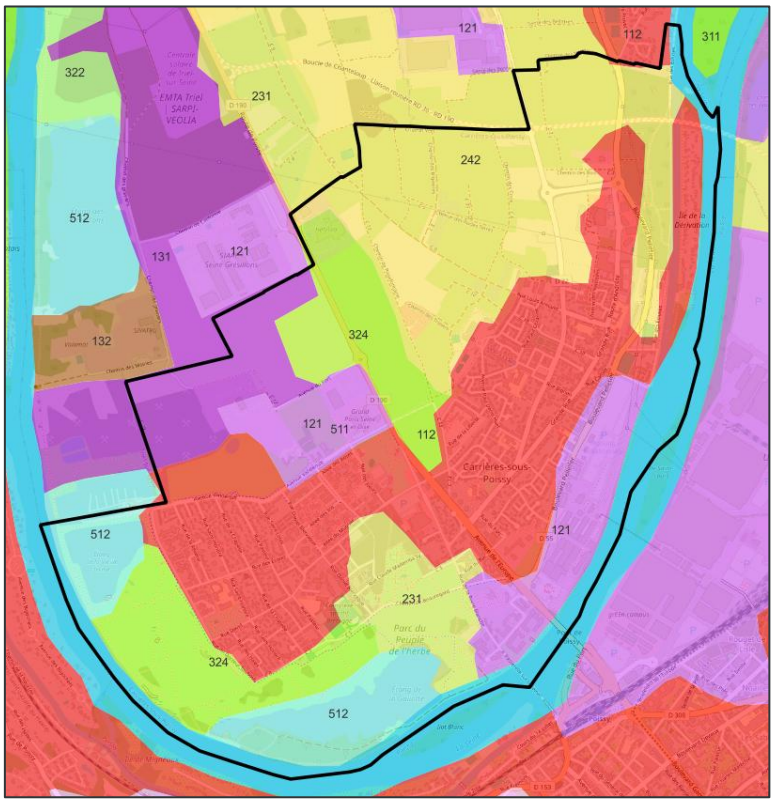

Figure 33 CLC 2018 land cover pattern for CS1.

In the next step, using GIS analytical tools, the mean temperature values were calculated for each land-use type. The temperature regulation potential was calculated by relating the mean temperature values to the highest intended mean value for a given land use. The calculation results are presented in Table 32.

Funded by the European Union

Table 32 Cooling potential of land cover – CS1.

CLC 2018 Land Cover class	Mean T [°C]	Cooling potential [°C]
Water courses	24.6	6.8
Mixed forest	24.7	6.7
Water bodies	26.0	5.4
Transitional woodland-shrub	28.8	2.6
Discontinuous urban fabric	29.3	2.1
Pastures	30.2	1.2
Industrial or commercial units	30.8	0.6
Mineral extraction sites	31.1	0.3
Complex cultivation patterns	31.4	0.0

The results were then normalised to a scale from 1 to 10, where 1 denotes no potential and 10 the highest potential of the ESS. The projected temperature value for the analysed land-use scenarios was adopted assuming that Scenario 1 corresponds to mixed forests, Scenario 2 to industrial or commercial units, and Scenario 3 to pastures. The results of the potential analysis for each scenario are presented in Table 33.

Table 33 Evaluation of cooling potential for analysed Scenarios – CS1.

Corine Land Cover Class	Cooling potential [-]
Discontinuous urban fabric	3.8
Industrial or commercial units	1.8
Scenario 2 - Industrial scenario, photovotaic panels	**1.8**
Mineral extraction sites	1.4
Pastures	2.5
Scenario 3 - Recreational, meadows, pastures	**2.5**
Complex cultivation patterns	1.0
Mixed forest	9.8
Scenario 1 - NBS, forests	**9.8**
Transitional woodland-shrub	4.4
Water courses	10.0
Water bodies	8.1

6.1.6 Cultural- direct, in-situ and outdoor interactions with living systems (ESS6)

The first stage of the analysis involved collecting detailed data on the location of residential areas and areas meeting the criteria for green spaces providing recreational opportunities. Baseline mapping was undertaken using the Urban Atlas LCLU 2018 (https://land.copernicus.eu/local/urban-atlas/urban-atlas-2018). Within the administrative boundaries of the units Vieux-Charmont and Carrieres-Sous-Poissy communes, the following land cover classes have been identified as green recreation areas: forests (deciduous forests (CLC 311), coniferous forests (CLC 312), mixed forests CLC 313); green urban areas (CLC 141), water (CLC 511, CLC 512).

Funded by the European Union

The potential for providing recreational services was also assessed for areas that may be converted into green areas in the future:

- The area of the contaminated case study site (brownfield CS 1)
- Land without current use (CLC 133)
- Mineral extraction and dump sites (CLC 131)

The potential for recreational use was assessed using the number of residents within 300 meters of a green recreational area (> 1 ha). This indicator allows for an assessment of how many people will use the area in question for recreational purposes. The greater the number of residents within a 300 m radius, the greater the potential of the area in terms of this ecosystem service. The quantifying indicator required the use of High-Resolution Population Density Maps. The dataset was developed by use techniques to identify buildings from publicly accessible mapping services to create the most accurate population datasets (TIECKE, et al. 2017). The disadvantage of this dataset is that it assigns residents to buildings with industrial and service functions.

In the quantitative analyses of the cultural services indicator, the number of inhabitants within areas that do not serve a residential function (e.g industrial areas) was not considered.

An analysis of the potential of existing and potential green areas to provide recreational functions showed that analyzed, brownfield, does not have significant potential to provide cultural functions. This is due to the distance of the area from densely populated residential areas.

The future use for recreational purposes will provide 293 residents with access to this type of area. Within the analysed administrative boundaries, there are green areas with a recreational function that serve recreational function for 17 736 residents (forest areas along the river)

In the south-eastern part of the Carrieres-Sous-Poissy communes, there are areas where mining operations are conducted (Mineral extraction and dump sites). These areas are located near densely populated residential areas (>10). Redevelopment of these areas for recreational purposes will increase accessibility for 8 076 residents. With regard to these values, the development of the analysed contaminated site (CS1) will not result in a significant increase in the availability of green areas for residents. The potential of existing and potential green areas with recreational functions on a scale of 1 to 10 is shown in the figure below (Figure 34).

Funded by the European Union

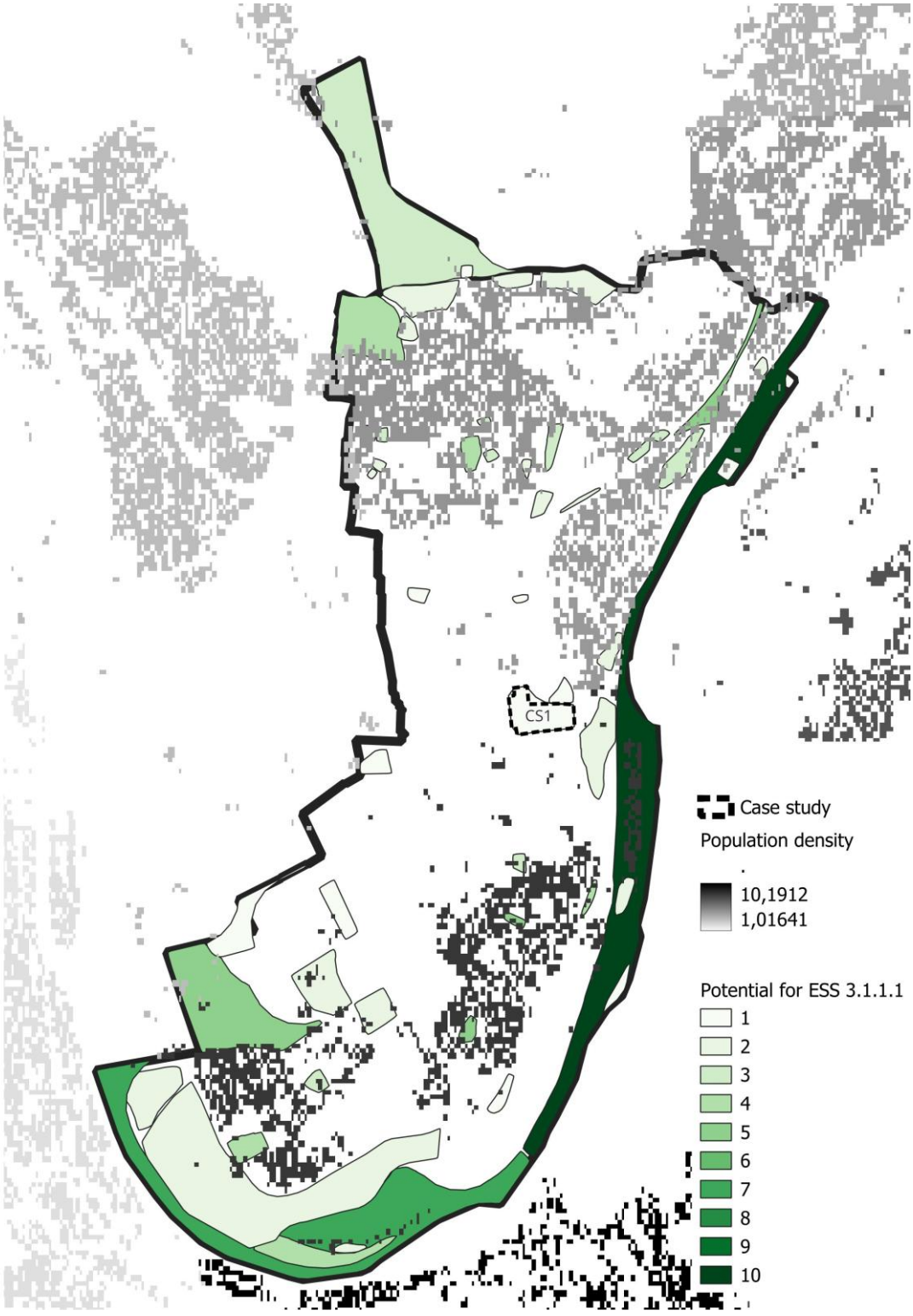

Figure 34 Cultural services: Interactions with natural environment for CS1.

In the adopted land use options, only the scenario 1 (Afforestation) and scenario 3 (Grassland cover), meet the criteria for green areas with a recreational function. Compared to other green areas within the administrative boundaries of, this scenario has very little potential for providing cultural services (Table 34).

Funded by
the European Union

Table 34 A summary of ESS6 results for the different CS1 land-use scenarios.

Land-use scenario	Scenario 1	Scenario 2	Scenario 3
ESS6 [Number of residents within 300 meters of a green recreational area]	293	0	293

6.1.7 Energy properties (ESS7)

The performance of photovoltaic installations for CS1 was estimated using an application provided by the EC: Photovoltaic Geographical Information System [https://re.jrc.ec.europa.eu/pvg_tools/en/tools.html]. This application provides data on solar radiation and energy production from photovoltaic (PV) systems globally. Following the application instructions, the performance of photovoltaic installations was estimated based on the assumption presented in Table 35.

Table 35 Assumptions and settings used for PV calculation for CS1.

PV Performance Modelling Parameters						
Solar radiation database:	PV technology:	Installed peak PV power	System loss	Mounting position	Slope	Azimuth:
PVGIS-SARAH3	Crystalline Silicon (original)	1 kWp	14%	Free-standing	35°	0°

In Table 36, the CS1 is characterised in relation to the analysis conducted.

Table 36 Site characteristic.

Case Study	Coordinates (center)		Elevation	Area [ha]
	Latitude	Longitude		
CS1	48.960	2.0400	41	7

To estimate the electricity production capacity for this CS1, the maximum feasible installed PV capacity (kWp) was determined from the available area. For the purposes of the analysis, it was assumed that 1 kWp corresponds to a PV system area of 6 m². Because the full area could not be developed under real conditions (e.g., spacing between modules, internal roads, technical buildings, fencing, and grid infrastructure), a Surface Coverage Ratio (α = 50%) was used to reflect practical land take. This value was derived from an assessment of operating photovoltaic farms with total areas ranging from 27 ha to 300 ha.

Table 37 shows the calculated performance of PV installations for CS1. The estimated yearly in-plane irradiation is 1 417.06 kWh/m², taking into account factors such as system losses (14%). The annual electricity production is determined to be 1 133.78 kWh per 1 kWp installed. Table 37 presents the estimated value of electricity production, considering the surface area calculated using the Ideal Value Model and near-real conditions determined by the Surface Coverage Ratio. Under ideal conditions, the annual energy production could reach 13.2 GWh. Based on the Surface Coverage Ratio, the annual energy production is projected to be 6.6 GWh.

Table 37 Yearly PV energy production for CS1.

Yearly PV energy production [kWh]	1 133.78

Funded by the European Union

Yearly in-plane irradiation [kWh/m^2]		1 417.06
Year-to-year variability [kWh]		47.25
Changes in output due to		
-Angle of incidence [%]		-3.03
-Spectral effects [%]		1.68
Temperature and low irradiance [%]		-5.64
Total loss [%]		-19.99
Max. kWp needed [kWp]		11 667
Energy production (Ideal Value Model)	GWh/y	13.2
Energy production (Surface Coverage Ratio)	GWh/y	6.6

Figure 35 shows a report from the Photovoltaic Geographical Information System application (estimating annual energy production for CS1).

Figure 35 CS1 – Performance of grid-connected PV.

The ESS7 results for CS1 are summarized in the table below (Table 38).

Table 38 A summary of ESS7 (Energy properties) results for the different CS1 land-use scenarios.

Land-use scenario	Scenario 1	Scenario 2	Scenario 3
ESS7: Potential energy production [GWh/y].	0.0	6.0	0.0

Funded by the European Union

6.2 Ecosystem services assessment for CS2

In this section, the valuation of ESS for CS2 (Kozani, GR – EL53) was presented in the context of local site conditions and the analysed land-use scenarios. At the same time, a harmonised data preparation approach was applied to ensure comparability of results across case studies.

6.2.1 Biomass production (ESS1)

The ESS1 assessment for CS2 was based on the EP indicator (GJ·ha^{-1}·year^{-1}), derived from the annual above-ground biomass increment AGBinc (t d.m.·ha^{-1}·year^{-1}) using the equation:

$$EP = AGBinc \times CV$$

Where:
- CV is the calorific value of the biomass (GJ·t^{-1} d.m.), adopted in line with the ESS1 service card,
- AGBin above-ground biomass AGBinc (t d.m.·ha^{-1}·year^{-1}),
- EP is energy potential.

For Greece, consistent and comparable AGBinc data at the regional (NUTS2) level were not available. The accessible results referred mainly to the northern part of the country and to conditions associated with high productivity (Table 39).

Table 39 Annual biomass production on different types of land in Greece.

Land type	Value	Units	Method / notes	Source
Deciduous forest	7.19	t/ha/year	Aboveground net primary productivity (ANPP) estimated from allometry + management plan data; stand-scale production; Value is ANPP/aboveground production for beech forest case study; not national mean for all deciduous forests.	[Zianis, D., & Mencuccini, M., 2025]
Poplar monoculture (Populus)	16.54	t/ha/year	Clone productivity reported for Greece (review of breeding/biomass trials);Clone-specific reported yield; not national average across all poplar plantations.	[Aravanopoulos, F. A. (2010]
Mixed forests	-	-	No reliable value found in the searched sources (explicit mean annual biomass increment for mixed forests in Greece).	
Coniferous forests	-	-	No reliable value found in the searched sources (explicit mean annual biomass increment for coniferous forests in Greece).	
Grassland / meadow cultivation	-	-	No reliable value found in the searched sources (accessible, citable annual biomass yield/increment statement).	

According to the data limitations, a harmonisation approach was applied for the forest scenario (afforestation) (Broad-leaved Forest and Coniferous Forest). Net annual increment (NAI; m^3·ha^{-1}·year^{-1}) was used as the starting point and was converted to AGBinc using a conversion factor derived from the reference dataset. This solution ensured that the ESS1 assessment remained comparable across the report and reduced the risk of overestimating results based on fragmented local data. Table below (Table 40) presents the AGBinc and CV values, together with the resulting EP, assigned to CLC classes and scenarios in CS2.

For the poplar plantations scenario,

$$AGBinc = 15.00 \text{ t d.m.} \cdot ha^{-1} \cdot year^{-1}$$

was applied within the harmonised approach. The available literature for poplar largely refers to plantations managed under particularly favourable growth conditions (e.g., northern regions or intensively irrigated sites) and reports values around 16.54 t d.m.·ha^{-1}·year^{-1}, which could lead to inflated parameters for CS2. To maintain comparability between case studies and avoid transferring values representative of exceptionally high productivity into CS2, AGBinc = 15.00 t d.m.·ha^{-1}·year^{-1} was adopted as a common upper value for poplar, consistent with the highest value applied across the full CS dataset.

For the scenario 2 (grasslands), AGBinc values were adopted at the NUTS2 level and were selected to match local climatic conditions and land-use intensity, so that regional constraints on biomass production were properly reflected. For example, for EL30 (Attica), a range of 1-3 t d.m.·ha^{-1}·year^{-1} was assumed for dry Mediterranean pastures, where production is strongly limited by water deficit and a shorter period of intensive growth (Table 40).

Table 40 Estimated annual above-ground biomass increment (AGBinc) for grasslands in NUTS2 regions – assumptions and literature-based justification.

NUTS2	Region	Type of grassland	Estimated AGB increase (t DM·ha^{-1}·yr^{-1})	Rationale (climate / intensity)	Citations
EL30	Attyka	dry pastures	1–3	Dry Mediterranean pastures: strong water limitation and a shorter period of intensive growth	[Shi et al., 2023], [Obermeier et al., 2018], [Tao et al., 2015]

Table 41 presents the input data used to calculate ESS1 (biomass production) for CS2, including AGBinc, CV and the resulting EP values for each land-cover component considered in the scenarios.

Table 41 Calculation parameters for the biomass energy potential for CS2 (EL53).

CLC clasification	Couling Land Cover	AGBinc (tDM/ha/yr)	CV (GJ/tDM)	EP (GJ/ha/yr)
3.1.1	Broad-leaved forest	2.56	18.5	47.4
1.4.1	Green urban areas -grassland or lawns	3.00	17.5	52.5
1.2.1	Industrial - PV installation (80% grassland)	2.40	17.5	42.0
3.1.2	Coniferous forest	2.57	18.5	47.5
3.2.4	Transitional woodland/shrub (poplar plantations)	15.00	18.6	278.4
1.2.1	Industrial - buildings and halls (20% grassland)	0.60	17.5	10.5

Table 42 provides a scenario-level summary of ESS1 results for CS2 by compiling the EP outcomes across the defined land-use scenarios. The reported values enable comparison between scenarios under a consistent calculation framework and a harmonised set of biomasses increment assumptions

Table 42 A summary of ESS1 (Biomass production) results for the different CS2 land-use scenarios.

Land-use scenario	Scenario 1	Scenario 2	Scenario 3
Energy potential [GJ/ha/year]	278.4	42	52.5

Funded by the European Union

6.2.2 Regulation of soil quality (ESS2)

In this section, the ESS2 indicator (regulation of soil quality) for CS2 was estimated as the potential for metal accumulation in plant biomass under the analysed land-use scenarios. As part of the literature review, concentration ranges of several metals in plant biomass were compiled e.g. cadmium, lead, zinc, copper, and nickel. However, for valuation purposes, one representative metal was selected: cadmium (Cd). Cadmium is frequently reported in environmental studies, it has no nutrient function (unlike Zn or Cu), and its accumulation in plant tissues provides a useful indicator of contamination pressure. In addition, Cd is often more mobile and more readily translocated to above-ground plant parts than Pb, which increases its suitability for scenario comparisons based on AGB.

As part of the parameterisation of metal concentrations in conifer biomass, relevant literature sources were reviewed. Data for needles are widely available, but they show high variability depending on species, site conditions, anthropogenic pressure, and the age of the assimilatory tissues. At the same time, many studies focus on needles or bark as biomonitors and do not provide comparable values for stem wood, nor a consistent "needles versus stem wood" dataset for the full set of metals. For this reason, instead of averaging results from heterogeneous studies, an approach based on one internally consistent dataset was adopted, covering both needles and stem wood analysed with the same methodology. The study by Skonieczna et al. (2014) was selected as the baseline source. In that work, 15 *Pinus sylvestris* trees from five stands were analysed. The investigated forests were located in an area influenced by anthropogenic pressures, but not in the immediate vicinity of point emission sources.

For the assessment, mean concentrations of Cd, Zn, Pb, and Cu were introduced for needles (as a representative of the "leaf" fraction) and for stem wood (as a representative of the "stem" fraction). Cadmium was then used for the subsequent valuation step.

For poplar plantations, several literature sources were reviewed. As in other cases, it was found that experimental conditions were often not comparable between studies. Therefore, the focus was placed on a single publication that reported concentrations in poplar leaves and shoots in a format suitable for comparison across case studies

Based on the reviewed evidence, Pilipović et al. (2019) was adopted as the source of ESS2 parameters for poplar plantations, as it provides a coherent empirical dataset covering both leaves and shoots/stems, analysed using the same methodology and under the same experimental conditions. This allowed the "leaf versus wood/shoots" fractions to be separated directly, without merging heterogeneous studies and without additional assumption-based conversions. In addition, the study reports several metals (including Cd, Zn, Pb, and Cu) in a way that supported the selection of values representative of moderate anthropogenic pressure, thereby improving comparability between land-use scenarios within the ESS2 assessment.

For Scenario with grassland, an above-ground biomass (AGB)-based approach was applied, using metal concentration ranges in herbaceous plant tissues as reported in the literature. To reflect the typical spread of values associated with different levels of anthropogenic influence, three pressure levels were compiled (moderate, heavy, and extreme), representing, respectively, urban and transport impacts, post-mining areas, and locations in the immediate vicinity of smelters.

Funded by the European Union

However, for the purpose of the ESS2 valuation, the moderate contamination variant was adopted, as it was considered representative of the common anthropogenic background conditions observed across the CS landscape and the analysed land-use scenarios. This choice reduced the influence of extreme concentration values that could otherwise dominate the result, and it ensured that differences in ESS2 were driven primarily by land-cover type and AGB magnitude rather than by exceptional, localised point sources of pollution.

The input data used for CS2 are identical to those described for CS1 in Section 6.1.2. Table 43 provides a concise overview of the heavy metal concentration datasets applied in the biomass assessment and includes references to the corresponding detailed tables in Section 6.1.2

Table 43 Heavy metal concentrations in biomass used for ESS2 parameterisation (data sources and table references).

No.	Heavy metal concentrations in the biomass	Reference table
1	Broadleaf species	Table 16 Heavy metal concentrations in the biomass of broadleaf species.
2	Conifer species	Table 17 Heavy metal concentrations in the biomass of conifer species.
3	Poplar and willow crops.	Table 18 Heavy metal concentrations in the biomass of poplar and willow crops.
4	Grassland species	Table 19 Heavy metal concentrations in the aboveground biomass of grassland species.

Table 44 presents the input parameters and calculation outputs used to estimate the ESS2 indicator for CS2 (EL53), expressed as the potential annual Cd accumulation in above-ground plant biomass. It combines AGBinc values (from ESS1) with tissue Cd concentrations and harvest fractions to derive Cd concentration in harvested biomass and the resulting Cd removal per hectare and year, in accordance with the methodology described in Section 4.3

Table 44 Calculation sheet for ESS2 (Cd): biomass increment, concentration assumptions and annual removal.

Corine Land Cover	AGBinc (tDM/ha/yr) [from ESS1]	f_leaf (season harvest) [0-1]	Cd_C_leaf (mg/kg DM) [input]	Cd_C_stem (mg/kg DM) [input]	Cd_C_harvest (mg/kg DM) [calc]	Cd_Removal (g/ha/yr) [calc]
Broad-leaved forest	2.56	0.2	0.4	0.1	0.16	0.4
Green urban areas - grassland or lawns	3.00	1	0.75		0.75	2.3
Industrial - PV installation (80% grassland)	2.40	1	0.6		0.6	1.4
Coniferous forest	2.57	0.2	0.1	0.24	0.28	0.5
Transitional woodland/shrub (poplar plantations)	15.00	0.2	7.85	3.25	4.17	62.6
Industrial - buildings and halls (20% grassland)	0.60	1	0.15		0.15	0.1

Table 45 summarises the ESS2 results for CS2 across the analysed land-use scenarios. Values are reported as the estimated potential annual pollutant (Cd) accumulation in above-ground biomass (g/ha/year) enabling direct comparison between scenarios under a consistent parameter set.

Funded by the European Union

Table 45 A summary of ESS2 (Regulation of soil quality) results for the different CS2 land-use scenarios.

Land-use scenario	Scenario 1	Scenario 2	Scenario 3
Potential annual pollutant accumulation [g/ha/year]	62.6	1.4	2.3

6.2.3 Mitigation of climate change (carbon dioxide sequestration) (ESS3)

The assessment of ESS3 was conducted using annual carbon sequestration as the principal indicator, expressed in tonnes of CO_2 per hectare per year (t CO_2/ha/year). Total carbon sequestration was estimated by summing the carbon accumulated in above-ground biomass and below-ground biomass and then converting this combined value into CO_2 equivalents. The methodological approach was consistent with the carbon allocation models developed for poplar plantations, as outlined earlier in the ESS3 section of the document.

The estimation of the annual above-ground biomass increment (AGBinc) followed the same procedure applied in ESS1, which involved reviewing and analysing available data sources, including scientific literature, forest inventory data, and indirect indicators. For the Servio Municipal Unit, Prosilio Kozani site in Greece (CS2), the available data were fragmented and methodologically inconsistent, reflecting differing definitions of production, growth indicators, typological classifications, and measurement units. As a result, direct comparisons between land cover types were limited. To ensure coherence across the deliverable, AGBinc values were therefore derived from harmonized data presented in the study “Improved large-area forest increment information in Europe through harmonization of National Forest Inventories” (Forest Ecology and Management, 562, 121913), which provides comparable annual growth estimates for most European countries and forest types.

The annual below-ground biomass increment (BGBinc) was calculated from AGBinc using the ratio between above- and below-ground biomass increments (AGBinc/BGBinc). The applied root-to-shoot ratios were based on findings from the literature, including Oliveira Rodríguez et al. (2018) and the Intergovernmental Panel on Climate Change (2003, 2006), selected due to their standardized methodologies across countries, ensuring a consistent estimation of BGBinc. Based on these sources, the ratio used for the industrial and commercial land-use scenario was assumed to represent approximately 20% of the grassland AGBinc-to-BGBinc ratio, while the scenario involving ground-mounted photovoltaic installations was assumed to retain 80% of the grassland coverage value (Table 46).

Table 46 Sources used for the estimation of below ground - above ground ratio (%).

CS2 (GRC) - types of management	AGBinc - BGBinc ratio (%)	Sources
Broad-leaf forest	0.43	IPCC (2003) Annex 3A.1.8
Coniferous forest	0.46	
Grassland	1.58	IPCC (2003) Annex 3A.1.8 Mokany, Raison & Prokushkin (2006)
Poplar cultivation	0.21	Oliveira (2018)

After calculating the values of the BGBinc from the ratio and the AGBinc values provided, the results were added and multiplied by the C fraction to account for the carbon content. The carbon content values in dry matter are assumed at approx. 50% values, supported by literature.

In the next step the results were converted to the CO_2 equivalent by multiplying the final value by 3.67 (ratio of the atomic mass of the molecules). The indicator reflects the annual flow of carbon sequestration associated with biomass growth, rather than long-term carbon stock changes (Table 47).

Table 47 Sources used for the estimation of C fraction of carbon content in dry mass.

CS2 (GRC) - types of management	C fraction of carbon content in dry matter	Source/Reference
Broad-leaf forest	0.46	IPCC (2003) Annex 3A.1 Dupouey (2010)
Coniferous forest	0.46	
Grassland	0.48	Shiferaw, Kassawmar, Zeleke (2022)
Poplar cultivation	0.48	Shiferaw, Kassawmar & Zeleke (2022)

The results for the region of Servio Municipal Unit, Prosilio Kozani site in Greece (CS2) show that the annual carbon sequestration for broadleaf forests is about 6,187 t (CO_2/ha/year), 11,194 t (CO_2/ha/year) for coniferous forest and the highest value for annual carbon sequestration resulted in poplar plantation at 30,641 t (CO_2/ha/year) for the. Grassland coverage was at a 13,635 t (CO_2/ha/year). Those results were used to provide background land use values for the evaluation of the values for Scenarios 1, 2 and 3.

ESS: MITIGATION OF CLIMATE CHANGE						
PL	Średnia roczna ilość biomasy nadziemnej z hektara (tDM/ha/yr)	Stosunek biomasy poniżej - powyżej gruntu	Średnia roczna ilość biomasy korzennej z hektara (tDM/ha/yr)	Średnie stężenie węgla w biomasie (%)	Sekwestracja węgla (kg/year/ha)	Roczna sekwestracja węgla wyrażona w t (CO_2/ha/year)
ENG	Average anual amount of above-ground biomass from ha (tDM/ha/yr)	Below ground - above ground ratio	Average annual amount of below biomass from ha (tDM/ha/yr)	Biomass mean concentration of carbon (%)	Carbon sequestration (t/year/ha)	Annual carbon sequestration expressed in t (CO_2/ha/year)
						Conversion factor from Carbon (C) to CO_2 equivalent
						3,67
CS2 (GRC) - Servio Municipal Unit, Prosilio Kozani						
Forest_broadleaf_poplar	2,56	0,43	1,102	0,46	1,686	6,187
Grassland	3,00	1,58	4,740	0,48	3,715	13,635
PV_groundmounted (80% grassland)	2,40	1,58	3,792	0,48	2,972	10,908
coniferous	2,57	1,58	4,061	0,46	3,050	11,194
poplar cultivation	15,00	0,21	3,150	0,46	8,349	30,641
Industrial of commercial units (20% grassland)	0,60	1,58	0,948	0,48	0,743	2,727

Figure 36 Calculations concerning the ESS3 indicator – annual carbon sequestration expressed in t (CO_2/ha/year) for the Servio Municipal Unit, Prosilio Kozani site in Greece (CS2).

For the Scenario 1 – NBS, the value of poplar plantations was assumed. The 2nd Scenario = industrial scenario for ESS3 considered 80% vegetation in AGBinc and BGBinc value due to a decreased but still present level of low-vegetation growth. For Scenario 3, the value of grasslands was assumed as an option for low-vegetation, recreational approach (Table 48).

Table 48 A summary of ESS3 - Annual carbon sequestration expressed in t CO_2/ha/year for the different CS2 land-use scenarios.

Land-use scenario	Scenario 1 - NBS, forests	Scenario 2 - Industrial scenario, photovoltaic panels	Scenario 3 - Recreational, meadows, pastures
ESS3 - Annual carbon sequestration expressed in t CO_2/ha/year	30.641	10.908	13.635

Funded by the European Union

6.2.4 Air quality mitigation (ESS4)

The evaluation of ESS4 analyses the capacity of tree and shrub canopies in urban, peri-urban, and rehabilitated post-industrial landscapes to remove air pollutants—especially particulate matter (PM10 and PM2.5)—via dry deposition processes. The key indicator applied is the annual removal of PM10, expressed in tonnes per hectare per year (t/ha/year). This methodology is based on the dry deposition model introduced by Tallis et al. (2011)., where:

$$\text{Absorption of } PM_{10} = \text{Flux (V) x Surface (SA) x Period (t) } (t/km^2/year)$$

where:

- Flux is the pollutant to the surface (amount removed per unit area and time), calculated by multiplying the deposition velocity of the pollutant (m/s), which depends on canopy structure and wind speed and the concentration of the pollutant in the atmosphere.
- Surface is the considered surface area multiplied by the surface area index functioning in a given area (LAI).
- Period accounts for the period of analysis in days, multiplied by the proportion of dry days and the proportion of non-leaf days.

The total annual pollutant removal is calculated by integrating deposition fluxes over the vegetated surface area of each land-use scenario. The above contributes to the calculation as follows:

- V = deposition velocity (m/s) x pollutant conc. (µg/m³)
  - Flux (µg/m³) was then converted to daily flux by multiplying it by 86400
- SA = LAI (m²/m²) x area of land considered (m²)
- t = period of analysis (days) x proportion of dry days (fraction) x proportion of on-leaf days (fraction)
  - Afterwards the absorption of PM_{10} was converted from (µg/m²/year) to (t/km²/year) by $x10^6$

The data for the Servio Municipal Unit, Prosilio Kozani site in Greece (CS2) involved land use scenarios for the broad-leaf forest, coniferous forest, mixed forest, pastures, grasslands and photovoltaic farm. For each component of the model, a literature review was conducted to establish the most suitable range of standardized values to ensure comparability. In instances where specific data for a component was unavailable, an average was derived from countries or regions with similar ecosystem types, allowing the results to remain compatible.

Regarding the deposition velocity by land use type, no data was found in the research for the Servio Municipal Unit, Prosilio Kozani region, however, comparable data were used from European, U.S. and Italian databases to provide a baseline. Data gathered from Marando et al. (2016), investigated deposition velocity in various vegetation types in mediterranean climate, its main reference point being Rome, Italy, using the i-Tree Eco dry deposition model (Table 49):

Table 49 Estimated deposition velocity in mediterranean climate by Marando et al. (2016).

Vegetation Type	Deposition Velocity (cm s^{-1})	Additional observations
Broadleaf trees (in-leaf)	0.5–1.5	Higher during full leaf area
Coniferous trees	1.0–2.0	Year-round interception
Grass/shrubs	0.2–0.8	Lower aerodynamic roughness

Another study by Mariarosa et al. (2019) provided information in dry deposition modelling and validation in urban and suburban Italy, representative of mediterranean and temperate climate (Table 50).

Funded by the European Union

Table 50 Estimated deposition velocity in regions managed as low-vegetation or industrial/urban sites by Mariarosa et al. (2019).

Land use type	Deposition Velocity (cm s^{-1})	Additional observations
Industrial surfaces	0.1–0.5	Smooth surfaces lower deposition
Suburban vegetation	0.3–1.2	Higher roughness enhances capture
Grasslands	0.2–0.6	Moderate

Considering the site at Servio Municipal Unit, Prosilio Kozani lays in the mediterranean climate belt, the above values were averaged for each land use type and used for further calculations.

The next component researched for the model was the pollutant concentration (μg/m^3). The values were provided from the WHO 2013, EU policy ranges and local monitoring such as Air Quality Index were used, which proved at a 25-45 μg m^{-3} value. An average of 35 μg m^{-3} was used.

Regarding the surface area, the values of the leaf area index (LAI) in various types of land use were taken into consideration (Table 51). Due to the lack of specific data regarding the above-mentioned land use types for the region, European and global data were considered.

Table 51 References for the leaf area index concerning chosen types of land use.

Land use type	LAI values	Represented region	Sources / References
Broad-leaf forest	5–8 (max values) 3–6 (urban average 3–4.5) 2–10 (broad global range)	France (temperate deciduous) Primarily U.S., global review Global synthesis	Le Dantec, Dufrêne, Saugier (2000) Nowak et al. (2017) Parker (2020)
Coniferous forest	6–11 3–6 (urban average 3–4.5) 2–10 (broad global range)	Pacific Northwest, U.S. Primarily U.S., global review Global synthesis	Turner et al. (2000) Nowak et al. (2017) Parker (2020)
Mixed forest	3–7 typical; up to 9 dense stands	Europe (multi-site comparison)	Sinan & Hasenauer (2025)
Pasture/ Grassland/ Shrub	2.0–4.5 (Wetland shrubs lower (2–3), wooded wetland stands up to 4.5)	Poland (Central Europe)	Leśny et al. (2007)

Area assumed for the calculation at this stage was a m2, after conversion km2. Regarding the period component, it was calculated by taking average of the range of the vegetation period for each type of land use. For the Prosilio Kozani site, the middle of the range was used from the mediterranean values (Table 52).

Table 52 Number of vegetative days for each land use type according to the climate type.

Land Use Type	Boreal	Temperate	Mediterranean	Subtropical	References/Sources
Coniferous Forest	120–180	180–220	200–240	250–300	EMEP (2016) GIOŚ (2018) Langner, Kull & Endlicher (2011) Chen (2015). Khan & Perlinger (2017) Vivanco et al. (2021)
Broadleaf Forest	140–190	190–220	220–260	280–320	
Grassland	150–190	200–240	220–300	280–320	
Cropland	140–180	180–220	250–320	280–330	

For the scenario regarding industrial land use type, including photovoltaic farm, the vegetative period was assumed the same as for a grassland. The proportion of dry days was assumed at

Funded by the European Union

60% according to Chervenkov & Slavov (2021), while the proportion of on-leaf days was assumed at 100%, due to already exclusively selected vegetative dry periods.

The results for the region of Servio Municipal Unit, Prosilio Kozani in Greece (CS1) presented in the figure below (Figure 37) show that the annual absorption of PM10 are as follows: 26,13 t/km²/year for broad-leaf forest, 41,91 t/km²/year for coniferous forest, 35,26 t/km²/year for mixed forest, 5,17 t/km²/year for pastures, 2,83 t/km²/year for grasslands and 0,57 t/km²/year for industrial land use/photovoltaic farm. Those results were used to provide background land use values for the evaluation of the values for Scenarios 1, 2 and 3.

For the Scenario 1 – NBS solutions the value of broad-leaf forest was assumed. Concerning Scenario 2, the industrial/photovoltaic land use was considered and for Scenario 3 the values for pastures were assumed, as shown in the table below (Table 53).

ESS: AIR PURIFICATION							
Seconds/day (s)	86 400						
		CS2 (GRC) - Servio Municipal Unit, Prosilio Kozani					
PL	EN	Broad-leaf forest	Coniferous forest	Mixed forest	Pasture	Grassland	Photovoltaic farm
Prędkość osiadania (m/s)	Deposition velocity (m/s)	0,010	0,015	0,013	0,005	0,004	0,001
Stężenie PM10 (µg/m³)	Pollutant conc. (µg/m³)	35,000	35,000	35,000	35,000	35,000	35,000
Przepływ (µg/m²/s) = Prędkość osiadania (m/s) x Stężenie PM10 (µg/m³)	**Flux (µg/m²/s) =** deposition velocity (m/s) x pollutant conc. (µg/m³)	0,350	0,525	0,455	0,175	0,140	0,035
Dzienny przepływ (µg/m²/dzień)	**Daily flux (µg/m²/day)**	30240	45360	39312	15120	12096	3024
Wskaźnik powierzchni (m²/m²)	Surface area index (LAI) (m²/m²)	6,000	7,000	6,500	2,000	1,500	1,200
Powierzchnia brana pod uwagę (m²)	Area of land (m²)	1,000	1,000	1,000	1,000	1,000	1,000
Powierzchnia (m²) = Wskaźnik powierzchni (m²/m²) x Powierzchnia brana pod uwagę (m²)	**Surface (m2) =** LAI (m²/m²) x area of land (m²)	6,000	7,000	6,500	2,000	1,500	1,200
Okres kwitnienia liści	Vegetation period (days)	240,000	220,000	230,000	285,000	260,000	260,000
Odsetek dni suchych	Proportion of dry days (fraction)	0,600	0,600	0,600	0,600	0,600	0,600
Odsetek dni wchłaniania przez dojrzały liść	Proportion of on-leaf days (fraction)	1,000	1,000	1,000	1,000	1,000	1,000
Okres = Okres kwitnienia liści (dni) x Odsetek dni suchych x Odsetek dni wchłaniania przez dojrzały	**Period =** period of analysis (days) x proportion of dry days (fraction) x proportion of on-leaf days	144,000	132,000	138,000	171,000	156,000	156,000
Wchłanianie PM10 (µg/m²/rok)	**Absorption of PM10 = Flux x Surface x Period (µg/m²/year)**	26127360	41912640	35262864	5171040	2830464	566092,8
Wchłanianie PM10 (t/km²/rok)	**Absorption of PM10 = Flux x Surface x Period (t/km²/year)**	**26,13**	**41,91**	**35,26**	**5,17**	**2,83**	**0,57**

Figure 37 Summary of the calculations involved in the calculations for ESS4 indicator – Absorption of PM10.

Funded by the European Union

Table 53 A summary of ESS4 - Annual removal of particulate matter PM10 particles [t/km²/year] results for the different CS2 land-use scenarios.

Land-use scenario	Scenario 1	Scenario 2	Scenario 3
ESS4 – Annual removal of PM10, expressed as [t/km²/year]	26.13	0.57	5.17

6.2.5 Temperature regulation (ESS5)

The assessment of temperature regulation potential was based on Landsat 8 satellite data processed into a Land Surface Temperature (LST) map using the ASTER database. The Advanced Spaceborne Thermal Emission and Reflection Radiometer Global Emissivity Database (ASTER GED) was developed by National Aeronautics and Space Administration's (NASA) Jet Propulsion Laboratory (JPL), California Institute of Technology. The ASTER GED product provides global emissivity maps of the Earth's land surface in five spectral bands. In addition to the mean emissivity and standard deviation maps for all five ASTER thermal infrared bands, the product also provides maps for mean land surface temperature (LST) and standard deviation.

The analysis focused on the day with the highest air temperature recorded in the last 10 years. For CS2, this was 2.08.2021. The analysis was carried out for the entire Servia Municipal Unit, within which CS2 is located. The study area was divided into land-use categories according to CLC 2018 (Corine Land Cover). The following (Figure 38) land-use categories were identified: coniferous forest (312), broad-leaved forest (311), mixed forest (313), water bodies (512), inland marshes (411), transitional woodland-shrub (324), land principally occupied by agriculture, with significant areas of natural vegetation (243), natural grasslands (321), complex cultivation patterns (242), discontinuous urban fabric (112), mineral extraction sites (131), non-irrigated arable land (211), pastures (231), industrial or commercial units (121), permanently irrigated land (212), sclerophyllous vegetation (323).

Funded by the European Union

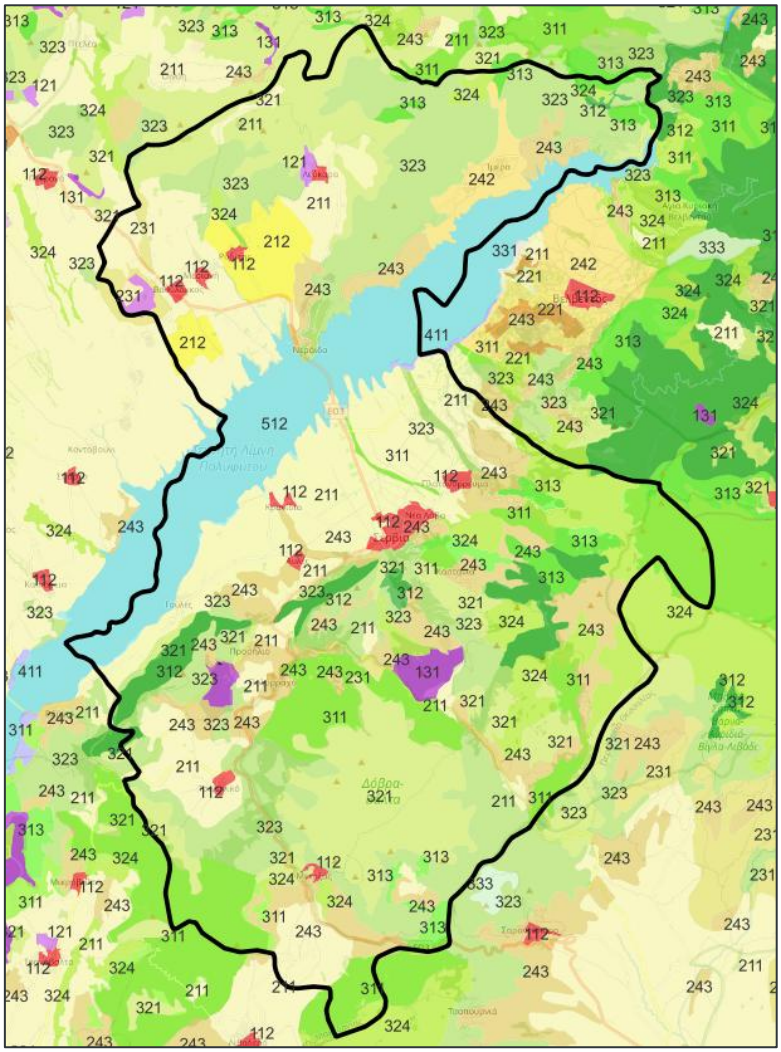

Figure 38 CLC 2018 land cover pattern for CS2.

In next step, using GIS analytical tools, the mean temperature values were calculated for each land-use type. The temperature regulation potential was calculated by relating the mean temperature values to the highest intended mean value for a given land use. The calculation results are presented in Table 54.

Table 54 Cooling potential of land cover – CS2.

CLC 2018 Land Cover class	Mean T [°C]	Cooling potential [°C]
Coniferous forest	37.3	12.9
Broad-leaved forest	38.9	11.3
Mixed forest	38.9	11.3
Water bodies	40.2	10.0
Inland marshes	42.0	8.2
Transitional woodland-shrub	42.4	7.8
Sclerophyllous vegetation	43.9	6.3
Land principally occupied by agriculture, with significant areas of natural vegetation	45.0	5.2
Natural grasslands	45.9	4.3

Funded by the European Union

CLC 2018 Land Cover class	Mean T [°C]	Cooling potential [°C]
Complex cultivation patterns	47.0	3.2
Discontinuous urban fabric	48.1	2.2
Mineral extraction sites	48.2	2.0
Non-irrigated arable land	48.6	1.6
Permanently irrigated land	48.6	1.6
Pastures	48.7	1.5
Industrial or commercial units	50.2	0.0

The results were then normalised to a scale from 1 to 10, where 1 denotes no potential and 10 the highest potential of the ecosystem service. The projected temperature value for the analysed land-use scenarios was adopted assuming that Scenario 1 corresponds to mixed forests, Scenario 2 to industrial or commercial units, and Scenario 3 to pastures. The results of the potential analysis for each scenario are presented in Table 55.

Table 55 Evaluation of cooling potential for analysed Scenarios – CS2.

Corine Land Cover Class	Cooling potential [-]
Discontinuous urban fabric	2.5
Industrial or commercial units	1.0
Secenario 2 - Industrial scenario, photovotaic panels	**1.0**
Mineral extraction sites	2.4
Non-irrigated arable land	2.1
Permanently irrigated land	2.1
Pastures	2.0
Secenario 3 - Recreational, meadows, pastures	**2.0**
Complex cultivation patterns	3.2
Land principally occupied by agriculture, with significant areas of natural vegetation	4.6
Broad-leaved forest	8.9
Coniferous forest	10.0
Mixed forest	8.9
Secenario 1 - NBS, forests	**8.9**
Natural grasslands	4.0
Sclerophyllous vegetation	5.4
Transitional woodland-shrub	6.4
Inland marshes	6.7
Water bodies	8.0

6.2.6 Cultural- direct, in-situ and outdoor interactions with living systems (ESS6)

Due to the large size of the administrative unit, CLC data was used to assess its potential for recreational purposes. Following land cover classes have been identified as green recreation areas: deciduous forests (CLC 311), coniferous forests (CLC 312), mixed forests CLC 313),

Funded by the European Union

natural grasslands (CLC 321), sclerophyllous vegetation (CLC 323), transitional woodland-shrub (CLC 324), inland marshes (411).

The potential for providing recreational services was also assessed for the area of the contaminated area (CS 2). The brownfield site under analysis is located away from densely populated residential areas. The future use for recreational purposes will provide 13 residents with access to this type of area. Within the analysed administrative boundaries, there are green areas with a recreational function that serve recreational function for 648 residents (Sclerophyllous vegetation in the south- part of the administrative boundaries).

With regard to these values, the development of the analyzed contaminated site (CS2) will not result in a significant increase in the availability of green areas for residents. The potential of existing and potential green areas with recreational functions on a scale of 1 to 10 is shown in the figure below (Figure 39).

Funded by the European Union

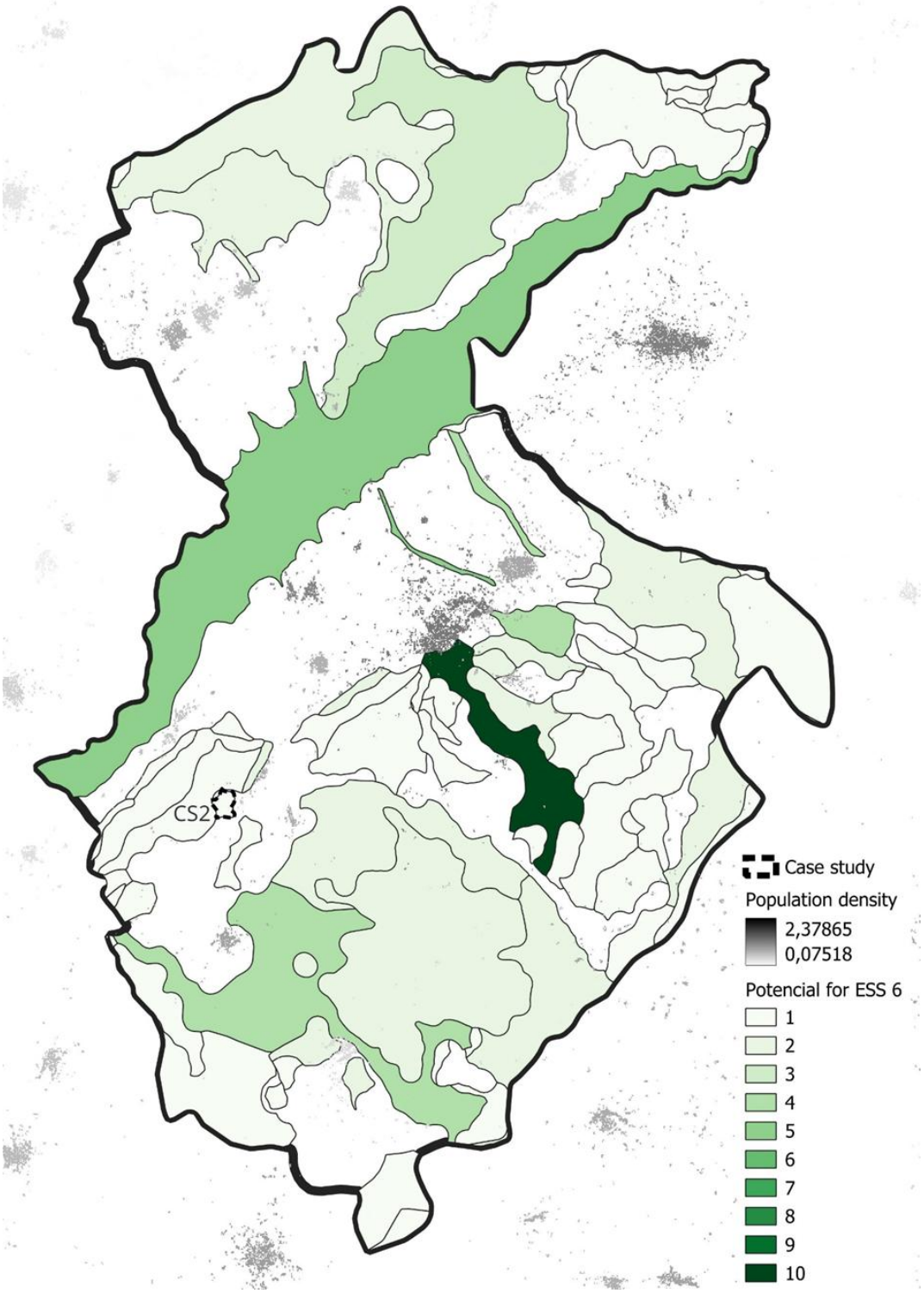

Figure 39 Cultural services: Interactions with natural environment for CS2.

In the adopted land use options, only the scenario 1 (Afforestation) and scenario 3 (Grassland cover), meet the criteria for green areas with a recreational function. Compared to other green areas within the analyzed administrative boundaries, this scenario has very little potential for providing cultural services (Table 56).

Funded by
the European Union

Table 56 A summary of ESS6 results for the different CS2 land-use scenarios.

Land-use scenario	Scenario 1	Scenario 2	Scenario 3
ESS6 [Number of residents within 300 meters of a green recreational area]	13	0	13

6.2.7 Energy properties (ESS7)

The performance of photovoltaic installations for CS2 was estimated using an application provided by the EC: Photovoltaic Geographical Information System [https://re.jrc.ec.europa.eu/pvg_tools/en/tools.html]. This application provides data on solar radiation and energy production from photovoltaic (PV) systems globally. Following the application instructions, the performance of photovoltaic installations was estimated based on the assumption presented in Table 57.

Table 57 Assumptions and settings used for PV calculation for CS2.

PV Performance Modelling Parameters						
Solar radiation database:	PV technology:	Installed peak PV power	System loss	Mounting position	Slope	Azimuth:
PVGIS-SARAH3	Crystalline Silicon (original)	1 kWp	14%	Free-standing	35°	0°

In the table below (Table 58), the CS2 is characterised in relation to the analysis conducted.

Table 58 Site characteristic.

Case Study	Coordinates (center)		Elevation	Area [ha]
	Latitude	Longitude		
CS2	40.144	21.932	622	33.3

To estimate the electricity production capacity for this CS1, the maximum feasible installed PV capacity (kWp) was determined from the available area. For the purposes of the analysis, it was assumed that 1 kWp corresponds to a PV system area of 6 m². Because the full area could not be developed under real conditions (e.g., spacing between modules, internal roads, technical buildings, fencing, and grid infrastructure), a Surface Coverage Ratio (α = 50%) was used to reflect practical land take. This value was derived from an assessment of operating photovoltaic farms with total areas ranging from 27 ha to 300 ha. Table below (Table 59) shows the calculated performance of PV installations for CS2. The estimated yearly in-plane irradiation is 1 758.27 kWh/m², taking into account factors such as system losses (14%). The annual electricity production is determined to be 1 363.18 kWh per 1 kWp installed. The table presents the estimated value of electricity production, considering the surface area calculated using the Ideal Value Model and near-real conditions determined by the Surface Coverage Ratio. Under ideal conditions, the annual energy production could reach 75.7 GWh. Based on the Surface Coverage Ratio, the annual energy production is projected to be 37.6 GWh.

Table 59 Yearly PV energy production for CS2.

Yearly PV energy production [kWh]	1 363.18
Yearly in-plane irradiation [kWh/m^2]	1 758.27

Funded by the European Union

Year-to-year variability [kWh]		50.07
Changes in output due to		
-Angle of incidence [%]		-2.64
-Spectral effects [%]		0.84
Temperature and low irradiance [%]		-8.18
Total loss [%]		-22.47
Max. kWp needed [kWp]		55 500
Energy production (Ideal Value Model)	75.7	13.2
Energy production (Surface Coverage Ratio)	37.6	6.6

Figures below (Figure 40) show a report from the Photovoltaic Geographical Information System application (estimating annual energy production for CS2).

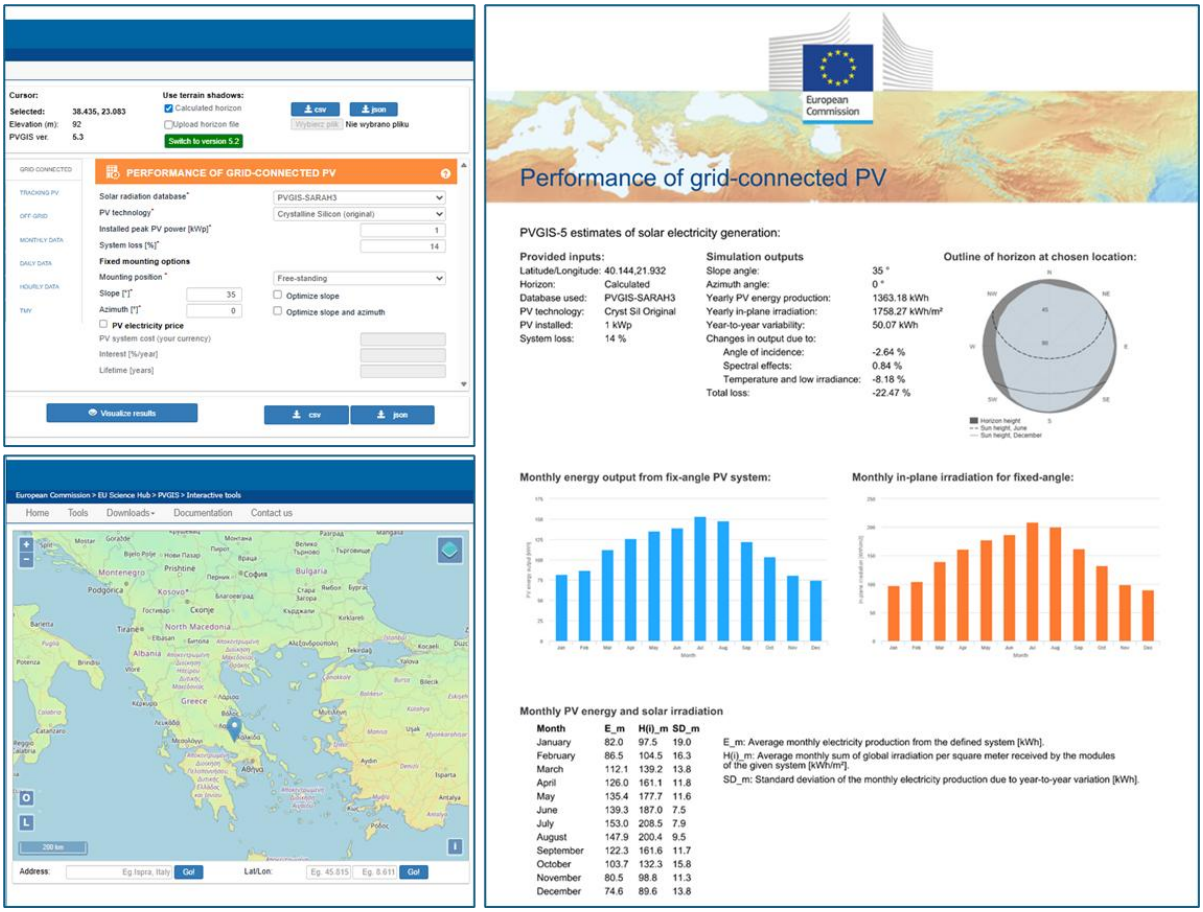

Figure 40 CS2 – Performance of grid-connected PV.

The ESS7 results for CS2 are summarised in the table below (Table 60).

Table 60 A summary of ESS7 (Energy properties) results for the different CS2 land-use scenarios.

Land-use scenario	Scenario 1	Scenario 2	Scenario 3
ESS7: Potential energy production [GWh/y].	0.0	37.6	0.0

Funded by the European Union

6.3 Ecosystem services assessment for CS3

In this section, the valuation of ESS for CS3 (Odiel Basin, ES – ES61) was presented with reference to local site conditions and the analysed redevelopment scenarios, while maintaining consistent calculation assumptions across the entire report

6.3.1 Biomass production (ESS1)

The ESS1 assessment for CS3 was based on the EP indicator derived from AGBinc using the relationship :

$$EP = AGBinc \times CV$$

Where:
- CV is the calorific value of the biomass (GJ·t^{-1} d.m.), adopted in line with the ESS1 service card,
- AGBin above-ground biomass AGBinc (t d.m.·ha^{-1}·year^{-1}),
- EP is energy potential.

Available studies on biomass increment in forests were reviewed (Table 61), however, a wide range of values was identified, largely due to definitional and methodological differences. In several sources, biomass increment is not reported directly; instead, carbon sequestration is provided (e.g., Mg C·ha^{-1}·year^{-1}) and then converted to dry biomass using an assumed carbon fraction (e.g., CF = 0.47 following IPCC). This additional conversion step further limits comparability between studies.

Therefore, consistent with the approach applied throughout the report, harmonised results from the publication “Improved large-area forest increment information in Europe through harmonisation of National Forest Inventories” (Forest Ecology and Management, 562, 121913) were adopted as both the input dataset and the reference benchmark. This source provides comparable AGB increment data at the country and forest-type levels after harmonising definitions and methodology.

Table 61 Annual biomass production on different types of land in Spain.

Land type	Value	Unit	Carbon fraction (t C / t d.m.)	Mean annual biomass increment (computed)	Computed unit	Biomass definition	Method / notes	Source (full reference)
Deciduous broadleaved forest	1.065	Mg C/ha/yr	0.47	2.266	t /ha/yr	Dry biomass increment computed from reported carbon sequestration using IPCC CF=0.47.	Computed value shown as dry matter biomass increment; do not interpret as aboveground-only unless specified. .	[González-Díaz, et al., 2019]
Deciduous broadleaved forest	0.715	Mg C/ha/yr	0.47	1.521	t /ha/yr			
Deciduous broadleaved forest	2.048	Mg C/ha/yr	0.47	4.357	t /ha/yr			
Deciduous broadleaved forest	1.363	Mg C/ha/yr	0.47	2.900	t /ha/yr			
Deciduous broadleaved forest	2.614	Mg C/ha/yr	0.47	5.562	t /ha/yr			

Land type	Value	Unit	Carbon fraction (t C / t d.m.)	Mean annual biomass increment (computed)	Computed unit	Biomass definition	Method / notes	Source (full reference)
Deciduous broadleaved forest	2.729	Mg C/ha/yr	0.47	5.806	t /ha/yr			
Coniferous forest	0.728	Mg C/ha/yr	0.47	1.549	t /ha/yr			
Coniferous forest	2.040	Mg C/ha/yr	0.47	4.340	t /ha/yr			
Coniferous forest	1.708	Mg C/ha/yr	0.47	3.634	t /ha/yr			
Coniferous forest	0.010	Mg C/ha/yr	0.47	0.021	t/ha/yr			
Coniferous forest	1.302	Mg C/ha/yr	0.47	2.770	t/ha/yr			
Coniferous forest	1.818	Mg C/ha/yr	0.47	3.868	t /ha/yr			
Coniferous forest	1.881	Mg C/ha/yr	0.47	4.002	t /ha/yr			
Poplar monoculture (short rotation coppice)	10.900	Mg dry biomass/ha/yr		10.900	t /ha/yr	Dry biomass production (materia seca) – mean	Average production for management scenario 'deficiente (D)'; Q1–Q99 5.6–14.3	6º Congreso Forestal Español, paper 6CFE01-095
Poplar monoculture (short rotation coppice)	15.300	Mg dry biomass/ha/yr		15.300	t /ha/yr	Dry biomass production (materia seca) – mean	Average production for management scenario 'apropiada (P)'; Q1–Q99 8.3–19.2	6º Congreso Foresta l Español, paper 6CFE01-095
Grassland / meadow (dehesa natural pastures)	1000 – 2700	kg DM/ha/yr			t /ha/yr (optional conversion)	Annual pasture production (dry matter)	Range depends on site condition and year (citing López-Díaz et al. 2009). Deterministic unit conversion: 1000–2700 kg DM/ha/yr = 1.0–2.7 t DM/ha/yr.	AGFORWARD system description: Iberian Dehesas, Spain (Moreno & Cáceres)

Funded by the European Union

For Spain, the following AGBinc values were applied: 2.24 t d.m.·ha^{-1}·year^{-1} for coniferous forests and 2.05 t d.m.·ha^{-1}·year^{-1} for broadleaved forests, with CV = 18.5 GJ per t d.m. (Table 62).

Table 62 Parameters for the biomass energy potential for CS3 (ES61).

CLC clasification	Couling Land Cover	AGBinc (tDM/ha/yr)	CV (GJ/tDM)	EP (GJ/ha/yr)
3.1.1	Broad-leaved forest	2.05	18.5	37.9
1.4.1	Green urban areas -grassland or lawns	3.00	17.5	52.5
1.2.1	Industrial - PV installation (80% grassland)	2.40	17.5	42.0
3.1.2	Coniferous forest	2.24	18.5	41.4
3.2.4	Transitional woodland/shrub (poplar plantations)	13.10	18.6	243.1
1.2.1	Industrial buildings and halls (20% grassland)	0.60	17.5	10.5

The AGBinc value for the scenario 1 (poplar plantations) was adopted from literature on poplar plantations, where dry biomass production is reported directly. Two values were compiled (10.9 and 15.3 t d.m.·ha^{-1}·year^{-1}), reflecting different management variants. For the calculations, an intermediate value of 13.10 t d.m.·ha^{-1}·year^{-1} was applied as representative for the scenario (CV = 18.6 GJ per t d.m.). For the 2nd scenario (grassland)

AGBinc = 3.00 t d.m.·ha^{-1}·year^{-1}

and **CV = 17.5 GJ per t d.m.**

were adopted as working values, reflecting relatively productive grassland conditions within the analysed setting (Table 63).

Table 63 Estimated annual above-ground biomass increment (AGBinc) for grasslands in NUTS2 regions – assumptions and literature-based justification.

NUTS2	Region	Grassland type	Estimated AGB inc (td.m.·ha^{-1}·yr^{-1})	Factors	Citations
ES61	Andalusia	Mediterranean grasslands	**2-4**	Mediterranean seasonally dry grasslands: water limitation, shorter growing season, and lower productivity than temperate meadows	[Shi et al., 2023] [Obermeier et al., 2018]

For industrial classes, fixed grassland equivalent shares were assumed in accordance with the methodology of the report: for PV installations, 80% of the area with a grassland function was assumed (AGBinc = 2.40 t d.m.·ha^{-1}·year^{-1}), while for built-up areas (buildings and halls) 20% of the grassland equivalent (AGBinc = 0.60 t DM·ha^{-1}·year^{-1}) was assumed, with a constant CV = 17.5 GJ/t DM. The final results are presented in Table 64.

Table 64 A summary of ESS1 (Biomass production) results for the different CS3 land-use scenarios.

Land-use scenario	Scenario 1	Scenario 2	Scenario 3
Energy potential [GJ/ha/year]	243	42	52.5

Funded by the European Union

6.3.2 Regulation of soil quality (ESS2)

In this section, the ESS2 indicator (regulation of soil quality) for CS3 was estimated as the potential for metal accumulation in plant biomass under the analysed land-use scenarios. As part of the literature review, concentration ranges of several metals in plant biomass were compiled e.g. cadmium, lead, zinc, copper, and nickel. However, for valuation purposes, one representative metal was selected: cadmium (Cd). Cadmium is frequently reported in environmental studies, it has no nutrient function (unlike Zn or Cu), and its accumulation in plant tissues provides a useful indicator of contamination pressure. In addition, Cd is often more mobile and more readily translocated to above-ground plant parts than Pb, which increases its suitability for scenario comparisons based on AGB.

As part of the parameterisation of metal concentrations in conifer biomass, relevant literature sources were reviewed. Data for needles are widely available, but they show high variability depending on species, site conditions, anthropogenic pressure, and the age of the assimilatory tissues. At the same time, many studies focus on needles or bark as biomonitors and do not provide comparable values for stem wood, nor a consistent "needles versus stem wood" dataset for the full set of metals. For this reason, instead of averaging results from heterogeneous studies, an approach based on one internally consistent dataset was adopted, covering both needles and stem wood analysed with the same methodology. The study by Skonieczna et al. (2014) was selected as the baseline source. In that work, 15 *Pinus sylvestris* trees from five stands were analysed. The investigated forests were located in an area influenced by anthropogenic pressures, but not in the immediate vicinity of point emission sources.

For the assessment, mean concentrations of Cd, Zn, Pb, and Cu were introduced for needles (as a representative of the "leaf" fraction) and for stem wood (as a representative of the "stem" fraction). Cadmium was then used for the subsequent valuation step.

For poplar plantations, several literature sources were reviewed. As in other cases, it was found that experimental conditions were often not comparable between studies. Therefore, the focus was placed on a single publication that reported concentrations in poplar leaves and shoots in a format suitable for comparison across case studies

Based on the reviewed evidence, Pilipović et al. (2019) was adopted as the source of ESS2 parameters for poplar plantations, as it provides a coherent empirical dataset covering both leaves and shoots/stems, analysed using the same methodology and under the same experimental conditions. This allowed the "leaf versus wood/shoots" fractions to be separated directly, without merging heterogeneous studies and without additional assumption-based conversions. In addition, the study reports several metals (including Cd, Zn, Pb, and Cu) in a way that supported the selection of values representative of moderate anthropogenic pressure, thereby improving comparability between land-use scenarios within the ESS2 assessment.

For Scenario with grassland, an above-ground biomass (AGB)-based approach was applied, using metal concentration ranges in herbaceous plant tissues as reported in the literature. To reflect the typical spread of values associated with different levels of anthropogenic influence, three pressure levels were compiled (moderate, heavy, and extreme), representing, respectively, urban and transport impacts, post-mining areas, and locations in the immediate vicinity of smelters.

Funded by
the European Union

However, for the purpose of the ESS2 valuation, the moderate contamination variant was adopted, as it was considered representative of the common anthropogenic background conditions observed across the CS landscape and the analysed land-use scenarios. This choice reduced the influence of extreme concentration values that could otherwise dominate the result, and it ensured that differences in ESS2 were driven primarily by land-cover type and AGB magnitude rather than by exceptional, localised point sources of pollution.

The input data used for CS3 are identical to those described for CS1 in Section 6.1.2. Table below (Table 65) provides a concise overview of the heavy metal concentration datasets applied in the biomass assessment and includes references to the corresponding detailed tables in Section 6.1.2

Table 65 Heavy metal concentrations in biomass used for ESS2 parameterisation (data sources and table references).

No.	Heavy metal concentrations in the biomass	Reference table
1	Broadleaf species	Table 16 Heavy metal concentrations in the biomass of broadleaf species.
2	Conifer species	Table 17 Heavy metal concentrations in the biomass of conifer species.
3	Poplar and willow crops.	Table 18 Heavy metal concentrations in the biomass of poplar and willow crops.
4	Grassland species	Table 19 Heavy metal concentrations in the aboveground biomass of grassland species.

Table below (Table 66) presents the input parameters and calculation outputs used to estimate the ESS2 indicator for CS3 (ES61), expressed as the potential annual cadmium (Cd) accumulation in above-ground plant biomass. It combines AGBinc values (from ESS1) with tissue Cd concentrations and harvest fractions to derive Cd concentration in harvested biomass and the resulting Cd removal per hectare and year, in accordance with the methodology described in Section 4.3

Table 66 Calculation sheet for EES2 (Cd): biomass increment, concentration assumptions and annual removal.

Corine Land Cover	AGBinc (tDM/ha/yr) [from ESS1]	f_leaf (season harvest) [0-1]	Cd_C_leaf (mg/kg DM) [input]	Cd_C_stem (mg/kg DM) [input]	Cd_C_harvest (mg/kg DM) [calc]	Cd_Removal (g/ha/yr) [calc]
Broad-leaved forest	2.05	0.2	0.4	0.1	0.16	0.3
Green urban areas - grassland or lawns	3.00	1	0.75		0.75	2.3
Industrial - PV installation (80% grassland)	2.40	1	0.6		0.6	1.4
Coniferous forest	2.24	0.2	0.1	0.24	0.212	0.5
Transitional woodland/shrub (poplar plantations)	13.10	0.2	7.85	3.25	4.17	54.6
Industrial - buildings and halls (20% grassland)	0.60	1	0.15		0.15	0.1

Table below (Table 67) summarises the ESS2 results for CS3 across the analysed land-use scenarios. Values are reported as the estimated potential annual pollutant (Cd) accumulation in above-ground biomass (g/ha/year) enabling direct comparison between scenarios under a consistent parameter set.

Table 67 A summary of ESS2 (Regulation of soil quality) results for the different CS3 land-use scenarios.

Land-use scenario	Scenario 1	Scenario 2	Scenario 3
Potential annual pollutant accumulation [g/ha/year]	54.6	1.4	2.3

6.3.3 Mitigation of climate change (carbon dioxide sequestration) (ESS3)

Evaluation for ESS3 was based on annual carbon sequestration expressed in t CO_2/ha/year as its indicator. Total carbon sequestration was calculated as the sum of above-ground biomass and below-ground carbon accumulation, which was later converted to CO_2 equivalent. The methodology followed the carbon allocation models for poplar plantations, as specified in the ESS3 card earlier in the document.

Acquiring information about the AGBinc followed the same procedure as described in ESS1, which involved analysing the accessible sources of data such as literature, inventory data and indirect indicators. For the Minas de Riotinta, Odiel Basin site in Spain (CS3) the data proved methodologically inconsistent and dispersed, which resulted in various definitions of production, growth, typological ranges or units. Therefore, a direct comparison between the coverage types was limited. The values for AGBinc across the deliverable are based on the harmonized data sourced from the "Improved large-area forest increment information in Europe through harmonization of National Forest Inventories" (Forest Ecology and Management, 562, 121913), which provided comparable results regarding the annual growth across most of the countries regarding forest types.

The BGBinc value was derived from the AGBinc value by using the AGBinc / BGBinc, annual above- and below-ground biomass ratio. The root-to-shoot ratio was based upon the literature findings such as Oliveira Rodríguez et al. (2018) and Intergovernmental Panel on Climate Change in 2003 and 2006 due to their unified methodology across countries, to best estimate the BGBinc. Based on those findings, the ratio for industrial and commercial land use scenario was calculated based on the value of about 20% of the grassland AGBinc to BGBinc ratio, and the scenario assuming the ground-mounted photovoltaic farm designation accounted for 80% of the grassland coverage value. The literature data collected for the analysis are summarised in the Table 68 and Table 69.

Table 68 Sources used for the estimation of below ground - above ground ratio (%).

CS3 (ESP) - types of management	AGBinc - BGBinc ratio (%)	Sources
Broad-leaf forest	0.43	IPCC (2003) Annex 3A.1.8
Coniferous forest	0.46	
Grassland	3.50	Cañellas & San Miguel Ayanz (2000)
Poplar cultivation	0.21	Oliveira (2018)

After calculating the values of the BGBinc from the ratio and the AGBinc values provided, the results were added and multiplied by the C fraction to account for the carbon content. The carbon content values in dry matter are assumed at approx. 50% values, supported by literature.

In the next step the results were converted to the CO_2 equivalent by multiplying the final value by 3,67 (ratio of the atomic mass of the molecules). The indicator reflects the annual flow of carbon sequestration associated with biomass growth, rather than long-term carbon stock changes.

Funded by the European Union

Table 69 Sources used for the estimation of C fraction of carbon content in dry mass.

CS3 (ESP) - types of management	C fraction of carbon content in dry matter	Source/Reference
Broad-leaf forest	0.46	IPCC (2003) Annex 3A.1 Dupouey (2010)
Coniferous forest	0.46	
Grassland	0.48	Shiferaw, Kassawmar, Zeleke (2022)
Poplar cultivation	0.48	Shiferaw, Kassawmar & Zeleke (2022)

The results for the region of Minas de Riotinto, Odiel Basin site in Spain (CS3) (Figure 41) show that the annual carbon sequestration for broadleaf forests is about 4,949 t (CO_2/ha/year), 5,521 t (CO_2/ha/year) for coniferous forest and the highest value for annual carbon sequestration resulted in poplar plantation at 26,760 t (CO_2/ha/year) for the. Grassland coverage was similar at a 23,782 t (CO_2/ha/year). Those results were used to provide background land use values for the evaluation of the values for Scenarios 1, 2 and 3.

ESS: MITIGATION OF CLIMATE CHANGE

PL	Średnia roczna ilość biomasy nadziemnej z hektara (tDM/ha/yr)	Stosunek biomasy poniżej - powyżej gruntu	Średnia roczna ilość biomasy korzennej z hektara (tDM/ha/yr)	Średnie stężenie węgla w biomasie (%)	Sekwestracja węgla (kg/year/ha)	Roczna sekwestracja węgla wyrażona w t (CO_2/ha/year)
ENG	Average anual amount of above-ground biomass from ha (tDM/ha/yr)	Below ground - above ground ratio	Average annual amount of below biomass from ha (tDM/ha/yr)	Biomass mean concentration of carbon (%)	Carbon sequestration (t/year/ha)	Annual carbon sequestration expressed in t (CO_2/ha/year)
						Conversion factor from Carbon (C) to CO_2 equivalent
						3,67
CS3 (ESP) - Minas de Riotinta, Odiel Basin						
Forest_broadleaf_poplar	2,05	0,43	0,882	0,46	1,348	4,949
Grassland	3,00	3,50	10,500	0,48	6,480	23,782
PV_groundmounted (80% grassland)	2,40	1,58	3,792	0,48	2,972	10,908
coniferous	2,24	0,46	1,030	0,46	1,504	5,521
poplar cultivation	13,10	0,21	2,751	0,46	7,291	26,760
Industrial of commercial units (20% grassland)	0,60	1,58	0,948	0,48	0,743	2,727

Figure 41 Calculations concerning the ESS3 indicator – annual carbon sequestration expressed in t (CO_2/ha/year) for the Minas de Riotinto, Odiel Basin site in Spain (CS3).

For the Scenario 1 – NBS solutions, the value of poplar plantations was assumed. The 2nd Scenario = industrial scenario for ESS3 considered 80% vegetation in AGBinc value due to a decreased but still present level of low-vegetation growth. For Scenario 3, the value of grasslands was assumed as an option for low-vegetation, recreational approach. The summary results of the ESS3 assessment are presented in Table 70.

Table 70 A summary of ESS3 - Annual carbon sequestration expressed in t CO_2/ha/year for the different CS3 land-use scenarios.

Land-use scenario	Scenario 1	Scenario 2	Scenario 3
ESS3 - Annual carbon sequestration expressed in t CO_2/ha/year	26,760	10,908	23,782

6.3.4 Air quality mitigation (ESS4)

The assessment of ESS4 examines how tree and shrub canopies in urban, peri-urban, and restored post-industrial environments remove air pollutants -particularly particulate matter (PM10 and PM2.5) - through dry deposition. The primary metric used is the yearly removal of PM10,

Funded by the European Union

reported in kilograms per hectare per year (kg/ha/year). This approach follows the dry deposition framework developed by Tallis et al. (2011)., where:

$$\text{Absorption of } PM_{10} = \text{Flux (V) x Surface (SA) x Period (t) } (t/km^2/year)$$

where:

- Flux is the pollutant to the surface (amount removed per unit area and time), calculated by multiplying the deposition velocity of the pollutant (m/s), which depends on canopy structure and wind speed and the concentration of the pollutant in the atmosphere.
- Surface is the considered surface area multiplied by the surface area index functioning in a given area (LAI).
- Period accounts for the period of analysis in days, multiplied by the proportion of dry days and the proportion of non-leaf days.

The total annual pollutant removal is calculated by integrating deposition fluxes over the vegetated surface area of each land-use scenario. The above contributes to the calculation as follows:

- V = deposition velocity (m/s) x pollutant conc. (µg/m³)
  - Flux (µg/m³) was then converted to daily flux by multiplying it by 86400
- SA = LAI (m²/m²) x area of land considered (m²)
- t = period of analysis (days) x proportion of dry days (fraction) x proportion of on-leaf days (fraction)
  - Afterwards the absorption of PM_{10} was converted from (µg/m²/year) to (t/km²/year) by $x10^6$

The data for the Minas de Riotinto, Odiel Basin site in Spain (CS3) involved land use scenarios for the broad-leaf forest, coniferous forest, mixed forest, pastures, grasslands and photovoltaic farm. For each component of the model, a literature review was conducted to establish the most suitable range of standardized values to ensure comparability. In instances where specific data for a component was unavailable, an average was derived from countries or regions with similar ecosystem types, allowing the results to remain compatible. Regarding the deposition velocity by land use type, no data was found in the research for the Minas de Riotinto, Odiel Basin region, however, comparable data were used from European, U.S. and Italian databases to provide a baseline. Data gathered from Marando et al. (2016), investigated deposition velocity in various vegetation types in mediterranean climate, its main reference point being Rome, Italy, using the i-Tree Eco dry deposition model (Table 71).

Table 71 Estimated deposition velocity in mediterranean climate by Marando et al. (2016).

Vegetation Type	Deposition Velocity (cm s^{-1})	Additional observations
Broadleaf trees (in-leaf)	0.5–1.5	Higher during full leaf area
Coniferous trees	1.0–2.0	Year-round interception
Grass/shrubs	0.2–0.8	Lower aerodynamic roughness

Another study by Mariarosa et al. (2019) provided information in Dry deposition modelling and validation in urban and suburban Italy, representative of mediterranean and temperate climate (Table 72).

Table 72 Estimated deposition velocity in regions managed as low-vegetation or industrial/urban sites by Mariarosa et al. (2019).

Land use type	Deposition Velocity (cm s^{-1})	Additional observations
Industrial surfaces	0.1–0.5	Smooth surfaces lower deposition
Suburban vegetation	0.3–1.2	Higher roughness enhances capture
Grasslands	0.2–0.6	Moderate

Considering the site at Minas de Riotinto, Odiel Basin lays in the mediterranean climate belt, the above values were averaged for each land use type and used for further calculations. The next

Funded by
the European Union

component researched for the model was the pollutant concentration (µg/m³). The values were based on investigations by Pérez-Vizcaín et al. (2026), which proved at a 25-45 µg m^{-3} value. An average of 35 µg m^{-3} was used. Regarding the surface area, the values of the leaf area index (LAI) in various types of land use were taken into consideration. Due to the lack of specific data regarding the above-mentioned land use types for the region, European and global data were considered (Table 73).

Table 73 References for the leaf area index concerning chosen types of land use.

Land use type	LAI values	Represented region	Sources / References
Broad-leaf forest	5–8 (max values) 3–6 (urban average 3–4.5) 2–10 (broad global range)	France (temperate deciduous) Primarily U.S., global review Global synthesis	Le Dantec, Dufrêne, Saugier (2000) Nowak et al. (2017) Parker (2020)
Coniferous forest	6–11 3–6 (urban average 3–4.5) 2–10 (broad global range)	Pacific Northwest, U.S. Primarily U.S., global review Global synthesis	Turner et al. (2000) Nowak et al. (2017) Parker (2020)
Mixed forest	3–7 typical; up to 9 dense stands	Europe (multi-site comparison)	Sinan & Hasenauer (2025)
Pasture/ Grassland/ Shrub	2.0–4.5 (Wetland shrubs lower (2–3), wooded wetland stands up to 4.5)	Poland (Central Europe)	Leśny et al. (2007)

Area assumed for the calculation at this stage was a m^2, after conversion km^2. Regarding the period component, it was calculated by taking average of the range of the vegetation period for each type of land use. Based on the data presented in Table 74 for the Minas de Riotinto site, the middle of the range was used from the mediterranean values.

Table 74 Number of vegetative days for each land use type according to the climate type.

Land Use Type	Boreal	Temperate	Mediterranean	Subtropical	References/Sources
Coniferous Forest	120–180	180–220	200–240	250–300	EMEP (2016) GIOŚ (2018) Langner, Kull & Endlicher (2011) Chen (2015). Khan & Perlinger (2017) Vivanco et al. (2021)
Broadleaf Forest	140–190	190–220	220–260	280–320	
Grassland	150–190	200–240	220–300	280–320	
Cropland	140–180	180–220	250–320	280–330	

For the scenario regarding industrial land use type, including photovoltaic farm, the vegetative period was assumed the same as for a grassland. The proportion of dry days was assumed at 60% according to Chervenkov & Slavov (2021), while the proportion of on-leaf days was assumed at 100%, due to already exclusively selected vegetative dry periods. The results for the region of Minas de Riotinto, Odiel Basin in Spain (CS3) presented in the figure below (Figure 42) show that the annual absorption of PM10 are as follows: 18,87 t/km²/year for broad-leaf forest, 38,92 t/km²/year for coniferous forest, 29,39 t/km²/year for mixed forest, 7,00 t/km²/year for pastures, 5,11 t/km²/year for grasslands and 0,61 t/km²/year for industrial land use/photovoltaic farm. Those results were used to provide background land use values for the evaluation of the values for Scenarios 1, 2 and 3 (Figure 42). For the Scenario 1 – NBS solutions the value of broad-leaf forest was assumed. Concerning Scenario 2, the industrial/photovoltaic land use was considered and for Scenario 3 the values for pastures were assumed, as shown in (Table 75).

Funded by the European Union

ESS: AIR PURIFICATION							
Seconds/day (s)	86 400						
		CS3 (ESP) - Minas de Riotinta, Odiel Basin					
PL	EN	Broad-leaf forest	Coniferous forest	Mixed forest	Pasture	Grassland	Photovoltaic farm
Prędkość osiadania (m/s)	Deposition velocity (m/s)	0,010	0,015	0,013	0,005	0,004	0,001
Stężenie PM10 (µg/m^3)	Pollutant conc. (µg/m^3)	35,000	35,000	35,000	35,000	35,000	35,000
Przepływ (µg/m^2/s) = Prędkość osiadania (m/s) x Stężenie PM10 (µg/m^3)	**Flux (µg/m^2/s) =** deposition velocity (m/s) x pollutant conc. (µg/m^3)	0,350	0,525	0,455	0,175	0,140	0,035
Dzienny przepływ (µg/m^2/dzień)	**Daily flux (µg/m^2/day)**	30240	45360	39312	15120	12096	3024
Wskaźnik powierzchni (m^2/m^2)	Surface area index (LAI) (m^2/m^2)	4,000	6,000	5,000	2,500	2,500	1,200
Powierzchnia brana pod uwagę (m^2)	Area of land (m^2)	1,000	1,000	1,000	1,000	1,000	1,000
Powierzchnia (m^2) = Wskaźnik powierzchni (m^2/m^2) x Powierzchnia brana pod uwagę (m^2)	**Surface (m2) =** LAI (m^2/m^2) x area of land (m^2)	4,000	6,000	5,000	2,500	2,500	1,200
Okres kwitnienia liści	Vegetation period (days)	240,000	220,000	230,000	285,000	260,000	260,000
Odsetek dni suchych	Proportion of dry days (fraction)	0,650	0,650	0,650	0,650	0,650	0,650
Odsetek dni wchłaniania przez dojrzały liść	Proportion of on-leaf days (fraction)	1,000	1,000	1,000	1,000	1,000	1,000
Okres = Okres kwitnienia liści (dni) x Odsetek dni suchych x Odsetek dni wchłaniania przez dojrzały	**Period =** period of analysis (days) x proportion of dry days (fraction) x proportion of on-leaf days	156,000	143,000	149,500	185,250	169,000	169,000
Wchłanianie PM10 (µg/m^2/rok)	**Absorption of PM10 = Flux x Surface x Period (µg/m^2/year)**	18869760	38918880	29385720	7002450	5110560	613267,2
Wchłanianie PM10 (t/km^2/rok)	**Absorption of PM10 = Flux x Surface x Period (t/km^2/year)**	**18,87**	**38,92**	**29,39**	**7,00**	**5,11**	**0,61**

Figure 42 Summary of the calculations involved in the calculations for ESS4 indicator – Absorption of PM10.

Table 75 A summary of ESS4 - Annual removal of PM10 [t/km²/year] results for the different CS3 land-use scenarios.

Land-use scenario	Scenario 1	Scenario 2	Scenario 3
ESS4 – Annual removal of PM10, expressed as [t/km²/year]	18.87	0.61	5.11

Funded by the European Union

6.3.5 Temperature regulation (ESS5)

The assessment of temperature regulation potential was based on Landsat 8 satellite data processed into a Land Surface Temperature (LST) map using the ASTER database. The Advanced Spaceborne Thermal Emission and Reflection Radiometer Global Emissivity Database (ASTER GED) was developed by National Aeronautics and Space Administration's (NASA) Jet Propulsion Laboratory (JPL), California Institute of Technology. The ASTER GED product provides global emissivity maps of the Earth's land surface in five spectral bands. In addition to the mean emissivity and standard deviation maps for all five ASTER thermal infrared bands, the product also provides maps for mean land surface temperature (LST) and standard deviation.

The analysis focused on the day with the highest air temperature recorded in the last 10 years. For CS3, this was 15.08.2021. The analysis was carried out for the entire Minas de Riotinto Municipality, within which CS3 is located. The study area was divided into land-use categories according to CLC 2018 (Corine Land Cover). The following (Figure 43) land-use categories were identified: water bodies (512), pastures (231), fruit trees and berry plantations (222), transitional woodland-shrub (324), natural grasslands (321), land principally occupied by agriculture, with significant areas of natural vegetation (243), coniferous forest (312), mixed forest (313), sparsely vegetated areas (333), discontinuous urban fabric (112), industrial or commercial units (121), mineral extraction sites (131), sclerophyllous vegetation (323).

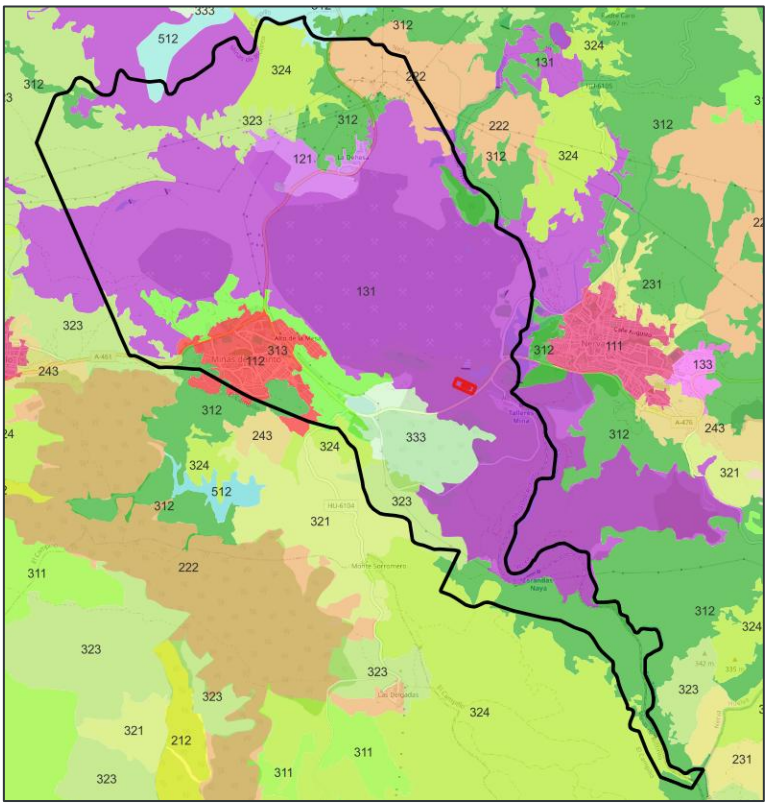

Figure 43 CLC 2018 land cover pattern for CS3.

In next step, using GIS analytical tools, the mean temperature values were calculated for each land-use type. The temperature regulation potential was calculated by relating the mean temperature values to the highest intended mean value for a given land use. The calculation results are presented in Table 76.

Funded by the European Union

Table 76 Cooling potential of land cover – CS3.

CLC 2018 Land Cover class	Mean T [°C]	Cooling potential [°C]
Water bodies	40.1	7.5
Pastures	43.2	4.4
Fruit trees and berry plantations	44.8	2.8
Transitional woodland-shrub	45.2	2.4
Natural grasslands	45.7	1.9
Land principally occupied by agriculture, with significant areas of natural vegetation	45.9	1.7
Coniferous forest	46.1	1.5
Mixed forest	46.2	1.4
Sparsely vegetated areas	46.3	1.3
Sclerophyllous vegetation	46.3	1.3
Discontinuous urban fabric	46.4	1.2
Industrial or commercial units	47.3	0.3
Mineral extraction sites	47.6	0.0

The results were then normalised to a scale from 1 to 10, where 1 denotes no potential and 10 the highest potential of the ecosystem service. The projected temperature value for the analysed land-use scenarios was adopted assuming that Scenario 1 corresponds to mixed forests, Scenario 2 to industrial or commercial units, and Scenario 3 to pastures. The results of the potential analysis for each scenario are presented in Table 77.

Table 77 Evaluation of cooling potential for analysed Scenarios – CS3.

Corine Land Cover Class	Cooling potential [-]
Discontinuous urban fabric	2.4
Industrial or commercial units	1.4
Secenario 2 - Industrial scenario, photovotaic panels	**1.4**
Mineral extraction sites	1.0
Fruit trees and berry plantations	4.4
Pastures	6.3
Secenario 3 - Recreational, meadows, pastures	**6.3**
Land principally occupied by agriculture, with significant areas of natural vegetation	3.0
Coniferous forest	2.8
Mixed forest	2.7
Secenario 1 - NBS, forests	**2.7**
Natural grasslands	3.3
Transitional woodland-shrub	3.9
Sclerophyllous vegetation	2.6
Sparsely vegetated areas	2.5
Water bodies	10.0

Funded by the European Union

6.3.6 Cultural – direct, in-situ and outdoor interactions with living systems (ESS6)

Due to the large size of the administrative unit, CLC data was used to assess its potential for recreational purposes. Following land cover classes have been identified as green recreation areas: coniferous forests (CLC 312), mixed forests CLC 313), natural grasslands (CLC 321), sclerophyllous vegetation (CLC 323), transitional woodland-shrub (CLC 324), sparsely vegetated areas, inland marshes (CLC 411), water bodies (CLC 512).

The potential for providing recreational services was also assessed for the area of the contaminated area (CS 3). The brownfield is located away from densely populated residential areas. The future use for recreational purposes will not provide access to this type of area for residents (0). Within the analysed administrative boundaries, there are green areas with a recreational function that serve recreational function for 1578 residents (Natural grasslands directly adjacent to inhabited areas in the east part of the administrative boundaries).

With regard to these values, the development of the analysed contaminated site (CS3) will not provide an increase in the availability of green areas for residents. The potential of existing and potential green areas with recreational functions on a scale of 1 to 10 is shown in the Figure 44.

Funded by the European Union

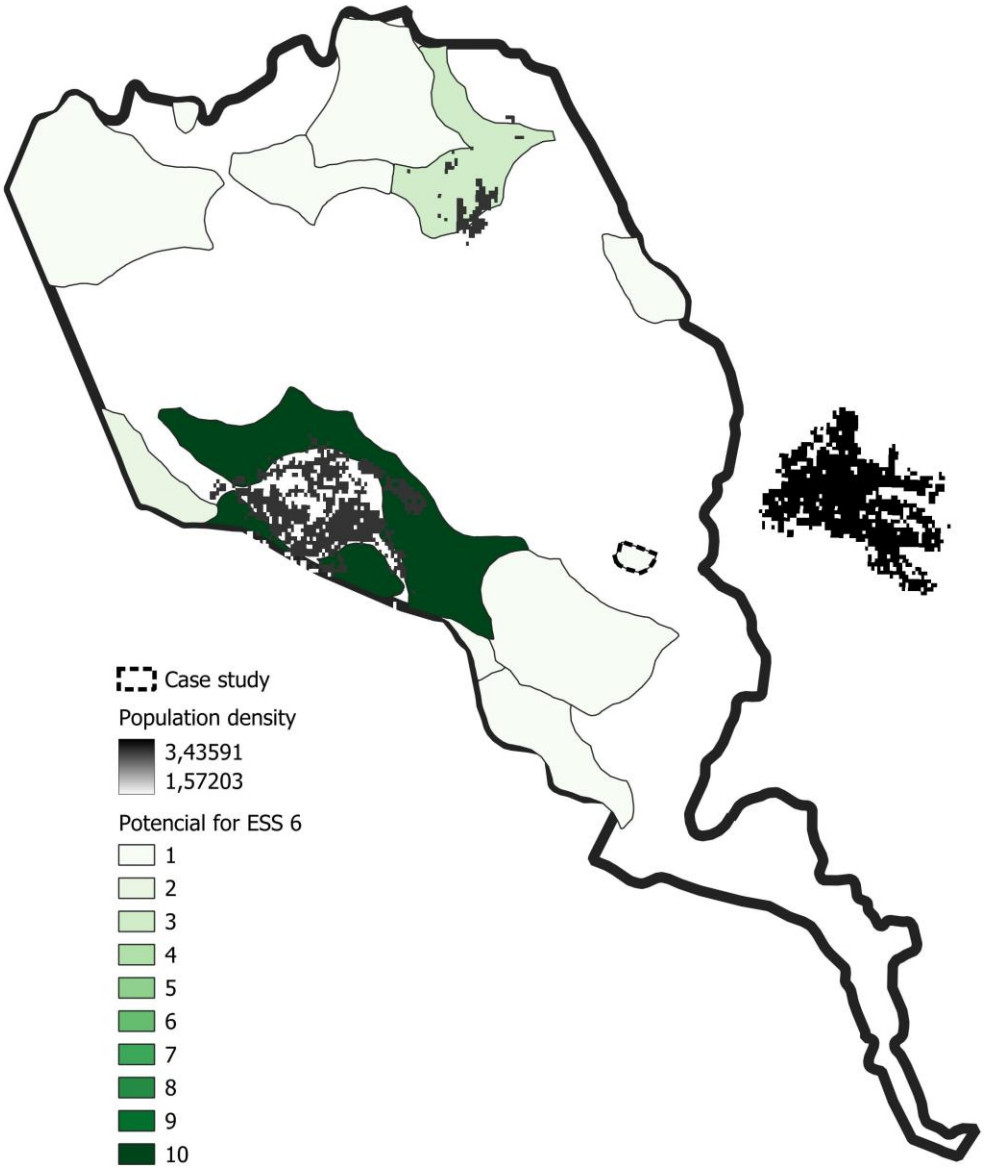

Figure 44 Cultural services: Interactions with natural environment for CS3.

In the adopted land use options, only the scenario 1 (Afforestation) and scenario 3 (Grassland cover), meet the criteria for green areas with a recreational function. However, neither scenario will increase access to green recreational areas (Table 78).

Table 78 A summary of ESS6 results for the different CS3 land-use scenarios.

Land-use scenario	Scenario 1	Scenario 2	Scenario 3
ESS6 [Number of residents within 300 meters of a green recreational area]	0	0	0

Funded by
the European Union

6.3.7 Energy production (ESS7)

The performance of photovoltaic installations for CS3 was estimated using an application provided by the EC: Photovoltaic Geographical Information System [https://re.jrc.ec.europa.eu/pvg_tools/en/tools.html]. This application provides data on solar radiation and energy production from photovoltaic (PV) systems globally. Following the application instructions, the performance of photovoltaic installations was estimated based on the assumption presented in Table 79.

Table 79 Assumptions and settings used for PV calculation for CS3.

PV Performance Modelling Parameters						
Solar radiation database:	PV technology:	Installed peak PV power	System loss	Mounting position	Slope	Azimuth:
PVGIS-SARAH3	Crystalline Silicon (original)	1 kWp	14%	Free-standing	35°	0°

In Table 80, the CS3 is characterised in relation to the analysis conducted.

Table 80 Site characteristic.

Case Study	Coordinates (center)		Elevation	Area [ha]
	Latitude	Longitude		
CS3	37.691	-6.567	334	4.9

To estimate the electricity production capacity for this CS3, the maximum feasible installed PV capacity (kWp) was determined from the available area. For the purposes of the analysis, it was assumed that 1 kWp corresponds to a PV system area of 6 m². Because the full area could not be developed under real conditions (e.g., spacing between modules, internal roads, technical buildings, fencing, and grid infrastructure), a Surface Coverage Ratio (α = 50%) was used to reflect practical land take. This value was derived from an assessment of operating photovoltaic farms with total areas ranging from 27 ha to 300 ha.

Table below (Table 81) show shows the calculated performance of photovoltaic installations for CS3. The estimated yearly in-plane irradiation is 2 101.64 kWh/m², taking into account factors such as system losses (14%). The annual electricity production is determined to be 1 609.17 per 1 kWp installed.The table presents the estimated value of electricity production, considering the surface area calculated using the Ideal Value Model and near-real conditions determined by the Surface Coverage Ratio.Under ideal conditions, the annual energy production could reach 13.1 GWh. Based on the Surface Coverage Ratio, the annual energy production is projected to be 6.5 GWh.

Table 81 Yearly PV energy production for CS3.

Yearly PV energy production [kWh]	1 609.17
Yearly in-plane irradiation [kWh/m^2]	2 101.64
Year-to-year variability [kWh]	48.18
Changes in output due to	
-Angle of incidence [%]	-2.6
-Spectral effects [%]	0.57
Temperature and low irradiance [%]	-9.1

Funded by the European Union

Total loss [%]		-23.43
Max. kWp needed [kWp]		8 167
Energy production (Ideal Value Model)	13.1	13.2
Energy production (Surface Coverage Ratio)	6.5	6.6

Figure 45 show a report from the Photovoltaic Geographical Information System application (estimating annual energy production for CS3).

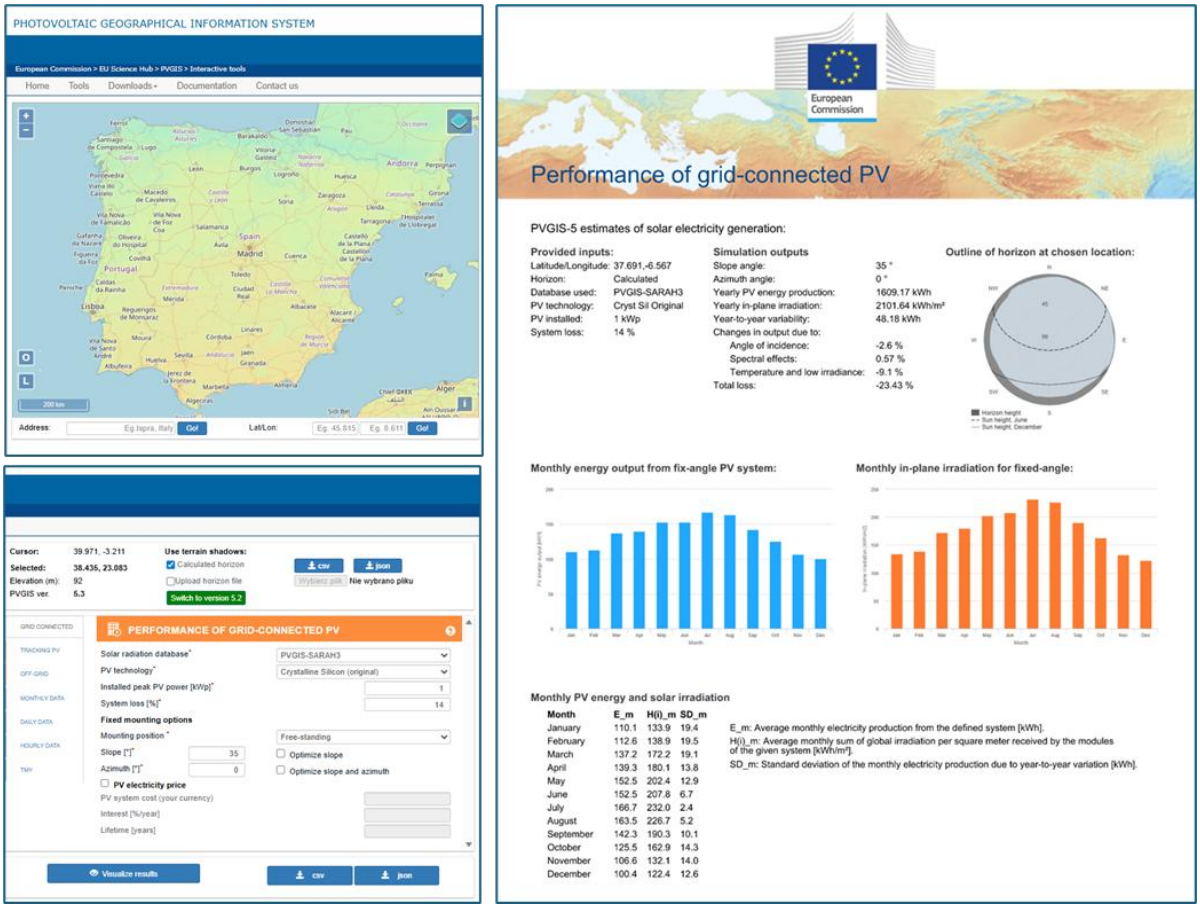

Figure 45 CS2 – Performance of grid-connected PV.

The ESS7 results for CS3 are summarised in the Table 82.

Table 82 A summary of ESS7 (Energy properties) results for the different CS3 land-use scenarios.

Land-use scenario	Scenario 1	Scenario 2	Scenario 3
ESS7: Potential energy production [GWh/y].	0.0	6.5	0.0

Funded by the European Union

6.4 Ecosystem services assessment for CS4

In this section, the valuation of ESS for CS4 (Upper Silesia, PL – PL22) was presented, considering the local site context and the analysed land-use scenarios, while applying a harmonised data-processing methodology to ensure comparability of results.

6.4.1 Biomass production (ESS1)

The assessment of ESS1 (*biomass production*) for CS4 is based on the energy potential indicator EP (GJ·ha^{-1}·year^{-1}). EP is derived from the annual increment of above-ground biomass AGBinc (t d.m.·ha^{-1}·year^{-1}) using the following relationship:

$$EP = AGBinc \times CV \ [GJ \cdot ha^{-1} \cdot year^{-1}]$$

Where:
- CV is the calorific value of the biomass (GJ·t^{-1} d.m.), adopted in line with the ESS1 service card,
- AGBin above-ground biomass AGBinc (t d.m.·ha^{-1}·year^{-1}),
- EP is energy potential.

For Poland, relatively extensive information on forest stand increment is available, including inventory-based datasets and national studies. Selected results are presented in the table below (Table 83). However, these sources differ in their definitions (e.g., the biomass fractions covered and how increment is expressed) and in reporting formats, which limits their direct use as input data for comparative calculations across case studies. Therefore, the national sources were used only for a basic consistency check (to confirm the expected order of magnitude). For the actual calculations, harmonised values from "Improved large-area forest increment information in Europe through harmonisation of National Forest Inventories" (Forest Ecology and Management, 562, 121913) were applied, in line with the approach used throughout the report. This ensured that ESS1 results remained comparable across all case studies and reduced the risk of methodological inconsistencies.

Table 83 Annual biomass production on different types of land in Poland.

Land type	Biomass increment value (t/ha/year)	Method / Notes (very short)	Source
Coniferous	6.60 t/ha/yr	Harmonised NFI; gross annual increment (GAI7) by forest type	[Gschwantner et al., 2024]
Broadleaved	6.77 t/ha/yr	Harmonised NFI; gross annual increment (GAI7) by forest type	[Gschwantner et al., 2024]
Mixed	6.98 t/ha/yr	Harmonised NFI; gross annual increment (GAI7) by forest type	[Gschwantner et al., 2024]
Poplar monoculture (energy plantations; Poland practice example)	7.7 t/ha/yr (and 1.7 t/ha/yr for unmanaged)	Reported yields for poplar energy plantations (management vs none)	[Niemczyk M., 2017]
Grasslands / permanent meadows (hay-equivalent)	4.46 t/ha/yr (hay-equivalent)	Official national agri report; "in hay equivalent"; conversion factor	[GUS, 2020]
Grasslands / meadows (hay yield; peer-reviewed summary of GUS)	5.18 t/ha/yr (hay)	Peer-reviewed paper; values based on GUS	[Gabryszuk et al., 2021]

For the poplar plantations scenario, AGBinc was taken from literature sources that report dry biomass production directly (t d.m.·ha^{-1}·year^{-1}).The source literature data are presented in Table 84). Because reported values vary substantially between studies (due to differences in cultivars,

plantation age, water availability, and management practices), the assessment was not based on a single extreme result. Instead, a working value representative of moderate conditions under the analysed scenario was applied. This approach maintained parameter consistency across case studies and reduced the risk of overestimating EP based on data from intensively irrigated plantations or sites with exceptionally favourable growing conditions.

Table 84 Parameters for calculating the energy potential of biomass for CS4 (PL22).

CLC clasification	Couling Land Cover	AGBinc (tDM/ha/yr)	CV (GJ/tDM)	EP (GJ/ha/yr)
3.1.1	Broad-leaved forest	6.77	18.5	125.2
1.4.1	Green urban areas -grassland or lawns	5.00	17.5	87.5
1.2.1	Industrial PV installation (80% grassland)	4.00	17.5	70.0
3.1.2	Coniferous forest	6.60	18.5	122.1
3.2.4	Transitional woodland/shrub (poplar plantations)	10.50	18.6	194.9
1.2.1	Industrial buildings and halls (20% grassland)	1.00	17.5	17.5
2.1.1	Non-irrigated arable land - Brassica juncae	9.00	17.5	157.5
2.1.1	Non-irrigated arable land - Lablab purpureus	n.d.	n.d.	n.d.

For the scenario with grasslands, AGBinc was defined based on the typical productivity of meadows under a temperate climate. A working range consistent with literature for the PL22 region (Silesia) was adopted, i.e., 4–6 t d.m.·ha^{-1}·year^{-1}, reflecting values reported for temperate lowland meadows and field experiments (including FACE: type studies and higher-productivity variants) (Table 85).

For industrial classes, a simplified methodological assumption was applied using fixed grassland-equivalent shares: 80% of the area was treated as having a grassland function for PV installations, while a 20% grassland equivalent was assumed for built-up areas (buildings and halls), in line with the report assumptions.

Table 85 Estimated annual above-ground biomass increment (AGBinc) for grasslands in NUTS2 regions – assumptions and literature-based justification.

NUTS2	Region	Type of grassland	Estimated AGB increase (t DM·ha^{-1}·yr^{-1})	Rationale (climate / intensity)	Citations
PL22	Silesia	temperate lowland meadows	4–6	Climate similar to Southern–Central Europe; evidence from FACE experiments and fertilised grasslands indicates an increase on the order of 4–7 t DM·yr^{-1}	[Obermeier et al., 2018 ; Andresen et al., 2018]

A summary results of ESS1 assessment for CS4 are presented in Table 86.

Table 86 A summary of ESS1 (Biomass production) results for the different CS4 land-use scenarios.

Land-use scenario	Scenario 1	Scenario 2	Scenario 3
Energy potential [GJ/ha/year]	194.9	70	87.5

Funded by the European Union

6.4.2 Regulation of soil quality (ESS2)

In this section, the ESS2 indicator (regulation of soil quality) for CS4 was estimated as the potential for metal accumulation in plant biomass under the analysed land-use scenarios. As part of the literature review, concentration ranges of several metals in plant biomass were compiled e.g. cadmium, lead, zinc, copper, and nickel. However, for valuation purposes, one representative metal was selected: cadmium (Cd). Cadmium is frequently reported in environmental studies, it has no nutrient function (unlike Zn or Cu), and its accumulation in plant tissues provides a useful indicator of contamination pressure. In addition, Cd is often more mobile and more readily translocated to above-ground plant parts than Pb, which increases its suitability for scenario comparisons based on AGB.

As part of the parameterisation of metal concentrations in conifer biomass, relevant literature sources were reviewed. Data for needles are widely available, but they show high variability depending on species, site conditions, anthropogenic pressure, and the age of the assimilatory tissues. At the same time, many studies focus on needles or bark as biomonitors and do not provide comparable values for stem wood, nor a consistent "needles versus stem wood" dataset for the full set of metals. For this reason, instead of averaging results from heterogeneous studies, an approach based on one internally consistent dataset was adopted, covering both needles and stem wood analysed with the same methodology. The study by Skonieczna et al. (2014) was selected as the baseline source. In that work, 15 *Pinus sylvestris* trees from five stands were analysed. The investigated forests were located in an area influenced by anthropogenic pressures, but not in the immediate vicinity of point emission sources.

For the assessment, mean concentrations of Cd, Zn, Pb, and Cu were introduced for needles (as a representative of the "leaf" fraction) and for stem wood (as a representative of the "stem" fraction). Cadmium was then used for the subsequent valuation step.

For poplar plantations, several literature sources were reviewed. As in other cases, it was found that experimental conditions were often not comparable between studies. Therefore, the focus was placed on a single publication that reported concentrations in poplar leaves and shoots in a format suitable for comparison across case studies

Based on the reviewed evidence, Pilipović et al. (2019) was adopted as the source of ESS2 parameters for poplar plantations, as it provides a coherent empirical dataset covering both leaves and shoots/stems, analysed using the same methodology and under the same experimental conditions. This allowed the "leaf versus wood/shoots" fractions to be separated directly, without merging heterogeneous studies and without additional assumption-based conversions. In addition, the study reports several metals (including Cd, Zn, Pb, and Cu) in a way that supported the selection of values representative of moderate anthropogenic pressure, thereby improving comparability between land-use scenarios within the ESS2 assessment.

For Scenario with grassland, an above-ground biomass (AGB)-based approach was applied, using metal concentration ranges in herbaceous plant tissues as reported in the literature. To reflect the typical spread of values associated with different levels of anthropogenic influence, three pressure levels were compiled (moderate, heavy, and extreme), representing, respectively, urban and transport impacts, post-mining areas, and locations in the immediate vicinity of smelters.

Funded by the European Union

However, for the purpose of the ESS2 valuation, the moderate contamination variant was adopted, as it was considered representative of the common anthropogenic background conditions observed across the CS landscape and the analysed land-use scenarios. This choice reduced the influence of extreme concentration values that could otherwise dominate the result, and it ensured that differences in ESS2 were driven primarily by land-cover type and AGB magnitude rather than by exceptional, localised point sources of pollution.

The input data used for CS4 are identical to those described for CS1 in Section 6.1.2. Table 87 provides a concise overview of the heavy metal concentration datasets applied in the biomass assessment and includes references to the corresponding detailed tables in Section 6.1.2

Table 87 Heavy metal concentrations in biomass used for ESS2 parameterisation (data sources and table references).

No.	Heavy metal concentrations in the biomass	Reference table
1	Broadleaf species	Table 16 Heavy metal concentrations in the biomass of broadleaf species.
2	Conifer species	Table 17 Heavy metal concentrations in the biomass of conifer species.
3	Poplar and willow crops.	Table 18 Heavy metal concentrations in the biomass of poplar and willow crops.
4	Grassland species	Table 19 Heavy metal concentrations in the aboveground biomass of grassland species.

Table 88 presents the input parameters and calculation outputs used to estimate the ESS2 indicator for CS4 (PL22) expressed as the potential annual cadmium (Cd) accumulation in above-ground plant biomass. It combines AGBinc values (from ESS1) with tissue Cd concentrations and harvest fractions to derive Cd concentration in harvested biomass and the resulting Cd removal per hectare and year, in accordance with the methodology described in Section 4.3

Table 88 Calculation sheet for ESS2 (Cd): biomass increment, concentration assumptions and annual removal.

Corine Land Cover	AGBinc (tDM/ha/yr) [from ESS1]	f_leaf (season harvest) [0-1]	Cd_C_leaf (mg/kg DM) [input]	Cd_C_stem (mg/kg DM) [input]	Cd_C_harvest (mg/kg DM) [calc]	Cd_Removal (g/ha/yr) [calc]
Broad-leaved forest	6.77	0.2	0.4	0.1	0.16	1.1
Green urban areas - grassland or lawns	5.00	1	0.75	-	0.75	3.8
Industrial - PV installation (80% grassland)	4.00	1	0.6	-	0.6	2.4
Coniferous forest	6.60	0.2	0.1	0.24	0.212	1.4
Transitional woodland/shrub (poplar plantations)	10.50	0.2	7.85	3.25	4.17	43.8
Industrial - buildings and halls (20% grassland)	1.00	1	0.15	-	0.15	0.2

Table 89 summarises the ESS2 results for CS4 across the analysed land-use scenarios. Values are reported as the estimated potential annual pollutant (Cd) accumulation in above-ground biomass (g/ha/year) enabling direct comparison between scenarios under a consistent parameter set.

Funded by the European Union

Table 89 A summary of ESS2 (Regulation of soil quality) results for the different CS4 land-use scenarios.

Land-use scenario	Scenario 1	Scenario 2	Scenario 3
Potential annual pollutant accumulation [g/ha/year]	43.8	2.4	3.8

6.4.3 Mitigation of climate change (carbon dioxide sequestration) (ESS3)

The ESS3 assessment relied on annual carbon sequestration as the primary indicator, expressed in tonnes of CO_2 per hectare per year (t CO_2/ha/year). Total sequestration was estimated by summing carbon accumulation in above-ground and below-ground biomass and subsequently converting this total into CO_2 equivalents. The approach was aligned with the carbon allocation models developed for poplar plantations, as described earlier in the ESS3 methodological framework.

The estimation of annual above-ground biomass increment (AGBinc) followed the same methodology applied in ESS1, involving a review and analysis of available sources such as scientific literature, national forest inventory data, and indirect indicators. In the case of the Miasteczko Śląskie, Huta Cynku site in Poland (CS4), the collected data were fragmented and methodologically inconsistent, with differing definitions of production, growth metrics, typological classifications, and units of measurement. This limited the possibility of making direct comparisons between land cover categories. To ensure consistency across the deliverable, AGBinc values were therefore derived from harmonized data presented in the study “Improved large-area forest increment information in Europe through harmonization of National Forest Inventories” (Forest Ecology and Management, 562, 121913), which provides comparable annual forest growth estimates for most European countries and forest types.

The annual below-ground biomass increment (BGBinc) was calculated from the AGBinc using the ratio between above- and below-ground biomass increments (AGBinc/BGBinc)(Table 90). The applied root-to-shoot ratios were based on literature sources, including Oliveira Rodríguez et al. (2018) and the Intergovernmental Panel on Climate Change (2003, 2006), selected for their standardized and internationally consistent methodologies. According to these references, the ratio used for the industrial and commercial land-use scenario was assumed to represent approximately 20% of the grassland AGBinc-to-BGBinc ratio, whereas the scenario involving ground-mounted photovoltaic installations was assumed to retain 80% of the grassland coverage value.

Table 90 Sources used for the estimation of below ground - above ground ratio (%).

CS4 (PL) - types of management	AGBinc - BGBinc ratio (%)	Sources
Broad-leaf forest	0.35	Bijak, Zasada & Bronisz (2013)
Coniferous forest	0.30	GIOŚ (2019)
Grassland	1.58	IPCC (2003) Annex 3A.1.8 Mokany, Raison & Prokushkin (2006)
Poplar cultivation	0.21	Oliveira (2018)

After calculating the values of the BGBinc from the ratio and the AGBinc values provided, the results were added and multiplied by the C fraction to account for the carbon content (Table 91).

Funded by the European Union

The carbon content values in dry matter are assumed at approx. 50% values, supported by literature.

In the next step the results were converted to the CO_2 equivalent by multiplying the final value by 3,67 (ratio of the atomic mass of the molecules). The indicator reflects the annual flow of carbon sequestration associated with biomass growth, rather than long-term carbon stock changes.

Table 91 Sources used for the estimation of C fraction of carbon content in dry mass.

CS4 (PL) - types of management	C fraction of carbon content in dry matter	Source/Reference
Broad-leaf forest	0.46	IPCC (2003) Annex 3A.1 Dupouey (2010)
Coniferous forest	0.46	
Grassland	0.48	Shiferaw, Kassawmar, Zeleke (2022)
Poplar cultivation	0.48	Shiferaw, Kassawmar & Zeleke (2022)

The results for the region of Miasteczko Śląskie, Huta Cynku site in Poland (CS4) show that the annual carbon sequestration for broadleaf forests is about 16,100 t (CO_2/ha/year), 15,115 t (CO_2/ha/year) for coniferous forest and for poplar plantation the results were 17,567 t (CO_2/ha/year). Grassland coverage scored the highest at a 22,725 t (CO_2/ha/year). The results presented in the Figure 46 were used to provide background land use values for the evaluation of the values for Scenarios 1, 2 and 3.

ESS: MITIGATION OF CLIMATE CHANGE

PL	Średnia roczna ilość biomasy nadziemnej z hektara (tDM/ha/yr)	Stosunek biomasy poniżej - powyżej gruntu	Średnia roczna ilość biomasy korzennej z hektara (tDM/ha/yr)	Średnie stężenie węgla w biomasie (%)	Sekwestracja węgla (kg/year/ha)	Roczna sekwestracja węgla wyrażona w t (CO_2/ha/year)
ENG	Average anual amount of above-ground biomass from ha (tDM/ha/yr)	Below ground - above ground ratio	Average annual amount of below biomass from ha (tDM/ha/yr)	Biomass mean concentration of carbon (%)	Carbon sequestration (t/year/ha)	Annual carbon sequestration expressed in t (CO_2/ha/year)
						Conversion factor from Carbon (C) to CO_2 equivalent
						3,67
CS4 (PL) - Miasteczko Śląskie, Huta Cynku						
Forest_broadleaf_poplar	6,77	0,35	2,370	0,48	4,387	16,100
Grassland	5,00	1,58	7,900	0,48	6,192	22,725
PV_groundmounted (80% grassland)	4,00	1,58	6,320	0,48	4,954	18,180
coniferous	6,60	0,30	1,980	0,48	4,118	15,115
poplar cultivation	8,60	0,21	1,806	0,46	4,787	17,567
Industrial of commercial units (20% grassland)	1,00	1,58	1,580	0,48	1,238	4,545

Figure 46 Calculations concerning the ESS3 indicator – annual carbon sequestration expressed in t (CO_2/ha/year) for the Miasteczko Śląskie, Huta Cynku site in Poland (CS4).

For the Scenario 1 – NBS solutions, the value of poplar plantations was assumed. The 2nd Scenario = industrial scenario for ESS3 considered 80% vegetation in AGBinc and BGBinc value due to a decreased but still present level of low-vegetation growth. For Scenario 3, the value of grasslands was assumed as an option for low-vegetation, recreational approach. The results obtained within ESS3 assessment for CS4 are presented inTable 92.

Table 92 A summary of ESS3 - Annual carbon sequestration expressed in t CO_2/ha/year for the different CS4 land-use scenarios.

Land-use scenario	Scenario 1	Scenario 2	Scenario 3
ESS3 - Annual carbon sequestration expressed in t CO_2/ha/year	17.567	18.180	22.725

Funded by the European Union

6.4.4 Air quality mitigation (ESS4)

Evaluation of ESS4 considers the removal of atmospheric pollutants (specifically particulate matter PM_{10} and $PM_{2.5}$) by tree and shrub canopies in urban, peri-urban and rehabilitated post-industrial areas through dry deposition processes. The main indicator is the annual removal of particulate matter PM_{10} particles expressed in kg/ha/year. The methodology is based on the dry deposition mode, established by Tallis et al. (2011), where:

$$\text{Absorption of } PM_{10} = \text{Flux (V) x Surface (SA) x Period (t) (t/km}^2\text{/year)}$$

where:

- Flux is the pollutant to the surface (amount removed per unit area and time), calculated by multiplying the deposition velocity of the pollutant (m/s), which depends on canopy structure and wind speed and the concentration of the pollutant in the atmosphere.
- Surface is the considered surface area multiplied by the surface area index functioning in given area (LAI).
- Period accounts for the period of analysis in days, multiplied by the proportion of dry days and the proportion of non-leaf days.

The total annual pollutant removal is calculated by integrating deposition fluxes over the vegetated surface area of each land-use scenario. The above contributes to the calculation as follows:

- V = deposition velocity (m/s) x pollutant conc. (µg/m³)
  - Flux (µg/m³) was then converted to daily flux by multiplying it by 86400
- SA = LAI (m²/m²) x area of land considered (m²)
- t = period of analysis (days) x proportion of dry days (fraction) x proportion of on-leaf days (fraction)
  - Afterwards the absorption of PM_{10} was converted from (µg/m²/year) to (t/km²/year) by $x10^6$

The data for the Miasteczko Śląskie, Huta Cynku site in Poland (CS4) involved land use scenarios for the broad-leaf forest, coniferous forest, mixed forest, pastures, grasslands and photovoltaic farm. For each of the components of the model, the literature research was carried out to scope the best range of unified results to produce comparable values. In some cases, it was not possible to gather data regarding each of the components of the model, in which case an average was used from the data regarding countries or regions in the world with closest ecosystem type, for the results to be compatible. Regarding the deposition velocity by land use type, data used was based on Schrader & Brümmer (2014) and middle ranges for values for each land use type were used for calculations (Table 93):

Table 93 Estimated deposition deposition velocity in mediterranean climate by Schrader & Brümmer et al. (2016).

Land Use Type	Median Deposition Velocity ($cm \cdot s^{-1}$)	Additional observations
Broad-leaf forest (deciduous)	~0.9–1.1 cm s^{-1}	Higher vegetative roughness and stomatal uptake yield enhanced deposition relative to low vegetation
Coniferous forest	~2.1–2.2 cm s^{-1}	Dense, needle-like foliage increases turbulence and interception, yielding the highest observed v_e among forests
Mixed forest	~1.2–1.5 cm s^{-1}	Intermediate between broadleaf and coniferous forests due to mixed canopy structure
Grasslands	~0.7–1.0 cm s^{-1}	Lower roughness than forests, moderate interception via blades; similar range applies to pastures
Urban (vegetation)	~0.8 cm s^{-1}	Urban green spaces show intermediate deposition efficiency
Pastures/Agricultural fields	~0.4–1.0 cm s^{-1}	Includes pastures and cropland; lower than forested sites

Funded by the European Union

For industrial land use including photovoltaic farm, smooth surfaces with minimal yield dry deposition like bare soil were taken into the consideration at an approx. 0,2 cm s^{-1}. The next component researched for the model was the pollutant concentration (µg/m^3). The values for pollutant concentrations recovered for the region were based on Sówka et al. (2019) and Kuklinska, Wolska & Namiesnik (2015). The value was estimated at 35–60 µg/m^3 middle of the range at 47,5 was assumed. Regarding the surface area, the values of the leaf area index (LAI) in various types of land use were taken into consideration. Due to the lack of specific data regarding the above-mentioned land use types for the region, European and global data were considered (Table 94).

Table 94 References for the leaf area index concerning chosen types of land use.

Land use type	LAI values	Represented region	Sources / References
Broad-leaf forest	5–8 (max values) 3–6 (urban average 3–4.5) 2–10 (broad global range)	France (temperate deciduous) Primarily U.S., global review Global synthesis	Le Dantec, Dufrêne, Saugier (2000) Nowak et al. (2017) Parker (2020)
Coniferous forest	6–11 3–6 (urban average 3–4.5) 2–10 (broad global range)	Pacific Northwest, U.S. Primarily U.S., global review Global synthesis	Turner et al. (2000) Nowak et al. (2017) Parker (2020)
Mixed forest	3–7 typical; up to 9 dense stands	Europe (multi-site comparison)	Sinan & Hasenauer (2025)
Pasture/ Grassland/ Shrub	2.0–4.5 (Wetland shrubs lower (2–3), wooded wetland stands up to 4.5)	Poland (Central Europe)	Leśny et al. (2007)

Area assumed for the calculation at this stage was a m^2, after conversion a km^2. Regarding the period component, it was calculated assuming middle range of the vegetation period for each type of land use based on findings by Tomczyk & Szyga-Pluta (2016). Table 95 presents the temperate values which were used for Miasteczko Śląskie assessment.

Table 95 Number of vegetative days based on land use in Poland according to Tomczyk & Szyga-Pluta (2016).

Land Use / Vegetation Type	Typical Vegetation Period (days per year)	Additional observations
Broad-leaf Forest	210–230	Vegetation period in lowland Southern Poland resembling national average; forests begin growth earlier and extend slightly longer due to microclimate
Coniferous Forest	210–230	Evergreen conifers remain photosynthetically active throughout most of the thermal period; start/end tied to temperature
Mixed Forest	210–230	Intermediate; combination of deciduous and evergreen behaviour extends green season
Pastures	200–225	Grass pastures enter growth with warming temperatures and maintain growth until first frost; alike regional thermal season length
Grasslands	200–225	Herbaceous grasslands follow thermal growing season (≥ 5 °C) and are active through spring–autumn

For the scenario regarding industrial land use type, including photovoltaic farm, the vegetative period was assumed the same as for a grassland. The proportion of dry days was assumed at 60% according to Chervenkov & Slavov (2021), while the proportion of on-leaf days was assumed at 100%, due to already exclusively selected vegetative dry periods.
The results for the region of Miasteczko Śląskie site Poland (CS4) presented in the Figure 47 show that the annual absorption of PM10 are as follow: 26,00 t/km^2/year for broad-leaf forest, 79,63

Funded by the European Union

t/km²/year for coniferous forest, 52,82 t/km²/year for mixed forest, 7,34 t/km²/year for pastures, 6,29 t/km²/year for grasslands and 0,63 t/km²/year for industrial land use/photovoltaic farm. Those results were used to provide background land use values for the evaluation of the values for Scenarios 1, 2 and 3.

For the Scenario 1 – NBS solutions the value of broad-leaf forest was assumed. Concerning Scenario 2, the industrial/photovoltaic land use was considered and for Scenario 3 the values for pastures were assumed, as shown in the Table 96.

ESS: AIR PURIFICATION							
Seconds/day (s)	86 400						
		CS4 (PL) - Miasteczko Śląskie, Huta Cynku					
PL	EN	Broad-leaf forest	Coniferous forest	Mixed forest	Pasture	Grassland	Photovoltaic farm
Prędkość osiadania (m/s)	Deposition velocity (m/s)	0,008	0,021	0,015	0,007	0,008	0,001
Stężenie PM10 (µg/m³)	Pollutant conc. (µg/m³)	47,500	47,500	47,500	47,500	47,500	47,500
Przepływ (µg/m²/s) = Prędkość osiadania (m/s) x Stężenie PM10 (µg/m³)	**Flux (µg/m²/s) =** deposition velocity (m/s) x pollutant conc. (µg/m³)	0,380	0,998	0,713	0,333	0,380	0,048
Dzienny przepływ (µg/m²/dzień)	**Daily flux (µg/m²/day)**	32832	86184	61560	28728	32832	4104
Wskaźnik powierzchni (m²/m²)	Surface area index (LAI) (m²/m²)	6,000	7,000	6,500	2,000	1,500	1,200
Powierzchnia brana pod uwagę (m²)	Area of land (m²)	1,000	1,000	1,000	1,000	1,000	1,000
Powierzchnia (m²) = Wskaźnik powierzchni (m²/m²) x Powierzchnia brana pod uwagę (m²)	**Surface (m2) =** LAI (m²/m²) x area of land (m²)	6,000	7,000	6,500	2,000	1,500	1,200
Okres kwitnienia liści	Vegetation period (days)	220,000	220,000	220,000	213,000	213,000	213,000
Odsetek dni suchych	Proportion of dry days (fraction)	0,600	0,600	0,600	0,600	0,600	0,600
Odsetek dni wchłaniania przez dojrzały liść	Proportion of on-leaf days (fraction)	1,000	1,000	1,000	1,000	1,000	1,000
Okres = Okres kwitnienia liści (dni) x Odsetek dni suchych x Odsetek dni wchłaniania przez dojrzały	**Period =** period of analysis (days) x proportion of dry days (fraction) x proportion of on-leaf days	132,000	132,000	132,000	127,800	127,800	127,800
Wchłanianie PM10 (µg/m²/rok)	**Absorption of PM10 = Flux x Surface x Period (µg/m²/year)**	26002944	79634016	52818480	7342877	6293894	629389,4
Wchłanianie PM10 (t/km²/rok)	**Absorption of PM10 = Flux x Surface x Period (t/km²/year)**	**26,00**	**79,63**	**52,82**	**7,34**	**6,29**	**0,63**

Figure 47 Summary of the calculations involved in the calculations for ESS4 indicator – Absorption of PM10.

Funded by the European Union

Table 96 A summary of ESS4 - Annual removal of PM10 [t/km²/year] results for the different CS4 land-use scenarios.

Land-use scenario	Scenario 1	Scenario 2	Scenario 3
ESS4 – Annual removal of PM10, expressed as [t/km²/year]	26.00	0.63	7.34

6.4.5 Temperature regulation (ESS5)

The assessment of temperature regulation potential was based on Landsat 8 satellite data processed into an Land Surface Temperature (LST) map using the ASTER database. The Advanced Spaceborne Thermal Emission and Reflection Radiometer Global Emissivity Database (ASTER GED) was developed by National Aeronautics and Space Administration's (NASA) Jet Propulsion Laboratory (JPL), California Institute of Technology. The ASTER GED product provides global emissivity maps of the Earth's land surface in five spectral bands. In addition to the mean emissivity and standard deviation maps for all five ASTER thermal infrared bands, the product also provides maps for mean land surface temperature (LST) and standard deviation.

The analysis focused on the day with the highest air temperature recorded in the last 10 years. For CS4, this was 19.08.2023.The analysis was carried out for the entire Miasteczko Śląskie Municipality, within which CS4 is located. The study area was divided into land-use categories according to CLC 2018 (Corine Land Cover). The following land-use categories were identified: discontinuous urban fabric (112), industrial or commercial units (121), road and rail networks and associated land (122),construction sites (133),non-irrigated arable land (211), pastures (231), complex cultivation patterns (242), broad-leaved forest (311), coniferous forest (312), mixed forest (313), transitional woodland-shrub (324) (Figure 48).

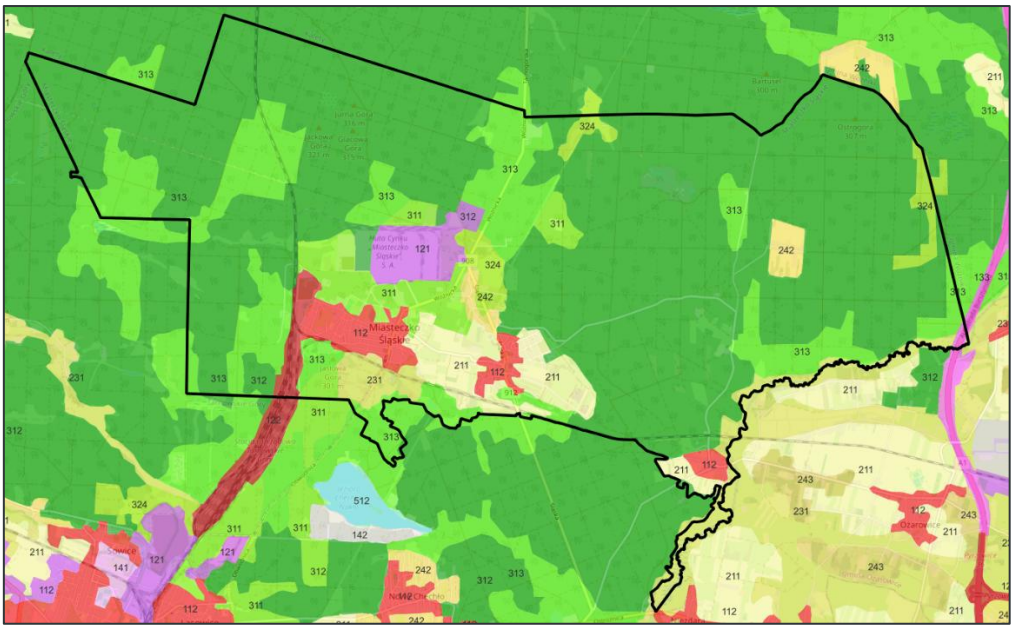

Figure 48 CLC 2018 land cover pattern for CS4.

In next step, using GIS analytical tools, the mean temperature values were calculated for each land-use type. The temperature regulation potential was calculated by relating the mean

Funded by the European Union

temperature values to the highest intended mean value for a given land use. The calculation results are presented in Table 97.

Table 97 Cooling potential of land cover – CS4.

CLC 2018 Land Cover class	Mean T [°C]	Cooling potential [°C]
Coniferous forest	28.9	7.5
Mixed forest	29.2	7.1
Pastures	30.2	6.2
Broad-leaved forest	30.2	6.1
Construction sites	30.6	5.7
Transitional woodland-shrub	30.9	5.4
Non-irrigated arable land	30.9	5.4
Road and rail networks and associated land	31.0	5.4
Complex cultivation patterns	31.8	4.5
Discontinuous urban fabric	32.7	3.6
Industrial or commercial units	36.4	0.0

The results were then normalised to a scale from 1 to 10, where 1 denotes no potential and 10 the highest potential of the ecosystem service. The projected temperature value for the analysed land-use scenarios was adopted assuming that Scenario 1 corresponds to mixed forests, Scenario 2 to industrial or commercial units, and Scenario 3 to pastures. The results of the potential analysis for each scenario are presented in Table 98.

Table 98 Evaluation of cooling potential for analysed Scenarios – CS4.

Corine Land Cover Class	Cooling potential [-]
Discontinuous urban fabric	5.4
Industrial or commercial units	1.0
Secenario 2 - Industrial scenario, photovotaic panels	**1.0**
Road and rail networks and associated land	7.4
Construction sites	7.9
Non-irrigated arable land	7.5
Pastures	8.5
Secenario 3 - Recreational, meadows, pastures	**8.5**
Complex cultivation patterns	6.5
Broad-leaved forest	8.4
Coniferous forest	10.0
Mixed forest	9.6
Secenario 1 - NBS, forests	**9.6**
Transitional woodland-shrub	7.5

Funded by the European Union

6.4.6 Cultural- direct, in-situ and outdoor interactions with living systems (ESS6)

Due to the large size of the administrative unit, CLC data was used to assess its potential for recreational purposes. Following land cover classes have been identified as green recreation areas: broad-leaved forest (CLC 311), coniferous forests (CLC 312), mixed forests CLC 313), transitional woodland-shrub (CLC 324), inland marshes (CLC 411), water bodies (CLC 512).

The potential for providing recreational services was also assessed for the area of the contaminated area (CS 4). The brownfield is located away from densely populated residential areas. The future use for recreational purposes will not provide access to this type of area for residents (0). Within the analysed administrative boundaries, there are green areas with a recreational function that serve recreational function for 5061 residents (Broad-leaved forest directly adjacent to inhabited areas in the central part of the administrative boundaries).

The potential of existing and potential green areas with recreational functions on a scale of 1 to 10 is shown in the Figure 49.

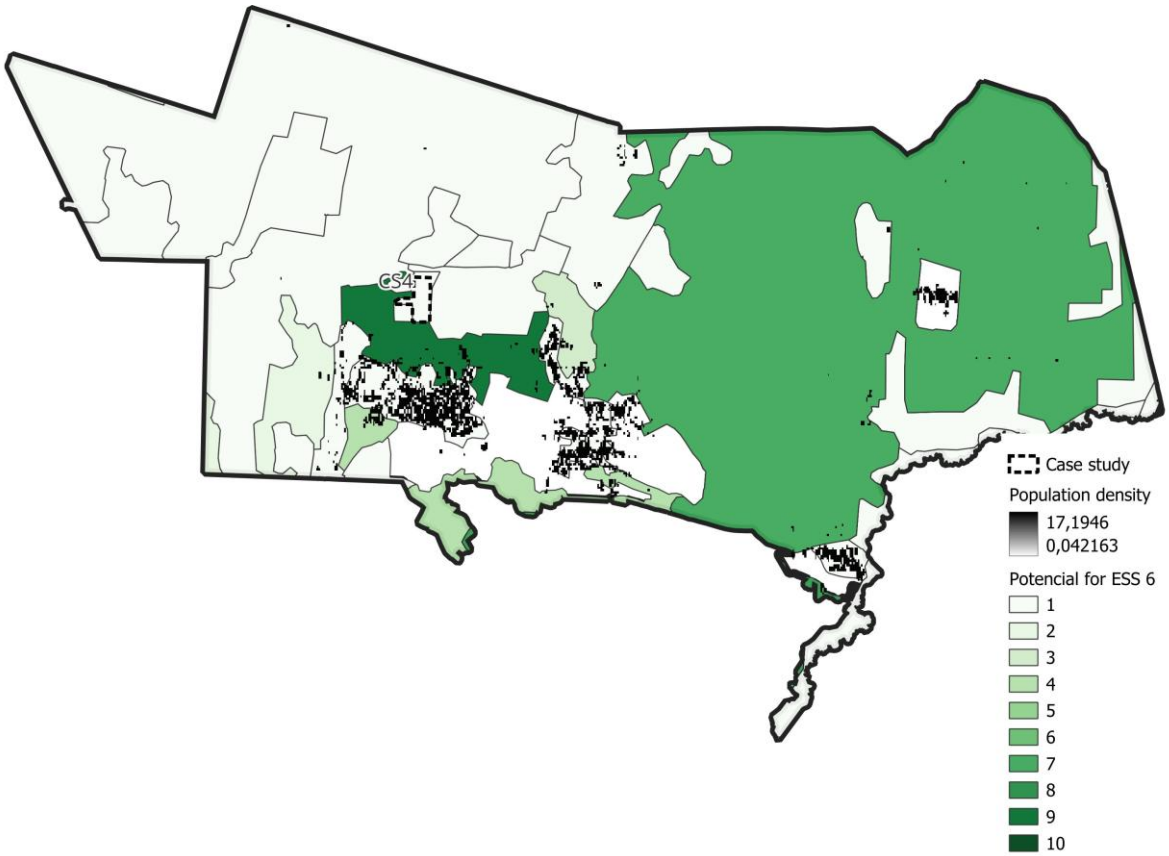

Figure 49 Cultural services: Interactions with natural environment for CS4.

In the adopted land use options, only the scenario 1 (Afforestation) and scenario 3 (Grassland cover), meet the criteria for green areas with a recreational function. However, neither scenario will increase access to green recreational areas (Table 99).

Table 99 A summary of ESS6 results for the different CS4 land-use scenarios.

Funded by
the European Union

Land-use scenario	Scenario 1	Scenario 2	Scenario 3
ESS6[Number of residents within 300 meters of a green recreational area]	0	0	0

6.4.7 Energy production (ESS7)

The performance of photovoltaic installations for CS4 was estimated using an application provided by the EC: Photovoltaic Geographical Information System [https://re.jrc.ec.europa.eu/pvg_tools/en/tools.html]. This application provides data on solar radiation and energy production from photovoltaic (PV) systems globally. Following the application instructions, the performance of photovoltaic installations was estimated based on the assumption presented in Table 100.

Table 100 Assumptions and settings used for PV calculation for CS4.

PV Performance Modelling Parameters						
Solar radiation database:	PV technology:	Installed peak PV power	System loss	Mounting position	Slope	Azimuth:
PVGIS-SARAH3	Crystalline Silicon (original)	1 kWp	14%	Free-standing	35°	0°

In Table 101, the CS4 is characterised in relation to the analysis conducted.

Table 101 Site characteristic.

Case Study	Coordinates (center)		Elevation	Area [ha]
	Latitude	Longitude		
CS4	50.503	18.916	293	14.9

To estimate the electricity production capacity for this CS3, the maximum feasible installed PV capacity (kWp) was determined from the available area. For the purposes of the analysis, it was assumed that 1 kWp corresponds to a PV system area of 6 m². Because the full area could not be developed under real conditions (e.g., spacing between modules, internal roads, technical buildings, fencing, and grid infrastructure), a Surface Coverage Ratio (α = 50%) was used to reflect practical land take. This value was derived from an assessment of operating photovoltaic farms with total areas ranging from 27 ha to 300 ha.

Table 102 shows the calculated performance of photovoltaic installations for CS4. The estimated yearly in-plane irradiation is 1 302.79 kWh/m², taking into account factors such as system losses (14%). The annual electricity production is determined to be 1 049.06 kWh per 1 kWp installed. The table presents the estimated value of electricity production, considering the surface area calculated using the Ideal Value Model and near-real conditions determined by the Surface Coverage Ratio. Under ideal conditions, the annual energy production could reach 26.1 GWh. Based on the Surface Coverage Ratio, the annual energy production is projected to be 13 GWh.

Table 102 Yearly PV energy production for CS4.

Yearly PV energy production [kWh]	1 049.06
Yearly in-plane irradiation [kWh/m^2]	1 302.79
Year-to-year variability [kWh]	52.84

Funded by the European Union

Changes in output due to		
-Angle of incidence [%]		-3.03
-Spectral effects [%]		1.7
Temperature and low irradiance [%]		-5.06
Total loss [%]		-19.48
Max. kWp needed [kWp]		24833
Energy production (Ideal Value Model)	26.1	13.2
Energy production (Surface Coverage Ratio)	13.0	6.6

Figure 50 show a report from the Photovoltaic Geographical Information System application (estimating annual energy production for CS4).

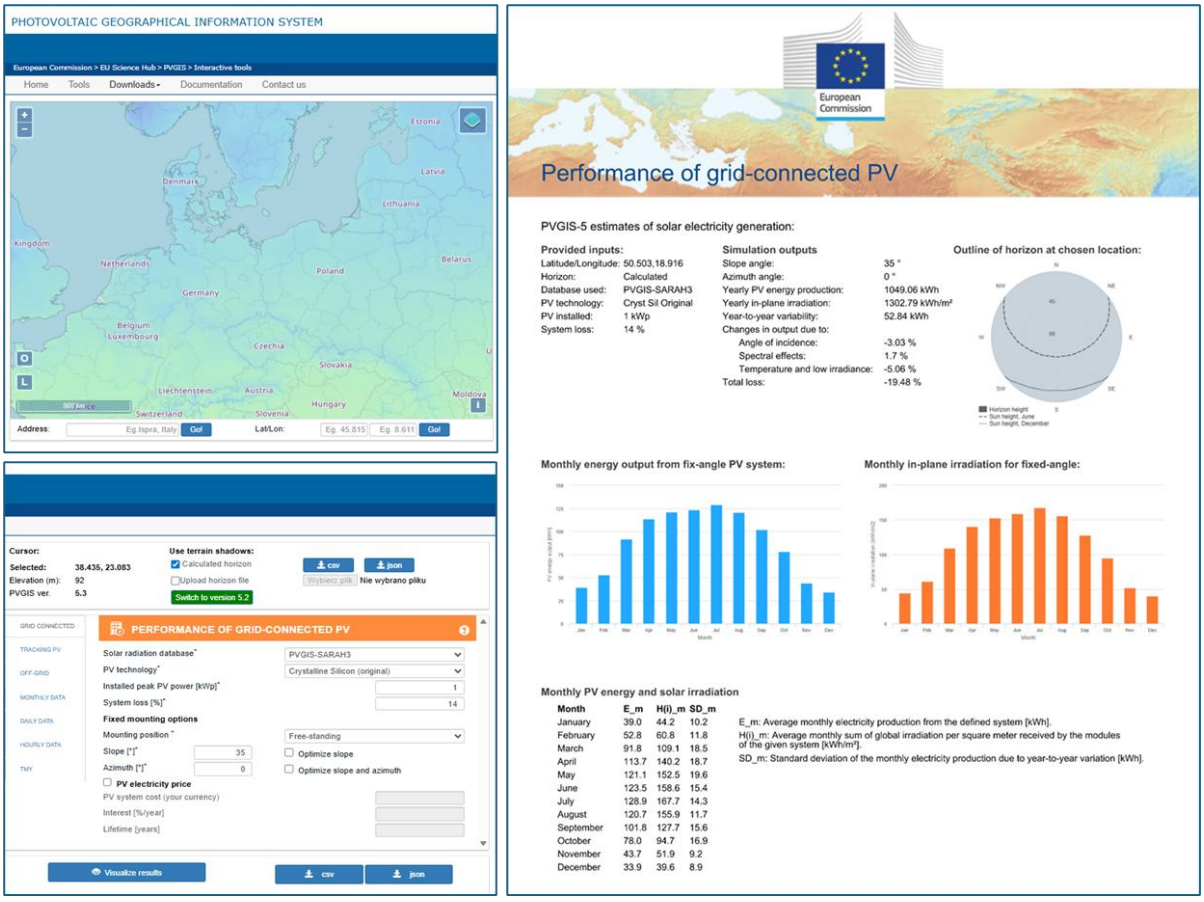

Figure 50 CS4– Performance of grid-connected PV.

The summary results of ESS7 assessment performed for CS4 are presented in Table 103.

Table 103 A summary of ESS7 (Energy properties) results for the different CS4 land-use scenarios.

Land-use scenario	Scenario 1	Scenario 2	Scenario 3
ESS7: Potential energy production [GWh/y].	0.0	13.0	0.0

Funded by the European Union

6.5 Ecosystem services assessment for CS5

In this section, the ESS valuation for CS5 (Galliera, IT – ITH5) is presented, embedded in the local site context and land-use scenarios, while maintaining the common calculation assumptions adopted across all case studies.

6.5.1 Biomass production (ESS1)

The ESS1 assessment for CS5 was based on the EP indicator (GJ/ha/year), derived from AGBinc (t d.m./ha/year) using the equation

$$EP = AGBinc \times CV \ [GJ \cdot ha^{-1} \cdot year^{-1}]$$

Where:
- CV is the calorific value of the biomass (GJ·t^{-1} d.m.), adopted in line with the ESS1 service card,
- AGBin above-ground biomass AGBinc (t d.m.·ha^{-1}·year^{-1}),
- EP is energy potential.

During data preparation, available sources on biomass increment were reviewed (inventory datasets and literature). Selected results are presented in Table 104. However, because consistent NUTS2-level data reported under the same increment definition were not available, and because substantial methodological differences were observed between sources, country-level values were adopted for the forest scenarios as a comparable benchmark.

Table 104 Annual biomass production on different types of land in Italy.

Land type	Biomass component	Value	Unit	Method /notes	Source (full citation)
Broadleaved	Not specified	3.0 - 3.2	Mg/ha/year	*No reliable value found in the searched sources (explicit mean annual biomass increment for*	[Gasparini et. al., 2022]
Coniferous	Not specified	5.40	Mg/ha/year	*No reliable value found in the searched sources (explicit mean annual biomass increment for*	
Forest (all forest types; Total Forest)	Aboveground tree biomass carbon increment (growth-related annual increase in C stock in AGB)	1.49	tC/ha/yr	Annual increase in carbon stock in aboveground tree biomass due to growth (as reported). **Value entered from Table 12.13 (Total Forest, per hectare).**	[Di Cosmo et. al., 2023]
Forest (all forest types; Total Forest)	Aboveground tree biomass (dry matter), derived from carbon using source-stated fraction	2.98	t(dry matter)/ha/yr	Conversion only using source statement: organic carbon in biomass ≈ half of dry weight, so dry biomass = 2 × carbon; Dry biomass increment computed as 2 × 1.49 tC/ha/yr = 2.98 tDM/ha/yr	[Gasparini et. al., 2022]

Land type	Biomass component	Value	Unit	Method /notes	Source (full citation)
Poplar monoculture (short rotation coppice; SRC) for woodchips	Harvestable aboveground biomass (dry matter), as reported	15	t(dry matter)/ha/yr	Reported biomass harvest/production per year for the SRC system in the study. Site- and management-specific; not a national mean.	[Manzone et. al., 2014]
Grassland / managed meadows (prati/pascoli)	Not specified	8.2	t(dry matter)/ha/yr	In order to estimate the DM yield, each herbage portion was collected with the self-loading wagons and then weighed; No explicit national/regional mean annual biomass increment for grassland located in this run.	[Dal Prà, et. al., 2023]
Non-irrigated arable land (Brassica napus)		13.7	t(dry matter)/ha/yr		[Del Gatto et. al., 2015]
Non-irrigated arable land (Brassica napus)		10.3 - 17.7			[Lazzeri et. al., 2009]
Non-irrigated arable land (Pisum sativum)		2.57 - 4.63			[Borreani et. al., 2007]

For Italy, harmonised values were applied after aligning increment definitions within the NFI-based comparison based on “Improved large-area forest increment information in Europe through harmonisation of National Forest Inventories” (Forest Ecology and Management, 562, 121913): 2.49 t d.m./ha/year for broadleaved forests and 3.05 t d.m./ha/year for coniferous forests. For the poplar plantations scenario, a representative value for energy plantations was adopted as a proxy, as no single, stable yield dataset is available that directly corresponds to the AGBinc indicator at the regional scale. The adopted level of 15.00 t d.m./ha/year falls within the typical ranges used for standardisation across case studies and therefore supports comparability of results (Table 105).

Table 105 ESS1 - parameters for the biomass energy potential for CS5 (ITH5).

CLC clasification	Couling Land Cover	AGBinc (tDM/ha/yr)	CV (GJ/tDM)	EP (GJ/ha/yr)
3.1.1	Broad-leaved forest	2.49	18.5	46.1
1.4.1	Green urban areas -grassland or lawns	8.50	17.5	148.8
1.2.1	Industrial - PV installation (80% grassland)	6.80	17.5	119.0
3.1.2	Coniferous forest	3.05	18.5	56.4
3.2.4	Transitional woodland/shrub (poplar plantations)	15.00	18.6	278.4
1.2.1	Industrial - buildings and halls (20% grassland)	1.70	17.5	29.8
2.1.1	Non-irrigated arable land - Brassica juncae	13.70	17.5	239.8

Funded by the European Union

For scenario with grasslands, a range representative of intensive meadows (often irrigated) in the ITH5 region (Emilia-Romagna) was adopted, i.e., 7–10 t d.m.·ha^{-1}·year^{-1}. This range was treated as an order-of-magnitude estimate driven by land-use type (intensive, fertilised, and irrigated grasslands) rather than by a single local statistic. In line with the report assumptions, the 3rd scenario (PV) was defined as an 80% grassland equivalent, while the industrial/commercial scenario was defined as a 20% grassland equivalent. The adopted AGBinc and CV parameters, together with the resulting EP values assigned to CLC classes and scenarios in CS5, are summarized in the Table 106 and Table 107.

Table 106 Estimated annual above-ground biomass increment (AGBinc) for grasslands in NUTS2 regions – assumptions and literature-based justification.

NUTS2	Region	Type of grassland	Estimated AGB increase (t DM·ha^{-1}·yr^{-1})	Rationale (climate / intensity)	Citations
ITH5	Emilia-Romagna	intensively managed meadows (often irrigated)	7–10	Intensive, irrigated meadows typically achieve much higher yields than semi-natural grasslands; evidence comes from European trials on intensively managed grasslands under high fertilisation.	[Feng et al., 2023], [Oddi et al., 2024],[Andresen et al., 2018]

Table 107 A summary of ESS1 (Biomass production) results for the different CS5 land-use scenarios.

Land-use scenario	Scenario 1	Scenario 2	Scenario 3
Energy potential [GJ/ha/year]	278.4	119	148.8

6.5.2 Regulation of soil quality (ESS2)

In this section, the ESS2 indicator (regulation of soil quality) for CS5 was estimated as the potential for metal accumulation in plant biomass under the analysed land-use scenarios. As part of the literature review, concentration ranges of several metals in plant biomass were compiled e.g. cadmium, lead, zinc, copper, and nickel. However, for valuation purposes, one representative metal was selected: cadmium (Cd). Cadmium is frequently reported in environmental studies, it has no nutrient function (unlike Zn or Cu), and its accumulation in plant tissues provides a useful indicator of contamination pressure. In addition, Cd is often more mobile and more readily translocated to above-ground plant parts than Pb, which increases its suitability for scenario comparisons based on AGB.

As part of the parameterisation of metal concentrations in conifer biomass, relevant literature sources were reviewed. Data for needles are widely available, but they show high variability depending on species, site conditions, anthropogenic pressure, and the age of the assimilatory tissues. At the same time, many studies focus on needles or bark as biomonitors and do not provide comparable values for stem wood, nor a consistent “needles versus stem wood” dataset for the full set of metals. For this reason, instead of averaging results from heterogeneous studies, an approach based on one internally consistent dataset was adopted, covering both needles and stem wood analysed with the same methodology. The study by Skonieczna et al. (2014) was selected as the baseline source. In that work, 15 *Pinus sylvestris* trees from five stands were

Funded by the European Union

analysed. The investigated forests were located in an area influenced by anthropogenic pressures, but not in the immediate vicinity of point emission sources.

For the assessment, mean concentrations of Cd, Zn, Pb, and Cu were introduced for needles (as a representative of the "leaf" fraction) and for stem wood (as a representative of the "stem" fraction). Cadmium was then used for the subsequent valuation step.

For poplar plantations, several literature sources were reviewed. As in other cases, it was found that experimental conditions were often not comparable between studies. Therefore, the focus was placed on a single publication that reported concentrations in poplar leaves and shoots in a format suitable for comparison across case studies

Based on the reviewed evidence, Pilipović et al. (2019) was adopted as the source of ESS2 parameters for poplar plantations, as it provides a coherent empirical dataset covering both leaves and shoots/stems, analysed using the same methodology and under the same experimental conditions. This allowed the "leaf versus wood/shoots" fractions to be separated directly, without merging heterogeneous studies and without additional assumption-based conversions. In addition, the study reports several metals (including Cd, Zn, Pb, and Cu) in a way that supported the selection of values representative of moderate anthropogenic pressure, thereby improving comparability between land-use scenarios within the ESS2 assessment.

For Scenario with grassland, an above-ground biomass (AGB)-based approach was applied, using metal concentration ranges in herbaceous plant tissues as reported in the literature. To reflect the typical spread of values associated with different levels of anthropogenic influence, three pressure levels were compiled (moderate, heavy, and extreme), representing, respectively, urban and transport impacts, post-mining areas, and locations in the immediate vicinity of smelters.

However, for the purpose of the ESS2 valuation, the moderate contamination variant was adopted, as it was considered representative of the common anthropogenic background conditions observed across the CS landscape and the analysed land-use scenarios. This choice reduced the influence of extreme concentration values that could otherwise dominate the result, and it ensured that differences in ESS2 were driven primarily by land-cover type and AGB magnitude rather than by exceptional, localised point sources of pollution.

The input data used for CS5 are identical to those described for CS1 in Section 6.1.2. Table 108 provides a concise overview of the heavy metal concentration datasets applied in the biomass assessment and includes references to the corresponding detailed tables in Section 6.1.2

Table 108 Heavy metal concentrations in biomass used for ESS2 parameterisation (data sources and table references).

No.	Heavy metal concentrations in the biomass	Reference table
1	Broadleaf species	Table 16 Heavy metal concentrations in the biomass of broadleaf species.
2	Conifer species	Table 17 Heavy metal concentrations in the biomass of conifer species.
3	Poplar and willow crops.	Table 18 Heavy metal concentrations in the biomass of poplar and willow crops.
4	Grassland species	Table 19 Heavy metal concentrations in the aboveground biomass of grassland species.

Funded by
the European Union

Table 109 presents the input parameters and calculation outputs used to estimate the ESS2 indicator for CS5 (ITH5) expressed as the potential annual cadmium (Cd) accumulation in above-ground plant biomass. It combines AGBinc values (from ESS1) with tissue Cd concentrations and harvest fractions to derive Cd concentration in harvested biomass and the resulting Cd removal per hectare and year, in accordance with the methodology described in Section 4.3

Table 109 Calculation sheet for ESS2 (Cd): biomass increment, concentration assumptions and annual removal.

Corine Land Cover	AGBinc (tDM/ha/yr) [from ESS1]	f_leaf (season harvest) [0-1]	Cd_C_leaf (mg/kg DM) [input]	Cd_C_stem (mg/kg DM) [input]	Cd_C_harvest (mg/kg DM) [calc]	Cd_Removal (g/ha/yr) [calc]
Broad-leaved forest	2.49	0.2	0.4	0.1	0.16	0.4
Green urban areas - grassland or lawns	8.50	1	0.75		0.75	6.4
Industrial - PV installation (80% grassland)	6.80	1	0.6		0.6	4.1
Coniferous forest	3.05	0.2	0.1	0.24	0.212	0.6
Transitional woodland/shrub (poplar plantations)	15.00	0.2	7.85	3.25	4.17	62.6
Industrial - buildings and halls (20% grassland)	1.70	1	0.15		0.15	0.3

In Table 110 presents the summarised results of the ESS2 assessment for CS5 across the analysed land-use scenarios. Values are reported as the estimated potential annual pollutant (Cd) accumulation in above-ground biomass (g/ha/year) enabling direct comparison between scenarios under a consistent parameter set.

Table 110 A summary of ESS2 (Regulation of soil quality) results for the different CS5 land-use scenarios.

Land-use scenario	Scenario 1	Scenario 2	Scenario 3
Potential annual pollutant accumulation [g/ha/year]	62.6	4.1	6.4

6.5.3 Mitigation of climate change (carbon dioxide sequestration) (ESS3)

Evaluation for ESS3 was based on annual carbon sequestration expressed in t CO_2/ha/year as its indicator. Total carbon sequestration was calculated as the sum of above-ground biomass and below-ground carbon accumulation, which was later converted to CO_2 equivalent. The methodology followed the carbon allocation models for poplar plantations, as specified in the ESS3 card earlier in the document.

Acquiring information about the AGBinc followed the same procedure as described in ESS1, which involved analysing the accessible sources of data such as literature, inventory data and indirect indicators. For the Maranello site in Italy (CS5) the data proved methodologically inconsistent and dispersed, which resulted in various definitions of production, growth, typological ranges or units. Therefore, a direct comparison between the coverage types was limited. The values for AGBinc across the deliverable are based on the harmonized data sourced from the “Improved large-area forest increment information in Europe through harmonization of National Forest Inventories”

Funded by the European Union

(Forest Ecology and Management, 562, 121913), which provided comparable results regarding the annual growth across most of the countries regarding forest types.

The BGBinc value was derived from the AGBinc value by using the AGBinc / BGBinc, annual above- and below-ground biomass ratio. The root-to-shoot ratio was based upon the literature findings such as Oliveira Rodríguez et al. (2018) and Intergovernmental Panel on Climate Change in 2003 and 2006 due to their unified methodology across countries, to best estimate the BGBinc (Table 111). Based on those findings, the ratio for industrial and commercial land use scenario was calculated based on the value of about 20% of the grassland AGBinc to BGBinc ratio, and the scenario assuming the ground-mounted photovoltaic farm designation accounted for 80% of the grassland coverage value.

Table 111 Sources used for the estimation of below ground - above ground ratio (%).

CS5 (IT) - types of management	AGBinc - BGBinc ratio (%)	Sources
Broad-leaf forest	0.43	IPCC (2003) Annex 3A.1.8
Coniferous forest	0.46	
Grassland	1.58	IPCC (2003) Annex 3A.1.8 Mokany, Raison & Prokushkin (2006)
Poplar cultivation	0.21	Oliveira (2018)

After calculating the values of the BGBinc from the ratio and the AGBinc values provided, the results were added and multiplied by the C fraction to account for the carbon content. The carbon content values in dry matter are assumed at approx. 50% values, supported by literature (Table 112).

In the next step the results were converted to the CO_2 equivalent by multiplying the final value by 3,67 (ratio of the atomic mass of the molecules). The indicator reflects the annual flow of carbon sequestration associated with biomass growth, rather than long-term carbon stock changes.

Table 112 Sources used for the estimation of C fraction of carbon content in dry mass.

CS5 (IT) - types of management	C fraction of carbon content in dry matter	Source/Reference
Broad-leaf forest	0.46	IPCC (2003) Annex 3A.1 Dupouey (2010)
Coniferous forest	0.46	
Grassland	0.48	Shiferaw, Kassawmar, Zeleke (2022)
Poplar cultivation	0.48	Shiferaw, Kassawmar & Zeleke (2022)

The results for the region of Maranello in Italy (CS5) show that the annual carbon sequestration for broadleaf forests is about 6,011 t (CO_2/ha/year), 7,518 t (CO_2/ha/year) for coniferous forest and for poplar plantation the results were 30,641 t (CO_2/ha/year) (Figure 51). Grassland coverage scored the highest at a 38,632 t (CO_2/ha/year). Those results were used to provide background land use values for the evaluation of the values for Scenarios 1, 2 and 3.

Funded by the European Union

ESS: MITIGATION OF CLIMATE CHANGE						
PL	Średnia roczna ilość biomasy nadziemnej z hektara (tDM/ha/yr)	Stosunek biomasy poniżej - powyżej gruntu	Średnia roczna ilość biomasy korzennej z hektara (tDM/ha/yr)	Średnie stężenie węgla w biomasie (%)	Sekwestracja węgla (kg/year/ha)	Roczna sekwestracja węgla wyrażona w t (CO_2/ha/year)
ENG	Average anual amount of above-ground biomass from ha (tDM/ha/yr)	Below ground - above ground ratio	Average annual amount of below biomass from ha (tDM/ha/yr)	Biomass mean concentration of carbon (%)	Carbon sequestration (t/year/ha)	Annual carbon sequestration expressed in t (CO_2/ha/year)
						Conversion factor from Carbon (C) to CO_2 equivalent
						3,67
CS5 (IT) - Maranello						
Forest_broadleaf_poplar	2,49	0,43	1,0707	0,46	1,638	6,011
Grassland	8,50	1,58	13,43	0,48	10,526	38,632
PV_groundmounted (80% grassland)	6,80	1,58	10,744	0,48	8,421	30,906
coniferous	3,05	0,46	1,403	0,46	2,048	7,518
poplar cultivation	15,00	0,21	3,15	0,46	8,349	30,641
Industrial of commercial units (20% grassland)	1,70	1,58	2,686	0,48	2,105	7,726

Figure 51 Calculations concerning the ESS3 indicator – annual carbon sequestration expressed in t (CO_2/ha/year) for the region of Maranello in Italy (CS5).

For the Scenario 1 - NBS solutions, the value of poplar plantations was assumed. The 2nd Scenario = industrial scenario for ESS3 considered 80% vegetation in AGBinc and BGBinc value due to a decreased but still present level of low-vegetation growth. For Scenario 3, the value of grasslands was assumed as an option for low-vegetation, recreational approach. Summary results are presented in Table 113.

Table 113 A summary of ESS3 - Annual carbon sequestration expressed in t CO_2/ha/year for the different CS5 land-use scenarios.

Land-use scenario	Scenario 1	Scenario 2	Scenario 3
ESS3 - Annual carbon sequestration expressed in t CO_2/ha/year	30.641	30.906	38.632

6.5.4 Air quality mitigation (ESS4)

The assessment of ESS4 analyses the capacity of tree and shrub canopies in urban, peri-urban, and rehabilitated post-industrial landscapes to remove air pollutants-especially particulate matter (PM10 and PM2.5)-via dry deposition processes. The key indicator applied is the annual removal of PM10, expressed in kilograms per hectare per year (kg/ha/year). This methodology is based on the dry deposition model introduced by Tallis et al. (2011), where:

$$\text{Absorption of } PM_{10} = \text{Flux (V) x Surface (SA) x Period (t) (t/km}^2\text{/year)}$$

where:

- Flux is the pollutant to the surface (amount removed per unit area and time), calculated by multiplying the deposition velocity of the pollutant (m/s), which depends on canopy structure and wind speed and the concentration of the pollutant in the atmosphere.
- Surface is the considered surface area multiplied by the surface area index functioning in given area (LAI).
- Period accounts for the period of analysis in days, multiplied by the proportion of dry days and the proportion of non-leaf days.

The total annual pollutant removal is calculated by integrating deposition fluxes over the vegetated surface area of each land-use scenario. The above contributes to the calculation as follows:

- V = deposition velocity (m/s) x pollutant conc. (µg/m³)
  - Flux (µg/m³) was then converted to daily flux by multiplying it by 86400
- SA = LAI (m²/m²) x area of land considered (m²)

Funded by the European Union

- t = period of analysis (days) x proportion of dry days (fraction) x proportion of on-leaf days (fraction)
  - Afterwards the absorption of PM_{10} was converted from (µg/m²/year) to (t/km²/year) by x10^6

The data for the Maranello site in Italy (CS5) involved land use scenarios for the broad-leaf forest, coniferous forest, mixed forest, pastures, grasslands and photovoltaic farm. For each component of the model, a literature review was conducted to establish the most suitable range of standardized values to ensure comparability. In instances where specific data for a component was unavailable, an average was derived from countries or regions with similar ecosystem types, allowing the results to remain compatible. Regarding the deposition velocity by land use type, data gathered from Marando et al. (2016) investigated deposition velocity in various vegetation types in mediterranean climate, its main reference point being Rome, Italy, using the i-Tree Eco dry deposition model (Table 114):

Table 114 Estimated deposition velocity in mediterranean climate by Marando et al. (2016).

Vegetation Type	Deposition Velocity (cm s^{-1})	Additional observations
Broadleaf trees (in-leaf)	0.5–1.5	Higher during full leaf area
Coniferous trees	1.0–2.0	Year-round interception
Grass/shrubs	0.2–0.8	Lower aerodynamic roughness

Another study by Mariarosa et al. (2019) provided information in Dry deposition modelling and validation in urban and suburban Italy, representative of mediterranean and temperate climate (Table 115).

Table 115 Estimated deposition velocity in regions managed as low-vegetation or industrial/urban sites by Mariarosa et al. (2019).

Land use type	Deposition Velocity (cm s^{-1})	Additional observations
Industrial surfaces	0.1–0.5	Smooth surfaces lower deposition
Suburban vegetation	0.3–1.2	Higher roughness enhances capture
Grasslands	0.2–0.6	Moderate

Considering the site at Maranello lays in the mediterranean climate belt, the above values were averaged for each land use type and used for further calculations. The next component researched for the model was the pollutant concentration (µg/m³).

The values were provided from the WHO 2013, EU policy ranges and local monitoring such as Air Quality Index were used, which proved at a 30-50 µg m^{-3} value. Middle range of 40,0 µg m^{-3} was used. Regarding the surface area, the values of the leaf area index (LAI) in various types of land use were taken into consideration. Due to the lack of specific data regarding the above-mentioned land use types for the region, European and global data were considered (Table 116).

Table 116 References for the leaf area index concerning chosen types of land use.

Land use type	LAI values	Represented region	Sources / References
Broad-leaf forest	5–8 (max values) 3–6 (urban average 3–4.5) 2–10 (broad global range)	France (temperate deciduous) Primarily U.S., global review Global synthesis	Le Dantec, Dufrêne, Saugier (2000) Nowak et al. (2017) Parker (2020)
Coniferous forest	6–11 3–6 (urban average 3–4.5) 2–10 (broad global range)	Pacific Northwest, U.S. Primarily U.S., global review Global synthesis	Turner et al. (2000) Nowak et al. (2017) Parker (2020)

Funded by the European Union

Land use type	LAI values	Represented region	Sources / References
Mixed forest	3–7 typical; up to 9 dense stands	Europe (multi-site comparison)	Sinan & Hasenauer (2025)
Pasture/ Grassland/ Shrub	2.0–4.5 (Wetland shrubs lower (2–3), wooded wetland stands up to 4.5)	Poland (Central Europe)	Leśny et al. (2007)

Area assumed for the calculation at this stage was a m2, after conversion km2. Regarding the period component, it was calculated by taking average of the range of the vegetation period for each type of land use. For the Maranello site, the middle of the temperature range values were used for the calculations (Table 117).

Table 117 Number of vegetative days for each land use type according to the climate type.

Land Use Type	Boreal	Temperate	Mediterranean	Subtropical	References/Sources
Coniferous Forest	120–180	180–220	200–240	250–300	EMEP (2016) GIOŚ (2018) Langner, Kull & Endlicher (2011) Chen (2015). Khan & Perlinger (2017) Vivanco et al. (2021)
Broadleaf Forest	140–190	190–220	220–260	280–320	
Grassland	150–190	200–240	220–300	280–320	
Cropland	140–180	180–220	250–320	280–330	

For the scenario regarding industrial land use type, including photovoltaic farm, the vegetative period was assumed the same as for a grassland. The proportion of dry days was assumed at 60% according to Chervenkov & Slavov (2021), while the proportion of on-leaf days was assumed at 100%, due to already exclusively selected vegetative dry periods.

The results for the region of Maranello in Italy (CS5) presented in the figure below (Figure 52) show that the annual absorption of PM10 are as follows: 18,66 t/km²/year for broad-leaf forest, 43,55 t/km²/year for coniferous forest, 30,66 t/km²/year for mixed forest, 4,15 t/km²/year for pastures, 2,74 t/km²/year for grasslands and 0,55 t/km²/year for industrial land use/photovoltaic farm.

Those results were used to provide background land use values for the evaluation of the values for Scenarios 1, 2 and 3. For the Scenario 1 – NBS solutions the value of broad-leaf forest was assumed. Concerning Scenario 2, the industrial/photovoltaic land use was considered and for Scenario 3 the values for pastures were assumed, as shown in the Table 118.

Funded by the European Union

ESS: AIR PURIFICATION							
Seconds/day (s)	86 400						
		CS5 (IT) - Maranello					
PL	EN	Broad-leaf forest	Coniferous forest	Mixed forest	Pasture	Grassland	Photovoltaic farm
Prędkość osiadania (m/s)	Deposition velocity (m/s)	0,010	0,015	0,013	0,005	0,004	0,001
Stężenie PM10 (µg/m^3)	Pollutant conc. (µg/m^3)	40,000	40,000	40,000	40,000	40,000	40,000
Przepływ (µg/m^2/s) = Prędkość osiadania (m/s) x Stężenie PM10 (µg/m^3)	**Flux (µg/m^2/s) =** deposition velocity (m/s) x pollutant conc. (µg/m^3)	0,400	0,600	0,520	0,200	0,160	0,040
Dzienny przepływ (µg/m^2/dzień)	**Daily flux (µg/m^2/day)**	34560	51840	44928	17280	13824	3456
Wskaźnik powierzchni (m^2/m^2)	Surface area index (LAI) (m^2/m^2)	6,000	7,000	6,500	2,000	1,500	1,200
Powierzchnia brana pod uwagę (m^2)	Area of land (m^2)	1,000	1,000	1,000	1,000	1,000	1,000
Powierzchnia (m^2) = Wskaźnik powierzchni (m^2/m^2) x Powierzchnia brana pod uwagę (m^2)	**Surface (m2) =** LAI (m^2/m^2) x area of land (m^2)	6,000	7,000	6,500	2,000	1,500	1,200
Okres kwitnienia liści	Vegetation period (days)	150,000	200,000	175,000	200,000	220,000	220,000
Odsetek dni suchych	Proportion of dry days (fraction)	0,600	0,600	0,600	0,600	0,600	0,600
Odsetek dni wchłaniania przez dojrzały liść	Proportion of on-leaf days (fraction)	1,000	1,000	1,000	1,000	1,000	1,000
Okres = Okres kwitnienia liści (dni) x Odsetek dni suchych x Odsetek dni wchłaniania przez dojrzały	**Period =** period of analysis (days) x proportion of dry days (fraction) x proportion of on-leaf days	90,000	120,000	105,000	120,000	132,000	132,000
Wchłanianie PM10 (µg/m^2/rok)	**Absorption of PM10 = Flux x Surface x Period (µg/m^2/year)**	18662400	43545600	30663360	4147200	2737152	547430,4
Wchłanianie PM10 (t/km^2/rok)	**Absorption of PM10 = Flux x Surface x Period (t/km^2/year)**	**18,66**	**43,55**	**30,66**	**4,15**	**2,74**	**0,55**

Figure 52 Summary of the calculations involved in the calculations for ESS4 indicator – Absorption of PM10.

Table 118 A summary of ESS4 - ESS4 – Annual removal of PM10 [t/km²/year] results for the different CS5 land-use scenarios.

Land-use scenario	Scenario 1	Scenario 2	Scenario 3
ESS4 – Annual removal of PM10, expressed as [t/km²/year]	18.66	0.55	4.15

Funded by the European Union

6.5.5 Temperature regulation (ESS5)

The assessment of temperature regulation potential was based on Landsat 8 satellite data processed into an Land Surface Temperature (LST) map using the ASTER database. The Advanced Spaceborne Thermal Emission and Reflection Radiometer Global Emissivity Database (ASTER GED) was developed by National Aeronautics and Space Administration's (NASA) Jet Propulsion Laboratory (JPL), California Institute of Technology. The ASTER GED product provides global emissivity maps of the Earth's land surface in five spectral bands. In addition to the mean emissivity and standard deviation maps for all five ASTER thermal infrared bands, the product also provides maps for mean land surface temperature (LST) and standard deviation.

The analysis focused on the day with the highest air temperature recorded in the last 10 years. For CS5, this was 4.08.2017. The analysis was carried out for the entire Maranello Municipality, within which CS5 is located. The study area was divided into land-use categories according to CLC 2018 (Corine Land Cover). The following land-use categories were identified: broad-leaved forest (311), natural grasslands (321), transitional woodland-shrub (324), land principally occupied by agriculture, with significant areas of natural vegetation (243), sparsely vegetated areas (333), sport and leisure facilities (142), complex cultivation patterns (242), discontinuous urban fabric (112),non-irrigated arable land (211), industrial or commercial units (121), annual crops associated with permanent crops (241) (Figure 53).

Mixed forests (313) and Pastures (231) located closest to CS5 were also included in the analysis, because this land-cover category did not occur within the boundaries of the commune under study.

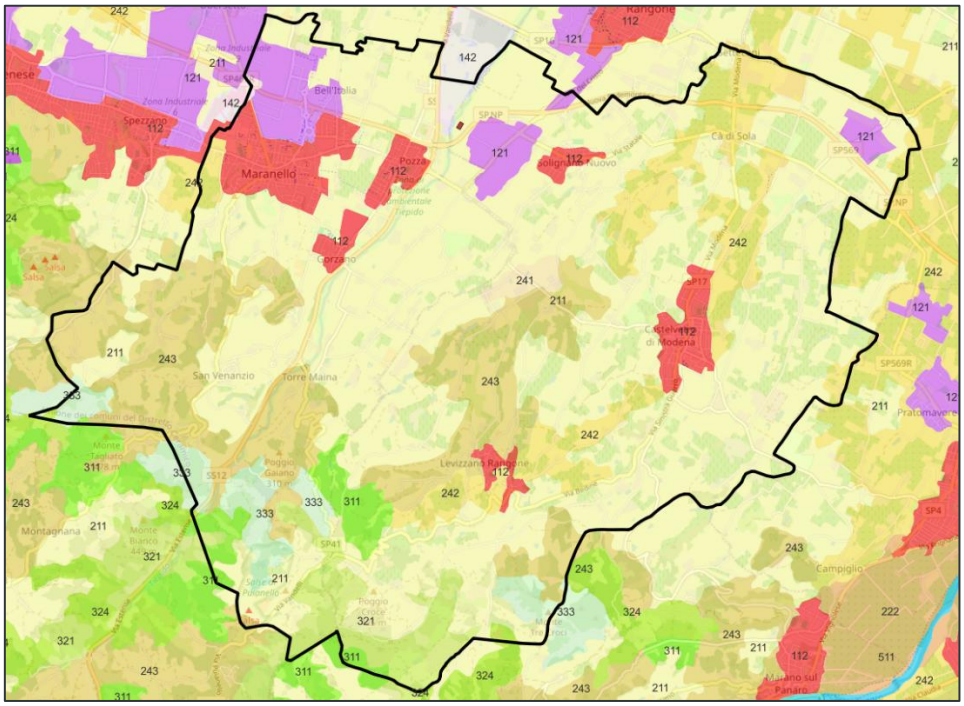

Figure 53 CLC 2018 land cover pattern for CS5.

In next step, using GIS analytical tools, the mean temperature values were calculated for each land-use type. The temperature regulation potential was calculated by relating the mean

temperature values to the highest intended mean value for a given land use. The calculation results are presented in Table 119.

Table 119 Cooling potential of land cover – CS5.

CLC 2018 Land Cover class	Mean T [°C]	Cooling potential [°C]
Mixed forest	29.5	17.0
Pastures	32.9	13.6
Broad-leaved forest	40.5	6.0
Natural grasslands	42.1	4.4
Transitional woodland-shrub	42.4	4.1
Land principally occupied by agriculture, with significant areas of natural vegetation	42.7	3.8
Sparsely vegetated areas	43.1	3.4
Sport and leisure facilities	43.5	3.0
Complex cultivation patterns	44.1	2.4
Annual crops associated with permanent crops	44.4	2.1
Discontinuous urban fabric	44.9	1.7
Non-irrigated arable land	45.0	1.5
Industrial or commercial units	46.5	0.0

The results were then normalised to a scale from 1 to 10, where 1 denotes no potential and 10 the highest potential of the ecosystem service. The projected temperature value for the analysed land-use scenarios was adopted assuming that Scenario 1 corresponds to mixed forests, Scenario 2 to industrial or commercial units, and Scenario 3 to pastures. The results of the potential analysis for each scenario are presented in Table 120.

Table 120 Evaluation of cooling potential for analysed Scenarios – CS5.

Corine Land Cover Class	Cooling potential [-]
Discontinuous urban fabric	1.9
Industrial or commercial units	1.0
Secenario 2 - Industrial scenario, photovotaic panels	**1.0**
Sport and leisure facilities	2.6
Non-irrigated arable land	1.8
Pastures	8.2
Secenario 3 - Recreational, meadows, pastures	**8.2**
Annual crops associated with permanent crops	2.1
Complex cultivation patterns	2.3
Land principally occupied by agriculture, with significant areas of natural vegetation	3.0
Broad-leaved forest	4.2
Mixed forest	10.0
Secenario 1 - NBS, forests	**10.0**
Natural grasslands	3.3
Transitional woodland-shrub	3.2
Sparsely vegetated areas	2.8

Funded by the European Union

6.5.6 Cultural- direct, in-situ and outdoor interactions with living systems (ESS6)

Baseline mapping was undertaken using the Urban Atlas LCLU 2018 (https://land.copernicus.eu/local/urban-atlas/urban-atlas-2018). Within the administrative boundaries of the units, the following land cover classes have been identified as green recreation areas forests (deciduous forests (CLC 311), coniferous forests (CLC 312), mixed forests CLC 313)), green urban areas (CLC 141), natural grassland (CLC 321) water (CLC 511, CLC 512).

The potential for providing recreational services was also assessed for areas that may be converted into green areas in the future:

- The area of the contaminated case study site (brownield CS 5)
- Land without current use (CLC 133)
- Mineral extraction and dump sites (CLC 131)

The brownfield is located in the vicinity of relatively densely populated residential areas. The future use for recreational purposes will provide 442 residents with access to this type of area. The brownfield is adjacent to Tiepido River. This is a protected area whose purpose is to preserve the natural ecological corridor of the river. The riverside landscape in this zone is characterized by rich vegetation. This area is very well known among fans of active recreation due to the so-called Percorso Natura Torrente Tiepido (Tiepido Stream Nature Trail). This grenn area also provides direct access to green spaces for 43 256 residents. This is the most important natural element ensuring access to green areas for the largest number of residents within the administrative boundaries. If the brownfild (CS) is developed as green recreation space, it will become part of this natural element with a recreational function (Tiepido Stream Nature Trail).

The potential of existing and potential green areas with recreational functions on a scale of 1 to 10 is shown in the Figure 54.

Funded by the European Union

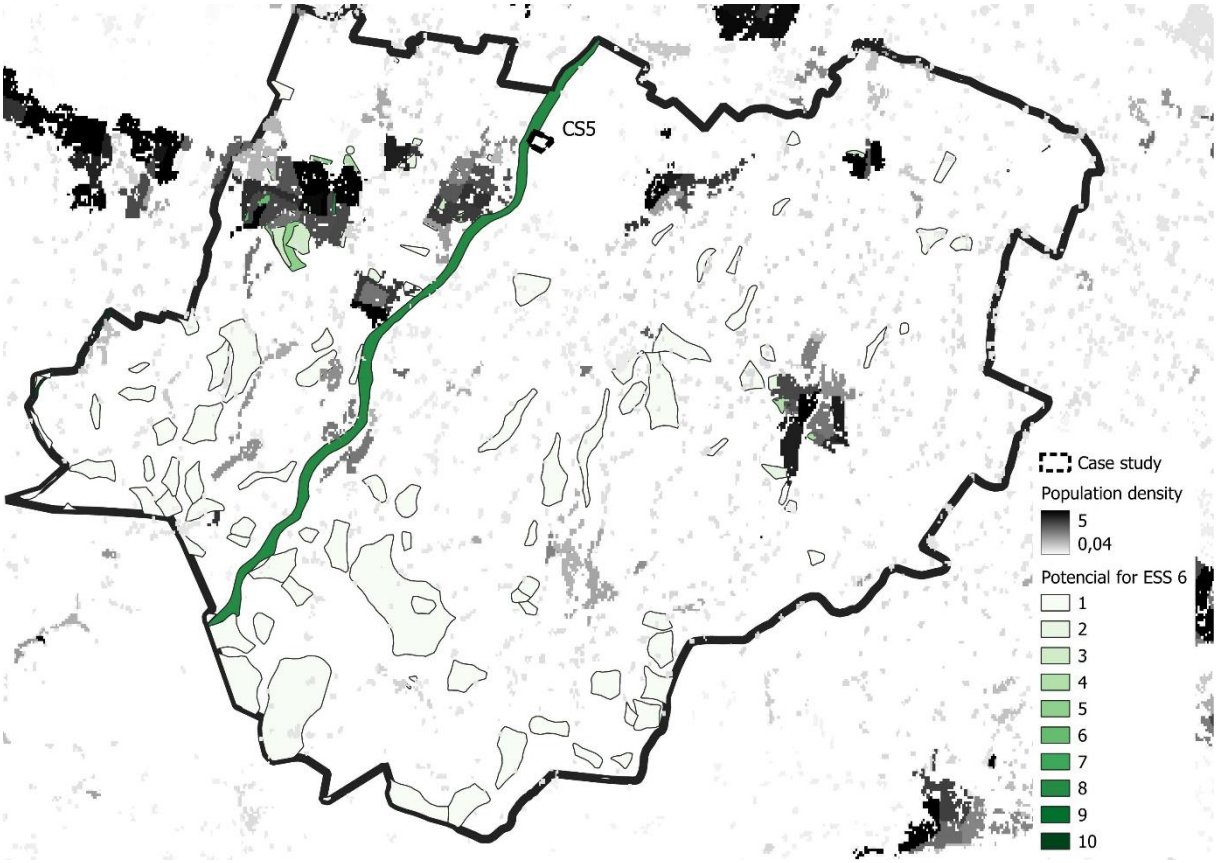

Figure 54 Cultural services: Interactions with natural environment for CS5

In the adopted land use options, only the scenario 1 (Afforestation) and scenario 3 (Grassland cover), meet the criteria for green areas with a recreational function. Compared to other green areas within the administrative boundaries, this scenario has little potential for providing cultural services (1,2). However, taking into account locations in the vicinity Tiepido River, the brownfield has high potential for providing recreational services (10). The summary results are presented in Table 121.

Table 121 A summary of ESS6results for the different CS5 land-use scenarios.

Land-use scenario	Scenario 1	Scenario 2	Scenario 3
ESS6[Number of residents within 300 meters of a green recreational area]	442 (43 698)	0	442 (43 698)

6.5.7 Energy production (ESS7)

The performance of photovoltaic installations for CS5 was estimated using an application provided by the EC: Photovoltaic Geographical Information System [https://re.jrc.ec.europa.eu/pvg_tools/en/tools.html]. This application provides data on solar radiation and energy production from photovoltaic (PV) systems globally. Following the application instructions, the performance of photovoltaic installations was estimated based on the assumption presented in Table 122.

Funded by
the European Union

Table 122 Assumptions and settings used for PV calculation for CS5.

PV Performance Modelling Parameters						
Solar radiation database:	PV technology:	Installed peak PV power	System loss	Mounting position	Slope	Azimuth:
PVGIS-SARAH3	Crystalline Silicon (original)	1 kWp	14%	Free-standing	35°	0°

In Table 123, the CS4 is characterised in relation to the analysis conducted.

Table 123 Site characteristic.

Case Study	Coordinates (center)		Elevation	Area [ha]
	Latitude	Longitude		
CS5	44.532	10.903	112	3.8

To estimate the electricity production capacity for this CS5, the maximum feasible installed PV capacity (kWp) was determined from the available area. For the purposes of the analysis, it was assumed that 1 kWp corresponds to a PV system area of 6 m². Because the full area could not be developed under real conditions (e.g., spacing between modules, internal roads, technical buildings, fencing, and grid infrastructure), a Surface Coverage Ratio (α = 50%) was used to reflect practical land take. This value was derived from an assessment of operating photovoltaic farms with total areas ranging from 27 ha to 300 ha. Table 124 shows the calculated performance of photovoltaic installations for CS5. The estimated yearly in-plane irradiation is 1 752.13 kWh/m², taking into account factors such as system losses (14%). The annual electricity production is determined to be 1 356.44 kWh per 1 kWp installed. The table presents the estimated value of electricity production, considering the surface area calculated using the Ideal Value Model and near-real conditions determined by the Surface Coverage Ratio. Under ideal conditions, the annual energy production could reach 8.6 GWh. Based on the Surface Coverage Ratio, the annual energy production is projected to be 4.3 GWh.

Table 124 Yearly PV energy production for CS5.

Yearly PV energy production [kWh]		1 356.44
Yearly in-plane irradiation [kWh/m^2]		1 752.13
Year-to-year variability [kWh]		71.21
Changes in output due to		
-Angle of incidence [%]		-2.71
-Spectral effects [%]		1.21
Temperature and low irradiance [%]		-8.58
Total loss [%]		-22.58
Max. kWp needed [kWp]		6333
Energy production (Ideal Value Model)	GWh/y	8.6
Energy production (Surface Coverage Ratio)	GWh/y	4.3

Figure 55 shows a report from the Photovoltaic Geographical Information System application (estimating annual energy production for CS5).

Funded by the European Union

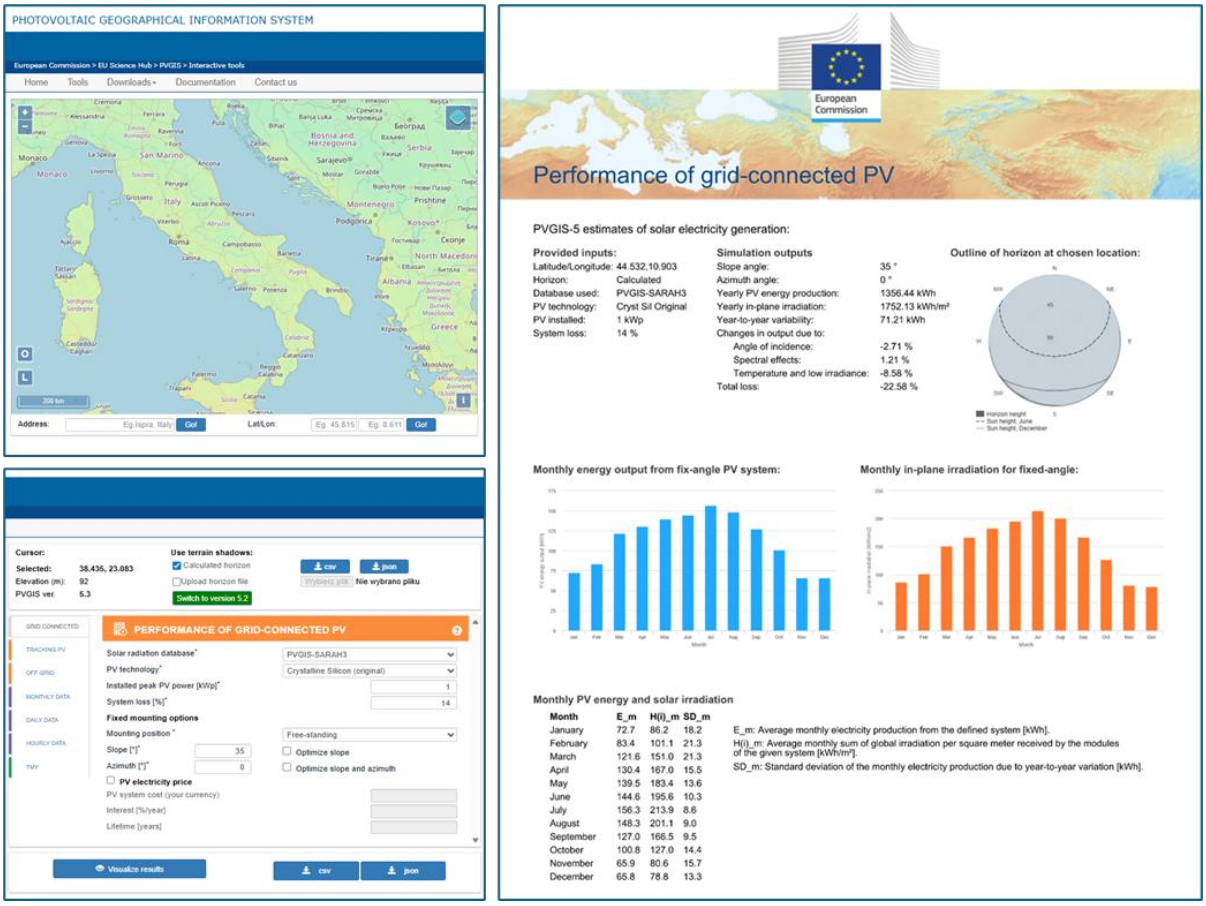

Figure 55 CS5– Performance of grid-connected PV

A summary of ESS7 (Energy properties) results for the different CS5 land-use scenarios are presented in Table 125.

Table 125 A summary of ESS7 (Energy properties) results for the different CS5 land-use scenarios.

Land-use scenario	Scenario 1	Scenario 2	Scenario 3
ESS7: Potential energy production [GWh/y].	0.0	4.3	0.0

Funded by
the European Union

6.6 Ecosystem services assessment for CS6

In this section, the valuation of ESS for CS6 (Vieux-Charmont, FR – FRC2) was presented in relation to local site conditions and the analysed scenarios, while maintaining a consistent data preparation methodology across the entire report.

6.6.1 Biomass production (ESS1)

The ESS1 assessment for CS6 was based on the EP indicator (GJ·ha^{-1}·year^{-1}), calculated from the annual above-ground biomass increment AGBinc (t d.m.·ha^{-1}·year^{-1}) using the equation:

$$EP = AGBinc \times CV \ [GJ \cdot ha^{-1} \cdot year^{-1}]$$

Where:

- CV is the calorific value of biomass (GJ·t^{-1} d.m.), adopted in line with the ESS1 service card.
- AGBin above-ground biomass AGBinc (t d.m.·ha^{-1}·year^{-1}),
- EP is energy potential.

During data preparation, available AGBinc sources were reviewed, including inventory datasets, literature, and proxy indicators. In practice, the information available for France was found to be fragmented and methodologically inconsistent, which limited the scope for direct comparisons between case studies. Therefore, consistent with the approach applied throughout the report, harmonised results from "Improved large-area forest increment information in Europe through harmonisation of National Forest Inventories" (Forest Ecology and Management, 562, 121913) were adopted as the reference benchmark. This publication provides comparable increment data (including AGB increment) at country and forest-type levels after harmonising definitions and calculation approaches (Table 126).

Table 126 Annual biomass production on different types of land in France.

Land type	Min (t/ha/year)	Max (t/ha/year)	Unit	Biomass type/notes	Sources
Broadleaved forests	4.03	4.03	t/ha/year	Above-ground biomass increment (GAI7)	[Gschwantner et. al., 2024]
Mixed forests	4.20	4.20	t/ha/year	Above-ground biomass increment (GAI7)	[Gschwantner et. al., 2024]
Coniferous forests	4.72	4.72	t/ha/year	Above-ground biomass increment (GAI7)	[Gschwantner et. al., 2024]
Poplar monoculture (poplar plantations)	4.20	5.40	m³/ha/year	Wood mass at 12% moisture (stem/wood proxy); wood density 350–450 kg/m³ (12% moisture)	[CIP, 2020]
Grassland – permanent productive grasslands	5.00	5.00	t/ha/year	Annual dry matter production (DM)	Étude de nouveaux gisements de biomasse végétale fermentescible, et des conditions de leur mobilisation pour la méthanisation Rapport
Grassland – temporary grasslands	6.00	6.00	t/ha/year	Annual dry matter production (DM)	
Grassland – permanent low-productive (estives)	1.50	1.50	t/ha/year	Annual dry matter production (DM)	

For CS6 (France), AGBinc values were adopted from the harmonised reference source "Improved large-area forest increment information in Europe through harmonisation of National Forest Inventories" (Forest Ecology and Management, 562, 121913): 4.72 t d.m.·ha^{-1}·year^{-1} for coniferous forests and 4.03 t d.m.·ha^{-1}·year^{-1} for broadleaved forests. For the poplar plantations scenario, AGBinc = 6.60 t d.m.·ha^{-1}·year^{-1} was applied as a working value (source data presented in Table 127). This parameter was derived by converting the typical volume increment of poplar stands in France (about 12–14 m³·ha^{-1}·year^{-1}) into dry biomass using a standard poplar wood density factor (approximately 0.47 t d.m./m³). The resulting estimate (around 6.6 t d.m.·ha^{-1}·year^{-1}) provided a clear and defensible input for EP calculations in a context where consistent regional datasets for poplar plantations were not available.

Table 127 ESS1 – Calculation parameters for the biomass energy potential for CS6 (FRC2).

CLC clasification	Couling Land Cover	AGBinc (tDM/ha/yr)	CV (GJ/tDM)	EP (GJ/ha/yr)
3.1.1	Broad-leaved forest	4.03	18.5	74.6
1.4.1	Green urban areas -grassland or lawns	4.00	17.5	70.0
1.2.1	Industrial - PV installation (80% grassland)	3.20	17.5	56.0
3.1.2	Coniferous forest	4.72	18.5	87.3
3.2.4	Transitional woodland/shrub (poplar plantations)	6.60	18.6	122.5
1.2.1	Industrial - buildings and halls (20% grassland)	0.80	17.5	14.0
2.1.1	Non-irrigated arable land - *Brassica juncae*	*n.d.*	*n.d.*	*n.d.*
2.1.1	Non-irrigated arable land - *Lablab purpureus*	*n.d.*	*n.d.*	*n.d.*

For scenario with grasslands (Scenario 3), a typology-based approach was applied. Instead of relying on administrative regional averages, indicative AGBinc values were assigned to specific meadow/pasture types using the literature summary prepared for the report. In this framing, AGBinc depended mainly on grassland type, management intensity, and water availability. For FRC2 (Bourgogne – Franche-Comté), a range of 3–5 t d.m.·ha^{-1}·year^{-1} was assumed for temperate and mountain meadows, and a working value of 4.00 t d.m.·ha^{-1}·year^{-1} was used in the calculations (Table 128).

Table 128 Estimated annual above-ground biomass increment (AGBinc) for grasslands in NUTS2 regions – assumptions and literature-based justification.

NUTS2	Region	Type of grassland	Estimated AGB increase (t DM·ha^{-1}·yr^{-1})	Rationale (climate / intensity)	Citations
FRC2	Bourgogne–Franche-Comté	temperate / mountain	3–5	Temperate and mountain meadows produce less biomass during the growing season than	[Shi et al., 2023],

Funded by the European Union

		meadows (grasslands)		intensively managed lowland meadows, but their overall biomass increase is in a similar range to other temperate meadows.	[Barrachina et al., 2015]

Scenario, where vegetation cover is only partial, coefficients were applied to reflect the assumed biologically active area: PV (ground-mounted) = 0.8 × grassland and industrial/commercial units = 0.2 × grassland (in terms of AGBinc). This keeps the scenarios comparable while accounting for the limited vegetated surface.

The summary results of ESS1 calculation for CS6 are presented in Table 129.

Table 129 A summary of ESS1 (Biomass production) results for the different CS6 land-use scenarios.

Land-use scenario	Scenario 1	Scenario 2	Scenario 3
Energy potential [GJ/ha/year]	122.5	56	70

6.6.2 Regulation of soil quality (ESS2)

In this section, the ESS2 indicator (regulation of soil quality) for CS6 was estimated as the potential for metal accumulation in plant biomass under the analysed land-use scenarios. As part of the literature review, concentration ranges of several metals in plant biomass were compiled e.g. cadmium, lead, zinc, copper, and nickel. However, for valuation purposes, one representative metal was selected: cadmium (Cd). Cadmium is frequently reported in environmental studies, it has no nutrient function (unlike Zn or Cu), and its accumulation in plant tissues provides a useful indicator of contamination pressure. In addition, Cd is often more mobile and more readily translocated to above-ground plant parts than Pb, which increases its suitability for scenario comparisons based on AGB.

As part of the parameterisation of metal concentrations in conifer biomass, relevant literature sources were reviewed. Data for needles are widely available, but they show high variability depending on species, site conditions, anthropogenic pressure, and the age of the assimilatory tissues. At the same time, many studies focus on needles or bark as biomonitors and do not provide comparable values for stem wood, nor a consistent “needles versus stem wood” dataset for the full set of metals. For this reason, instead of averaging results from heterogeneous studies, an approach based on one internally consistent dataset was adopted, covering both needles and stem wood analysed with the same methodology. The study by Skonieczna et al. (2014) was selected as the baseline source. In that work, 15 *Pinus sylvestris* trees from five stands were analysed. The investigated forests were located in an area influenced by anthropogenic pressures, but not in the immediate vicinity of point emission sources.

For the assessment, mean concentrations of Cd, Zn, Pb, and Cu were introduced for needles (as a representative of the “leaf” fraction) and for stem wood (as a representative of the “stem” fraction). Cadmium was then used for the subsequent valuation step.

For poplar plantations, several literature sources were reviewed. As in other cases, it was found that experimental conditions were often not comparable between studies. Therefore, the focus

was placed on a single publication that reported concentrations in poplar leaves and shoots in a format suitable for comparison across case studies

Based on the reviewed evidence, Pilipović et al. (2019) was adopted as the source of ESS2 parameters for poplar plantations, as it provides a coherent empirical dataset covering both leaves and shoots/stems, analysed using the same methodology and under the same experimental conditions. This allowed the "leaf versus wood/shoots" fractions to be separated directly, without merging heterogeneous studies and without additional assumption-based conversions. In addition, the study reports several metals (including Cd, Zn, Pb, and Cu) in a way that supported the selection of values representative of moderate anthropogenic pressure, thereby improving comparability between land-use scenarios within the ESS2 assessment.

For Scenario with grassland (Scenario 3), an above-ground biomass (AGB)-based approach was applied, using metal concentration ranges in herbaceous plant tissues as reported in the literature. To reflect the typical spread of values associated with different levels of anthropogenic influence, three pressure levels were compiled (moderate, heavy, and extreme), representing, respectively, urban and transport impacts, post-mining areas, and locations in the immediate vicinity of smelters.

However, for the purpose of the ESS2 valuation, the moderate contamination variant was adopted, as it was considered representative of the common anthropogenic background conditions observed across the CS landscape and the analysed land-use scenarios. This choice reduced the influence of extreme concentration values that could otherwise dominate the result, and it ensured that differences in ESS2 were driven primarily by land-cover type and AGB magnitude rather than by exceptional, localised point sources of pollution.

The input data used for CS6 are identical to those described for CS1 in Section 6.1.2. Table 130 provides a concise overview of the heavy metal concentration datasets applied in the biomass assessment and includes references to the corresponding detailed tables in Section 6.1.2

Table 130 Heavy metal concentrations in biomass used for ESS2 parameterisation (data sources and table references).

No.	Heavy metal concentrations in the biomass	Reference table
1	Broadleaf species	Table 16 Heavy metal concentrations in the biomass of broadleaf species.
2	Conifer species	Table 17 Heavy metal concentrations in the biomass of conifer species.
3	Poplar and willow crops.	Table 18 Heavy metal concentrations in the biomass of poplar and willow crops.
4	Grassland species	Table 19 Heavy metal concentrations in the aboveground biomass of grassland species.

Table 131 presents the input parameters and calculation outputs used to estimate the ESS2 indicator for CS6 (FRC2) expressed as the potential annual cadmium (Cd) accumulation in above-ground plant biomass. It combines AGBinc values (from ESS1) with tissue Cd concentrations and harvest fractions to derive Cd concentration in harvested biomass and the resulting Cd removal per hectare and year, in accordance with the methodology described in Section 4.3

Table 131 Calculation sheet for ESS2 (Cd): biomass increment, concentration assumptions and annual removal.

Funded by the European Union

Corine Land Cover	AGBinc (tDM/ha/yr) [from ESS1]	f_leaf (season harvest) [0-1]	Cd_C_leaf (mg/kg DM) [input]	Cd_C_stem (mg/kg DM) [input]	Cd_C_harvest (mg/kg DM) [calc]	Cd_Removal (g/ha/yr) [calc]
Broad-leaved forest	4.03	0.2	0.4	0.1	0.16	0.6
Green urban areas -grassland or lawns	4.00	1	0.75		0.75	3.0
Industrial - PV installation (80% grassland)	3.20	1	0.6		0.6	1.9
Coniferous forest	4.72	0.2	0.1	0.24	0.212	1.0
Transitional woodland/shrub (poplar plantations)	6.60	0.2	7.85	3.25	4.17	27.5
Industrial - buildings and halls (20% grassland)	0.80	1	0.15		0.15	0.1

Table 132 summarises the ESS2 results for CS6 across the analysed land-use scenarios. Values are reported as the estimated potential annual pollutant (Cd) accumulation in above-ground biomass (g/ha/year) enabling direct comparison between scenarios under a consistent parameter set.

Table 132 A summary of ESS2 (Regulation of soil quality) results for the different CS6 land-use scenarios.

Land-use scenario	Scenario 1	Scenario 2	Scenario 3
Potential annual pollutant accumulation [g/ha/year]	27.5	1.9	3.0

6.6.3 Mitigation of climate change (carbon dioxide sequestration) (ESS3)

The assessment of ESS3 was carried out using annual carbon sequestration as the key indicator, expressed in tonnes of CO_2 per hectare per year (t CO_2/ha/year). Total carbon sequestration was determined by combining carbon accumulation in above-ground biomass and below-ground biomass and subsequently converting the total into CO_2 equivalents. The methodology applied was consistent with the carbon allocation models developed for poplar plantations, as outlined earlier in the ESS3 section of the document.

The estimation of annual above-ground biomass increment (AGBinc) followed the same approach described under ESS1, which involved reviewing available data sources such as scientific literature, forest inventory databases, and indirect indicators. For the Vieux-Charmont site in France (CS6), the available data were fragmented and methodologically inconsistent, with differing definitions of production, growth parameters, typological classifications, and measurement units. Consequently, direct comparisons between land cover types were limited. To ensure consistency throughout the deliverable, AGBinc values were ultimately based on harmonized data from the study “Improved large-area forest increment information in Europe through harmonization of National Forest Inventories” (Forest Ecology and Management, 562, 121913), which provides comparable estimates of annual forest growth across most European countries and forest types.

The annual below-ground biomass increment (BGBinc) was derived from the AGBinc using the ratio between above- and below-ground biomass increments (AGBinc/BGBinc). The root-to-shoot

ratio applied was based on findings from the literature, including Oliveira Rodríguez et al. (2018) and the Intergovernmental Panel on Climate Change (2003, 2006), selected due to their standardized methodologies across countries, allowing for a consistent estimation of BGBinc (Table 133). Based on these sources, the ratio for the industrial and commercial land-use scenario was calculated as approximately 20% of the grassland AGBinc-to-BGBinc ratio, while the scenario assuming ground-mounted photovoltaic farm development accounted for 80% of the grassland coverage value.

Table 133 Sources used for the estimation of below ground - above ground ratio (%).

CS6 (FR) - types of management	AGBinc - BGBinc ratio (%)	Sources
Broad-leaf forest	0.43	IPCC (2003) Annex 3A.1.8
Coniferous forest	0.46	
Grassland	2.25	IPCC (2003) Annex 3A.1.8 Mokany, Raison & Prokushkin (2006)
Poplar cultivation	0.21	Oliveira (2018)

After calculating the values of the BGBinc from the ratio and the AGBinc values provided, the results were added and multiplied by the C fraction to account for the carbon content. The carbon content values in dry matter are assumed at approx. 50% values, supported by literature(Table 134).

In the next step the results were converted to the CO_2 equivalent by multiplying the final value by 3.67 (ratio of the atomic mass of the molecules). The indicator reflects the annual flow of carbon sequestration associated with biomass growth, rather than long-term carbon stock changes.

Table 134 Sources used for the estimation of C fraction of carbon content in dry mass.

CS6 (FR) - types of management	C fraction of carbon content in dry matter	Source/Reference
Broad-leaf forest	0.46	IPCC (2003) Annex 3A.1
Coniferous forest	0.46	Dupouey (2010)
Grassland	0.48	Shiferaw, Kassawmar, Zeleke (2022)
Poplar cultivation	0.48	Shiferaw, Kassawmar & Zeleke (2022)

The results for the region of Vieux-Charmont in France (CS6)(Figure 56) shows that the annual carbon sequestration for broadleaf forests is about 9.729 t (CO_2/ha/year), 11.634 t (CO_2/ha/year) for coniferous forest and for poplar plantation the results were 17,567 t (CO_2/ha/year). Grassland coverage scored the highest at a 22.901 t (CO_2/ha/year). Those results were used to provide background land use values for the evaluation of the values for Scenarios 1, 2 and 3.

Funded by
the European Union

ESS: MITIGATION OF CLIMATE CHANGE						
PL	Średnia roczna ilość biomasy nadziemnej z hektara (tDM/ha/yr)	Stosunek biomasy poniżej - powyżej gruntu	Średnia roczna ilość biomasy korzennej z hektara (tDM/ha/yr)	Średnie stężenie węgla w biomasie (%)	Sekwestracja węgla (kg/year/ha)	Roczna sekwestracja węgla wyrażona w t (CO_2/ha/year)
ENG	Average anual amount of above-ground biomass from ha (tDM/ha/yr)	Below ground - above ground ratio	Average annual amount of below biomass from ha (tDM/ha/yr)	Biomass mean concentration of carbon (%)	Carbon sequestration (t/year/ha)	Annual carbon sequestration expressed in t (CO_2/ha/year)
						Conversion factor from Carbon (C) to CO_2 equivalent
						3,67
CS6 (FR) - Vieux-Charmont						
Forest_broadleaf_poplar	4,03	0,43	1,733	0,46	2,651	9,729
Grassland	4,00	2,25	9,000	0,48	6,240	22,901
PV_groundmounted (80% grassland)	3,20	1,58	5,056	0,48	3,963	14,544
coniferous	4,72	0,46	2,171	0,46	3,170	11,634
poplar cultivation	8,60	0,21	1,806	0,46	4,787	17,567
Industrial of commercial units (20% grassland)	0,80	1,58	1,264	0,48	0,991	3,636

Figure 56 Calculations concerning the ESS3 indicator – annual carbon sequestration expressed in t (CO_2/ha/year) for the region of Vieux-Charmont in France (CS6).

For the Scenario 1 (afforestation, NBS solutions), the value of poplar plantations was assumed. The 2nd Scenario = industrial scenario for ESS3 considered 80% vegetation in AGBinc value due to a decreased but still present level of low-vegetation growth. For Scenario 3, the value of grasslands was assumed as an option for low-vegetation, recreational approach. The final results are summarized in Table 135.

Table 135 A summary of ESS3 - Annual carbon sequestration expressed in t CO_2/ha/year for the different CS6 land-use scenarios.

Land-use scenario	Scenario 1	Scenario 2	Scenario 3
ESS3 - Annual carbon sequestration expressed in t CO_2/ha/year	17.57	14.54	22.90

6.6.4 Air quality mitigation (ESS4)

Evaluation of ESS4 considers the removal of atmospheric pollutants (specifically particulate matter PM_{10} and $PM_{2.5}$) by tree and shrub canopies in urban, peri-urban and rehabilitated post-industrial areas through dry deposition processes. The main indicator is the annual removal of particulate matter PM_{10} particles expressed in kg/ha/year. The methodology is based on the dry deposition mode, established by Tallis et al. (2011), where:

$$\text{Absorption of } PM_{10} = \text{Flux (V) x Surface (SA) x Period (t) (t/km}^2\text{/year)}$$

where:

- Flux is the pollutant to the surface (amount removed per unit area and time), calculated by multiplying the deposition velocity of the pollutant (m/s), which depends on canopy structure and wind speed and the concentration of the pollutant in the atmosphere.
- Surface is the considered surface area multiplied by the surface area index functioning in given area (LAI).
- Period accounts for the period of analysis in days, multiplied by the proportion of dry days and the proportion of non-leaf days.

The total annual pollutant removal is calculated by integrating deposition fluxes over the vegetated surface area of each land-use scenario. The above contributes to the calculation as follows:

- V = deposition velocity (m/s) x pollutant conc. (µg/m³)
  - Flux (µg/m³) was then converted to daily flux by multiplying it by 86400
- SA = LAI (m²/m²) x area of land considered (m²)
- t = period of analysis (days) x proportion of dry days (fraction) x proportion of on-leaf days (fraction)

Funded by the European Union

- Afterwards the absorption of PM_{10} was converted from (µg/m²/year) to (t/km²/year) by x10^6

The data for the Vieux-Charmont site in France (CS6) involved land use scenarios for the broad-leaf forest, coniferous forest, mixed forest, pastures, grasslands and photovoltaic farm. For each of the components of the model, the literature research was carried out to scope the best range of unified results to produce comparable values. In some cases, it was not possible to gather data regarding each of the components of the model, in which case an average was used from the data regarding countries or regions in the world with closest ecosystem type, for the results to be compatible.

Regarding the deposition velocity by land use type, no data was found in the research for the Vieux-Charmont region, however, comparable data were used from European, U.S. and Italian databases to provide a baseline. Data gathered from Marando et al. (2016), investigated deposition velocity in various vegetation types in mediterranean climate, its main reference point being Rome, Italy, using the i-Tree Eco dry deposition model (Table 136):

Table 136 Estimated deposition velocity in mediterranean climate by Marando et al. (2016).

Vegetation Type	Deposition Velocity (cm s^{-1})	Additional observations
Broadleaf trees (in-leaf)	0.5–1.5	Higher during full leaf area
Coniferous trees	1.0–2.0	Year-round interception
Grass/shrubs	0.2–0.8	Lower aerodynamic roughness

Another study by Mariarosa et al. (2019) provided information in Dry deposition modelling and validation in urban and suburban Italy, representative of mediterranean and temperate climate (Table 137).

Table 137 Estimated deposition velocity in regions managed as low-vegetation or industrial/urban sites by Mariarosa et al. (2019).

Land use type	Deposition Velocity (cm s^{-1})	Additional observations
Industrial surfaces	0.1–0.5	Smooth surfaces lower deposition
Suburban vegetation	0.3–1.2	Higher roughness enhances capture
Grasslands	0.2–0.6	Moderate

Other studies which represented estimation of deposition velocity on a global scale in temperate and boreal regions, their focus on U.S and central Europe. Lovett (1994) investigated particle deposition velocity in coniferous forests, deciduous forests and grasslands, with results stated below (Table 138).

Table 138 Estimated deposition velocity in temperate and boreal climate by Lovett (1994).

Land Use	Particle Deposition Velocity (cm s^{-1})	Additional observations
Coniferous forest	1.0–3.0	High canopy roughness
Deciduous forest	0.5–2.0	Seasonal variation
Grassland	0.1–0.5	Lower surface roughness

Considering the site in Vieux-Charmont site in France lays in the temperate climate belt, a cross-study synthesis was performed to best account for the values of deposition velocity for the different types of vegetation in Vieux-Charmont region, and an average of below values (Table 139) was used for following calculations.

Funded by the European Union

Table 139 Cross-Study Synthesis Deposition Velocity by Land Use Type.

Land Use	PM10 (cm s^{-1})	Represented regions	Sources/Reference
Broad-leaf forest	0.5–2.0	North America, Italy	Marando et al. (2016) Lovett (1994) Nowak et al. (2013) U.S. Forest Service. i-Tree Eco (2011). Mariarosa et al. (2019)
Coniferous forest	1.0–3.0	North America, Europe	
Grassland/ Pasture	0.1–0.5	North America, Europe	
Industrial land cover	0.1–0.5	Italy	

The next component researched for the model was the pollutant concentration (µg/m³). The values for pollutant concentrations could not be recovered for the region; however, estimates were based on the information gathered over a period from the Airparif (2022) reports, and investigations by Borlaza-Lacoste et. al. (2022). Based on these results, a pollution concentration of 20 µg/m³ was assumed.

Regarding the surface area, the values of the leaf area index (LAI) in various types of land use were taken into consideration. Due to the lack of specific data regarding the above-mentioned land use types for the region, European and global data were considered, see Table 140.

Table 140 References for the leaf area index concerning chosen types of land use.

Land use type	LAI values	Represented region	Sources / References
Broad-leaf forest	5–8 (max values) 3–6 (urban average 3–4.5) 2–10 (broad global range)	France (temperate deciduous) Primarily U.S., global review Global synthesis	Le Dantec, Dufrêne, Saugier (2000) Nowak et al. (2017) Parker (2020)
Coniferous forest	6–11 3–6 (urban average 3–4.5) 2–10 (broad global range)	Pacific Northwest, U.S. Primarily U.S., global review Global synthesis	Turner et al. (2000) Nowak et al. (2017) Parker (2020)
Mixed forest	3–7 typical; up to 9 dense stands	Europe (multi-site comparison)	Sinan & Hasenauer (2025)
Pasture/ Grassland/ Shrub	2.0–4.5 (Wetland shrubs lower (2–3), wooded wetland stands up to 4.5)	Poland (Central Europe)	Leśny et al. (2007)

Area assumed for the calculation at this stage was a m^2, after conversion km^2. Regarding the period component, it was calculated by taking average of the range of the vegetation period for each type of land use. The temperature values used for calculation performed for the Vieux-Charmont are presented in Table 141.

Table 141 Number of vegetative days for each land use type according to the climate type.

Land Use Type	Boreal	Temperate	Mediterranean	Subtropical	References/Sources
Coniferous Forest	120–180	180–220	200–240	250–300	EMEP (2016) GIOŚ (2018) Langner, Kull & Endlicher (2011) Chen (2015). Khan & Perlinger (2017) Vivanco et al. (2021)
Broadleaf Forest	140–190	190–220	220–260	280–320	
Grassland	150–190	200–240	220–300	280–320	
Cropland	140–180	180–220	250–320	280–330	

For the scenario regarding industrial land use type, including photovoltaic farm, the vegetative period was assumed the same as for a grassland. The proportion of dry days was assumed at

60% according to Chervenkov & Slavov (2021), while the proportion of on-leaf days was assumed at 100%, due to already exclusively selected vegetative dry periods.

The results for the region of Vieux-Charmont site in France (CS6) presented in the Figure 57 show that the annual absorption of PM10 are as follow: 12.13 t/km²/year for broad-leaf forest, 29.03 t/km²/year for coniferous forest, 20.05 t/km²/year for mixed forest, 1.24 t/km²/year for pastures, 1.03 t/km²/year for grasslands and 0.27 t/km²/year for industrial land use/photovoltaic farm. Those results were used to provide background land use values for the evaluation of the values for Scenarios 1, 2 and 3. For the Scenario 1 (afforestration, NBS solutions) the value of broad-leaf forest was assumed. Concerning Scenario 2, the industrial/photovoltaic land use was considered and for Scenario 3 the values for pastures were assumed, as shown in the Table 142.

ESS: AIR PURIFICATION							
Seconds/day (s)	86 400						
		CS6 (FR) - Vieux-Charmont					
PL	EN	Broad-leaf forest	Coniferous forest	Mixed forest	Pasture	Grassland	Photovoltaic farm
Prędkość osiadania (m/s)	Deposition velocity (m/s)	0,013	0,020	0,017	0,003	0,003	0,001
Stężenie PM10 (µg/m³)	Pollutant conc. (µg/m³)	20,000	20,000	20,000	20,000	20,000	20,000
Przepływ (µg/m²/s) = Prędkość osiadania (m/s) x Stężenie PM10 (µg/m³)	**Flux (µg/m²/s) =** deposition velocity (m/s) x pollutant conc. (µg/m³)	0,260	0,400	0,340	0,060	0,060	0,020
Dzienny przepływ (µg/m²/dzień)	**Daily flux (µg/m²/day)**	22464	34560	29376	5184	5184	1728
Wskaźnik powierzchni (m²/m²)	Surface area index (LAI) (m²/m²)	6,000	7,000	6,500	2,000	1,500	1,200
Powierzchnia brana pod uwagę (m²)	Area of land (m²)	1,000	1,000	1,000	1,000	1,000	1,000
Powierzchnia (m²) = Wskaźnik powierzchni (m²/m²) x Powierzchnia brana pod uwagę (m²)	**Surface (m2) =** LAI (m²/m²) x area of land (m²)	6,000	7,000	6,500	2,000	1,500	1,200
Okres kwitnienia liści	Vegetation period (days)	150,000	200,000	175,000	200,000	220,000	220,000
Odsetek dni suchych	Proportion of dry days (fraction)	0,600	0,600	0,600	0,600	0,600	0,600
Odsetek dni wchłaniania przez dojrzały liść	Proportion of on-leaf days (fraction)	1,000	1,000	1,000	1,000	1,000	1,000
Okres = Okres kwitnienia liści (dni) x Odsetek dni suchych x Odsetek dni wchłaniania przez dojrzały	**Period =** period of analysis (days) x proportion of dry days (fraction) x proportion of on-leaf days	90,000	120,000	105,000	120,000	132,000	132,000
Wchłanianie PM10 (µg/m²/rok)	**Absorption of PM10 = Flux x Surface x Period (µg/m²/year)**	12130560	29030400	20049120	1244160	1026432	273715,2
Wchłanianie PM10 (t/km²/rok)	**Absorption of PM10 = Flux x Surface x Period (t/km²/year)**	**12,13**	**29,03**	**20,05**	**1,24**	**1,03**	**0,27**

Figure 57 Summary of the calculations involved in the calculations for ESS4 indicator – Absorption of PM10.

Funded by the European Union

Table 142 A summary of ESS4 - Annual removal of PM10 [t/km²/year] results for the different CS6 land-use scenarios.

Land-use scenario	Scenario 1	Scenario 2	Scenario 3
ESS4 – Annual removal of PM10, expressed as [t/km²/year]	12.3	0.27	1.24

6.6.5 Temperature regulation (ESS5)

The assessment of temperature regulation potential was based on Landsat 8 satellite data processed into an Land Surface Temperature (LST) map using the ASTER database. The Advanced Spaceborne Thermal Emission and Reflection Radiometer Global Emissivity Database (ASTER GED) was developed by National Aeronautics and Space Administration's (NASA) Jet Propulsion Laboratory (JPL), California Institute of Technology. The ASTER GED product provides global emissivity maps of the Earth's land surface in five spectral bands. In addition to the mean emissivity and standard deviation maps for all five ASTER thermal infrared bands, the product also provides maps for mean land surface temperature (LST) and standard deviation.

The analysis focused on the day with the highest air temperature recorded in the last 10 years. For CS6, this was 22.08.2019.The analysis was carried out for the entire Vieux-Charmont and Grand-Charmont Municipalities, within which CS6 is located. The study area was divided into land-use categories according to CLC 2018 (Corine Land Cover). The following land-use categories were identified: broad-leaved forest (311), water bodies (512), sport and leisure facilities (142), non-irrigated arable land (211), complex cultivation patterns (242), discontinuous urban fabric (112), industrial or commercial units (121) (Figure 58).

Mixed forests (313) and Pastures (231) located closest to CS6 were also included in the analysis, because this land-cover category did not occur within the boundaries of the commune under study.

Funded by the European Union

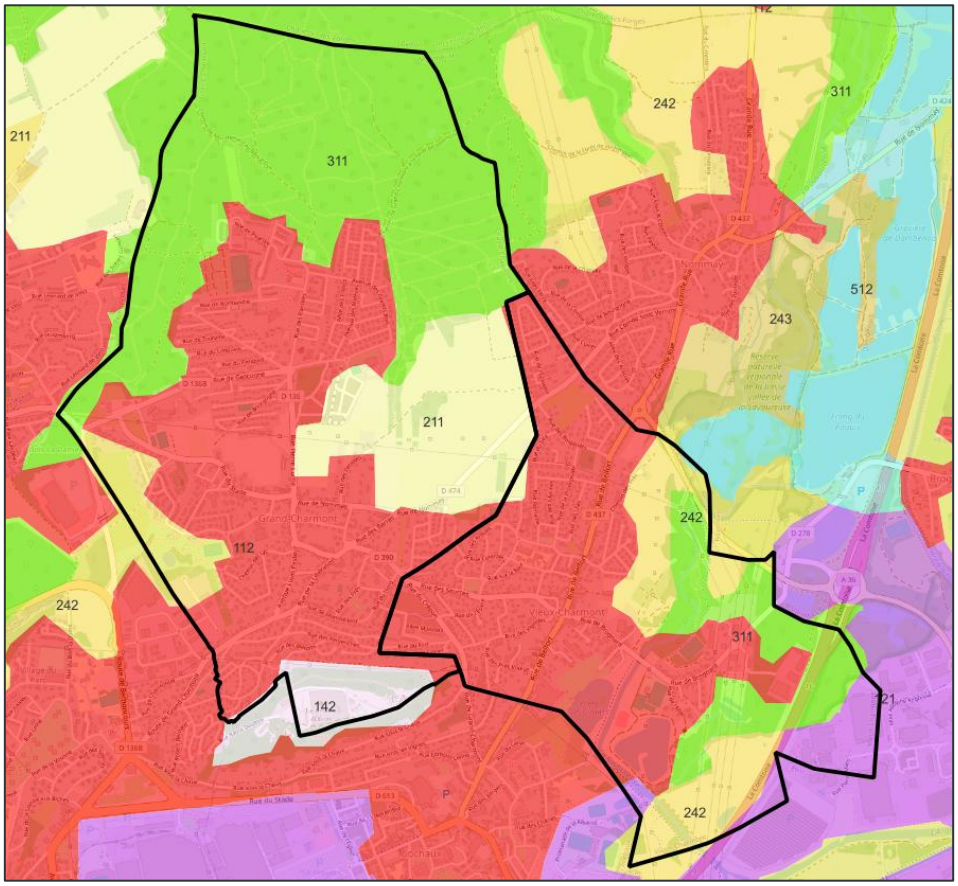

Figure 58 CLC 2018 land cover pattern for CS6.

In next step, using GIS analytical tools, the mean temperature values were calculated for each land-use type. The temperature regulation potential was calculated by relating the mean temperature values to the highest intended mean value for a given land use. The calculation results are presented in Table 143.

Table 143 Cooling potential of land cover – CS6.

CLC 2018 Land Cover class	Mean T [°C]	Cooling potential [°C]
Mixed forest	36.6	14.9
Broad-leaved forest	40.3	11.1
Water bodies	41.3	10.2
Pastures	42.1	9.4
Sport and leisure facilities	42.6	8.9
Non-irrigated arable land	44.1	7.3
Complex cultivation patterns	44.7	6.7
Discontinuous urban fabric	46.1	5.4
Industrial or commercial units	51.5	0.0

The results were then normalised to a scale from 1 to 10, where 1 denotes no potential and 10 the highest potential of the ecosystem service. The projected temperature value for the analysed land-use scenarios was adopted assuming that Scenario 1 corresponds to mixed forests, Scenario 2 to industrial or commercial units, and Scenario 3 to pastures. The results of the potential analysis for each scenario are presented in Table 144.

Funded by
the European Union

Table 144 Evaluation of cooling potential for analysed Scenarios – CS6.

Corine Land Cover Class	Cooling potential [-]
Discontinuous urban fabric	4.3
Industrial or commercial units	1.0
Secenario 2 - Industrial scenario, photovotaic panels	**1.0**
Sport and leisure facilities	6.4
Non-irrigated arable land	5.4
Pastures	6.7
Secenario 3 - Recreational, meadows, pastures	**6.7**
Annual crops associated with permanent crops	
Complex cultivation patterns	5.1
Broad-leaved forest	7.7
Mixed forest	10.0
Secenario 1 - NBS, forests	**10.0**
Water bodies	7.2

6.6.6 Cultural- direct, in-situ and outdoor interactions with living systems (ESS6)

Baseline mapping was undertaken using the Urban Atlas LCLU 2018 (https://land.copernicus.eu/local/urban-atlas/urban-atlas-2018). Within the administrative boundaries of the units, the following land cover classes have been identified as green recreation areas forests (deciduous forests (CLC 311), coniferous forests (CLC 312), mixed forests CLC 313)), green urban areas (CLC 141), natural grassland (CLC 321), water (CLC 511, CLC 512).

The potential for providing recreational services was also assessed for areas that may be converted into green areas in the future:

- The area of the contaminated case study site (CS 6)
- Land without current use (CLC 133)
- Mineral extraction and dump sites (CLC 131)

The area of the contaminated case study site is located within the urban park (Parc des Alliares). The park is located on a former industrial wasteland once heavily contaminated with heavy metals and hydrocarbons. The main method of combating soil pollution in Parc des Alliaires is phytoremediation Officially opened in 2023, it now serves two main purposes:

- Scientific: It acts as a pilot project studying how plants can purify soil in urban areas.
- Public: It is an accessible park featuring educational trails that explain the ongoing ecological restoration process to visitors.

The area within a 300-meter buffer of the park's border is inhabited by 2696. In addition, the area is adjacent to green areas with recreational functions, providing this service to a significant number of residents (water bodies -1205 and green urban area – 3263).

Within the analysed administrative boundaries, there are green areas with a recreational function that serve recreational function for 8717 residents (Forest adjacent to inhabited areas in the west part of the administrative unit).

Funded by the European Union

The potential of existing and potential green areas with recreational functions on a scale of 1 to 10 is shown in the Figure 59.

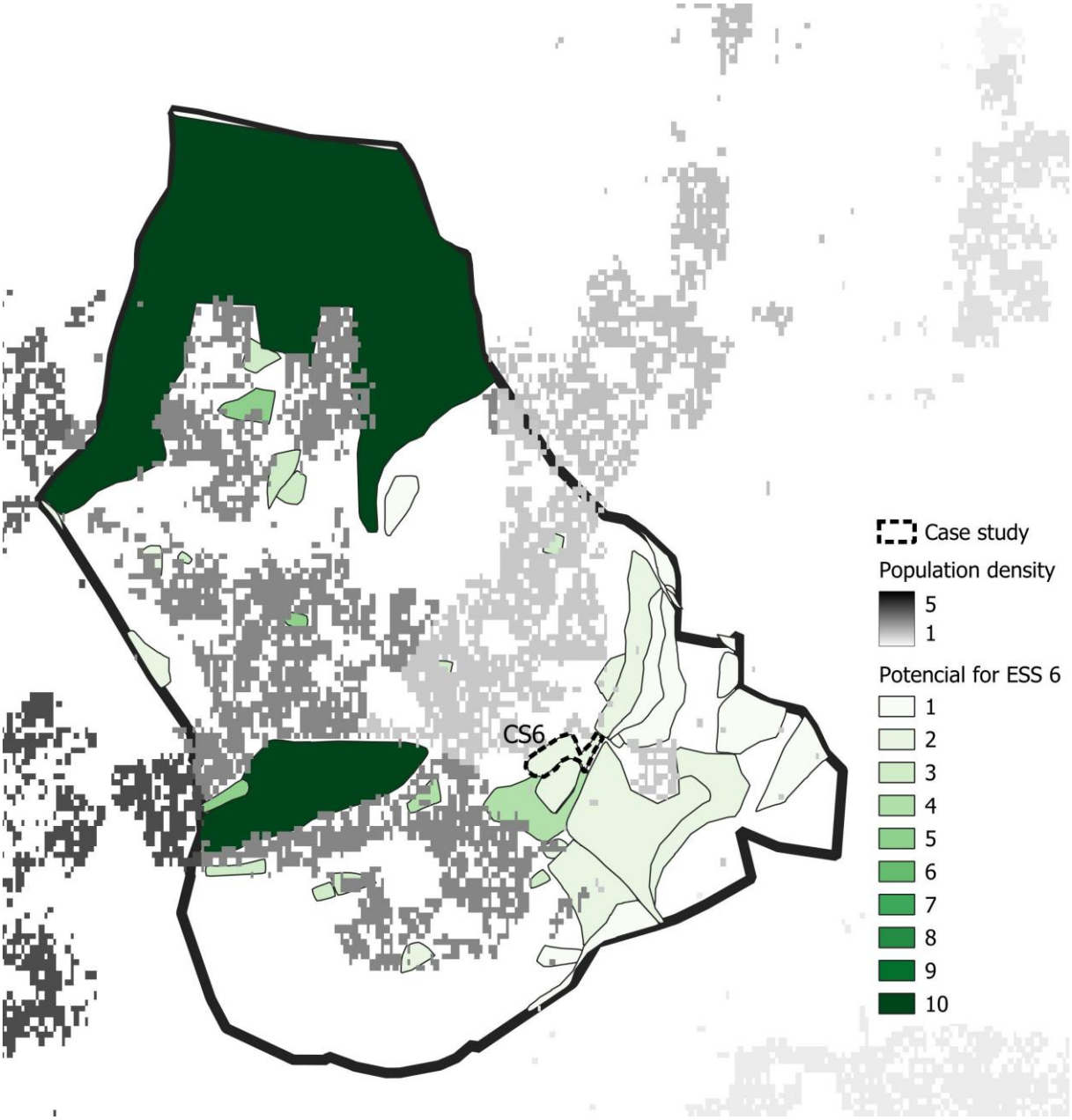

Figure 59 Cultural services: Interactions with natural environment for CS6.

In the adopted land use options, only the scenario 1 (Afforestation) and scenario 3 (Grassland cover), meet the criteria for green areas with a recreational function. Compared to other green areas within the administrative boundaries, this scenario has significant potential for providing cultural services (3,8). This potential is enhanced by the vicinity of green areas with recreational functions (8,4). Summary results of the ESS6 assessment are presented in Table 145.

Table 145 A summary of ESS6results for the different CS6 land-use scenarios.

Land-use scenario	Scenario 1	Scenario 2	Scenario 3

Funded by
the European Union

ESS6[Number of residents within 300 meters of a green recreational area]	2696 (7164)	0	2696 (7164)

6.6.7 Energy production (ESS7)

The performance of photovoltaic installations for CS6 was estimated using an application provided by the EC: Photovoltaic Geographical Information System [https://re.jrc.ec.europa.eu/pvg_tools/en/tools.html]. This application provides data on solar radiation and energy production from photovoltaic (PV) systems globally. Following the application instructions, the performance of photovoltaic installations was estimated based on the assumption presented in Table 146.

Table 146 Assumptions and settings used for PV calculation for CS6.

PV Performance Modelling Parameters						
Solar radiation database:	PV technology:	Installed peak PV power	System loss	Mounting position	Slope	Azimuth:
PVGIS-SARAH3	Crystalline Silicon (original)	1 kWp	14%	Free-standing	35°	0°

In Table 147, the CS6 is characterised in relation to the analysis conducted.

Table 147 Site characteristic.

Case Study	Coordinates (center)		Elevation	Area [ha]
	Latitude	Longitude		
CS6	47.521	6.8400	317	3.4

To estimate the electricity production capacity for this CS6, the maximum feasible installed PV capacity (kWp) was determined from the available area. For the purposes of the analysis, it was assumed that 1 kWp corresponds to a PV system area of 6 m². Because the full area could not be developed under real conditions (e.g., spacing between modules, internal roads, technical buildings, fencing, and grid infrastructure), a Surface Coverage Ratio (α = 50%) was used to reflect practical land take. This value was derived from an assessment of operating photovoltaic farms with total areas ranging from 27 ha to 300 ha. Table below show the calculated performance of photovoltaic installations for CS6. The estimated yearly in-plane irradiation is 1 483.38 kWh/m², taking into account factors such as system losses (14%). The annual electricity production is determined to be 1 177.1 kWh per 1 kWp installed. Table 148 presents the estimated value of electricity production, considering the surface area calculated using the Ideal Value Model and near-real conditions determined by the Surface Coverage Ratio. Under ideal conditions, the annual energy production could reach 6.7 GWh. Based on the Surface Coverage Ratio, the annual energy production is projected to be 3.3 GWh.

Table 148 Yearly PV energy production for CS6.

Yearly PV energy production [kWh]	1 177.1
Yearly in-plane irradiation [kWh/m^2]	1 483.38
Year-to-year variability [kWh]	68.06
Changes in output due to	--
-Angle of incidence [%]	-2.89

-Spectral effects [%]		1.51
Temperature and low irradiance [%]		-6.4
Total loss [%]		-20.65
Max. kWp needed [kWp]		5667
Energy production (Ideal Value Model)	GWh/y	6.7
Energy production (Surface Coverage Ratio)	GWh/y	3.3

Figure 60 shows a report from the Photovoltaic Geographical Information System application (estimating annual energy production for CS6).

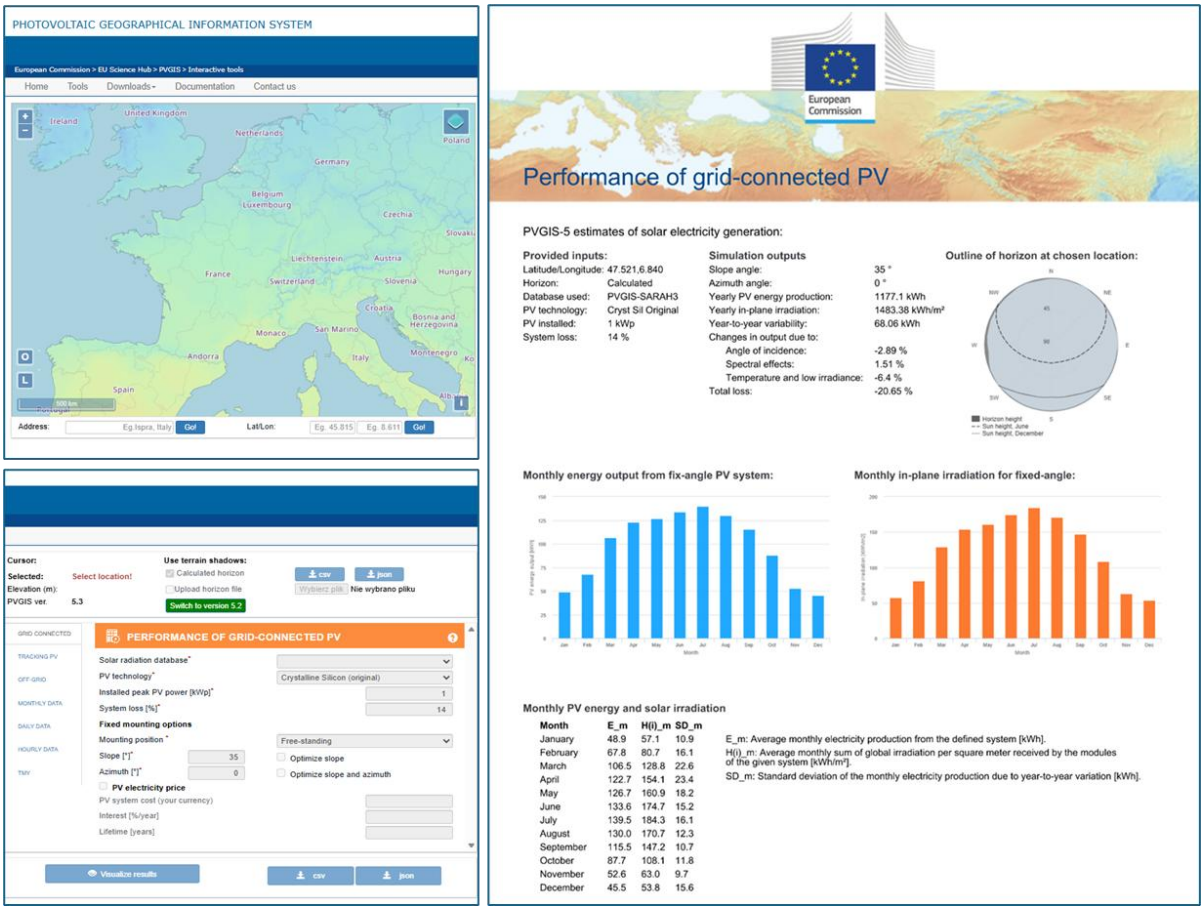

Figure 60 CS6– Performance of grid-connected PV.

A summary results of the ESS7 assessment performed for CS are presented in Table 149.

Table 149 A summary of ESS7 (Energy properties) results for the different CS5 land-use scenarios.

Land-use scenario	Scenario 1	Scenario 2	Scenario 3
ESS7: Potential energy production [GWh/y]	0.0	3.3	0.0

Funded by the European Union

6.7 Ecosystem services assessment for CS7

In this section, the ESS valuation for CS7 (Lavrion, GR – EL30) is presented in the local context of the site and land-use scenarios, while using a harmonised data-preparation approach to ensure comparability across all CS.

6.7.1 Biomass production (ESS1)

In this section the ESS1 was calculated as

$$EP = AGBinc \times CV \ [GJ \cdot ha^{-1} \cdot year^{-1}]$$

Where:
- CV is the calorific value of the biomass (GJ·t^{-1} d.m.), adopted in line with the ESS1 service card,
- AGBin above-ground biomass AGBinc (t d.m.·ha^{-1}·year^{-1}),
- EP is energy potential.

in line with the ESS1 service card (section 4.3). For Greece (CS7), the same approach as in CS2 was applied. Because consistent AGBinc data were not available at country or regional level under a single increment definition, an intermediate approach was adopted in which AGBinc was derived from NAI (a working variant developed for GR within the project). This ensured that results remained comparable across the entire report (Table 150).

Table 150 Annual biomass production on different types of land in Greece.

Land type	Value	Units	Method / notes	Source
Deciduous forest	7.19	t/ha/year	Aboveground net primary productivity (ANPP) estimated from allometry + management plan data; stand-scale production; Value is ANPP/aboveground production for beech forest case study; not national mean for all deciduous forests.	[Zianis & Mencuccini, 2005]
Poplar monoculture (Populus)	16.54	t/ha/year	Clone productivity reported for Greece (review of breeding/biomass trials);Clone-specific reported yield; not national average across all poplar plantations.	[Aravanopoulos, F.A., 2010]
Mixed forests	*n.d.*	*n.d.*	*No reliable value found in the searched sources (explicit mean annual biomass increment for mixed forests in Greece).*	*n.d.*
Coniferous forests	*n.d.*	*n.d.*	*No reliable value found in the searched sources (explicit mean annual biomass increment for coniferous forests in Greece).*	*n.d.*
Grassland / meadow cultivation	*n.d.*	*n.d.*	*No reliable value found in the searched sources (accessible, citable annual biomass yield/increment statement).*	*n.d.*

For the poplar plantations scenario AGBinc = 15.00 t d.m.·ha^{-1}·year^{-1} was adopted for poplar plantations as a harmonisation value (a common upper level for poplar across the full CS dataset). This value was applied because stable and comparable regional data for poplar plantations in Greece were not available, and the literature shows strong variability depending on water conditions and plantation management (Table 151).

Table 151 SS1 – Calculation parameters for the biomass energy potential for Greece (EL30).

CLC clasification	Couling Land Cover	AGBinc (tDM/ha/yr)	CV (GJ/tDM)	EP (GJ/ha/yr)
3.1.1	Broad-leaved forest	2.28	18.5	42.1
1.4.1	Green urban areas -grassland or lawns	2.00	17.5	35.0
1.2.1	Industrial - PV installation (80% grassland)	1.60	17.5	28.0

CLC clasification	Couling Land Cover	AGBinc (tDM/ha/yr)	CV (GJ/tDM)	EP (GJ/ha/yr)
3.1.2	Coniferous forest	2.24	18.5	41.5
3.2.4	Transitional woodland/shrub (poplar plantations)	15.00	18.56	278.4
1.2.1	Industrial - buildings and halls (20% grassland)	0.40	17.5	7.0

For scenario with grasslands, values representative of dry Mediterranean pastures in the EL30 region (Attica) were adopted (Table 152). This was treated as a realistic order-of-magnitude estimate for scenarios operating under strong water limitation and a short growing season. In line with the carried assumptions, the PV scenario was defined as an 80% grassland equivalent, while the industrial/commercial scenario was defined as a 20% grassland equivalent.

Table 152 Estimated annual above-ground biomass increment (AGBinc) for grasslands in NUTS2 regions – assumptions and literature-based justification.

NUTS2	Region	Type of grassland	Estimated AGB increase (t DM·ha^{-1}·yr^{-1})	Rationale (climate / intensity)	Citations
EL30	Attica	dry pastures (dry grasslands)	1–3	Dry Mediterranean pastures: strong water limitation and a shorter period of intensive growth	(Shi et al., 2023; Obermeier et al., 2018; Tao et al., 2015)

The summary results of the analysis are presented in the Table 153.

Table 153 A summary of ESS1 (Biomass production) results for the different CS7 land-use scenarios.

Land-use scenario	Scenario 1	Scenario 2	Scenario 3
Energy potential [GJ/ha/year]	278.4	28	35

6.7.2 Regulation of soil quality (ESS2)

In this section, the ESS2 indicator (regulation of soil quality) for CS7 was estimated as the potential for metal accumulation in plant biomass under the analysed land-use scenarios. As part of the literature review, concentration ranges of several metals in plant biomass were compiled e.g. cadmium, lead, zinc, copper, and nickel. However, for valuation purposes, one representative metal was selected: cadmium (Cd). Cadmium is frequently reported in environmental studies, it has no nutrient function (unlike Zn or Cu), and its accumulation in plant tissues provides a useful indicator of contamination pressure. In addition, Cd is often more mobile and more readily translocated to above-ground plant parts than Pb, which increases its suitability for scenario comparisons based on AGB.

As part of the parameterisation of metal concentrations in conifer biomass, relevant literature sources were reviewed. Data for needles are widely available, but they show high variability depending on species, site conditions, anthropogenic pressure, and the age of the assimilatory tissues. At the same time, many studies focus on needles or bark as biomonitors and do not provide comparable values for stem wood, nor a consistent “needles versus stem wood” dataset for the full set of metals. For this reason, instead of averaging results from heterogeneous studies, an approach based on one internally consistent dataset was adopted, covering both needles and stem wood analysed with the same methodology. The study by Skonieczna et al. (2014) was

Funded by the European Union

selected as the baseline source. In that work, 15 *Pinus sylvestris* trees from five stands were analysed. The investigated forests were located in an area influenced by anthropogenic pressures, but not in the immediate vicinity of point emission sources. For the assessment, mean concentrations of Cd, Zn, Pb, and Cu were introduced for needles (as a representative of the "leaf" fraction) and for stem wood (as a representative of the "stem" fraction). Cadmium was then used for the subsequent valuation step.

For poplar plantations, several literature sources were reviewed (see section 6.1.2). As in other cases, it was found that experimental conditions were often not comparable between studies. Therefore, the focus was placed on a single publication that reported concentrations in poplar leaves and shoots in a format suitable for comparison across case studies

Based on the reviewed evidence, Pilipović et al. (2019) was adopted as the source of ESS2 parameters for poplar plantations, as it provides a coherent empirical dataset covering both leaves and shoots/stems, analysed using the same methodology and under the same experimental conditions. This allowed the "leaf versus wood/shoots" fractions to be separated directly, without merging heterogeneous studies and without additional assumption-based conversions. In addition, the study reports several metals (including Cd, Zn, Pb, and Cu) in a way that supported the selection of values representative of moderate anthropogenic pressure, thereby improving comparability between land-use scenarios within the ESS2 assessment.

For Scenario with grassland, an above-ground biomass (AGB)-based approach was applied, using metal concentration ranges in herbaceous plant tissues as reported in the literature. To reflect the typical spread of values associated with different levels of anthropogenic influence, three pressure levels were compiled (moderate, heavy, and extreme), representing, respectively, urban and transport impacts, post-mining areas, and locations in the immediate vicinity of smelters.

However, for the purpose of the ESS2 valuation, the moderate contamination variant was adopted, as it was considered representative of the common anthropogenic background conditions observed across the CS landscape and the analysed land-use scenarios. This choice reduced the influence of extreme concentration values that could otherwise dominate the result, and it ensured that differences in ESS2 were driven primarily by land-cover type and AGB magnitude rather than by exceptional, localised point sources of pollution.

The input data used for CS7 are identical to those described for CS1 in Section 6.1.1. Table 154 provides a concise overview of the heavy metal concentration datasets applied in the biomass assessment and includes references to the corresponding detailed tables in Section 6.1.1

Table 154 Heavy metal concentrations in biomass used for ESS2 parameterisation (data sources and table references).

No.	Heavy metal concentrations in the biomass	Reference table
1	Broadleaf species	Table 16 Heavy metal concentrations in the biomass of broadleaf species.
2	Conifer species	Table 17 Heavy metal concentrations in the biomass of conifer species.
3	Poplar and willow crops.	Table 18 Heavy metal concentrations in the biomass of poplar and willow crops.
4	Grassland species	Table 19 Heavy metal concentrations in the aboveground biomass of grassland species.

Funded by the European Union

Table 155 presents the input parameters and calculation outputs used to estimate the ESS2 indicator for CS7 (EL30) expressed as the potential annual cadmium (Cd) accumulation in above-ground plant biomass. It combines AGBinc values (from ESS1) with tissue Cd concentrations and harvest fractions to derive Cd concentration in harvested biomass and the resulting Cd removal per hectare and year, in accordance with the methodology described in Section 4.3

Table 155 Calculation sheet for ESS2 (Cd): biomass increment, concentration assumptions and annual removal.

Couling Land Cover	AGBinc (tDM/ha/yr) [from ESS1]	f_leaf (season harvest) [0-1]	Cd_C_leaf (mg/kg DM) [input]	Cd_C_stem (mg/kg DM) [input]	Cd_C_harvest (mg/kg DM) [calc]	Cd_Removal (g/ha/yr) [calc]
Broad-leaved forest	2.28	0.2	0.4	0.1	0.16	0.4
Green urban areas - grassland or lawns	2.00	1	0.75		0.75	1.5
Industrial - PV installation (80% grassland)	1.60	1	0.6		0.6	1.0
Coniferous forest	2.24	0.2	0.1	0.24	0.212	0.5
Transitional woodland/shrub (poplar plantations)	15.00	0.2	7.85	3.25	4.17	62.6
Industrial - buildings and halls (20% grassland)	0.40	1	0.15		0.15	0.1

Table 156 summarises the ESS2 results for CS7 across the analysed land-use scenarios. Values are reported as the estimated potential annual pollutant (Cd) accumulation in above-ground biomass (g/ha/year) enabling direct comparison between scenarios under a consistent parameter set.

Table 156 A summary of ESS2 (regulation of soil quality) results for the different CS7 land-use scenarios.

Land-use scenario	Scenario 1	Scenario 2	Scenario 3
Potential annual pollutant accumulation [g/ha/year]	62.6	1.0	1.5

6.7.3 Mitigation of climate change (carbon dioxide sequestration) (ESS3)

The assessment of ESS3 was conducted using annual carbon sequestration, expressed in tonnes of CO_2 per hectare per year (t CO_2/ha/year), as the main indicator. Total carbon sequestration was estimated by summing carbon accumulation in above-ground biomass and below-ground biomass and subsequently converting this total into CO_2 equivalents. The approach was consistent with the carbon allocation models developed for poplar plantations, as outlined previously in the ESS3 methodological framework.

The estimation of annual above-ground biomass increment (AGBinc) followed the same approach described under ESS1, which included reviewing available data sources such as scientific literature, forest inventory datasets, and indirect indicators. For the Lavreotiki Municipal Unit site in Greece (CS7), the available data were fragmented and methodologically inconsistent, with differing definitions of production, growth metrics, typological classifications, and units of measurement. As a result, direct comparisons between land cover types were constrained. To ensure consistency across the deliverable, AGBinc values were ultimately derived from

Funded by the European Union

harmonized data provided by the study "Improved large-area forest increment information in Europe through harmonization of National Forest Inventories" (Forest Ecology and Management, 562, 121913), which offers comparable annual forest growth estimates across most European countries and forest types.

The BGBinc value was derived from the AGBinc value by using the AGBinc / BGBinc, annual above- and below-ground biomass ratio. The root-to-shoot ratio was based upon the literature findings such as Oliveira Rodríguez et al. (2018) and Intergovernmental Panel on Climate Change in 2003 and 2006 due to their unified methodology across countries, to best estimate the BGBinc (Table 157). Based on those findings, the ratio for industrial and commercial land use scenario was calculated based on the value of about 20% of the grassland AGBinc to BGBinc ratio, and the scenario assuming the ground-mounted photovoltaic farm designation accounted for 80% of the grassland coverage value.

Table 157 Sources used for the estimation of below ground - above ground ratio (%).

CS7 (GRC) - types of management	AGBinc - BGBinc ratio (%)	Sources
Broad-leaf forest	0.43	IPCC (2003) Annex 3A.1.8
Coniferous forest	0.46	
Grassland	1.58	IPCC (2003) Annex 3A.1.8 Mokany, Raison & Prokushkin (2006)
Poplar cultivation	0.21	Oliveira (2018)

After calculating the values of the BGBinc from the ratio and the AGBinc values provided, the results were added and multiplied by the C fraction to account for the carbon content. The carbon content values in dry matter are assumed at approx. 50% values, supported by literature (Table 158).

In the next step the results were converted to the CO_2 equivalent by multiplying the final value by 3.67 (ratio of the atomic mass of the molecules). The indicator reflects the annual flow of carbon sequestration associated with biomass growth, rather than long-term carbon stock changes.

Table 158 Sources used for the estimation of C fraction of carbon content in dry mass.

CS7 (GRC) - types of management	C fraction of carbon content in dry matter	Source/Reference
Broad-leaf forest	0.46	IPCC (2003) Annex 3A.1 Dupouey (2010)
Coniferous forest	0.46	
Grassland	0.48	Shiferaw, Kassawmar, Zeleke (2022)
Poplar cultivation	0.48	Shiferaw, Kassawmar & Zeleke (2022)

The results for the region of Lavreotiki Municipal Unit in Greece (CS7) show that the annual carbon sequestration for broadleaf forests is about 9.729 t (CO_2/ha/year), 11.634 t (CO_2/ha/year) for coniferous forest and for poplar plantation the results were 17.567 t (CO_2/ha/year)(Figure 61). Grassland coverage scored the highest at a 22.901 t (CO_2/ha/year). Those results were used to provide background land use values for the evaluation of the values for Scenarios 1, 2 and 3.

Funded by the European Union

ESS: MITIGATION OF CLIMATE CHANGE						
PL	Średnia roczna ilość biomasy nadziemnej z hektara (tDM/ha/yr)	Stosunek biomasy poniżej - powyżej gruntu	Średnia roczna ilość biomasy korzennej z hektara (tDM/ha/yr)	Średnie stężenie węgla w biomasie (%)	Sekwestracja węgla (kg/year/ha)	Roczna sekwestracja węgla wyrażona w t (CO_2/ha/year)
ENG	Average anual amount of above-ground biomass from ha (tDM/ha/yr)	Below ground - above ground ratio	Average annual amount of below biomass from ha (tDM/ha/yr)	Biomass mean concentration of carbon (%)	Carbon sequestration (t/year/ha)	Annual carbon sequestration expressed in t (CO_2/ha/year)
						Conversion factor from Carbon (C) to CO_2 equivalent
						3,67
CS7 (GRC) Lavreotiki Municipal Unit						
Forest_broadleaf_poplar	2,28	0,43	0,979	0,46	1,497	5,494
Grassland	2,00	1,58	3,160	0,48	2,477	9,090
PV_groundmounted (80% grassland)	1,60	1,58	2,528	0,48	1,981	7,272
coniferous	2,24	0,46	1,032	0,46	1,507	5,530
poplar cultivation	8,60	0,21	1,806	0,46	4,787	17,567
Industrial of commercial units (20% grassland)	0,40	1,58	0,632	0,48	0,495	1,818

Figure 61 Calculations concerning the ESS3 indicator – annual carbon sequestration expressed in t (CO_2/ha/year) for the region of Lavreotiki Municipal Unit in Greece (CS7).

For the Scenario 1 – NBS solutions, the value of poplar plantations was assumed. The 2nd Scenario = industrial scenario for ESS3 considered 80% vegetation in AGBinc value due to a decreased but still present level of low-vegetation growth. For Scenario 3, the value of grasslands was assumed as an option for low-vegetation, recreational approach. The summary results are presented in Table 159.

Table 159 A summary of ESS3 results for the different CS7 land-use scenarios.

Land-use scenario	Scenario 1	Scenario 2	Scenario 3
ESS3 - Annual carbon sequestration expressed in t CO_2/ha/year	17.567	7.272	9.090

6.7.4 Air quality mitigation (ESS4)

The evaluation of ESS4 analyzes the capacity of tree and shrub canopies in urban, peri-urban, and rehabilitated post-industrial landscapes to remove air pollutants - especially particulate matter (PM10 and PM2.5) - via dry deposition processes. The key indicator applied is the annual removal of PM10, expressed in kilograms per hectare per year (kg/ha/year). This methodology is based on the dry deposition model introduced by Tallis et al. (2011)., where:

$$\text{Absorption of } PM_{10} = \text{Flux (V) x Surface (SA) x Period (t) (t/km}^2\text{/year)}$$

where:

- Flux is the pollutant to the surface (amount removed per unit area and time), calculated by multiplying the deposition velocity of the pollutant (m/s), which depends on canopy structure and wind speed and the concentration of the pollutant in the atmosphere.
- Surface is the considered surface area multiplied by the surface area index functioning in given area (LAI).
- Period accounts for the period of analysis in days, multiplied by the proportion of dry days and the proportion of non-leaf days.

The total annual pollutant removal is calculated by integrating deposition fluxes over the vegetated surface area of each land-use scenario. The above contributes to the calculation as follows:

- V = deposition velocity (m/s) x pollutant conc. (µg/m³)
  - Flux (µg/m³) was then converted to daily flux by multiplying it by 86400
- SA = LAI (m²/m²) x area of land considered (m²)
- t = period of analysis (days) x proportion of dry days (fraction) x proportion of on-leaf days (fraction)
  - Afterwards the absorption of PM_{10} was converted from (µg/m²/year) to (t/km²/year) by x10^6

Funded by the European Union

The data for the Lavreotiki Municipal Unit site in Greece (CS7) involved land use scenarios for the broad-leaf forest, coniferous forest, mixed forest, pastures, grasslands and photovoltaic farm. For each component of the model, a literature review was conducted to establish the most suitable range of standardized values to ensure comparability. In instances where specific data for a component was unavailable, an average was derived from countries or regions with similar ecosystem types, allowing the results to remain compatible. Regarding the deposition velocity by land use type, no data was found in the research for the Lavreotiki Municipal Unit region, however, comparable data were used from European, U.S. and Italian databases to provide a baseline. Data gathered from Marando et al. (2016), investigated deposition velocity in various vegetation types in mediterranean climate, its main reference point being Rome, Italy, using the i-Tree Eco dry deposition model (Table 160):

Table 160 Estimated deposition velocity in mediterranean climate by Marando et al. (2016).

Vegetation Type	Deposition Velocity (cm s^{-1})	Additional observations
Broadleaf trees (in-leaf)	0.5–1.5	Higher during full leaf area
Coniferous trees	1.0–2.0	Year-round interception
Grass/shrubs	0.2–0.8	Lower aerodynamic roughness

Another study by Mariarosa et al. (2019) provided information in Dry deposition modelling and validation in urban and suburban Italy, representative of mediterranean and temperate climate (Table 161).

Table 161 Estimated deposition velocity in regions managed as low-vegetation or industrial/urban sites by Mariarosa et al. (2019).

Land use type	Deposition Velocity (cm s^{-1})	Additional observations
Industrial surfaces	0.1–0.5	Smooth surfaces lower deposition
Suburban vegetation	0.3–1.2	Higher roughness enhances capture
Grasslands	0.2–0.6	Moderate

Considering the site at Lavreotiki Municipal Unit lays in the mediterranean climate belt, the above values were averaged for each land use type and used for further calculations. The next component researched for the model was the pollutant concentration (µg/m^3). The values were provided from the WHO 2013, EU policy ranges and local monitoring such as Air Quality Index were used, which proved at a 30-55 µg m^{-3} value. Middle range of 42.5 µg m^{-3} was used. Regarding the surface area, the values of the leaf area index (LAI) in various types of land use were taken into consideration. Due to the lack of specific data regarding the above-mentioned land use types for the region, European and global data were considered.

Table 162 References for the leaf area index concerning chosen types of land use.

Land use type	LAI values	Represented region	Sources / References
Broad-leaf forest	5–8 (max values) 3–6 (urban average 3–4.5) 2–10 (broad global range)	France (temperate deciduous) Primarily U.S., global review Global synthesis	Le Dantec, Dufrêne, Saugier (2000) Nowak et al. (2017) Parker (2020)
Coniferous forest	6–11 3–6 (urban average 3–4.5) 2–10 (broad global range)	Pacific Northwest, U.S. Primarily U.S., global review Global synthesis	Turner et al. (2000) Nowak et al. (2017) Parker (2020)
Mixed forest	3–7 typical; up to 9 dense stands	Europe (multi-site comparison)	Sinan & Hasenauer (2025)

Funded by the European Union

Land use type	LAI values	Represented region	Sources / References
Pasture/ Grassland/ Shrub	2.0–4.5 (Wetland shrubs lower (2–3), wooded wetland stands up to 4.5)	Poland (Central Europe)	Leśny et al. (2007)

Area assumed for the calculation at this stage was a m^2, after conversion km^2. Regarding the period component, it was calculated by taking average of the range of the vegetation period for each type of land use. For the Lavreotiki Municipal Unit site, the midpoint of the Mediterranean range was used for the assessment (Table 161).

Table 163 Number of vegetative days for each land use type according to the climate type.

Land Use Type	Boreal	Temperate	Mediterranean	Subtropical	References/Sources
Coniferous Forest	120–180	180–220	200–240	250–300	EMEP (2016) GIOŚ (2018) Langner, Kull & Endlicher (2011) Chen (2015). Khan & Perlinger (2017) Vivanco et al. (2021)
Broadleaf Forest	140–190	190–220	220–260	280–320	
Grassland	150–190	200–240	220–300	280–320	
Cropland	140–180	180–220	250–320	280–330	

For the scenario regarding industrial land use type (Scenario 2), including photovoltaic farm, the vegetative period was assumed the same as for a grassland. The proportion of dry days was assumed at 60% according to Chervenkov & Slavov (2021), while the proportion of on-leaf days was assumed at 100%, due to already exclusively selected vegetative dry periods. The results for the region of Lavreotiki Municipal Unit in Greece (CS1) presented in the Figure 62 show that the annual absorption of PM10 are as follows: 21.15 t/km²/year for broad-leaf forest, 43.62 t/km²/year for coniferous forest, 32.94 t/km²/year for mixed forest, 7.85 t/km²/year for pastures, 5.73 t/km²/year for grasslands and 0.69 t/km²/year for industrial land use/photovoltaic farm. Those results were used to provide background land use values for the evaluation of the values for Scenarios 1, 2 and 3. For the Scenario 1 – NBS solutions the value of broad-leaf forest was assumed. Concerning Scenario 2, the industrial/photovoltaic land use was considered and for Scenario 3 the values for pastures were assumed, as shown in the Table 164.

Funded by the European Union

ESS: AIR PURIFICATION							
Seconds/day (s)	86 400						
		CS7 (GRC) Lavreotiki Municipal Unit					
PL	EN	Broad-leaf forest	Coniferous forest	Mixed forest	Pasture	Grassland	Photovoltaic farm
Prędkość osiadania (m/s)	Deposition velocity (m/s)	0,010	0,015	0,013	0,005	0,004	0,001
Stężenie PM10 (µg/m^3)	Pollutant conc. (µg/m^3)	42,500	42,500	42,500	42,500	42,500	42,500
Przepływ (µg/m^2/s) = Prędkość osiadania (m/s) x Stężenie PM10 (µg/m^3)	**Flux (µg/m^2/s) =** deposition velocity (m/s) x pollutant conc. (µg/m^3)	0,425	0,638	0,553	0,213	0,170	0,043
Dzienny przepływ (µg/m^2/dzień)	**Daily flux (µg/m^2/day)**	36720	55080	47736	18360	14688	3672
Wskaźnik powierzchni (m^2/m^2)	Surface area index (LAI) (m^2/m^2)	4,000	6,000	5,000	2,500	2,500	1,200
Powierzchnia brana pod uwagę (m^2)	Area of land (m^2)	1,000	1,000	1,000	1,000	1,000	1,000
Powierzchnia (m^2) = Wskaźnik powierzchni (m^2/m^2) x Powierzchnia brana pod uwagę (m^2)	**Surface (m2) =** LAI (m^2/m^2) x area of land (m^2)	4,000	6,000	5,000	2,500	2,500	1,200
Okres kwitnienia liści	Vegetation period (days)	240,000	220,000	230,000	285,000	260,000	260,000
Odsetek dni suchych	Proportion of dry days (fraction)	0,600	0,600	0,600	0,600	0,600	0,600
Odsetek dni wchłaniania przez dojrzały liść	Proportion of on-leaf days (fraction)	1,000	1,000	1,000	1,000	1,000	1,000
Okres = Okres kwitnienia liści (dni) x Odsetek dni suchych x Odsetek dni wchłaniania przez dojrzały	**Period =** period of analysis (days) x proportion of dry days (fraction) x proportion of on-leaf days	144,000	132,000	138,000	171,000	156,000	156,000
Wchłanianie PM10 (µg/m^2/rok)	**Absorption of PM10 = Flux x Surface x Period (µg/m^2/year)**	21150720	43623360	32937840	7848900	5728320	687398,4
Wchłanianie PM10 (t/km^2/rok)	**Absorption of PM10 = Flux x Surface x Period (t/km^2/year)**	**21,15**	**43,62**	**32,94**	**7,85**	**5,73**	**0,69**

Figure 62 Summary of the calculations involved in the calculations for ESS4 indicator – Absorption of PM10.

Table 164 A summary of ESS4 - Annual removal of PM10 [t/km²/year] results for the different CS7 land-use scenarios.

Land-use scenario	Scenario 1	Scenario 2	Scenario 3
ESS4 – Annual removal of PM10, expressed as [t/km²/year]	21.15	0.69	7.85

Funded by the European Union

6.7.5 Temperature regulation (ESS5)

The assessment of temperature regulation potential was based on Landsat 8 satellite data processed into an Land Surface Temperature (LST) map using the ASTER database. The Advanced Spaceborne Thermal Emission and Reflection Radiometer Global Emissivity Database (ASTER GED) was developed by National Aeronautics and Space Administration's (NASA) Jet Propulsion Laboratory (JPL), California Institute of Technology. The ASTER GED product provides global emissivity maps of the Earth's land surface in five spectral bands. In addition to the mean emissivity and standard deviation maps for all five ASTER thermal infrared bands, the product also provides maps for mean land surface temperature (LST) and standard deviation.

The analysis focused on the day with the highest air temperature recorded in the last 10 years. For CS7, this was 2.07.2017. The analysis was carried out for the entire Lavreotiki Municipal Unit, within which CS7 is located.

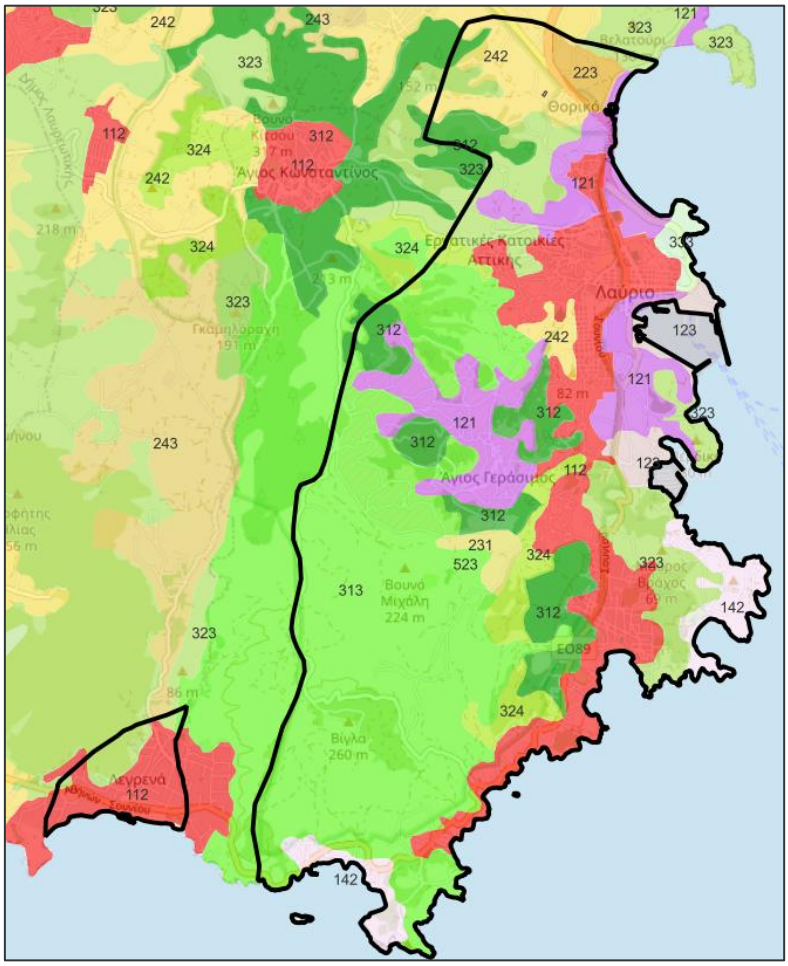

Figure 63 CLC 2018 land cover pattern for CS7.

The study area was divided into land-use categories according to CLC 2018 (Corine Land Cover). The following land-use categories were identified: sport and leisure facilities (142); sparsely vegetated areas (333), port areas (123), coniferous forest (312), mixed forest (313), discontinuous urban fabric (112), industrial or commercial units (121), transitional woodland-shrub (324),complex cultivation patterns (242),land principally occupied by agriculture, with

Funded by
the European Union

significant areas of natural vegetation (243),pastures (231),olive groves (223) and sclerophyllous vegetation (323) (Figure 63).

In next step, using GIS analytical tools, the mean temperature values were calculated for each land-use type. The temperature regulation potential was calculated by relating the mean temperature values to the highest intended mean value for a given land use. The calculation results are presented in Table 165.

Table 165 Cooling potential of land cover – CS7.

CLC 2018 Land Cover class	Mean T [°C]	Cooling potential [°C]
Sport and leisure facilities	37.3	7.4
Sparsely vegetated areas	38.5	6.3
Port areas	39.2	5.5
Coniferous forest	41.7	3.0
Mixed forest	42.1	2.6
Discontinuous urban fabric	42.3	2.4
Sclerophyllous vegetation	42.7	2.1
Olive groves	42.8	1.9
Industrial or commercial units	42.9	1.9
Transitional woodland-shrub	42.9	1.8
Complex cultivation patterns	44.2	0.5
Land principally occupied by agriculture, with significant areas of natural vegetation	44.6	0.1
Pastures	44.7	0.0

The results were then normalised to a scale from 1 to 10, where 1 denotes no potential and 10 the highest potential of the ecosystem service. The projected temperature value for the analysed land-use scenarios was adopted assuming that Scenario 1 corresponds to mixed forests, Scenario 2 to industrial or commercial units, and Scenario 3 to pastures. The results of the potential analysis for each scenario are presented in Table 166.

Table 166 Evaluation of cooling potential for analysed Scenarios – CS7.

Corine Land Cover Class	Cooling potential [-]
Discontinuous urban fabric	4.0
Industrial or commercial units	3.3
Secenario 2 - Industrial scenario, photovotaic panels	**3.3**
Port areas	7.7
Sport and leisure facilities	10.0
Olive groves	3.3
Pastures	1.0
Secenario 3 - Recreational, meadows, pastures	**1.0**
Complex cultivation patterns	1.6
Land principally occupied by agriculture, with significant areas of natural vegetation	1.1
Coniferous forest	4.7
Mixed forest	4.1
Secenario 1 - NBS, forests	**4.1**

Funded by the European Union

Sclerophyllous vegetation	3.5
Transitional woodland-shrub	3.1
Sparsely vegetated areas	8.6

6.7.6 Cultural- direct, in-situ and outdoor interactions with living systems (ESS6)

Baseline mapping was undertaken using the Urban Atlas LCLU 2018 Within the administrative boundaries the following land cover classes have been identified as green recreation areas forests (deciduous forests (CLC 311), coniferous forests (CLC 312), mixed forests CLC 313)), herbaceous vegetation associations (CLC 321), water (CLC 511, CLC 512).

The potential for providing recreational services was also assessed for areas that may be converted into green areas in the future:

- The area of the contaminated case study site (brownfield CS 7)
- Land without current use (CLC 133)

The future use of the brownfield for recreational purposes will provide 399 residents with access to this type of area. The brownfield adjacent to a green area in whose 300 m buffer zone lives 1233 residents. Within the analysed administrative boundaries, there are green areas with a recreational function that serve recreational function for 9364 residents (green areas along the coast). The potential of existing and potential green areas with recreational functions on a scale of 1 to 10 is shown in the Figure 64.

Funded by
the European Union

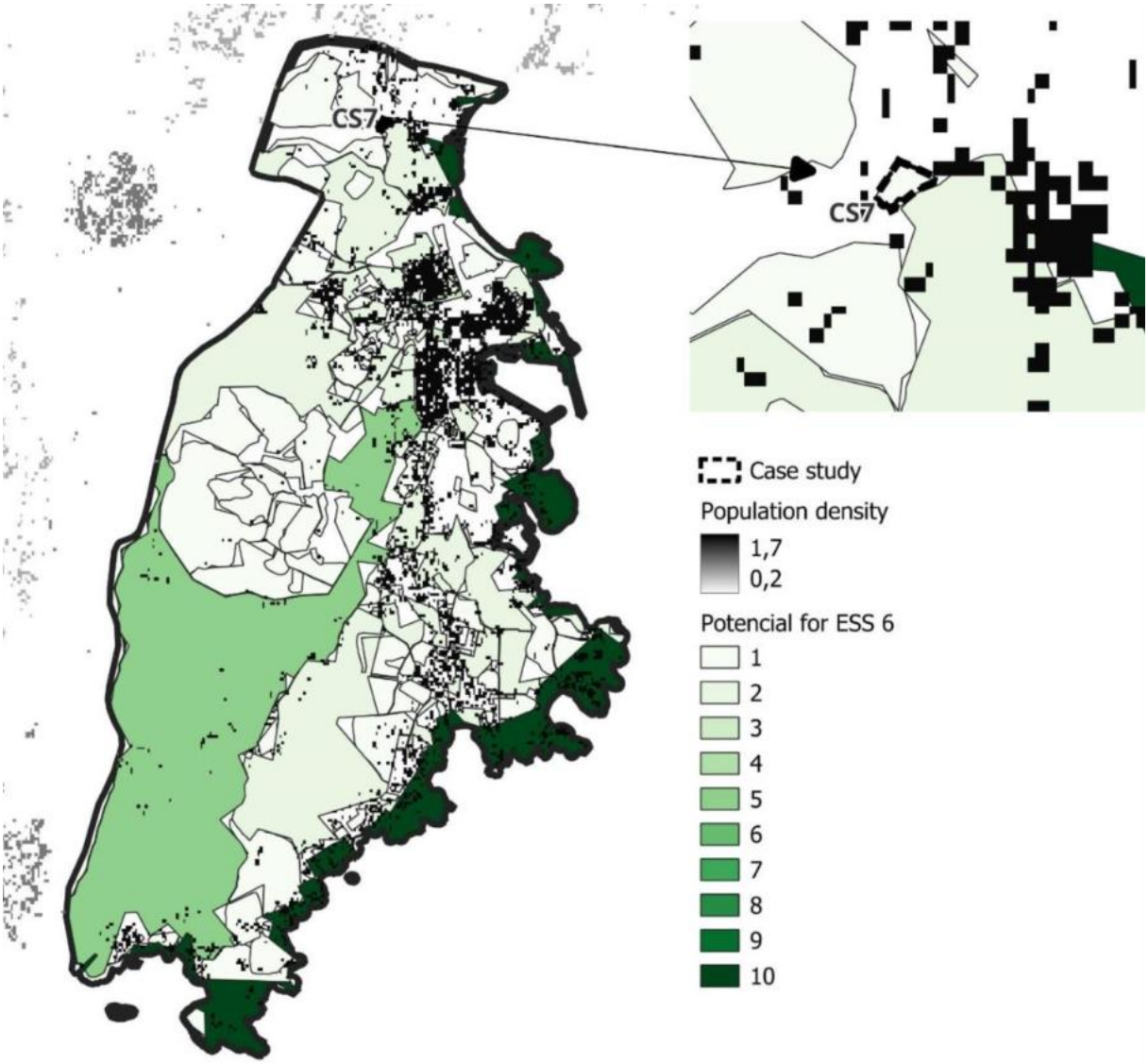

Figure 64 Cultural services: Interactions with natural environment for CS1.

In the adopted land use options, only the scenario 1 (Afforestation) and scenario 3 (Grassland cover), meet the criteria for green areas with a recreational function. Compared to other green areas within the administrative boundaries, this scenario has little potential for providing cultural services (1,4). The adjacent green area slightly increases this potential (2,6) (Table 167)

Table 167 A summary of ESS6 results for the different CS7 land-use scenarios.

Land-use scenario	Scenario 1	Scenario 2	Scenario 3
ESS6[Number of residents within 300 meters of a green recreational area]	399 (1632)	0	399 (1632)

6.7.7 Energy production (ESS7)

The performance of photovoltaic installations for CS7 was estimated using an application provided by the EC: Photovoltaic Geographical Information System

[https://re.jrc.ec.europa.eu/pvg_tools/en/tools.html]. This application provides data on solar radiation and energy production from photovoltaic (PV) systems globally. Following the application instructions, the performance of photovoltaic installations was estimated based on the assumption presented in Table 168.

Table 168 Assumptions and settings used for PV calculation for CS7.

PV Performance Modelling Parameters						
Solar radiation database:	PV technology:	Installed peak PV power	System loss	Mounting position	Slope	Azimuth:
PVGIS-SARAH3	Crystalline Silicon (original)	1 kWp	14%	Free-standing	35°	0°

In Table 169, the CS7 is characterised in relation to the analysis conducted.

Table 169 Site characteristic.

Case Study	Coordinates (center)		Elevation	Area [ha]
	Latitude	Longitude		
CS7	37.734	24.045	9	0.7

To estimate the electricity production capacity for this CS7, the maximum feasible installed PV capacity (kWp) was determined from the available area. For the purposes of the analysis, it was assumed that 1 kWp corresponds to a PV system area of 6 m². Because the full area could not be developed under real conditions (e.g., spacing between modules, internal roads, technical buildings, fencing, and grid infrastructure), a Surface Coverage Ratio (α = 50%) was used to reflect practical land take. This value was derived from an assessment of operating photovoltaic farms with total areas ranging from 27 ha to 300 ha. Table 170 shows the calculated performance of photovoltaic installations for CS7. The estimated yearly in-plane irradiation is 2 083.53 kWh/m², taking into account factors such as system losses (14%). The annual electricity production is determined to be 1 607.92 kWh per 1 kWp installed. The table presents the estimated value of electricity production, considering the surface area calculated using the Ideal Value Model and near-real conditions determined by the Surface Coverage Ratio. Under ideal conditions, the annual energy production could reach 1.9 GWh. Based on the Surface Coverage Ratio, the annual energy production is projected to be 0.9 GWh.

Table 170 Yearly PV energy production for CS7.

Yearly PV energy production [kWh]		1 607.92
Yearly in-plane irradiation [kWh/m^2]		2 083.53
Year-to-year variability [kWh]		29.22
Changes in output due to		
-Angle of incidence [%]		-2.63
-Spectral effects [%]		0.44
Temperature and low irradiance [%]		-8.25
Total loss [%]		-22.83
Max. kWp needed [kWp]		1 167
Energy production (Ideal Value Model)	GWh/y	1.9
Energy production (Surface Coverage Ratio)	GWh/y	0.9

Funded by the European Union

Figure 65 shows a report from the Photovoltaic Geographical Information System application (estimating annual energy production for CS7).

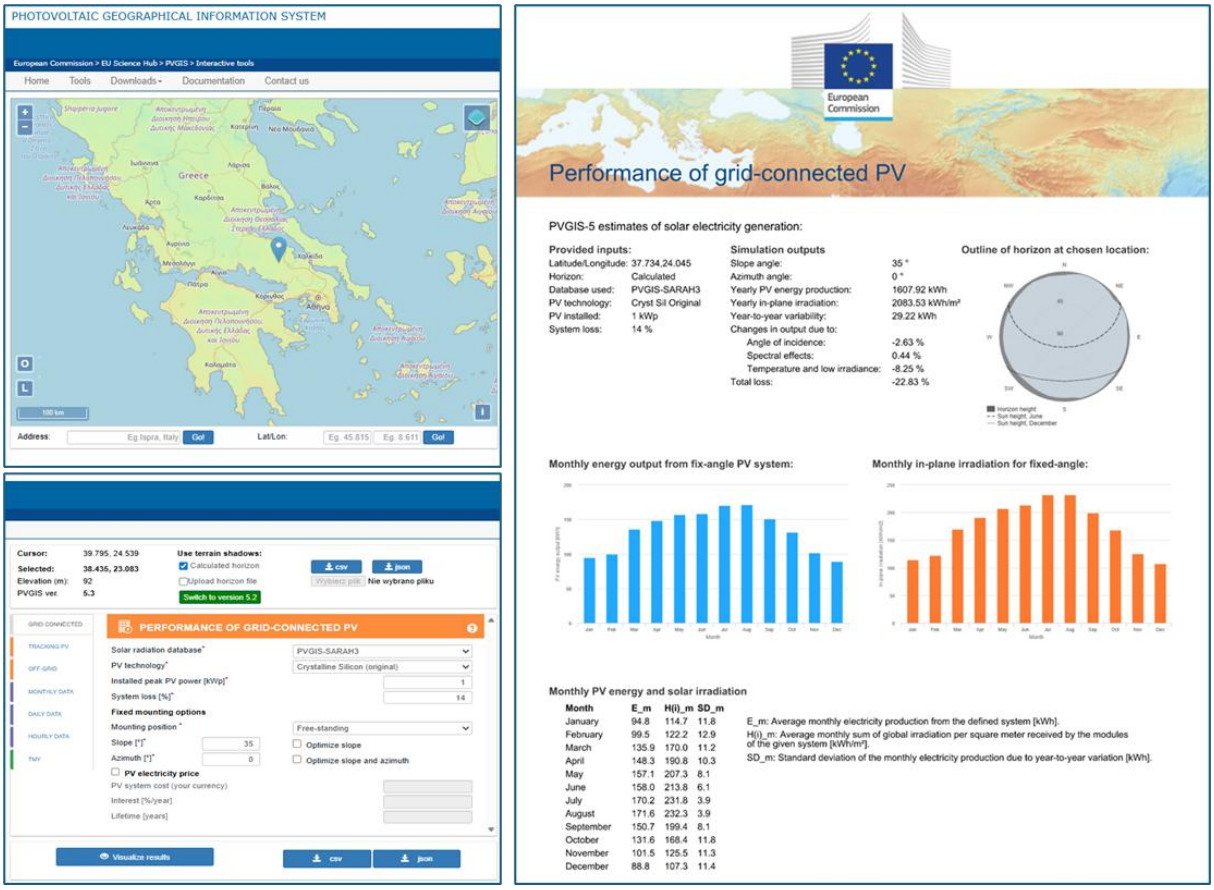

Figure 65 CS7– Performance of grid-connected PV.

A summary results for the ESS7 assessment are presented in Table 171.

Table 171 A summary of ESS7 (Energy properties) results for the different CS7 land-use scenarios.

Land-use scenario	Scenario 1	Scenario 2	Scenario 3
ESS7: Potential energy production [GWh/y].	0.0	0.9	0.

Funded by the European Union

7 Discussion

7.1 Comparison of ESS results across all CS and potential land-use scenarios

The consolidated results for all analyzed CS (CS1–CS7), assessed under the three future land-use scenarios, are presented in the corresponding tables: CS1 (Table 173), CS2 (Table 174), CS3 (Table 175), CS4 (Table 176), CS5 (Table 177), CS6 (Table 178) and CS7 (Table 179). For each ESS, the tables report normalized values to enable direct comparison of outcomes between CS despite differences in local context, data availability, and absolute magnitudes. To support interpretation, the normalized results are expressed on a 1–10 scale, where 1 indicates no potential and 10 indicates very high potential. In addition, a color scale was applied to the 1–10 classes to provide a clear visual overview of spatial and scenario-related patterns. The color legend used for this purpose is provided in theTable 172.

Table 172 Legend for the colour-coded ESS potential scale.

Score	Color code	Site potential to provide an ESS
1		**No potential**
2		**Extremely low potential**
3		**Very low potential**
4		**Low potential**
5		**Moderately low potential**
6		**Medium potential**
7		**Moderate potential**
8		**Moderately high potential**
9		**High potential**
10		**Very high potential**

Scenario 1	Afforestration (NBS, forests)
Scenario 2	Industrial scenario (photovotaic panels)
Scenario 3	Grassland, meadows, pastures (recreational)

Table 173 Summary table of CS1 potential to provide ESS across alternative future land-use scenarios.

ESS ID	Ecosystem Service (EDAPHOS)	Scenario 1	Scenario 2	Scenario 3
ESS 1	Biomass production	7.0	5.4	6.8
ESS 2	Regulation of soil quality	10.0	1.5	1.6
ESS 3	Mitigation of climate change (carbon dioxide sequestration)	3.6	7.6	10.0
ESS 4	Air quality mitigation	4.7	1.0	1.6
ESS 5	Temperature regulation	9.8	1.7	2.5
ESS 6	Direct in-situ regulation & Educational	1.0	1.0	1.0
ESS 7	Energy properties	1.0	10	1.0

Table 174 Summary table of CS2 potential to provide ESS across alternative future land-use scenarios.

ESS ID	Ecosystem Service (EDAPHOS)	Scenario 1	Scenario 2	Scenario 3
ESS 1	Biomass production	10.0	2.1	2.4
ESS 2	Regulation of soil quality	10.0	1.2	1.3
ESS 3	Mitigation of climate change (carbon dioxide sequestration)	10.0	3.6	4.5
ESS 4	Air quality mitigation	6.6	1.0	2.0
ESS 5	Temperature regulation	8.9	1.0	2.0
ESS 6	Direct in-situ regulation & Educational	1.2	1.0	1.0
ESS 7	Energy properties	1.0	10.0	1.0

Table 175 Summary table of CS3 potential to provide ESS across alternative future land-use scenarios.

ESS ID	Ecosystem Service (EDAPHOS)	Scenario 1	Scenario 2	Scenario 3
ESS 1	Biomass production	10.0	2.2	2.6
ESS 2	Regulation of soil quality	10.0	1.2	1.3
ESS 3	Mitigation of climate change (carbon dioxide sequestration)	10.0	4.1	9.0
ESS 4	Air quality mitigation	5.2	1.0	2.5
ESS 5	Temperature regulation	2.7	1.3	6.2
ESS 6	Direct in-situ regulation & Educational	1.0	1.0	1.0
ESS 7	Energy properties	1.0	10.0	1.0

Table 176 Summary table of CS4 potential to provide ESS across alternative future land-use scenarios.

ESS ID	Ecosystem Service (EDAPHOS)	Scenario 1	Scenario 2	Scenario 3
ESS 1	Biomass production	10.0	3.7	4.6
ESS 2	Regulation of soil quality	10.0	1.5	1.7
ESS 3	Mitigation of climate change (carbon dioxide sequestration)	3.7	3.8	10.0
ESS 4	Air quality mitigation	3.9	1.0	1.7
ESS 5	Temperature regulation	9.6	1.0	8.5
ESS 6	Direct in-situ regulation & Educational	1.0	1.0	1.0
ESS 7	Energy properties	1.0	10.0	1.0

Table 177 Summary table of CS5 potential to provide ESS across alternative future land-use scenarios.

ESS ID	Ecosystem Service (EDAPHOS)	Scenario 1	Scenario 2	Scenario 3
ESS 1	Biomass production	10.0	4.2	5.3
ESS 2	Regulation of soil quality	10.0	1.5	1.9
ESS 3	Mitigation of climate change (carbon dioxide sequestration)	7.8	7.9	10.0
ESS 4	Air quality mitigation	4.8	1.0	1.7
ESS 5	Temperature regulation	10.0	1.0	8.2
ESS 6	Direct in-situ regulation & Educational	10.0	1.0	1.0
ESS 7	Energy properties	1.0	10	1.0

Funded by the European Union

Table 178 Summary table of CS6 potential to provide ESS across alternative future land-use scenarios.

ESS ID	Ecosystem Service (EDAPHOS)	Scenario 1	Scenario 2	Scenario 3
ESS 1	Biomass production	10.0	4.5	5.6
ESS 2	Regulation of soil quality	10.0	1.6	1.9
ESS 3	Mitigation of climate change (carbon dioxide sequestration)	7.5	6.1	10.0
ESS 4	Air quality mitigation	4.7	1.0	1.3
ESS 5	Temperature regulation	10.0	1.0	6.7
ESS 6	Direct in-situ regulation & Educational	8.4	1.0	3.8
ESS 7	Energy properties	1.0	10.0	1.0

Table 179 Summary table of CS7 potential to provide ESS across alternative future land-use scenarios.

ESS ID	Ecosystem Service (EDAPHOS)	Scenario 1	Scenario 2	Scenario 3
ESS 1	Biomass production	10.0	1.7	1.9
ESS 2	Regulation of soil quality	10.0	1.1	1.2
ESS 3	Mitigation of climate change (carbon dioxide sequestration)	10.0	4.1	4.1
ESS 4	Air quality mitigation	5.3	1.0	2.5
ESS 5	Temperature regulation	4.1	3.3	1.0
ESS 6	Direct in-situ regulation & Educational	2.6	1	1.3
ESS 7	Energy properties	1.0	10.0	1.0

7.2 Interpretation of ESS assessment results

ESS1 – Biomass production (energy potential)

Under the adopted parameterisation, the scenario ranking for EES1 is consistent across all CS's (CS1–CS7). *Scenario 1* (NBS / forest-based land cover, including poplar plantations) achieves the highest values because forest and woody-crop options provide the largest above-ground biomass increment (AGBinc), which translates directly into higher energy potential (EP). This ordering remains stable even though the CS differ in their environmental and climatic contexts, because the scenario definition systematically assigns the highest AGBinc to NBS/woody vegetation options. *Scenario 3* (grassland-based/recreational uses such as meadows and pastures) ranks second, reflecting the working AGBinc values for productive grasslands. *Scenario 2* (industrial redevelopment with ground-mounted PV) is lowest. However, the difference relative to *Scenario 3* is generally small because the PV scenario assumes 80% grass cover, with vegetation maintained under and between panel rows, meaning that a substantial share of biomass production potential is retained and the reduction is mainly driven by the smaller biologically active fraction defined in the scenario.

ESS2 – Regulation of soil quality (Cd accumulation in biomass)

The same ranking is obtained for EES2 across CS1–CS7. *Scenario 1* obtained better results because the indicator is determined by the combined effect of biomass increment and tissue Cd concentrations (and the harvest allocation), which together define the estimated potential annual Cd accumulation in above-ground biomass. Although the absolute values differ between CS due to local conditions and the concentration datasets used, the overall pattern is consistent. *Scenario 1* ranks highest because, under the adopted assumptions, it provides the greatest biomass

Funded by the European Union

increment. *Scenario 3* typically ranks second, in line with the assumed grassland AGBinc and the concentration inputs selected to represent moderate anthropogenic pressure. *Scenario 2* ranks lowest but remains close to *Scenario 3* for the same structural reason as in ESS1: the PV scenario is parameterised as predominantly grass-covered (80%), with vegetation maintained under and between panel rows, so vegetation-based accumulation capacity is reduced only in proportion to the assumed non-vegetated fraction rather than being eliminated.

ESS3 – Mitigation of climate change

For the ESS3 indicator which investigates the mitigation of climate change through the annual carbon sequestration expressed in t CO_2/ha/year, across the seven case studies, the values vary substantially by both location and land-use scenario. In CS1, values range from 9.805 to 22.725 t CO_2/ha/year, with Scenario 3 delivering the highest performance, while in CS2, sequestration peaks at 30.641 t CO_2/ha/year under the NBS forest *scenario* and drops to 10.908 under the industrial scenario.

A similar pattern is observed in CS3, where the NBS scenario reaches 26.760, compared to a minimum of 10.908 in the industrial option. In CS4 and CS6, *Scenario 3* again provides the highest values (22.725 and 22.901 respectively), while their lowest values occur under either the NBS or industrial scenarios (17.567 and 14.544). CS5 stands out with consistently high sequestration across all scenarios and the overall maximum of 38.632 t CO_2/ha/year in *Scenario 3*. Conversely, the overall minimum is recorded in CS7, where the industrial scenario yields just 7.272 t CO_2/ha/year, confirming that both site-specific conditions and land-use choices strongly influence annual carbon sequestration potential.

ESS4 – Air purification

Considering the ESS4 - Air purification where the annual removal of particulate matter PM10 particles expressed as t/km²/year serves as an indicator, *Scenario 1* (NBS – poplar plantation) consistently delivers the highest annual removal of PM10, clearly outperforming the industrial and recreational alternatives. In CS1, PM10 removal declines sharply from 13.95 t/km²/year under forests to just 0.17 in the industrial scenario, while in CS2, the NBS scenario reaches 26.13 compared to only 0.57 under photovoltaic land use. In CS3, and CS4 similar conclusions can be drawn, as the forest-based solutions achieve 18.87 and 26.00 respectively, while industrial scenarios remain below 1 t/km²/year. CS5 and CS6 follow the same trend, though with comparatively lower forest values (18.66 and 12.3), again dropping to near-minimal levels under industrial use. The overall maximum PM10 removal is recorded in CS2 (26.13 t/km²/year under *Scenario 1*), closely followed by CS4 (26.00), while the absolute minimum occurs in CS1 under the industrial scenario (0.17 t/km²/year). Conversely, CS7 shows a strong forest performance (21.15) and the highest recreational value (7.85), reinforcing that nature-based forest solutions consistently maximize particulate matter removal across diverse territorial contexts.

ESS5 – Temperature regulation

Across the 7CS, temperature regulation potential is strongly scenario-dependent. In most CS, *Scenario 1* (NBS – poplar plantation) shows the highest cooling potential, while *Scenario 2* (industrial/PV) is consistently the lowest. *Scenario 3* (meadow/grassland) typically provides an intermediate cooling effect, but its performance varies by site context and land-cover characteristics. A clear pattern emerges from the scenario-specific values, e.g. *Scenario 2* (industrial/PV) remains low across all CS (≈ 1.0–3.3), indicating limited cooling capacity compared

Funded by the European Union

with green or semi-natural land covers. In contrast, *Scenario 1* (afforestation) shows high values in CS1, CS2, CS4, CS5, and CS6 (≈ 8.9–10.0), confirming forest-based options as the most effective for temperature regulation in these settings. *Scenario 3* (grassland/meadow) displays the widest range (≈ 1.0–8.5), reaching very high levels in CS4–CS6, while remaining low in CS7. Two site-specific deviations were noted. In CS3, the grassland scenario (6.3) exceeds the forest scenario (2.7), suggesting that the forest-related land-cover class applied there has comparatively low cooling performance under the adopted mapping assumptions. In CS7, all three scenarios show moderate-to-low cooling potential (*Scenario 1*: 4.1, *Scenario 2*: 3.3, *Scenario 3*: 1.0), indicating stronger constraints from the local land-cover context. Finally, performed analyses demonstrated that water bodies (water courses) achieve very high cooling potential (up to ~10 where present), highlighting the importance of blue infrastructure as a strong co-determinant of local temperature regulation within administrative units

ESS6 - Cultural- direct, in-situ and outdoor interactions with living systems

Across the 7CS (CS1–CS7), ESS6 was only supported under *Scenario 1* (afforestation) and *Scenario 3* (grassland), because these options meet the criteria for green areas with a recreational function. *Scenario 2* (industrial/PV development) did not qualify as a recreational green-area option and therefore did not contribute to ESS6 in the assessed framing. Overall, the results show that site location relative to residential areas and the presence of nearby recreational green infrastructure were the main determinants of cultural-service potential and of any measurable increase in residents' access. In most cases, the analysed areas are located away from densely populated neighbourhoods and are located in administrative units that already contain recreational green areas serving hundreds to several thousand residents. As a result, introducing afforestation or grassland on the contaminated sites typically did not materially increase the availability of recreational green space at the local scale (CS2, CS3, CS4), or produced only a very small increase (CS1: access for 13 residents; CS7: access for 399 residents). Two sites clearly differed from this general pattern (CS5 & CS6). CS5 showed high recreational potential due to its adjacency to the Tiepido River ecological corridor and the "Percorso Natura Torrente Tiepido" trail, meaning that converting the site to a green option could integrate it into an established and highly used recreational system (reported high potential score). CS6 is already embedded in an urban-park setting (Parc des Alliaires, opened in 2023), where recreational and educational use is an explicit function; here, the cultural-service potential is further strengthened by dense nearby population and adjacent recreational green areas.

ESS7 - Energy properties

Based on the ESS7 assessment results it can be concluded that the average value of yearly in-plane irradiation for all areas is 1 699.83 kWh/m²; however, the maximum value set to 2 101.64 kWh/m² is found in CS3 (Odiel Basin Area – ESSP), while the lowest is set to 1 302.79 kWh/m² in CS4 (Upper Silesia Coal Basin – PL). Due to constant model conditions across each CS, a yearly PV energy production parameter was used to estimate the energy production potential between each CS. The maximum yearly PV energy production set to 1 609.17 kWh is found in CS3. The lowest value, set to 1 049.06 kWh, is found in CS4. Energy production estimations should consider the feasibility of the investment; therefore, the calculations include the Surface Coverage Ratio, which takes into account the distance between PV modules; roads, and technological buildings construction; fencing; energy infrastructure, etc. The projected annual energy production ranges from 1.9 GWh to 75.7 GWh. Considering the Surface Coverage Ratio, the highest estimated

Funded by
the European Union

energy production is 37.6 GWh in CS2 (Kozani – GR), while the lowest is 0.9 GWh in CS7 (Lavrio – GR).

Funded by
the European Union

8 Recommendations

In EDAPHOS, the work delivered under Task 2.2 brought together two strands of evidence that are central for deciding "*what can realistically be done"* on contaminated and degraded sites. One strand focuses on soil condition and risk-relevant constraints, the other translates land-use alternatives into comparable ecosystem service outcomes across the seven case studies. The scenario comparison (forest-based NBS, grassland/recreational uses, and industrial redevelopment with PV) showed which benefits tend to be consistently associated with particular land-cover choices, and where outcomes are driven mainly by local context - especially for cultural benefits and some regulating functions.

This combination of risk-informed constraints and scenario-based ESS results is what allowed the recommendations to be formulated in a practical way. It highlights where low-disturbance options are typically robust, where public-facing or productive uses remain conditional *on site* evidence, and where uncertainty needs to be managed through phased implementation and monitoring. In that sense, Task 2.2 provides an evidence link that can be directly carried forward into the next project steps. It supports scenario selection and design choices, helps target additional investigations where they genuinely change decisions, and provides a consistent narrative that can be reused when moving from assessment into appraisal, planning, stakeholder discussion, and follow-up monitoring activities.

Across post-industrial and contaminated land, the most defensible redevelopment pathways are those that deliver benefits while remaining bounded by exposure control, mobilization risk, and realistic long-term stewardship. Options that increase soil disturbance, intensify public presence, or generate secondary material streams should be treated as conditional and justified only where site evidence demonstrates that risks are controlled and governance is durable. Redevelopment concepts gain clarity and robustness when organized through a compartment-based land-use logic. Areas with persistent constraints are most credibly aligned with low-occupancy, low-disturbance functions such as stabilizing green cover, controlled habitat creation, buffer zones, and technical infrastructure. Where constraints are lower and safety is verifiable, multifunctional uses become plausible, including recreation and education, but only where access is genuinely deliverable and enforceable rather than inferred from nominal land-cover change.

NBS approaches can deliver high value when they are implemented in a way that does not create new exposure pathways. They are most effective when they stabilise contaminated soils, reduce dust and erosion, and support local microclimate regulation, while remaining fully compatible with contaminant control measures. If there is a realistic risk that contaminants could be taken up by vegetation, bioaccumulate, or be mobilised during maintenance activities, a more robust option is to use hybrid or engineered solutions. In such cases, ecological features should be placed in controlled compartments (e.g., capped or isolated zones) and managed against clear performance indicators, with maintenance requirements that can be reliably delivered.

Renewable energy redevelopment is often compatible with disturbed land and can support economic reuse with limited soil interaction, provided that designs incorporate runoff and erosion control, minimal ground disturbance, and clear operational governance. Energy yield expectations should be tied to irradiation conditions and layout feasibility (spacing, access roads, fencing, grid connection, safety infrastructure). Any biomass-related energy narrative remains strictly conditional on contaminant-safe feedstock and chain-of-custody safeguards, so that redevelopment does not externalise risk into downstream users or environments.

Claims about cultural and recreational benefit are credible only when supported by real accessibility, safe routes, and integration into existing green networks. Where sites are remote, fenced, privately controlled, or poorly connected, land-cover change alone is unlikely to translate into meaningful cultural value. Where connection to corridors, trails, parks, or dense residential areas exists, the benefit proposition is stronger, provided that access, safety, and maintenance responsibilities are clearly assigned. Planning choices are more robust when treated as service bundles and trade-offs rather than single-metric optimisation. Maximising one outcome (for example energy production or carbon sequestration) can reduce others (such as accessibility, habitat continuity, or cooling) or increase maintenance and compliance burden. Preferred directions therefore tend to be those that achieve stable multi-benefit profiles under credible governance, even if they do not maximise any one indicator.

A minimum evidence package is a practical precondition for higher-intensity uses. Before endorsing public access, productive uses, or biomass handling, the site should be supported by targeted evidence on contaminant speciation and bioavailability, dust and runoff behavior, groundwater interactions, soil-function constraints, and ground stability, together with a realistic monitoring and stewardship plan. Where evidence is incomplete or uncertainty remains high, the precautionary baseline is restricted access and low-disturbance uses, with the possibility of later intensification once gaps are closed. Uncertainty should be treated as decision-relevant information, not as a technical detail. Where results depend on proxies, transferred parameters, or coarse spatial representations, they are best used for screening and prioritisation, while binding claims and fine-grained valuation require local validation. Approaches that remain defensible under plausible parameter ranges and operational constraints should be preferred over options whose attractiveness depends on optimistic assumptions.

Phased implementation is a pragmatic way to avoid lock-in under uncertainty. Early phases can focus on low-risk functions and controlled access while targeted monitoring and investigations are conducted; subsequent phases can expand to higher-intensity uses only when evidence confirms that risks are controlled and management capacity is secured. This approach reduces the probability of redesign, reputational risk, and non-compliance over the life cycle of the site.

Future research that most directly improves planning quality should prioritise transferable thresholds and decision triggers that connect monitoring observations to governance actions, particularly at the interface between contamination control and ecosystem function. The highest value additions are site-scale validation of cooling and air-quality regulation proxies, empirical understanding of accessibility and actual use for cultural services, and longitudinal evidence on how remediation and revegetation trajectories change service delivery and risk profiles over time.

Funded by
the European Union

References

Airparif. (2022). Air quality in the Paris region – Summary 2021. Airparif.

Algreen, M., Trapp, S., Rein, A. (2014). Phytoscreening and phytoextraction of heavy metals at Danish polluted sites using willow and poplar trees. Environmental Science and Pollution Research. 21. 8992–9001. 10.1007/s11356-013-2085-z

Ameller, J., Rinaudo, J.-D., & Merly, C. (2019). The contribution of economic science to brownfield redevelopment: A review. Integrated Environmental Assessment and Management, 16(2), 184–196. https://doi.org/10.1002/ieam.4233

Andresen, L. C., Yuan, N., Seibert, R., Moser, G., Kammann, C. I., Luterbacher, J., Erbs, M., Müller, C. (2018). Biomass responses in a temperate European grassland through 17 years of elevated CO2. Global Change Biology. 24(9). 3875-3885. 10.1111/gcb.13705

Andresen, L.C., Yuan, N., Seibert, R., Moser, G., Kammann, C.I., Luterbacher, J., Erbs, M., Müller, C. (2018). Biomass responses in a temperate European grassland through 17 years of elevated CO_2. Global Change Biology. 24(9). 3875–3885. 10.1111/gcb.13705.

Aravanopoulos, F. A. (2010). Breeding of fast growing forest tree species for biomass production in Greece. Biomass and bioenergy, 34(11), 1531-1537.

Asare, M. O., Száková, J., Tlustoš, P. (2023). Mechanisms of As, Cd, Pb, and Zn hyperaccumulation by plants and their effects on soil microbiome in the rhizosphere. Frontiers in Environmental Science. 11. 1157415. 10.3389/fenvs.2023.1157415

Bardos, R. P., Jones, S., Stephenson, I., Menger, P., Beumer, V., Neonato, F., Maring, L., Ferber, U., Track, T., & Wendler, K. (2016). Optimising value from the soft re-use of brownfield sites. Science of the Total Environment, 563–564, 769–782. https://doi.org/10.1016/j.scitotenv.2015.12.002

Bardos, R. P., Thomas, H. F., Smith, J. W. N., Harries, N. D., Evans, F., Boyle, R., Howard, T., Lewis, R., Thomas, A. O., Dent, V. L., & Haslam, A. (2020). Sustainability assessment framework and indicators developed by SuRF-UK for land remediation option appraisal. Remediation Journal, 31(1), 5–27. https://doi.org/10.1002/rem.21668

Bartke, S., Martinát, S., Klusáček, P., Pizzol, L., Alexandrescu, F., Frantál, B., Turečková, K., … & Zabeo, A. (2016). Targeted selection of brownfields from portfolios for sustainable regeneration: User experiences from five cases testing the TIMBRE Brownfield Prioritization Tool. Journal of Environmental Management, 184, 94–107. https://doi.org/10.1016/j.jenvman.2016.07.037

Baycu, G., Tolunay, D., Özden, H., Günebakan, S. (2006). Ecophysiological and seasonal variations in Cd, Pb, Zn, and Ni concentrations in the leaves of urban deciduous trees in Istanbul. Environmental Pollution. 143(3). 545–554. 10.1016/j.envpol.2005.10.050 Bierza, K., Bierza, W. (2024). The effect of industrial and urban dust pollution on the ecophysiology and leaf element concentration of Tilia cordata Mill. Environmental Science and Pollution Research. 31. 58413–58429. 10.1007/s11356-024-34999-9.

Borlaza-Lacoste, L.,Weber, S., Marsal, A., Uzu, G., Jacob, V., Besombes, J., Chatain, M., Conil, S., Jaffrezo, J. (2022). Nine-year trends of PM10 sources and oxidative potential in a rural background site in France. Atmospheric Chemistry and Physics. 22. 8701-8723. 10.5194/acp-22-8701-2022.

Borreani, G., Peiretti, P. G., & Tabacco, E. (2007). Effect of harvest time on yield and pre-harvest quality of semi-leafless grain peas (Pisum sativum L.) as whole-crop forage. Field Crops Research, 100(1), 1-9.

Budzyńska, S., Budka, A., Roszyk, E., Niedzielski, P., Mleczek, M. (2023). Trace of negative changes in environment recorded in cores of trees growing near busy city roads in Poznań, Poland – dendromonitoring of urban pollution. Ecological Indicators. 149. 110198. 10.1016/j.ecolind.2023.110198.

Calfapietra, C., Gielen, B., Galema, A., Lukac, M., Angelis, P., Moscatelli, M., Ceulemans, R., & Scarascia-Mugnozza, G. (2003). Free-air CO2 enrichment (FACE) enhances biomass production in a short-rotation poplar plantation.. Tree physiology, 23 12, 805-14 . https://doi.org/10.1093/treephys/23.12.805.

Cañellas Rey de Viñas, I., San Miguel Ayanz, A. (2000). Biomass of root and shoot systems of Quercus coccifera shrublands in Eastern Spain. Annals of Forest Science. 57(8). 803–810. 10.1051/forest:2000160. Cañellas I., Sixto H., Ceulemans R. (2018). Above- and below-ground biomass allocation in poplar short rotation plantations. Forest Ecology and Management, 428, 57–65.

Carabulea, V., Vrînceanu, N.O., Oprea, B.Ş., Costea, M., Plopeanu, G., Motelică, D.-M., Fudulu, I.D. (2024). A study regarding heavy metals in perennial grasses species harvested from permanent meadows in the Copşa Mică area, Romania. Annals of the University of Craiova - Agriculture, Montanology, Cadastre Series. 53(2). 10.52846/aamc.v53i2.1520.

Carvalho F., Lee H. K., Blaydes H., Treasure L., Harrison L. J., Montag H., Vucic K., Scurlock J., White P. C. L., Sharp S. P., Clarkson T., Armstrong A.(2024) Integrated policymaking is needed to deliver climate and ecological benefits from solar farms. Journal of Applied Ecology, Volume 62, Issue 7. https://doi.org/10.1111/1365-2664.14745

Carvalho F., Treasure L., Robinson S. J. B., Blaydes H., Exley G., Hayes R., Howell B., Keith A., Montag H., Parker G., Sharp S. P., Witten C., Armstrong A. (2023) Towards a standardized protocol to assess natural capital and

ecosystem services in solar parks. Ecological Solutions and Evidence Volume 4, Issue 1. https://doi.org/10.1002/2688-8319.12210

Chen,m., Y. Tan, X. Xu, Y. Lin (2023) Identifying ecological degradation and restoration zone based on ecosystem quality: A case study of Yangtze River Delta. Applied Geography, Volume 162, 103149. https://doi.org/10.1016/j.apgeog.2023.103149

Chervenkov, H., & Slavov, K. (2025). ETCCDI precipitation-based climate indices in the CMIP5 future climate projections over Southeast Europe. In ETCCDI precipitation-based climate indices in the CMIP5 future climate projections over Southeast Europe

CIP, 2020. Commission internationale du peuplier et autres arbres à croissance rapide [CIP], 2020. Technoquide de peupier.

Čeburnis, D., Steinnes, E. (2000). Conifer needles as biomonitors of atmospheric heavy metal deposition: comparison with mosses and precipitation, role of the canopy. Atmospheric Environment. 34(25). 4265–4271. 10.1016/S1352-2310(00)00213-2.

Costanza, R., d'Arge, R., de Groot, R., Farber, S., Grasso, M., Hannon, B., Limburg, K., Naeem, S., O'Neill, R.V., Paruelo, J., Raskin, R.G., Sutton, P., van den Belt, M. (1997). The value of the world's ecosystem services and natural capital. Nature. 387(6630). 253–260. 10.1038/387253a0.

Cundy, A. B., Bardos, R. P., Puschenreiter, M., Mench, M., Bert, V., Friesl-Hanl, W., Müller, I., Li, X. N., Weyens, N., Witters, N., & Vangronsveld, J. (2016). Brownfields to green fields: Realising wider benefits from practical contaminant phytomanagement strategies. Journal of Environmental Management, 184, 67–77. https://doi.org/10.1016/j.jenvman.2016.03.028

Dal Prà, A., Davolio, R., Immovilli, A., Burato, A., & Ronga, D. (2023). Plant composition and feed value of first cut permanent meadows. Agronomy, 13(3), 681.

Del Gatto, A., Melilli, M. G., Raccuia, S. A., Pieri, S., Mangoni, L., Pacifico, D., ... & Mengarelli, C. (2015). A comparative study of oilseed crops (Brassica napus L. subsp. oleifera and Brassica carinata A. Braun) in the biodiesel production chain and their adaptability to different Italian areas. Industrial Crops and Products, 75, 98-107.

Dère, C., Lamy, I., Jaulin, A., & Cornu, S. (2007). Long-term fate of exogenous metals in a sandy Luvisol subjected to intensive irrigation with raw wastewater. *Environmental Pollution*, *145*(1), 31–40. https://doi.org/10.1016/j.envpol.2006.04.002

Di Cosmo, L., Pilli, R., et al. (2022/2023). Forest Carbon Stock. In: Gasparini, P., Tabacchi, G. (eds) Italian National Forest Inventory: Methods and Results of the Third Survey (INFC2015). Springer.

Dickinson D.C., Hobbs R.J. (2016) Cultural ecosystem services: Characteristics, challenges and lessons for urban green space research. Ecosystem Services 179-194. https://doi.org/10.1016/j.ecoser.2017.04.014

Directive 2000/60/EC of the European Parliament and of the Council of 23 October 2000 establishing a framework for Community action in the field of water policy. (2000). Official Journal of the European Communities, L 327, 1–73. https://eur-lex.europa.eu/legal-content/EN/TXT/?uri=CELEX:32000L0060

Directive 2001/42/EC of the European Parliament and of the Council of 27 June 2001 on the assessment of the effects of certain plans and programmes on the environment. (2001). Official Journal of the European Communities, L 197, 30–37. https://eur-lex.europa.eu/legal-content/EN/TXT/?uri=CELEX:32001L0042

Directive 2004/35/EC of the European Parliament and of the Council of 21 April 2004 on environmental liability with regard to the prevention and remedying of environmental damage. (2004). Official Journal of the European Union, L 143, 56–75. https://eur-lex.europa.eu/legal-content/EN/TXT/?uri=CELEX:32004L0035

Directive 2006/118/EC of the European Parliament and of the Council of 12 December 2006 on the protection of groundwater against pollution and deterioration. (2006). Official Journal of the European Union, L 372, 19–31. https://eur-lex.europa.eu/legal-content/EN/TXT/?uri=CELEX:32006L0118

Directive 2009/147/EC of the European Parliament and of the Council of 30 November 2009 on the conservation of wild birds. (2010). Official Journal of the European Union, L 20, 7–25. https://eur-lex.europa.eu/legal-content/EN/TXT/?uri=CELEX:32009L0147

Directive 2010/75/EU of the European Parliament and of the Council of 24 November 2010 on industrial emissions (integrated pollution prevention and control). (2010). Official Journal of the European Union, L 334, 17–119. https://eur-lex.europa.eu/legal-content/EN/TXT/?uri=CELEX:32010L0075

Directive 2011/92/EU of the European Parliament and of the Council of 13 December 2011 on the assessment of the effects of certain public and private projects on the environment (as amended by Directive 2014/52/EU). (2012). Official Journal of the European Union, L 26, 1–21. https://eur-lex.europa.eu/legal-content/EN/TXT/?uri=CELEX:32011L0092

Dupouey, J. L., Pignard, G., Hamza, N., & Dhôte, J.-F. (2010). Estimating carbon stocks and fluxes in forest biomass: Application to the French case based upon National Forest Inventory data. In D. Loustau (Ed.), Forests, carbon cycle and climate change (pp. 101–129).

European Environment Agency (EEA). (2016). EMEP/EEA air pollutant emission inventory guidebook - 2016: Technical guidance to prepare national emission inventories. EEA Report 21/2016. 10.2800/247535.

Funded by the European Union

European Commission. (2011). Roadmap to a resource efficient Europe (COM(2011) 571 final). https://eur-lex.europa.eu/legal-content/EN/TXT/?uri=CELEX:52011DC0571

European Commission. (2020). EU biodiversity strategy for 2030: Bringing nature back into our lives (COM(2020) 380 final). https://eur-lex.europa.eu/legal-content/EN/TXT/?uri=CELEX:52020DC0380

European Commission. (2021a). EU soil strategy for 2030: Reaping the benefits of healthy soils for people, food, nature and climate (COM(2021) 699 final). https://eur-lex.europa.eu/legal-content/EN/TXT/?uri=CELEX:52021DC0699

European Commission. (2021b). Pathway to a healthy planet for all – EU action plan: "Towards zero pollution for air, water and soil" (COM(2021) 400 final). https://eur-lex.europa.eu/legal-content/EN/TXT/?uri=CELEX:52021DC0400

European Commission. (2023). Proposal for a directive of the European Parliament and of the Council on soil monitoring and resilience (Soil Monitoring Law) (COM(2023) 416 final). https://eur-lex.europa.eu/legal-content/EN/TXT/?uri=CELEX:52023PC0416

European Monitoring and Evaluation Programme (EMEP). (2016). Methods for estimating atmospheric deposition of heavy metals and particulate matter. Norwegian Meteorological Institute.

Fellet, G., Marchiol, L., Delle Vedove, G., Peressotti, A. (2019). Application of biochar on mine tailings: Effects and perspectives for land reclamation. Journal of Environmental Management. 231. 232–240. 10.1016/j.jenvman.2018.10.046.

Fermeglia, M., & Perisic, M. (2023). Nature-based solution to man-made problems: Fostering the uptake of phytoremediation and low-iLUC biofuels in the EU. Journal for European Environmental & Planning Law, 20(2), 145–167. https://doi.org/10.1163/18760104-20020007

Gabryszuk et al. (2021). Characteristics of grasslands and their use in Poland. Journal of Water and Land Development, 2021(…): p. 246 (PDF p.2). (Journal of Water and Land Development).

Gasparini, P., Di Cosmo, L., Floris, A., & De Laurentis, D. (2022). Italian National Forest Inventory—Methods and Results of the Third Survey: Inventario Nazionale delle Foreste e dei Serbatoi Forestali di Carbonio—Metodi e Risultati della Terza Indagine (p. 576). Springer Nature.

Geneletti, D., Scolozzi, R., Adem Esmail, B. (2018). Assessing ecosystem services and biodiversity tradeoffs across agricultural landscapes in a mountain region. International Journal of Biodiversity Science, Ecosystem Services & Management. 14(1). 188–208. 10.1080/21513732.2018.1526214.

Geneletti, D., Adem Esmail, B., Cortinovis, C., Arany, I., Balzan, M. V., van Beukering, P., … Veidemane, K. (2020). Ecosystem services mapping and assessment for policy- and decision-making: Lessons learned from a comparative analysis of European case studies. One Ecosystem. 5. e53111. 10.3897/oneeco.5.e53111.

GIOŚ. Poland's National Inventory Report 2019. Instytut Ochrony Środowiska – Państwowy Instytut Badawczy (2019). Root-to-shoot ratio for forest species Summary 2021.

Główny Inspektorat Ochrony Środowiska (GIOŚ). (2018). Review of methods that can be used in the assessment of atmospheric deposition. Chief Inspectorate of Environmental Protection, Poland.

González-Díaz, P. et al. (2019). A Multifactorial Approach to Value Supporting Ecosystem Services in Spanish Forests and Its Implications in a Warming World. Sustainability 11(2):358.

Grunewald, Karsten, et al. Proposal of indicators regarding the provision and accessibility of green spaces for assessing the ecosystem service "recreation in the city" in Germany. International Journal of Biodiversity Science, Ecosystem Services & Management, 2017, 13.2: 26-39.

Gschwantner, T., Riedel, T., Henning, L., Adame, P., Adolt, R., Aguirre, A., Westerlund, B. (2024). Improved large-area forest increment information in Europe through harmonisation of National Forest Inventories. Forest Ecology and Management, 562, 121913.

GUS, 2020, Główny Urząd Statystyczny. Rolnictwo w 2019 r. p. 49 (PDF page label). (Główny Urząd Statystyczny).

Haase, D. (2021). COVID-19 pandemic observations as a trigger to reflect on urban forestry in European cities under climate change: Introducing nature-society-based solutions. Urban Forestry & Urban Greening, 64, 127304. https://doi.org/10.1016/j.ufug.2021.127304

Haase, D., Kabisch, S., Haase, A., Andersson, E., Banzhaf, E., Baró, F., … & Wolff, M. (2017). Greening cities – To be socially inclusive? About the alleged paradox of society and ecology in cities. Habitat International, 64, 41–48. https://doi.org/10.1016/j.habitatint.2017.04.005

Handley, John. Providing Accessible Natural Greenspace in Towns and Cities. A Practical Guide to Assessing the Resource and Implementing Local Standards for Provision. Evaluation Draft. English Nature, 2003.

Hayes A. T., Jandaghian Z., Lacasse M. A., Gaur A., Lu H., Laouadi A., Ge H., Wang L. (2022) Nature-Based Solutions (NBSs) to Mitigate Urban Heat Island (UHI) Effects in Canadian Cities. Building Energy, Physics, Environment, and Systems. https://doi.org/10.3390/buildings12070925

Funded by the European Union

He D., Luo Y., Lu S., Liu M., Song Y., Lei L.(2018) Microplastics in soils: Analytical methods, pollution characteristics and ecological risks. TrAC Trends in Analytical Chemistry 163-172. https://doi.org/10.1016/j.trac.2018.10.006

He H., Chen J. (2011) Educational and enjoyment benefits of visitor education centers at botanical gardens. Biological Conservation 103-112. https://doi.org/10.1016/j.biocon.2012.01.048

IPBES. (2012). Resolution on the Intergovernmental Science-Policy Platform on Biodiversity and Ecosystem Services. Panama City, Panama, 21 April 2012.

Intergovernmental Panel on Climate Change (IPCC). (2003). Good Practice Guidance for Land Use, Land-Use Change and Forestry. Institute for Global Environmental Strategies (IGES) for the IPCC.Jacek, G., Rozan, A., Desrousseaux, M., & Combroux, I. (2022). Brownfields over the years: From definition to sustainable reuse. Environmental Reviews, 30(1), 50–60. https://doi.org/10.1139/er-2021-0017

Jakubiak, M., Panek, E., Urbański, K., Victória, S.S., Lach, S., Maciuk, K., Kopacz, M. (2025). Nature-Based Solutions in Sustainable Cities: Trace Metal Accumulation in Urban Forests of Vienna (Austria) and Krakow (Poland). Sustainability. 17(15). 7042. 10.3390/su17157042.

Juranović Cindrić, I., Zeiner, M., Starčević, A., et al. (2019). Metals in pine needles: characterisation of bio-indicators depending on species. International Journal of Environmental Science and Technology. 16. 4339–4346. 10.1007/s13762-018-2096-x.

Kabisch, N. (2019). Transformation of urban brownfields through co-creation: The multi-functional Lene-Voigt Park in Leipzig as a case in point. Urban Transformations, 1(1), 1–13. https://doi.org/10.1186/s42854-019-0002-6

Kabisch, N., Strohbach, M., Haase, D., & Kronenberg, J. (2016). Urban green space availability in European cities. Ecological indicators, 70, 586-596

Kandziora-Ciupa, M., Gospodarek, J., Nadgórska-Socha, A. (2022). Pollution and ecological risk assessment of heavy metals in forest soils with changes in the leaf traits and membrane integrity of Vaccinium myrtillus L. European Journal of Forest Research. 141. 409–419. 10.1007/s10342-022-01446-8.Khan F. N., Lukac M., Turner G., Godbold D. L. (2007) Elevated atmospheric CO2 changes phosphorus fractions in soils under a short rotation poplar plantation (EuroFACE). Soil Biology and Biochemistry 1716-1723. https://doi.org/10.1016/j.soilbio.2008.02.008

Khan, T., Perlinger, J. (2017). Evaluation of five dry particle deposition parameterizations for incorporation into atmospheric transport models, Geoscientific Model Development. 10. 3861-3888. 10.5194/gmd-10-3861-2017.

Kicińska, A., Gruszecka-Kosowska, A. (2016). Long-term changes of metal contents in two metallophyte species (Olkusz area of Zn-Pb ores, Poland). Environmental Monitoring and Assessment. 188. 339. 10.1007/s10661-016-5330-3.

Kicińska, A.J., Smreczak, B., Jadczyszyn, J. (2019). Soil Bioavailability of Cadmium, Lead, and Zinc in Areas of Zn-Pb Ore Mining and Processing (Bukowno, Olkusz). Journal of Ecological Engineering. 20(1). 84–92. 10.12911/22998993/93794.

Kotschik, P., Princz, J., Silva, C., Renaud, M., Martí-Roura, M., Brooks, B., … & Grenni, P. (2023). The upcoming European Soil Monitoring Law: An effective instrument for the protection of terrestrial ecosystems? Integrated Environmental Assessment and Management, 20(2), 316–321. https://doi.org/10.1002/ieam.4834

Kuklinska, K., Wolska, L., & Namiesnik, J. (2015). Air quality policy in the U.S. and the EU – A review. Atmospheric Pollution Research, 6(1), 129–137.

Langner M., Kull M., Endlicher W. R. (2011). Determination of PM_{10} deposition based on antimony flux to selected urban surfaces. Environ Pollut. 159 (8-9), 2028-34. doi: 10.1016/j.envpol.2011.01.017.

Laprise, M., Lufkin, S., & Rey, E. (2018). An operational monitoring tool facilitating the transformation of urban brownfields into sustainable neighborhoods. Building and Environment, 142, 221–233. https://doi.org/10.1016/j.buildenv.2018.06.005

Latini, A., Bacci, G., Teodoro, M., Mirabile Gattia, D., Bevivino, A., Trakal, L. (2019). The Impact of Soil-Applied Biochars From Different Vegetal Feedstocks on Durum Wheat Plant Performance and Rhizospheric Bacterial Microbiota in Low Metal-Contaminated Soil. Frontiers in Microbiology. 10. 2694. 10.3389/fmicb.2019.02694

Lazzeri, L., D'Avino, L., Mazzoncini, M., Antichi, D., Mosca, G., Zanetti, F., ... & Spugnoli, P. (2009). On farm agronomic and first environmental evaluation of oil crops for sustainable bioenergy chains. Italian Journal of Agronomy, 4(4), 171-180.

Le Dantec V., Dufrêne E., Saugier B. (2000). Interannual and spatial variation in maximum leaf area index of temperate deciduous stands, Forest Ecology and Management, 134 (1–3), 71-81.

Leśny, J., Szoszkiewicz, K., Juszczak, R., Olejnik, J. & Serba, T. (2007). Leaf area index of wood and shrub vegetation of wetland areas. Acta Agroph., 9(3), 673–684.

Leu S.,, M. Ben-Eli, A. Mor-Mussery (2021) Effects of grazing control on ecosystem recovery, biological productivity gains, and soil carbon sequestration in long-term degraded loess farmlands in the Northern Negev, Israel. Land Degradation & Development, 2580-2594. https://doi.org/10.1002/ldr.3923

Li C., Zhou K., Qin W., Tian C., Qi M., Yan X., Han W. (2019) A Review on Heavy Metals Contamination in Soil: Effects, Sources, and Remediation Techniques. Soil Sediment Contamination: An International Journal. https://doi.org/10.1080/15320383.2019.1592108

Li M, S. Liu, F. Wang, H. Liu, Y. Liu, Q. Wang (2021) Cost-benefit analysis of ecological restoration based on land use scenario simulation and ecosystem service on the Qinghai-Tibet Plateau. Global Ecology and Conservation, Volume 34. https://doi.org/10.1016/j.gecco.2022.e02006

Li Y., Niu S., Yu G. (2015) Aggravated phosphorus limitation on biomass production under increasing nitrogen loading: a meta-analysis. Global Change Biology 934-943. https://doi.org/10.1111/gcb.13125

Li, M., Heng, Q., Hu, C., Wang, Z., Jiang, Y., Wang, X., He, X., Yong, J., Dawoud, T., Rahman, S., Fan, J., & Zhang, Y. (2024). Phytoremediation efficiency of poplar hybrid varieties with diverse genetic backgrounds in soil contaminated by multiple toxic metals (Cd, Hg, Pb, and As).. Ecotoxicology and environmental safety, 283, 116843. https://doi.org/10.1016/j.ecoenv.2024.116843

Longato, D., Cortinovis, C., Albert, C., Geneletti, D. (2021). Practical applications of ecosystem services in spatial planning: Lessons learned from a systematic literature review. Environmental Science & Policy. 119. 72–84. 10.1016/j.envsci.2021.02.001 Louzon, M., Pauget, B., Gimbert, F., Morin-Crini, N., Wong, J. W. Y., Zaldibar, B., Natal-da-Luz, T., Neuwirthova, N., Thiemann, C., Sarrazin, B., Irazola, M., Amiot, C., Rieffel, D., Sousa, J. P., Chalot, M., & De Vaufleury, A. (2022). In situ and ex situ bioassays with *Cantareus aspersus* for environmental risk assessment of metal(loid) and PAH-contaminated soils. *Integrated Environmental Assessment and Management*, *18*(2), 539–554. https://doi.org/10.1002/ieam.4480

Lovett A.A., Dockerty T.L., Papathanasopoulou E., Beaumont N.J., Smith P. (2014) A framework for assessing the impacts on ecosystem services of energy provision in the UK: An example relating to the production and combustion life cycle of UK produced biomass crops (short rotation coppice and Miscanthus). Biomass and Bioenergy 311-321. https://doi.org/10.1016/j.biombioe.2015.10.001

Lovett, G. M. (1994). Atmospheric deposition of nutrients and pollutants in North America: An ecological perspective. Ecological Applications, 4(4), 629–650.

Lovett, G.M., Reiners, W.A., Olson, R.K. (2000). Factors regulating throughfall flux in a New Hampshire forested landscape. Atmospheric Environment. 34(27). 4527–4533. 10.1016/S1352-2310(00)00213-2.

Maes, J., et al. (2020). Mapping and Assessment of Ecosystems and their Services: An EU ecosystem assessment. EUR 30161 EN. Publications Office of the European Union. JRC120383. 10.2760/757183

Manzone M., Calvo A. (2015) Energy and CO2 analysis of poplar and maize crops for biomass production in north Italy. Renewable Energy 675-681. https://doi.org/10.1016/j.renene.2015.08.047

Manzone, M., Bergante, S., & Facciotto, G. (2014). Energy and economic evaluation of a poplar plantation for woodchips production in Italy. Biomass and Bioenergy, 60, 164–170.

Marando F., Heris M.P., Zulian G., Udías A., Mentaschi L., Chrysoulakis N., Parastatidis D., Maes J. (2021) Urban heat island mitigation by green infrastructure in European Functional Urban Areas. Sustainable Cities and Society. https://doi.org/10.1016/j.scs.2021.103564

Marando, F., Salvatori, E., Fusaro, L., & Manes, F. (2016). Removal of PM10 by Forests as a Nature-Based Solution for Air Quality Improvement in the Metropolitan City of Rome. Forests, 7(7), 150.

Mariarosa, G., Donateo, A., Buffa, P., Contini, D., Cervone, A., Lombardo, C., Rocchi, F. (2019). Atmospheric dry deposition processes of particles on urban and suburban surfaces: Modelling and validation works. Atmospheric Environment. 214. 116857. 10.1016/j.atmosenv.2019.116857.

Marmiroli, M., Pigoni, V., Savo Sardaro, M.L., Marmiroli, N. (2020). The effect of biochar and compost on the phytoremediation of a metal-contaminated soil by Miscanthus × giganteus. Science of the Total Environment. 703. 134701. 10.1016/j.scitotenv.2019.134701.

Martinát, S., Dvořák, P., Frantál, B., Klusáček, P., Kunc, J., Navrátil, J., Turečková, K., … & Reed, M. (2016). Sustainable urban development in a city affected by heavy industry and mining? Case study of brownfields in Karviná, Czech Republic. Journal of Cleaner Production, 118, 78–87. https://doi.org/10.1016/j.jclepro.2016.01.029

Martinho, V., Ferreira, A., Cunha, C., Pereira, J., Carreira, M., Castanheira, N., … & Ramos, T. (2024). Soil legislation and policies: Bibliometric analysis, systematic review and quantitative approaches with an emphasis on the specific cases of the European Union and Portugal. Heliyon, 10(14), e34307. https://doi.org/10.1016/j.heliyon.2024.e34307

Merwin, L., Umek, L., & Anastasio, A. (2022). Urban post-industrial landscapes have unrealized ecological potential. Restoration Ecology, 30(8), e13643. https://doi.org/10.1111/rec.13643

Mokany, K., Raison, R. J., & Prokushkin, A. S. (2006). Critical analysis of root:shoot partitioning and below-ground biomass in terrestrial biomes. Global Ecology and Biogeography, 15(5), 499–510. (providing a global dataset of R/S values).

Nechita, C., Iordache, A.M., Roba, C., Sandru, C., Zgavarogea, R., Camarero, J.J. (2025). Heavy Metal Health Risk Assessment in Picea abies L. Forests Along an Altitudinal Gradient in Southern Romania. Plants. 14(6). 968. 10.3390/plants14060968 Niemczyk M., 2017. Wydajne plantacje topolowe – szansa dla energetyki? Drwal, nr 2/2017. p. 46

Funded by the European Union

Niu, Z., Sun, L., Sun, T., Li, Y., Wang, H. (2018). Evaluation of phytoextracting cadmium and lead by Sedum alfredii Hance and the effects on soil microbial community in a field experiment. Ecotoxicology and Environmental Safety. 149. 296–302. 10.1016/j.ecoenv.2017.11.027.

Nowak, D. J., Hirabayashi, S., Bodine, A., & Greenfield, E. (2017). Tree and forest effects on air quality: A review. Environmental Pollution, 224, 1-1Tree and forest effects on air quality: A review.

Obermeier, W. A., Lehnert, L. W., Ivanov, M. A., Luterbacher, J., Bendix, J. (2018). Reduced Summer Aboveground Productivity in Temperate C3 Grasslands Under Future Climate Regimes. Earth's Future. 6(5). 716-729. 10.1029/2018EF000833

Obermeier, W.A., Lehnert, L.W., Ivanov, M.A., Luterbacher, J., Bendix, J. (2018). Reduced Summer Aboveground Productivity in Temperate C3 Grasslands Under Future Climate Regimes. Earth's Future. 6(5). 716–729. 10.1029/2018EF00083

Oliveira N., Rodríguez-Soalleiro R., Pérez-Cruzado C., Cañellas I., Sixto H., Ceulemans R. (2018). Above- and below-ground biomass allocation in poplar short rotation plantations. Forest Ecology and Management, 428, 57–65.

Oliveira S., Andrade H., Vaz T. (2011) The cooling effect of green spaces as a contribution to the mitigation of urban heat: A case study in Lisbon. Building and Environment 2186-2194. https://doi.org/10.1016/j.buildenv.2011.04.034

Orgiazzi, A., Panagos, P., Fernández-Ugalde, O., Wojda, P., Labouyrie, M., Ballabio, C., … & Jones, A. (2022). LUCAS Soil Biodiversity and LUCAS Soil Pesticides, new tools for research and policy development. European Journal of Soil Science, 73(5), e13299. https://doi.org/10.1111/ejss.13299

Palliwoda, J., Banzhaf, E., & Priess, J. A. (2020). How do the green components of urban green infrastructure influence the use of ecosystem services? Examples from Leipzig, Germany. Landscape Ecology, 35(5), 1127–1142. https://doi.org/10.1007/s10980-020-01004-w

Panagos, P., Broothaerts, N., Ballabio, C., Orgiazzi, A., Rosa, D., Borrelli, P., … & Jones, A. (2024). How the EU Soil Observatory is providing solid science for healthy soils. European Journal of Soil Science, 75(3), e13507. https://doi.org/10.1111/ejss.13507

Parker, G. (2020). Tamm review: Leaf Area Index (LAI) is both a determinant and a consequence of important processes in vegetation canopies. Forest Ecology and Management, 477, 118496. 10.1016/j.foreco.2020.118496.

Pérez-Vizcaíno P., Sánchez de la Campa A.M., Sánchez-Rodas D., Alastuey A., Querol X., de la Rosa J.D. (2026). PM10 chemical fingerprints and source assessment guiding air quality improvements by 2030 in Andalusia, southern Spain, Environmental Pollution, 388, 127347.

Pilipović, A., Zalesny, R., Rončević, S., Nikolič, N., Orlović, S., Beljin, J., & Katanić, M. (2019). Growth, physiology, and phytoextraction potential of poplar and willow established in soils amended with heavy-metal contaminated, dredged river sediments.. Journal of environmental management, 239, 352-365. https://doi.org/10.1016/j.jenvman.2019.03.072

Radojčić Redovniković, I., De Marco, A., Proietti, C., Hanousek, K., Sedak, M., Bilandžić, N., Jakovljević, T. (2017). Poplar response to cadmium and lead soil contamination. Ecotoxicology and Environmental Safety. 144. 482–489. 10.1016/j.ecoenv.2017.06.011

Redovniković, I., De Marco, A., Proietti, C., Hanousek, K., Sedak, M., Bilandžić, N., & Jakovljević, T. (2017). Poplar response to cadmium and lead soil contamination.. Ecotoxicology and environmental safety, 144, 482-489 . https://doi.org/10.1016/j.ecoenv.2017.06.011

Reed M. S, L. C. Stringer, A. J. Dougill, J. S. Perkins, J. R. Atlhopheng, K. Mulale, N. Favretto (2014) Reorienting land degradation towards sustainable land management: Linking sustainable livelihoods with ecosystem services in rangeland systems. Journal of Environmental Management, 472-485. https://doi.org/10.1016/j.jenvman.2014.11.010

Regulation (EU) 2020/852 of the European Parliament and of the Council of 18 June 2020 on the establishment of a framework to facilitate sustainable investment, and amending Regulation (EU) 2019/2088. (2020). Official Journal of the European Union, L 198, 13–43. https://eur-lex.europa.eu/legal-content/EN/TXT/?uri=CELEX:32020R0852

Regulation (EU) 2021/1119 of the European Parliament and of the Council of 30 June 2021 establishing the framework for achieving climate neutrality, and amending Regulations (EC) No 401/2009 and (EU) 2018/1999 (European Climate Law). (2021). Official Journal of the European Union, L 243, 1–17. https://eur-lex.europa.eu/legal-content/EN/TXT/?uri=CELEX:32021R1119

Robinson, D., Bentley, L., Jones, L., Feeney, C., Garbutt, A., Tandy, S., … & Emmett, B. (2024). Five decades' experience of long-term soil monitoring, and key design principles, to assist the EU soil health mission. European Journal of Soil Science, 75(5), e13570. https://doi.org/10.1111/ejss.13570

Rodríguez-Espinosa, T., Navarro-Pedreño, J., Lucas, I., Vidal, M., Bech, J., & Zorpas, A. (2021). Urban areas, human health and technosols for the green deal. Environmental Geochemistry and Health, 43(12), 5065–5086. https://doi.org/10.1007/s10653-021-00953-8

Sawidis, T., Breuste, J., Mitrovic, M., Pavlovic, P., Tsigaridas, K. (2011). Trees as bioindicator of heavy metal pollution in three European cities. Environmental Pollution. 159(12). 3560–3570. 10.1016/j.envpol.2011.08.033.

Schrader, F., & Brümmer, C. (2014). Land use specific ammonia deposition velocities: A review of recent studies (2004–2013). Water, Air, & Soil Pollution, 225, 2040

Semeraro T., Scarano A., Santino A., Emmanuel R., Lenucci M. (2021) An innovative approach to combine solar photovoltaic gardens with agricultural production and ecosystem services. Ecosystem Services Volume 56, 101450. https://doi.org/10.1016/j.ecoser.2022.101450

Semeraro T., Scarano A., Santino A., Emmanuel R., Lenucci M. (2021) An innovative approach to combine solar photovoltaic gardens with agricultural production and ecosystem services. Ecosystem Services Volume 56, 101450. https://doi.org/10.1016/j.ecoser.2022.101450

Shi, Y., Gao, J., Li, X., Brierley, G., Lin, C., & , X. (2023). Spatiotemporal Variability of Alpine Meadow Aboveground Biomass and Sustainable Grazing in Light of Climate Warming. Rangeland Ecology and Management, 90, 64 - 77.

Shiferaw H., Kassawmar T., Zeleke G. (2022) Above and belowground woody-biomass and carbon stock estimations at Kunzila watershed, Northwest Ethiopia, Trees, Forests and People, 7, 100204.

Sinan M., Hasenauer H. (2025). How to determine the leaf area index (LAI) of forests: A comparison of forest inventory versus satellite-driven estimates, Forest Ecosystems, 13, 100332. https://doi.org/10.1016/j.fecs.2025.100332.

Skonieczna, J., Małek, S., Polowy, K., Węgiel, A. (2014). Element content of Scots pine (Pinus sylvestris L.) stands of different densities. Drewno. 57(192). 77–87. 10.12841/wood.1644-3985.S13.05.

Sówka, I., Chlebowska-Styś, A., Pachurka, Ł., Rogula-Kozłowska, W., Mathews, B. (2019). Analysis of Particulate Matter Concentration Variability and Origin in Selected Urban Areas in Poland. Sustainability, 11(20), 5735. https://doi.org/10.3390/su11205735

Sun R., Chen L. (2016) Effects of green space dynamics on urban heat islands: Mitigation and diversification. Ecosystem Services 38-46. https://doi.org/10.1016/j.ecoser.2016.11.011

Sun Y., Wu G., Li P. (2024) Evaluation of Ecological Service Functions of Urban Greening Tree Species in Northern China Based on the Species-Specific Air Purification Index. Urban Forestry. https://doi.org/10.3390/f15101835

Sun, F.F., Wen, D.Z., Kuang, Y.W., et al. (2009). Concentrations of sulphur and heavy metals in needles and rooting soils of Masson pine (Pinus massoniana L.) trees growing along an urban–rural gradient in Guangzhou, China. Environmental Monitoring and Assessment. 154. 263–274. 10.1007/s10661-008-0394-3.

Suo, Y., Tang, N., Li, H., Corti, G., Jiang, L., Huang, Z., Zhang, Z., Huang, J., Wu, Z., Feng, C., & Zhang, X. (2021). Long-term effects of phytoextraction by a poplar clone on the concentration, fractionation, and transportation of heavy metals in mine tailings. Environmental Science and Pollution Research, 28, 47528 - 47539. https://doi.org/10.1007/s11356-021-13864-z

Suo, Y., Tang, N., Li, H., et al. (2021). Long-term effects of phytoextraction by a poplar clone on the concentration, fractionation, and transportation of heavy metals in mine tailings. Environmental Science and Pollution Research. 28. 47528–47539. 10.1007/s11356-021-13864-z.

Tao, Z., Guo, R., Gao, S., Guo, J., & Sun, W. (2015). Responses of Plant Community Composition and Biomass Production to Warming and Nitrogen Deposition in a Temperate Meadow Ecosystem. PLoS ONE, 10

TEEB. (2013). The Economics of Ecosystems and Biodiversity for Water and Wetlands. IEEP, London and Brussels; Ramsar Secretariat, Gland.

TEEB. (2015). TEEB for Agriculture & Food: an interim report. United Nations Environment Programme, Geneva, Switzerland

Tiecke, Tobias G., et al. Mapping the world population one building at a time. arXiv preprint arXiv:1712.05839, 2017). By combining this settlement data with census data, population maps with 30 meter resolution was created. (Source https://data.humdata.org/search?q=Meta+Population

Tomczyk, A. M., & Szyga-Pluta, K. (2016). Okres wegetacyjny w Polsce w latach 1971–2010 = Growing seasons in Poland in the period 1971–2010. Przegląd Geograficzny, 88(1).

Turner, D., Acker, S., Means, J., Garman, S. (2000). Assessing alternative allometric algorithms for estimating leaf area of Douglas-fir trees and stands. Forest Ecology and Management. 126. 61-76. 10.1016/S0378-1127(99)00083-3.

Vivanco, M. G., Garrido, J. L., Martín, F., Theobald, M. R., Gil, V., Santiago, J.-L., Lechón, Y., Gamarra, A. R., Sánchez, E., Alberto, A., Bailador, A. (2021). Assessment of the Effects of the Spanish National Air Pollution Control Programme on Air Quality. Atmosphere. 12(2). 158. 10.3390/atmos12020158

W. Wang, C. Xu, Y. Li (2024) Priority areas and benefits of ecosystem restoration in Beijing Environmental Science and Pollution Research, 83600- 83614. https://doi.org/10.1007/s11356-023-28255-9

Wales.Kabisch, N., Strohbach, M., Haase, D., Kronenberg, J,. Urban green space availability in European cities. Ecological Indicators 2016, 70:, 586-596.

Walston L. J., Li Y., Hartmann H. M., Macknick J., Hanson A., Nootenboom C., Lonsdorf E., Hellmann J. (2021) Modeling the ecosystem services of native vegetation management practices at solar energy facilities in the Midwestern United States Ecosystem Service Volume 47, 101227. https://doi.org/10.1016/j.ecoser.2020.101227

Walston L. J., Li Y., Hartmann H. M., Macknick J., Hanson A., Nootenboom C., Lonsdorf E., Hellmann J. (2021) Modeling the ecosystem services of native vegetation management practices at solar energy facilities in the Midwestern United States Ecosystem Service Volume 47, 101227 .https://doi.org/10.1016/j.ecoser.2020.101227.

Funded by the European Union

Wang C., Ren Z., Dong Y., Zhang P., Guo Y., Wang W., Bao G. (2022) Efficient cooling of cities at global scale using urban green space to mitigate urban heat island effects in different climatic regions. Urban Forestry & Urban Greening. https://doi.org/10.1016/j.ufug.2022.127635

Wang, L., Gao, Y., Zhang, H., et al. (2024). Phytoremediation of cadmium-contaminated soil by Bidens pilosa L.: Accumulation characteristics and ecological risk assessment. Ecotoxicology and Environmental Safety. 244. 114043. 10.1016/j.ecoenv.2024.114043.

Waza, A., Deguine, A., Soulemane H. N., Flament, P., Augustin, P., Cazier, F., Delbarre, H., Dewaele, D., Dieudonné, E., Fourmentin, M., Deboudt, K. (2025). Critical factors influencing PM10 and PM2.5 pollution episodes and their associated particle chemical composition and mixing state in a coastal multisources area. Atmospheric Environment. 365. 121676. 10.1016/j.atmosenv.2025.121676.

Wellbrock, N., Cools, N., Vos, B., Jandl, R., Lehtonen, A., Leitgeb, E., … & Šrámek, V. (2024). There is a need to better take into account forest soils in the planned soil monitoring law of the European Union. Annals of Forest Science, 81(1), 9. https://doi.org/10.1186/s13595-024-01238-7

World Health Organization Regional Office for Europe. (2013). Review of evidence on health aspects of air pollution: REVIHAAP project: technical report. WHO Regional Office for Europe.

Xu Y. , S. Dong, X. Gao, M. Yang, S. Li, H. Shen, J. Xiao, Y. Han, J. Zhang, Y. Li, Y. Zhi, Y. Yang, S. Liu, Q. Dong, H. Zhou, P. Stufkens (2019) Trade-offs and cost-benefit of ecosystem services of revegetated degraded alpine meadows over time on the Qinghai-Tibetan Plateau. Agriculture, Ecosystems & Environment, 130-138. https://doi.org/10.1016/j.agee.2019.04.015

Yan M., Wang L., Ren H., Zhang X. (2017) Biomass production and carbon sequestration of a short-rotation forest with different poplar clones in northwest China. Science of the Total Environment 1135-1140. https://doi.org/10.1016/j.scitotenv.2017.02.103

Zeiss, R., Eisenhauer, N., Orgiazzi, A., Rillig, M., Buscot, F., Jones, A., … & Guerra, C. (2022). Challenges of and opportunities for protecting European soil biodiversity. Conservation Biology, 36(5), e13930. https://doi.org/10.1111/cobi.13930

Zheng, B., & Masrabaye, F. (2023). Sustainable brownfield redevelopment and planning: Bibliometric and visual analysis. Heliyon, 9(2), e13280. https://doi.org/10.1016/j.heliyon.2023.e13280

Zhong, Q., Zhang, L., Zhu, Y., Konijnendijk, C. C., Han, J., Zhang, G., … & Li, Y. (2020). A conceptual framework for ex ante valuation of ecosystem services of brownfield greening from a systematic perspective. Ecosystem Health and Sustainability, 6(1), 1743206. https://doi.org/10.1080/20964129.2020.1743206

Zianis, D., & Mencuccini, M. (2005). Aboveground net primary productivity of a beech (Fagus moesiaca) forest: a case study of Naousa forest, northern Greece. Tree Physiology, 25(6), 713-722.

Funded by the European Union